Intracytoplasmic Lipid Droplets in High Grade Glioma – Metabolism and Target for Therapy

By

Robert John Murren

A thesis submitted to the University of Birmingham for the degree of DOCTOR OF PHILOSOPHY

UNIVERSITY OF BIRMINGHAM

Institute of Cancer and Genomic Sciences

College of Medical and Dental Sciences

University of Birmingham

February 2018

UNIVERSITY OF
BIRMINGHAM

University of Birmingham Research Archive

e-theses repository

This unpublished thesis/dissertation is copyright of the author and/or third parties. The intellectual property rights of the author or third parties in respect of this work are as defined by The Copyright Designs and Patents Act 1988 or as modified by any successor legislation.

Any use made of information contained in this thesis/dissertation must be in accordance with that legislation and must be properly acknowledged. Further distribution or reproduction in any format is prohibited without the permission of the copyright holder.

Abstract

Glioblastoma is a highly malignant and aggressive high grade glioma with a poor prognosis. The low survival rates stem from tumour progression, late intervention, ineffective therapies and drug resistance, requiring new therapeutic and diagnostic approaches. Lipid droplets are dynamic organelles suggested to be influential facets of cancer metabolism and biology in many tumours. In glioblastoma, lipid droplets have been associated with hypoxia, higher clinical grades and poor survival; however, the cellular pathways underlying lipid droplet metabolism remain unclear. Using a publically available database of grade 2 to 4 glioma gene expression, we observed that genes associated with lipid droplet metabolism were important prognostic survival and tumour progression indicators. Moreover, through confocal microscopy, flow cytometry and NMR-based methods, we observed that uptake of exogenous lipids and adipose triglyceride lipase-mediated lipid shuttling produced lipid droplets whilst autophagy was vital to lipid droplet breakdown. ATGL-mediated lipid shuttling was further observed to prevent unsaturated fatty acid oxidative damage. Finally, we investigated the effect of pharmacological lipid droplet manipulation and observed that autophagy inhibition can improve temozolomide and irradiation cytotoxicity. Taken together our data suggests that understanding lipid droplet metabolic pathways may generate prognostic bio-markers of survival and progression and improve current therapies.

Acknowledgements

It is my pleasure to acknowledge the help of several individuals who were instrumental in the completion of my PhD research.

First of all, I would like to thank Professor Andrew Peet for his invaluable help and guidance throughout my research and for helping me to see the way forward when I thought it had all gone wrong.

I also wish to thank Dr Daniel Tennant for taking me into his lab and imparting his vast knowledge of cellular metabolism.

My sincerest gratitude goes to Georgie Moseley and the Help Harry Help Others charity for funding this work. Their efforts to “help care, help cope and help cure” have been a constant inspiration.

Importantly, I would also like thank Christopher Bennett for his assistance with the HRMAS spectrometer and Haydn Munford for his assistance with the western blots. Further thanks also go to Haydn for the many nights as my drinking/coup partner and to Pip Evans for her saintly patience.

I am forever grateful to my family who have supported me throughout my life and offered a different kind of madness to escape to during the more stressful times.

Finally, I would like to thank the many others not mentioned by name.

Declaration

I confirm that this work is my own and that I have been involved in the design and conduct of this study, analysis of data and preparation of this thesis. The following aspects of this study were undertaken as part of collaboration:

1) Christopher Bennett assisted in the acquisition of HRMAS NMR spectra and provided subsequent quality control checks for peak assignment during analysis.

2) Haydn Munford assisted in the generation of the western blots, specifically the actin control blot.

3) STR profiling on extracted genomic DNA was performed by Eurofins, Germany

4) RNA sequencing on extracted mRNA was performed by Genomics Birmingham

I undertook all other experiments and statistical analyses within this study.

Table of Contents

List of Figures

Figure 5.4. Chloroquine pre-treatment can improve the cytotoxicity of irradiation.

List of Tables

List of Abbreviations

ACACA	Acetyl CoA carboxylase
ACLY	ATP citrate lyase
ACSS2	Acyl CoA synthetase
ATGL	Adipose triglyceride lipase
BCPC	Brain cancer progenitor cell
BODIPY	4,4-Difluoro-1,3,5,7,8-Pentamethyl-4-Bora-3a,4a-Diaza-s-Indacene
BPTES	Bis-2-(5-phenylacetamido-1,3,4-thiadiazol-2-yl)ethyl sulphide
CEPT1/CHPT1	Cholinephosphotransferases
CGI58	Comparative gene identification 58
CKA/B	Choline kinase A and B
CNS	Central nervous system
CPT1/2	Mitochondrial acyltransferases
CPMG	Carr-Purcell-Meiboom-Gill sequence
DAPI	4',6-diamidino-2-phenylindole
DMEM	Dulbecco's Modified Eagle's Medium
DMOG	Dimethyloxalylglycine

DMSO	Dimethyl Sulfoxide
EGFR	Epithelial growth factor receptor
EGFRvIII	Truncated EGFR
ER	Endoplasmic reticulum
ETNK1	Ethanolamine kinase 1
FABP	Fatty acid binding protein
FASN	Fatty acid synthase
FITC	Fluorecein isothiocyanate
FPKM	Fragments per kilobase of transcript per million reads
FSC	Forward scatter
GBM	Glioblastoma
GBW	Gehan-Breslow-Wilcoxon
GLS	Glutaminase
HIF	Hypoxia inducible factor
HIG2	Hypoxia inducible protein 2
HILPDA	Hypoxia inducible lipid droplet associated protein
HRMAS	High resolution magic angle spinning
HSL	Hormone sensitive lipase
H_2O_2	Hydrogen peroxide

IDH	Isocitrate dehydrogenase
IGV	Integrative genomics viewer
LDQ	Lipid droplet quantity
LPL	Lipoprotein lipase
LDL-R	Low density lipoprotein
MC	Log-rank/Mantel-Cox
MEFs	Mouse embryo fibroblasts
MGMT	O6-methylguanine DNA methyltransferase
MRS	Magnetic resonance spectroscopy
NF1	Neurofibromatosis type 1
NMR	Nuclear magnetic resonance
NOESY	Nuclear Overhauser effect spectroscopy
PI	Propidium Iodide
PLIN1	Perilipin 1
PLIN2	Adipophilin
PLIN3	TIP47
PTDSS1/2	Phosphatidylserine synthase
PTEN	Phosphatase tumour suppressor
RB1	Retinoblastoma protein 1

ROS	Reactive oxygen species
siAtg5	Atg5 siRNA
siNT	Non-targeting siRNA
siRNA	Small interfering RNA
SNP	Single nucleotide polymorphisms
SRB	Sulphorhodamine B
SSC	Side scatter
STR	Short tandem repeat
TAG	Triacylglycerol
TCA	Tricarboxylic acid cycle
TCGA	The cancer genome atlas
TIC	Tumour-initiating cell
VEGFR	Vascular endothelial growth factor receptor
VLDLR	Very low density lipoprotein uptake receptor
WHO	World health organisation
2-HG	2-hydroxyglutarate
3-MA	3-Methyladenine

Chapter 1

Introduction

1.1. Introduction

The world health organisation (WHO) reported that cancer was responsible for 8.8 million deaths in 2016, accounting for approximately a sixth of all deaths, and is a significant burden on medical resources (1). The category “Brain and CNS tumours” is comprised of many types of cancer including glioma, medulloblastoma, ependymoma, meningioma and metastases from other cancers localised to the brain. Although brain and CNS tumours represent a small percentage of cancer cases they contribute significantly to overall cancer mortality. Indeed, in 2014 brain and CNS tumours represented just 3% of all cases in the UK but had a 10 year survival of 14% (2). The majority of brain and CNS tumours occur in older patients, with 46% diagnosed in patients over 65 years (2); however, they also represent the most frequently occurring group of tumours in patients aged 0-19 (3). Although the mortality is far lower than their adult counterparts, brain and CNS tumours represent 40-50% of paediatric tumours (4) and are associated with the highest mortality rate in paediatric cancers. Despite significant research, little progress has been made in the improvement of treating many of these tumours and therefore effective novel therapeutic approaches have been long awaited.

1.2. Gliomas

1.2.1. Introduction to gliomas

The most common group of intrinsic CNS tumours is the gliomas, derived from glial cells which provide physical, metabolic and neurotrophic support to neurons within the brain (Figure 1.1.). Oligodendrocytes provide a myelin sheath similar to

peripheral nervous system Schwann cells (5) whilst microglia have a macrophage-like protective function (6). In contrast, astrocytes provide a diverse range of support including nutrient supply, brain repair and support for blood brain barrier endothelial cells (7). We have elected to focus upon astrocyte-derived gliomas, termed astrocytomas, which represent three quarters of all gliomas (8).

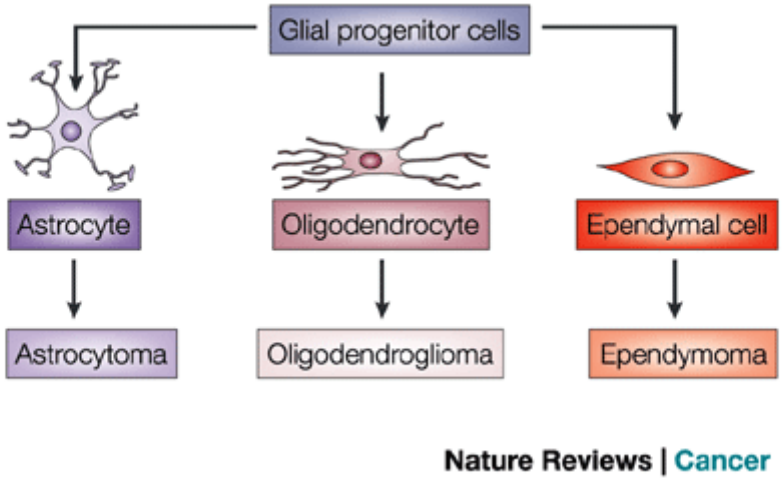

Figure 1.1. The glial progenitor cells and the corresponding tumours. Image from Rao et al. (292)

1.2.2. The WHO grading system

In contrast, to many cancers, brain tumours are separated by severity, progression and phenotype into representative groups called clinical grades as opposed to stages. The WHO classifies gliomas into 4 clinical grades of increasing severity (9). Grade 1 gliomas are well defined, have a low proliferative potential, rarely progress and are considered distinct from the other three glioma grades. Grade 2 gliomas also have low proliferative potential but are more invasive and infiltrative with more frequent recurrence and tumour progression. Similarly, grade 3 gliomas have increased infiltration and proliferation and are distinguished by increased malignant cytological indicators. Finally, grade 4 gliomas are highly invasive, aggressive and

necrotic and have a very poor survival. Previously tumour grade was predominantly classified through histology; however, the updated WHO glioma classification now includes molecular and genetic parameters within the definitions of glioma grades (9). Most notably, grade 2 and 3 gliomas are classified according to the mutational status of the metabolic IDH genes with IDH mutant tumours being the most frequent (10). As previously mentioned, grade 1 gliomas are considered notably distinct from the other glioma grades and therefore, in the interest of clarity, we have focussed upon grades 2 to 4.

1.2.3. Grade 2 gliomas

Grade 2 gliomas are predominantly slow growing diffuse astrocytomas with high differentiation (11) which most frequently present at the insular and supplementary motor area in Caucasian men aged approximately 40 years (12). The prognosis is relatively good with a 5 year survival of 47.4% (13) and tumours are characteristically noted to have ATRX loss and mutant IDH and TP53 (10). As previously mentioned, grade 2 tumours can progress to higher clinical grades and this has led to the proposal of an intermediate diffuse glioma between grades 2 and 3 (14).

1.2.4. Grade 3 gliomas

Grade 3 gliomas, most frequently presenting as anaplastic astrocytomas, can be difficult to define due to their similarities to grade 2 gliomas; however, the prognosis is inevitably poorer and more severe (15). 5 year survival is decreased to 27.3% in grade 3 gliomas (13) which are more aggressive, invasive and heterogeneous.

Indeed, grade 3 gliomas often display areas of high and low grade glioma biology (16). The frequency of tumour progression is also increased and it can be difficult to separate grade 3 and 4 gliomas by MRI and histology alone (17). Therefore, molecular markers such as the IDH, TP53 and NOTCH genes are used to complement histological markers and assist tumour classification.

1.2.5. Grade 4 gliomas

Grade 4 gliomas, known as glioblastoma (GBM), are the most common and severe group of gliomas accounting for 54% of all gliomas (8). The standard treatment regimen of surgery, radiotherapy and chemotherapy is largely ineffective (18-20) and the 5 year survival is less than 5% (13). These tumours are characteristically highly invasive, aggressive and proliferative and inadequate perfusion results in severely hypoxic areas forming necrotic foci surrounded by pseudopallisading cells (21-23). This stimulates the diffuse spread of cells throughout the entire brain, frequently generating new tumours and preventing effective resection. Indeed, some GBMs have a widely diffuse, infiltrative nature, in which cells are spread throughout the brain with no central foci (24).

GBMs are clinically delineated into two types, known as primary and secondary GBM, and are markedly distinct and believed to stem from different precursor cells (25). Primary GBMs are the most common type of GBM representing about 90% of all cases and are believed to occur spontaneously at grade 4 (9). These tumours are more invasive with a more rapid progression and worse prognosis. Moreover, they can be further subdivided into 4 sub-groups based upon several molecular features (26,27) (Figure 1.2.). The classical GBM sub-group is associated with alterations in

EGFR, PTEN, CDKN2A and NOTCH while the mesenchymal sub-group is associated with alterations in NF1, TP53, PTEN and MET. The pro-neural sub-group is similarly associated with alterations in PTEN and TP53 but also PDGFRA, IDH and PI3K whereas the neural subgroup is poorly defined but retains more similarity to normal brain structure. However, despite this, primary GBMs are not frequently associated with IDH and TP53 mutations. In contrast, to the spontaneous occurrence of primary GBMs at grade 4, secondary GBMs are believed to be the result of progression from lower tumour grades and retain the alterations in IDH and TP53 characteristic of grade 2 and 3 gliomas. Moreover, these tumours typically arise in younger patients and are associated with a better prognosis, emphasising the importance of these molecular markers across glioma grades.

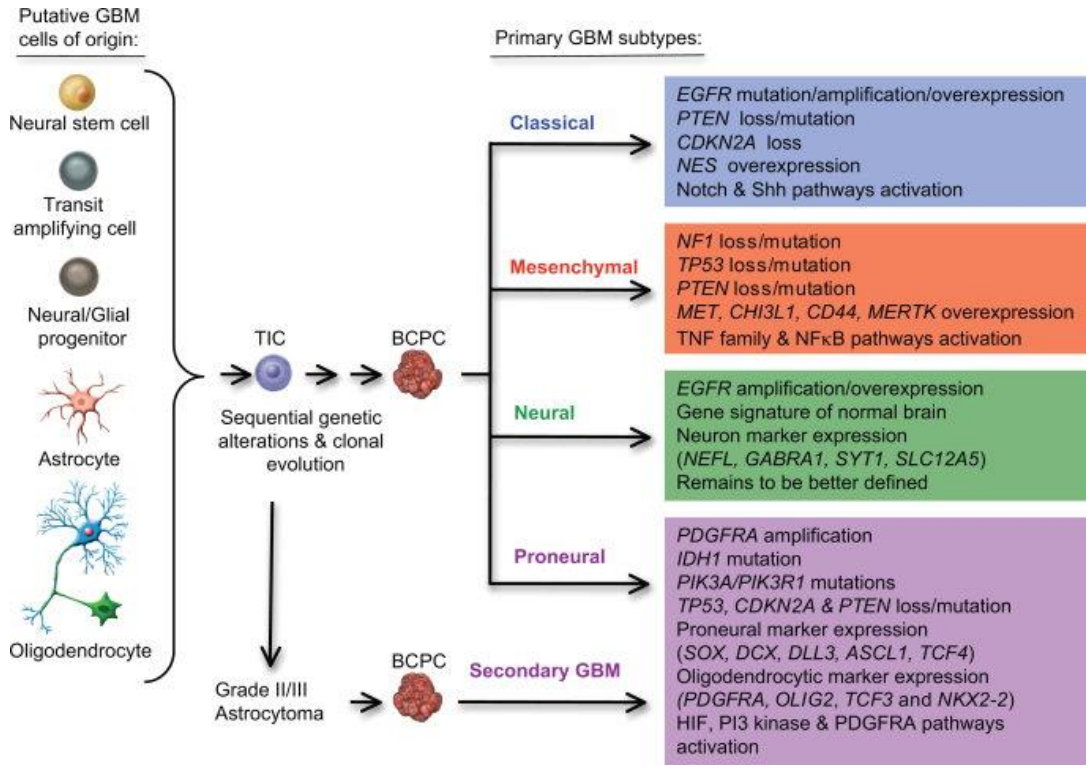

Figure 1.2. GBM can be split into primary and secondary GBM whilst primary GBM can be further divided by molecular subgroups. Image from Van Meir et al. (27). Tumour-initiating cell (TIC), Brain cancer progenitor cell (BCPC).

1.2.6. Molecular markers in gliomas

Several mutations are frequently observed in a large proportion of gliomas. For example GBMs have been noted to display mutations in the following proportions of tumours: PTEN (29%), TP53 (29%), EGFR (20%), NF1 (9%), RB1 (8%), IDH1 (5%) (28). Indeed, several of these mutations have particular importance as molecular markers of glioma grade.

1.2.6.1. IDH mutations

As previously mentioned, IDH mutations now define intra-grade tumour groups in gliomas due to the high frequency of observation. The IDH genes encode a group of isocitrate dehydrogenase enzymes 1, 2 and 3 and mutations in IDH 1 and 2 are observed in over 80% of grade 2 gliomas (29). IDH1 is located in the cytosol whilst IDH2 and 3 function within the mitochondria and together these enzymes carry out the synthesis of α-ketoglutarate from isocitrate in the tricarboxylic acid (TCA) cycle (30). Alternatively, IDH enzymes are also vital to glutamine-derived lipogenesis through reductive carboxylation, although the relatively slow kinetics of this pathway compared to oxidative glutamine metabolism mean that it only predominates in conditions in which oxidative metabolism is limiting, such as hypoxia (31). Finally, these enzymes may mediate electron and metabolite shutting between the mitochondria and cytosol and IDH1 mutations have been associated with reduced NADPH production (32). The diverse metabolic roles of the IDH enzymes therefore make them prime targets for subversion in tumorigenesis. Intriguingly mutations in IDH enzymes map exclusively to key structural residues within the active binding site, specifically three arginine residues critical to isocitrate binding (33). The choice

of amino acid that replaces the arginine appears unimportant implying that only physical active site structure and function disruption is required whilst obligatory heterozygosity suggests a gain of function effect. Indeed, the major effect of an IDH mutation may be the increased production of the oncometabolite 2-hydroxyglutarate (2-HG) which has neomorphic metabolic activity (Figure 1.3.). Although 2-HG is also produced by wildtype IDH enzymes as a minor product it is quickly cleared by a number of possible dehydrogenases. In contrast, the increased 2-HG production by mutant IDH enzymes overwhelms this process to the extent that 2-HG becomes one of the most abundant cellular metabolites. At such concentrations 2-HG dramatically alters the cellular metabolic and epigenetic profile and may promote tumorigenic activity (34). Indeed, mutations in IDH enzymes are understood to occur very early in glioma tumorigenesis and represent an important step within this process (35,36). Interestingly, IDH mutation is associated with improved survival and may also affect treatment efficacy (37). Nevertheless, due to the importance and frequency of these mutations, pharmacological inhibitors targeting oncogenic IDH enzymes are currently under trial (38).

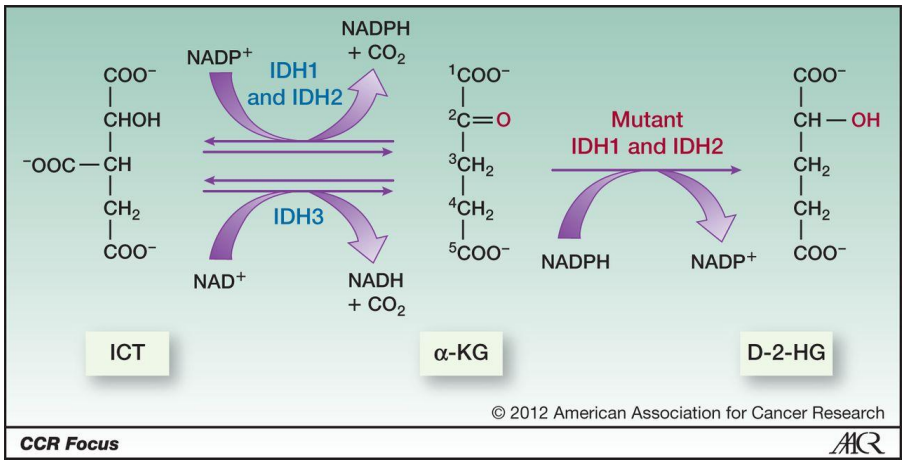

Figure 1.3. Mutant IDH enzymes have neomorphic metabolic activity. Image from Yang et al. (291)

1.4.6.2. TP53 mutations

Mutations in the TP53 tumour suppressor gene also represent one of the most common genetic alterations in grade 2 and 3 gliomas, mutated in up to 70% of cases (39). Indeed, glioma TP53 mutations occur almost invariably with IDH mutations (40). TP53 encodes the tumour suppressor p53 which is vital in many processes including DNA repair, cell cycle arrest and cell death (41,42). Mutations can result in loss of activity through protein degradation, truncation or suppression of the heterozygote wild type protein as a dominant negative oncogene. Mutations in TP53 are one of the most frequent genetic alteration observed in human cancers (43) and therefore its importance in gliomas is unsurprising. Nevertheless, the frequent association of TP53 and IDH mutations across glioma grades suggests a common importance in the process of glioma tumorigenesis.

1.4.6.3. Other common mutations

IDH and TP53 mutations represent the majority of genetic alterations in grade 2 and 3 gliomas; however, several other genes have been noted to occur with a high frequency at grade 4. Epidermal growth factor receptor (EGFR) gene amplification and mutation events cause constitutive activation and are the most common oncogenic alterations in GBM, amplified in up to 60% of cases (44). EGFR is a transmembrane tyrosine kinase receptor for epidermal growth factors which promotes growth, proliferation and angiogenesis through down-stream signalling pathways. The EGFR alteration that is observed most frequently in GBM is the EGFRvIII truncation which is constitutively active (45). Intriguingly this mutation is usually observed within a scattered subpopulation of the tumour surrounded by

tumour cells overexpressing wild-type EGFR (46). Although the late occurrence of this mutation could prevent diffuse migration and occurrence throughout the tumour, it has been suggested that expression of truncated EGFRvIII enhances the tumorigenic activity of the neighbouring tumours cells with amplified wild-type EGFR expression (47).

The phosphatase tumour suppressor PTEN is also mutated in GBM, occurring in 5-40% of cases and providing a prognostic marker in patients over 45 years (48). PTEN regulates re-entry into the cell cycle and loss of function genetic alterations to this gene often promote tumorigenic activity.

Neurofibromatosis type 1 is an autosomal dominant disorder characterised by mutations in the NF1 gene which suppresses the RAS kinase pathway. Mutations to this gene are oncogenic due to the role of NF1 in cell regulation and gliomas commonly occur in NF1 patients (49,50).

Mutation or loss of the alpha-thalassemia/mental retardation syndrome X-linked (ATRX) gene commonly occurs with IDH1 and TP53 mutation, mirroring their prognostic indication (51). Interestingly, loss of this gene lengthens cell mortality through telomerase lengthening and increases epigenetic instability through disruption of histone variant deposition (52,53).

Finally, epigenetic methylation of genes including tumour suppressors, growth regulators and drug resistance mechanisms provide interesting alterations throughout the glioma grades (54).

1.2.7. Tumour progression

Tumour progression presents one of the greatest challenges in glioma treatment as tumours become increasingly more aggressive and therapy resistant. Nevertheless, recurrent features across tumour grades such as alterations in the molecular markers IDH1 and TP53 may indicate aspects of an underlying progression route to higher clinical grades. TP53 and IDH1 mutations occur in the majority of grade 2 and 3 gliomas, although this is not reflected at grade 4. Indeed, IDH1 mutations occur in 83% of secondary GBMs but only 5% of primary GBMs (55). This suggests that these mutations are an important feature in the biology of a tumour progressing from a grade 2 glioma to a grade 4 secondary GBM but not a spontaneously occurring primary GBM. Moreover, IDH mutations occur very early in tumour progression often preceding other alterations in genes such as TP53 which again precede alterations in genes such as PTEN and EGFR (35,36). The occurrence of these mutations in an apparent common sequence shared by progressing tumours, again suggests that these genes may represent aspects of the tumour progression process (Figure 1.4.). These mutations are also stable molecular events, remaining throughout the transition from low to high grade, emphasising their oncogenic importance (56). However, despite the trends in mutation occurrence, a mechanistic link to tumour progression remains to be demonstrated. Although these genes clearly represent common alterations gained by tumours as they progress to higher clinical grades, the underlying features of tumour progression and a theoretical shared progression pathway remain uncertain. Nevertheless, it is reasonable to speculate that other genetic alterations may also contribute to or represent tumour progression and that, through understanding this process, we may be able to address and target the clinical problems associated with advancing tumour grade.

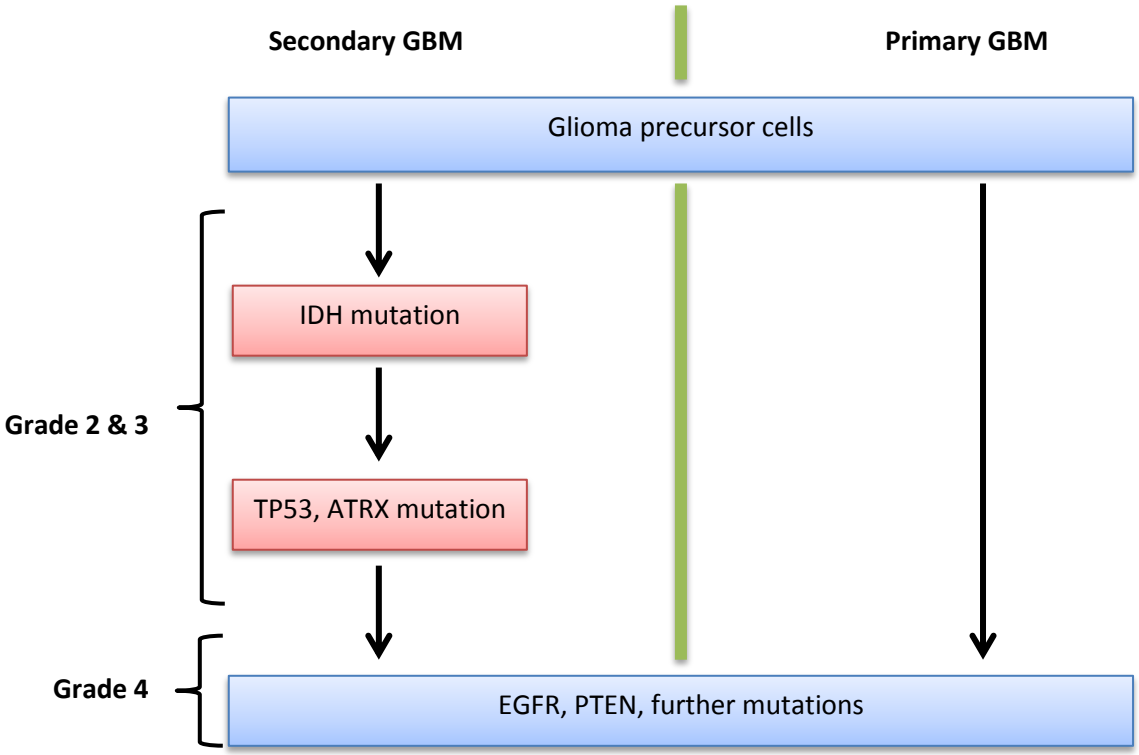

Figure 1.4. IDH, TP53 and ATRX mutations are associated with grade 2 and 3 gliomas and secondary GBM but not observed in primary GBM.

1.2.8. Glioma therapy and why it fails

Another major issue in the treatment of gliomas is ineffective therapies and therapy resistance. Standard therapy for gliomas is extensive resection with radiotherapy and adjuvant chemotherapy with regimen aggressiveness determined according to tumour grade and patient status (Figure 1.5.). Patient-specific variables such as old age and decreased vitality are important factors in determining the extent of treatment and can contraindicate high dose therapies and repeated surgeries. However, irrespective of aggressive therapies, this disease remains incurable due to intrinsic and acquired tumour resistance mechanisms. Extensive and early resection can improve patient survival with tumour resection over 90%, significantly increasing one year survival (57), although the infiltrative nature of gliomas means recurrence in

the surrounding tissue is inevitable. This is especially true in highly invasive GBM where complete resection is impossible. Radiotherapy also constitutes a standard feature in glioma treatment regimens; however, it is frequently resisted through a variety of cellular mechanisms. DNA repair enzymes are upregulated in response to radiation (58) and cell death can be inhibited (59). Indeed, Ape1 has been suggested to be of particular importance in gliomas due to its role in base excision repair (60) whilst EGFRvIII can upregulate DNA double strand break machinery (61). Similarly, cancer stem cells are known to have high radio-resistance (62) which can also be effected by the tumour microenvironment and oxygen concentration (63). Chemotherapy constitutes the final component in glioma treatment and relies predominantly on temozolomide. Temozolomide is an alkylating agent which methylates guanine at the O6 position, inducing cell death (64). However, this lesion can be removed by the DNA repair enzyme MGMT which is frequently upregulated in gliomas, limiting temozolomide efficacy (65). As such, the current treatment regimens of glioma remain ineffective and novel therapeutic approaches are required.

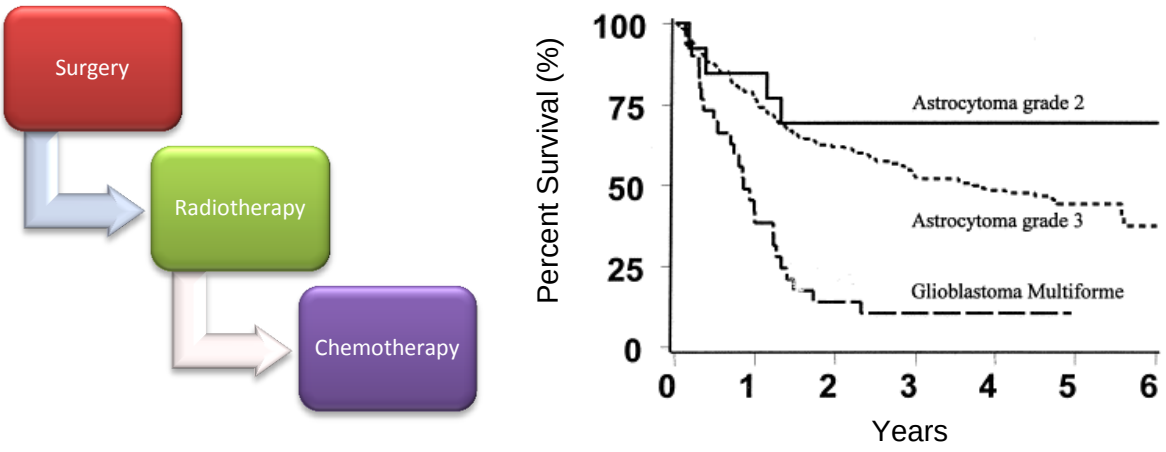

Figure 1.5. Surgery, radiotherapy and chemotherapy constitute the three major components of glioma treatment regimens and are escalated according to grade and tumour severity. Patient survival decreases according to clinical grade. Right image adapted from Prados et al. (295)

1.2.9. Novel therapeutics

Whilst current therapy efficacy remains low altered approaches will continue to be investigated, although these have been mostly limited to grade 3 and 4 glioma. Sloan et al. (66) reported in their systematic review that no novel therapies were being investigated for low grade gliomas (grades 1 and 2). Persistent hyperglycaemia was independently associated with poor survival and high recurrence in low grade gliomas implicating dietary options for improving current therapies (67). However, this remains to be further investigated. Consistent obstacles in the investigation of novel therapies in low grade gliomas remain cost and frequency of occurrence. Long follow up times increase study expense whilst low tumour frequency necessitates multi-centre studies. Moreover, the increased survival of these tumours compared to higher grades ensures novel therapeutics remain a lower priority in low grade gliomas.

In contrast, a variety of different approaches have been investigated in high grade gliomas. Several monoclonal antibodies targeting surface receptors to prevent down-stream activation or induce cell death have been trialled. Bevacizumab, an anti-VEGFR antibody, was designed to prevent neovascularisation but had no effect on survival (68). In contrast, AMG595, an anti-EGFRvIII antibody conjugated to a cytotoxic agent that is internalised upon binding, showed good *in vitro* and pre-clinical efficacy (69). However, cytotoxicity will be limited to the EGFRvIII subset of tumour cells and *in vivo* efficacy remains to be tested in clinical trials. Similarly, several synthetic glioma-associated antigen peptides, designed to stimulate the anti-tumour immune response, have passed the phase 1 clinical trial but require further investigation (70). Dendritic vaccines which mobilise the host's innate immune system against individual tumours have also been investigated in GBM but their

efficacy may be limited to a small patient sub-group (71). Moreover, oncolytic viruses such as herpes simplex and adenovirus which proliferate selectively in tumour cells and induce lysis are under current investigation (72) whilst antioxidants have shown inconsistent and unreliable results (73). As observed in many cancers, small molecule inhibitors have failed to reach expectations in gliomas and the EGFR tyrosine kinase inhibitor erlotinib (74) and an IDH1 mutant enzyme inhibitor (38) have shown limited efficacy. Despite extensive investigation, novel therapies have thus failed to provide significant breakthroughs and glioma therapy has remained unchanged. Therefore, many novel therapies are now targeting alternative key tumorigenic mechanisms in cancer biology, including tumour metabolism.

1.3. Tumour metabolism

1.3.1. Introduction to tumour metabolism

Altered metabolism is vital to support the increased demands of a tumour and is considered a “hallmark” of cancer (75). There are three main focuses for metabolic reprogramming; the production of energy (i.e. ATP), the maintenance of homeostatic reactions such as balancing the redox state and the generation of macromolecules and their pre-cursors for growth and proliferation. The increased metabolic activity of a tumour cell therefore requires an increased uptake of metabolic fuels such as glucose (76), acetate (77) and glutamine (78). Glucose uptake is dramatically increased in many cancers and provides a major source of energy (76). Glucose metabolism switches from linked glycolysis and oxidative phosphorylation to significantly increased glycolysis with subsequent production of lactate from pyruvate in a condition known as the Warburg effect (79,80). Although ATP production per

glucose molecule is lower, it is produced at a far quicker rate and can be maintained in the absence of oxygen providing a significant growth advantage within a tumour. Similarly, increased acetate metabolism provides an increased production of acetyl CoA to support a variety of metabolic processes (77). Exogenous glutamine can also be used to support several different cellular processes including the production of α-ketoglutarate for TCA cycle metabolism and reductive carboxylation or nitrogen donation for nucleotide biosynthesis (78). Indeed, many tumours, including some gliomas, are considered “glutamine addicted” emphasising the importance of glutamine in tumour metabolism (81,82). The increased tumour metabolic rate increases precursor supply for the production of macromolecules and drives upregulated growth and proliferation. Indeed, the importance of the subverted macromolecule production pathways in proliferation suggests they are key areas of tumour biology which must be understood to achieve real therapeutic progress.

1.3.2. Overview of the lipid class of macromolecules

Lipids represent a major class of macromolecules vital for life composed of three groups; isoprenoids, polyketides and acylglycerides/fatty acids (83). Isoprenoids are 5 carbon subunits such as steroids and bile acids whereas polyketides are a range of poly-β-ketoacid derived secondary metabolites containing aromatic and polycyclic groups. Acylglycerides and fatty acids represent the most universally important group of lipids. Fatty acids are comprised of long hydrocarbon chains with a distinct hydrophobic character that can be conferred to molecules such as proteins through conjugation. Moreover, they can be conjugated to glycerol “backbones” to produce acylglycerides including triglycerides and phospholipids. Fatty acids and

acylglycerides have a diverse range of roles including energy production through β-oxidation, protein modification and lipid signalling and are the major component of membranes as phospholipids. This investigation has focussed exclusively on the fatty acid and acylglyceride group of lipids to which the term “lipid” will refer to from hereon.

1.3.3. The importance of lipid metabolism in cancer

As previously discussed the activity of lipid metabolic pathways must be increased to meet the demands of energy production, signalling and biosynthesis in cancer and has long been established as a vital tumorigenic change (84). Indeed, lipid metabolism has been linked to the malignant phenotype of prostate cancer cells (85-87) and is an important factor in tumour growth and progression (88). Moreover, many lipid metabolic enzymes have been linked to prostate tumour growth (89,90) whilst obesity has been linked to patient survival (91). Similarly, lipid metabolism has been linked to metastatic disease in triple negative breast cancer (92) whilst lipid metabolism proteins have also been associated with decreased survival in several breast cancer subtypes (93). Altered lipid metabolism has been observed in nearly all cancers; however, the mechanism through which these changes aid tumorigenesis is often cancer-specific.

1.4. Lipid droplets

1.4.1. Introduction to lipid droplets

One major area of interest in cancer lipid metabolism is lipid droplets also known as mobile lipids, adiposomes, lipid bodies and magnetic resonance spectroscopy (MRS)-visible lipids. Although previously thought to be limited to large fat storage droplets within adipocytes, all human and animal cells have been observed to have the ability to form lipid droplets to some extent (94). These lipid-rich cytoplasmic organelles are involved in many cellular processes both physiological and pathological and can be visualised and detected with chemical staining and MRS (95). Classically lipid droplets were viewed as inert membrane bound stores of fatty acids awaiting catabolism; however, their complex metabolic roles and unique interactions with other organelles including the endoplasmic reticulum (ER), mitochondria and peroxisomes is such that they are now considered dynamic organelles (96). It is therefore unsurprising that they have been investigated in many diseases including atherosclerosis, obesity, heart disease, diabetes and viral pathogenesis. Most notably, lipid droplets have been linked with many types of cancer and are often considered negative pathological indicators and intrinsic to tumorigenic metabolism.

1.4.2. Lipid droplet composition

Membrane bilayers are inadequate for lipid storage as functionality and structural integrity can quickly be lost whilst high cytoplasmic lipid concentrations risk lipotoxic damage. Therefore, lipid droplets provide a system through which homeostasis can

be maintained. Lipid droplets are composed of a hydrophobic core of neutral lipids and cholesteryl esters surrounded by a single phospholipid monolayer membrane (Figure 1.6.). Pan et al. (97) observed that triglycerides within lipid droplets were composed of saturated, unsaturated and polyunsaturated fatty acids which were predominantly oleic and linoleic fatty acids. Interestingly, they also noted that the composition of lipid droplets is notably different to cell membranes due to the increased hydrophobic area of a droplet compared to a membrane bilayer. Similarly, Mirbahai et al. (98) observed that the polyunsaturated fatty acid concentration could increase in response to lipid droplet promoting conditions suggesting that these ratios are dynamic and condition-specific. Indeed, mobilisation of saturated fatty acids from lipid droplets for β-oxidation resulted in an increased proportion of monounsaturated fatty acids within the lipid droplet (99). It is therefore difficult to define lipid droplet contents from a general perspective as this can be cell type and condition specific and must be considered on a case by case basis.

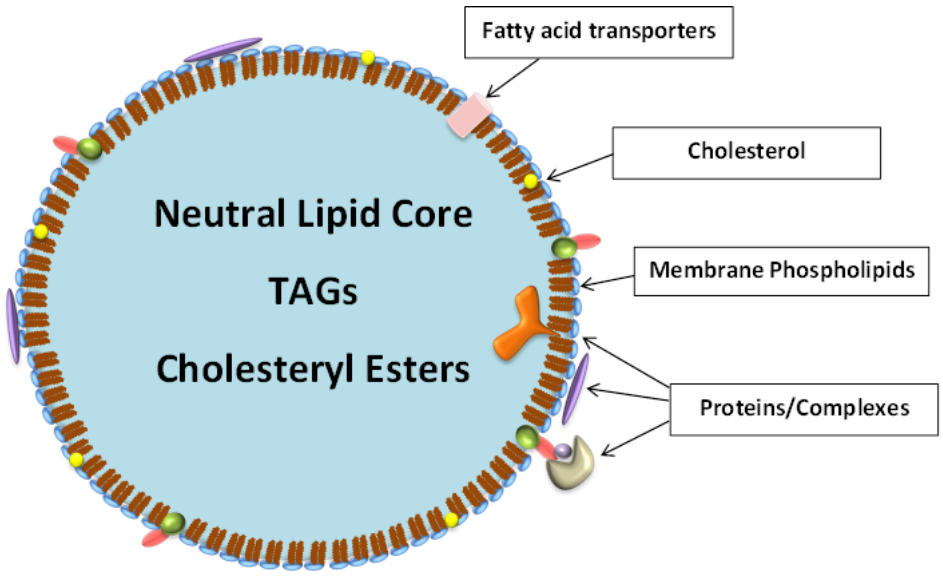

Figure 1.6. The major features in the structure and content of lipid droplets.

The amphipathic nature of phospholipids causes them to align at the lipid droplet surface to form a membrane and provide stability through emulsion principles (100,101). As surfactants they decrease surface tension and provide elasticity and flexibility, supported by their specialised structure. For example the hydrophilic head of phosphatidylcholine is cylindrical providing increased surface area and decreased surface tension compared to the conically shaped phosphatidylethanolamine.

1.4.3. Lipid droplet origin and size

Lipid droplets are thought to initially derive from the ER; however, the exact mechanism has remained poorly defined (96). A “lens” was observed between ER membranes and nascent lipid droplets suggesting a budding mechanism (102) which may involve apolipoprotein B-100 and the lipid droplet-associated protein TIP47 (103). Similarly, it has been suggested that small lipid droplets use ER enzymes to generate lipid content, requiring continued attachment to the ER (104). In contrast, large lipid droplets were suggested to relocate ER triglyceride synthesis enzymes such as GPAT4 to the lipid droplet surface suggesting ER independent mechanisms for mature lipid droplets (104). Interestingly, the ER membrane protein seipin has been shown to localise to the lipid droplet-ER contact site and control lipid and protein sorting in lipid droplet maturation; however, again the mechanism remains unclear (105-107). Moreover, larger lipid droplets have increased saturated fatty acids in the surrounding monolayer further supporting alterations in lipid droplet biology during maturation (108). Although our understanding of lipid droplet biogenesis remains limited, alterations to pre-existing lipid droplets appear to be of

far greater importance to lipid droplet functionality in health and disease and this is discussed in greater detail further in this review.

As previously mentioned, lipid droplet size can imply maturation status; however, it can also indicate metabolic activity and cell condition. Early reports suggested that lipid droplets were typically between 0.1-0.4 µm in diameter (109) and this has been supported in more recent studies (110). However, Pan et al. (110) also reported lipid droplet diameters up to 1µm and that the inverse association of droplet number to size was cell line-specific, further highlighting unique cell line-specific lipid droplet profiles. Cell condition can also affect lipid droplet size as intracellular lipid droplets within apoptotic cells and extracellular lipid droplets from necrotic cells can have diameters up to 2 µm and 10 µm respectively (111). Notably, however, detection of small droplets can be limited with current methodologies and lipid droplets with a diameter below 0.1 µm are considered NMR invisible (112).

1.4.4. Lipid droplet proteins

The single phospholipid layer and hydrophobic core of a lipid droplet prevents the anchoring of proteins via standard luminal insertion domains (96). Instead, lipid droplet-specific proteins have been suggested to often contain a hydrophobic hairpin domain for attachment (113). The most notable group associated with lipid droplets is the PAT family of proteins, named after the three main members perilipin 1, adipophilin and TIP47 (114). The PAT family of proteins shares a conserved PAT domain and encompasses the genes PLIN1 and PLIN2 and the isoforms PLIN3, PLIN4 and PLIN5; representing perilipin 1, adipophilin, TIP47, PLIN4 and PLIN5 respectively (Figure 1.7.).

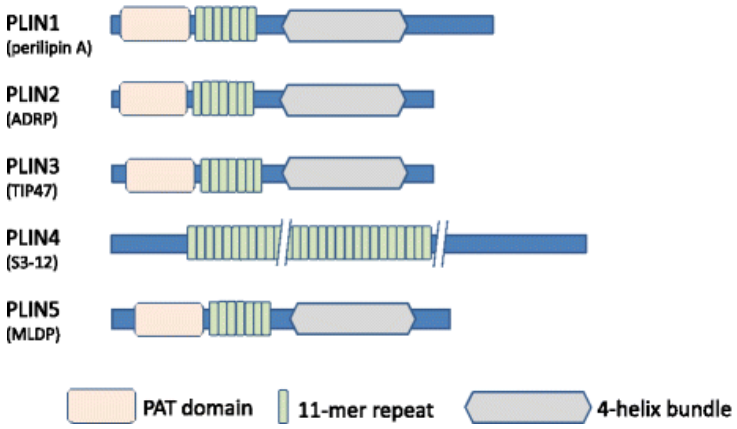

Figure 1.7. Protein structure remains similar throughout the PAT family of proteins. Image adapted from Itabe et al. (114).

Perilipin 1 is frequently associated with adipocytes but has been noted in many tissues (114). Through complexing with CGI58, a lipase activator protein, perilipin 1 prevents lipase activation and subsequently lipid droplets do not undergo lipolysis (115). However, once phosphorylated, perilipin 1 releases CGI58 and lipolysis is activated implicating perilipin 1 as a key regulator in inactivating lipid droplet metabolic pathways.

In contrast, adipophilin is expressed more ubiquitously (116) and is observed frequently in other tissues such as hepatocytes (117), macrophage foam cells (118), sebocytes (119) and epithelial cells (120). Adipophilin is thought to stabilise lipid droplets in high lipid conditions and is associated strongly with the metabolic process of autophagy (121). Indeed, it has been noted as an important lipid droplet marker in several cancers including renal cell carcinoma (122) and GBM (123). Interestingly, it is thought to often replace periliin 1 as lipid droplets mature and have a different role in the regulation of lipid droplet metabolism (114).

TIP47 is considered similar to adipophilin in role and structure but remains a distinct protein (114). Notably, neither adipophilin nor TIP47 bind to CGI58 (124) and therefore are believed to impact lipid droplet metabolism through an alternative mechanism.

Little is known regarding the biological functions of PLIN4; however, it is thought to have many similarities to perilipin 1 and is most notably distinct from other PLIN proteins through the absence of a PAT domain (114). Similarly, the role of PLIN5 is relatively unexplored; however, it has been associated with small lipid droplets and mitochondria in cardiomyocytes (125,126).

Hypoxia inducible protein 2 (HIG2) is encoded by the HILPDA gene and is an important lipid droplet-associated protein in hypoxic lipolytic regulation. Indeed, HIG2 has an established role in lipid utilisation (127) and hepatic (128) and macrophage (129) lipid storage. The HILPDA gene is a target of the hypoxic transcription factor HIF1α and is upregulated in hypoxia (130) which is also known to upregulate lipid droplet accumulation in GBM (123). Similarly, HILPDA is established as an important marker in renal cell carcinoma (131) and represents an important link between lipid droplets and hypoxia, discussed in greater detail in section 4.6.

Lipid droplets have also been associated with a wide variety of proteins from many different cellular pathways, reflecting the diversity of lipid droplet metabolism. This includes intracellular fatty acid transporters called fatty acid binding proteins (FABPs) (123), autophagy proteins (132) and a variety of organelle transport proteins such as SNARE (133), dynein (134) and microtubules (109,135). Together these proteins contribute towards the diverse functionality of lipid droplet metabolism.

1.4.5. Factors affecting lipid droplets

The large number of external and internal factors capable of influencing lipid droplets are a direct reflection of the diverse range of processes in which lipid droplets are involved. Environmental factors such as pH (95), oxidised lipids (136) and surrounding fatty acid content have been demonstrated to affect the number of lipid droplets. Similarly, lipid droplet number correlates positively with confluency (94) whist the core composition remains unchanged (112).

The effects of cell death on lipid droplet accumulation are frequently reported and cell stresses capable of inducing cell death, such as cytotoxic drugs, are known to induce lipid droplets (98,137). Indeed, increased numbers of lipid droplets has been proposed as a characteristic of the programmed cell death process, apoptosis (138). The characteristic increase in lipid droplet accumulation occurs early in the apoptotic process, preceding traditional markers and allowing the earlier detection of treatment responses compared to traditional apoptosis assays (98). Interestingly, apoptosis induces a decrease in malonyl CoA, expected to increase mitochondrial lipid uptake and β-oxidation and decrease lipid droplet number; however, the observation of an opposing effect suggests the involvement of other lipid droplet metabolic processes. Lipid droplets have also been linked to necrosis and are thought to be responsible for the high lipid content of necrotic GBM cores (94,98). Lipid droplets therefore represent interesting markers in cell death pathways but also a potential experimental pitfall from the accidental induction of death-related lipid droplet responses.

Hypoxia is a deficiency in the amount of oxygen reaching cells and is considered a hallmark of cancer (75) occurring in tumours with inadequate perfusion such as GBM

(23). Under sufficient oxygen conditions the α-subunits of the hypoxia inducible transcription factors, HIF1 and HIF2, are continuously targeted for proteasome degradation by the action of prolyl hydroxylases and the Von Hippel-Lindau protein. However, under hypoxic conditions the HIF α-subunits are stabilised and can form active dimers, activating numerous cellular mechanisms including angiogenesis and metabolic rewiring. Hypoxia is associated with lipid droplets in GBM in a HIF1α dependent manner (123) whilst in renal cell carcinoma HIF2α has been shown to induce PLIN2 expression and lipid droplet accumulation (122). Moreover, hypoxia stimulates several metabolic processes capable of fuelling lipogenesis including glycolysis (139,140) and reductive carboxylation (31,141,142). Indeed, hypoxia can also increase lipid uptake and promotes increased expression of the very low density lipoprotein uptake receptor (VLDL-R) in a HIF1α and HILPDA dependent manner (143). Due to the increased metabolic demand of a tumour cell and the high frequency of hypoxia within a tumour mass it is unsurprising that many of these pathways promote tumorigenesis in hypoxia and are strongly associated with lipid droplets.

1.4.6. Lipid droplet production mechanisms

Although lipid droplet biogenesis is relatively poorly understood, the metabolic mechanisms underlying lipid droplet accumulation have been investigated in many cell types and cancers.

1.4.6.1. Exogenous lipid uptake in lipid droplet production

A key biological source of lipids is the extracellular lipid pool, supplied *in vivo* by the circulatory system. Triglycerides and cholesterol are transported around the body from the intestines and liver in specialised vesicles called lipoproteins and chylomicrons (144). Typically very low density lipoproteins (VLDLs) are associated with endogenously produced lipids whereas chylomicrons are associated with exogenously acquired dietary lipids (144). These vesicles can be recognised by cell surface receptors whereupon they are degraded enzymatically by lipases such as lipoprotein lipase (LPL) and the contents internalised through specific transmembrane transporter proteins such as CD36 (145). The extracellular lipid pool is well characterised as an important source of lipids in many cancers. CD36 was observed to be important in breast cancer tissues (146) whilst CD36 and LPL in combination were noted as vital mediators in the uptake of exogenous lipoproteins in a number of cancers (147). Similarly, lipid uptake is increased in renal cell carcinoma and breast cancer through increased expression of low density lipoprotein receptor (143) and the associated protein LRP-1 (148) respectively. In both cases these upregulations are strongly associated with hypoxia and hypoxia-mimicking conditions, also known to increase exogenous lipid uptake (143). Ovarian and colon cancer cells have been observed to obtain exogenous lipids from the surrounding adipose tissue (149,150) whilst hypoxic prostate cancer cells were observed to have an increased uptake of extracellular lipid vesicles produced by normoxic cancer cells (151).These processes are important to fuelling lipid droplet production (Figure 1.8.) and GBM and breast cancer cell lines were observed to be reliant upon the uptake of exogenous serum lipids to produce lipid droplets in hypoxia (123). Interestingly, this study also indicated that this process relies upon the activity of FABPs to transport

intracellular lipids, a finding mirrored by Nieman et al. (150) who observed the importance of FABP4 in ovarian cancer cell lipid uptake. Giampietri et al. (152) also found that increased lipid uptake is responsible for increased lipid droplet accumulation in melanoma cancer stem cells suggesting that exogenous lipid uptake may correlate with a more aggressive cell phenotype.

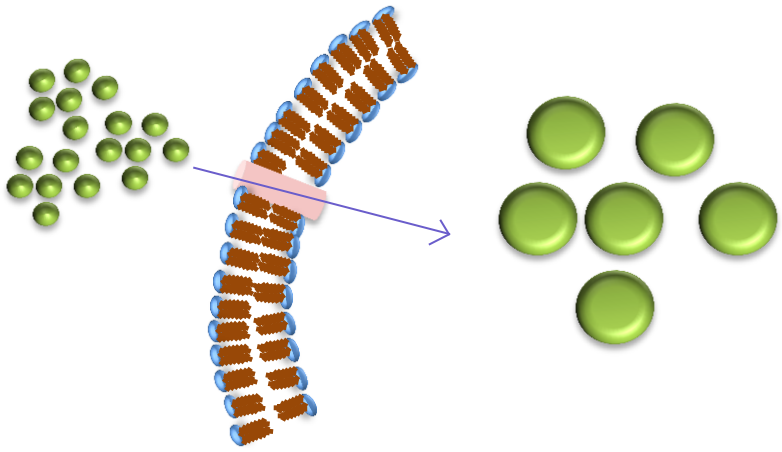

Figure 1.8. Exogenous lipid uptake. Lipids can be transported across cell membranes by transporters such as CD36 to enter the cell for lipid droplet production.

1.4.6.2. *De novo* fatty acid synthesis in lipid droplet production

Fatty acids can also be supplied through *de novo* fatty acid synthesis (Figure 1.9.), a pathway strongly linked to tumorigenesis. *De novo* fatty acid synthesis is the production of fatty acids from metabolic precursors such as glucose, acetate and glutamine (153). Glucose is converted to acetyl CoA and then citrate through glycolysis and the TCA cycle in order to be used for *de novo* fatty acid synthesis. Similarly, acetyl CoA can be produced from acetate by the enzyme acyl-CoA synthetase (ACSS2) and can also fuel *de novo* fatty acid synthesis. Glutamine can be converted to glutamate and α-ketoglutarate by glutaminase (GLS) and glutamate

dehydrogenase whereupon it enters the TCA cycle. α-ketoglutarate can then be converted to citrate through a reverse TCA cycle reaction known as reductive carboxylation which can provide up to 80% of acetyl CoA used in *de novo* fatty acid synthesis (31,154). Acetyl CoA is transported across the mitochondrial membrane as citrate where it is reconverted to acetyl CoA by ATP citrate lyase (ACLY). It is then converted to malonyl CoA by acetyl CoA carboxylase (ACACA) and forms the basic precursor for fatty acid synthesis. Fatty acid synthesis is performed by a multi-enzyme complex termed fatty acid synthase (FASN), composed of 7 simultaneously active enzymes encoded by the FASN gene. Through a process of condensation, reduction and thiolation, malonyl CoA is used to add repeated two carbon subunits and produce a fatty acid chain.

This process has been well established as an important aspect in cancer due to the increased lipid demands of a tumour and can be supported through a variety of genetic and metabolic alterations. Glycolysis is often increased in cancer through the Warburg effect providing an increased source of pyruvate for the generation of acetyl CoA (79) whilst cancer hallmarks such as hypoxia have been observed to increase fatty acid synthesis in several cancers (151,155). Similarly, the contribution of glutamine to fatty acid synthesis necessitates increased glutamine uptake which has been observed in many cancers including some gliomas (81,82). Moreover, many cancers have increased expression of fatty acid synthesis genes which are associated with poor prognosis (156). Indeed, FASN expression has been associated with increased colorectal cancer stage (157) whilst pancreatic cancer patients have been observed to have elevated serum FASN (158). ACLY associates with tumour specific cyclin E isoforms in invasive breast cancer cell lines and this association is required for *in vitro* transformation, migration and invasion and *in vivo*

tumour growth (159). Moreover, inhibition of ACLY attenuates proliferation and invasion and promotes apoptosis in osteosarcoma, prostate, cervical and lung cancer cell lines and mouse models (160). Similarly, ACACA expression is important in breast cancer survival (161) and inhibition of this enzyme can reduce proliferation and *de novo* lipogenesis in some GBM cell lines (162) whist ACSS2 has been observed to increase in hypoxia in breast and prostate cancer cells (163). The importance of the *de novo* fatty acid synthesis pathway in cancer is therefore clear and has been strongly associated with lipid droplets. Accioly et al. (136) observed that the CACO-2 colon cancer cell line requires *de novo* fatty acid synthesis to build lipid droplets and this could be interrupted with the FASN inhibitor C75. The importance of *de novo* fatty acid synthesis in lipid droplet production was supported in metastatic breast cancer by Wilmanski et al. (164) whilst Wang et al. (165) demonstrated that inhibited glutamine uptake reduced the number of lipid droplets in prostate cancer cells. However, Bensaad et al. (123) demonstrated that *de novo* fatty synthesis does not impact lipid droplet production in some GBM and breast cancer cell lines, indicating that this process is cell line and cancer-specific and requires further investigation.

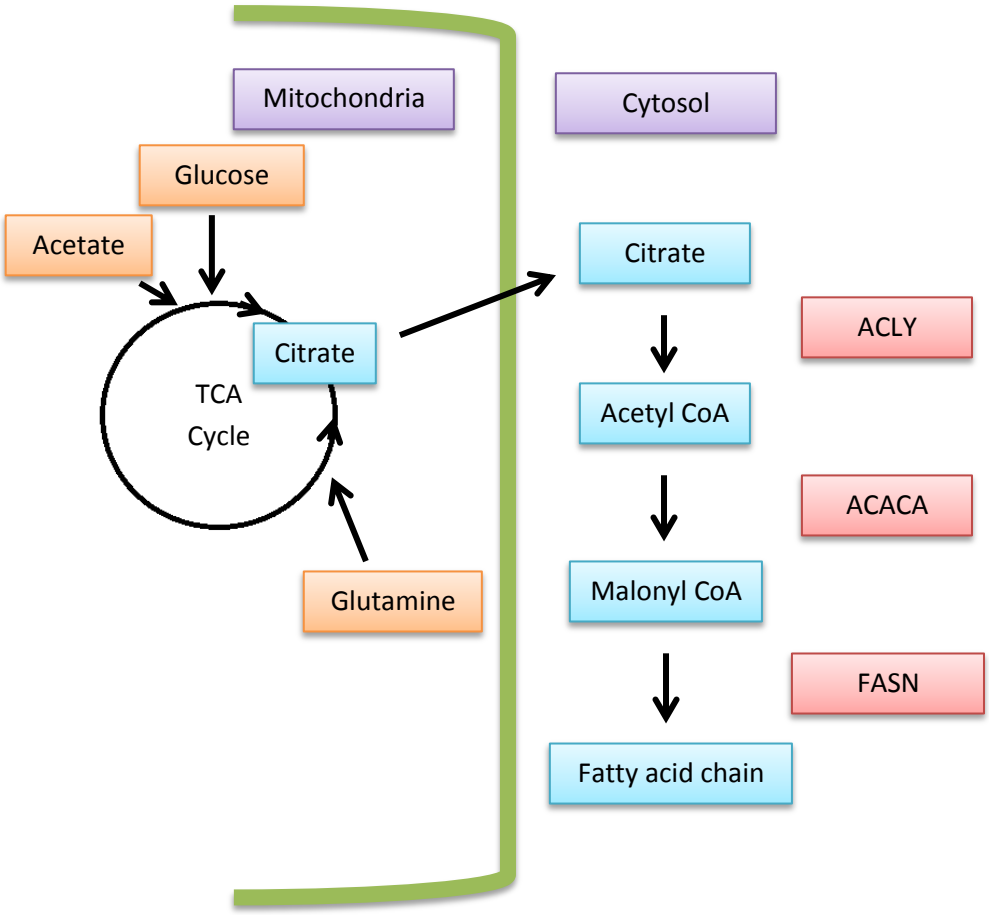

Figure 1.9. *De novo* fatty acid synthesis. Glucose, glutamine and acetate are all precursors for the production of fatty acids. Citrate is exported out of the mitochondria for fatty acid synthesis. ACLY, ACACA and FASN are vital enzymes in fatty acid synthesis.

1.4.6.3. Exogenous lipid uptake and *de novo* fatty acid synthesis are interlinked pathways

Increasing evidence suggests that exogenous lipid uptake and *de novo* fatty acid synthesis are intrinsically linked and must not be considered independently. The absence of the exogenous lipid pool increased *de novo* fatty acid synthesis in a number of cell lines (166) and was required for sensitivity to *de novo* fatty acid synthesis inhibition in prostate cancer cells (167). Similarly, hypoxia was observed to increase both *de novo* fatty acid synthesis and exogenous lipid uptake in prostate

cancer cells (151) supporting a complementary relationship between both pathways. Nevertheless, an inverse relationship has also been observed. Oncogenic Ras-activated cancer cells increased unsaturated fatty acid uptake at the expense of *de novo* fatty acid synthesis (168) whilst *de novo* fatty acid synthesis was increased at the expense of exogenous lipid uptake in breast and prostate cancer cells (163). This further demonstrates that, despite the clear importance of these pathways in cancer and lipid droplet metabolism, it is vital to understand these processes in specific cancers and experimental conditions.

1.4.6.4. Autophagy in lipid droplet production

The autophagy process has also been suggested as an important factor in lipid droplet production. Autophagy is the catabolic process of “self-digestion” wherein specialised endosomes called autophagosomes engulf intracellular content before lysosomal degradation (Figure 1.10.). There are 3 types of autophagy; macroautophagy, microautophagy and chaperone mediated autophagy and these are comprehensively reviewed by Galluzzi et al. (169). The best characterised form of autophagy is macroautophagy which is referred to as autophagy hereon. Autophagosomes form at the ER and can engulf organelles, misfolded proteins and excess macromolecular content in a targeted process (169). Lysosomes then fuse to form autophagolysosomes which digest the engulfed contents and release macromolecular building blocks and metabolites such as amino acids. This process can provide metabolites for energy production and macromolecule synthesis under starvation conditions as well as recycle and remove damaged organelles, maintaining organelle function and preventing cell death (170). In contrast,

autophagy is also believed to be a tumour suppressor and can initiate and enact autophagic cell death, a programmed cell death pathway similar to apoptosis (171). Autophagy is therefore an interesting oncological pathway and has been noted to be of importance in many cancers including GBM (172) and is under investigation as a therapeutic cancer target (173). Rambold et al. (174) observed that autophagy inhibition decreased lipid droplet replenishment in mouse embryo fibroblasts (MEFs) and hypothesised that lipid droplets were produced through autophagic organelle turnover. Similarly, Nguyen et al. (175) observed that autophagy-released lipids were transferred to lipid droplets by the enzyme DGAT1 in MEFs and provide a lipid buffering system to prevent lipotoxicity. However, these studies have not been replicated in human cancer cell lines and autophagy has been typically associated with lipid droplet breakdown in human tissues, discussed further in section 4.7.

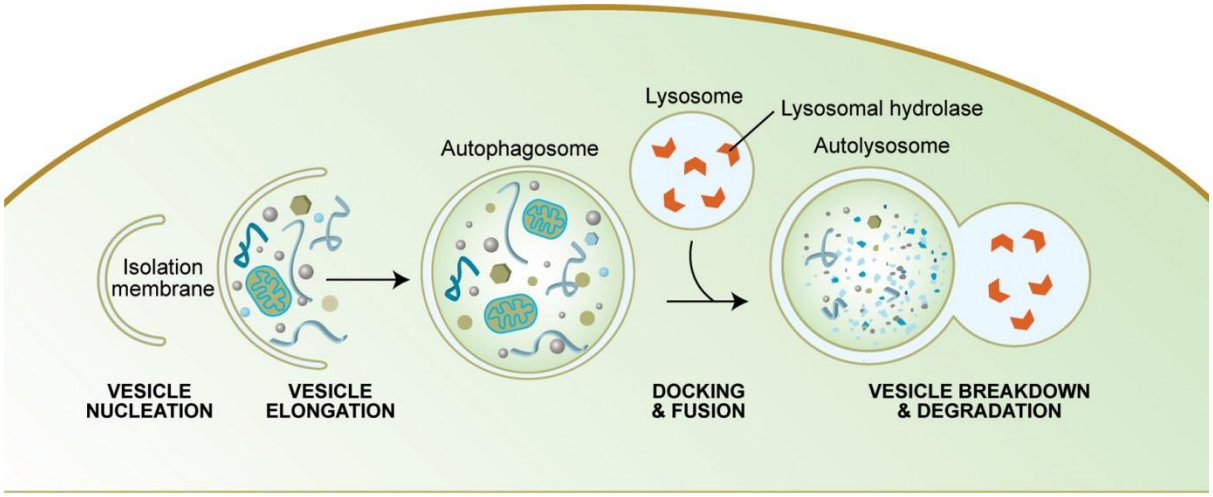

Figure 1.10. The process of autophagy. Autophagosomes engulf cellular components before fusing with lysosomes to degrade the vesicle contents. Image from Melendez et al. (293)

1.4.6.5. Lipolytic enzymes in lipid droplet production

Lipases have been reported to impact lipid droplet biogenesis (176) whilst secreted phospholipase A2 is thought to release fatty acids extracellularly for incorporation into lipid droplets (177). However, similarly to autophagy, lipases are typically associated with lipid droplet breakdown.

1.4.7. Lipid droplet breakdown mechanisms

1.4.7.1. Autophagy in lipid droplet breakdown

A type of autophagy, well characterised as a specialised lipid droplet breakdown mechanism, is termed lipophagy wherein lipid droplets are partially or entirely engulfed and degraded by autophagosomes (178). Lipophagy occurs in a wide range of tissues; however, it is best characterised in hepatocytes which frequently have high intracellular lipid content (179,180). Hepatic lipophagy is important in liver functionality and is tightly controlled by proteins such as the lipid droplet-associated protein adipophilin which is an established hepatic lipophagy inhibitor (181). Notably, adipophilin also prevents autophagic degradation of lipid droplets in pancreatic β-cells (182) whilst there are increased lipid droplets in neurons affected with Huntington's disease, known to have impaired autophagy (183). Interestingly, chaperone mediated autophagy has been observed as a lipid droplet breakdown mechanism in mouse fibroblasts, but is likely to be distinct from lipophagy (121). Lipophagy has also been established as an important mechanism of lipid droplet breakdown in many cancers including prostate (184), renal cell carcinoma (185,186), cervical (187) and ovarian cancer (188). Moreover, decreased autophagy was

observed to increase lipid droplet accumulation in lung cancer stem cells (152) further supporting a role for lipid droplets in more severe cancers.

1.4.7.2. Lipolytic enzymes in lipid droplet breakdown

In addition to lipophagy lipid droplets can be broken down by cytoplasmic lipases which enzymatically cleave fatty acid chains from lipids such as triglycerides in a structured sequence of lipolytic reactions. Adipose triglyceride lipase (ATGL) catalyses the initial rate limiting step of triglyceride hydrolysis, producing diacylglycerol and a single fatty acid (189). A second fatty acid chain is then removed by hormone sensitive lipase (HSL) to produce monoacylglycerol (190). Finally, monoglyceride lipase cleaves monoacylglycerol to produce a glycerol and a final fatty acid chain (191). As the initiating step, the activity of ATGL is most tightly regulated and requires activation by CGI58 for optimal enzymatic function (192). In contrast, CGI58 does not bind HSL which is regulated instead by ATGL activity. ATGL is known to localise to both cell membranes and lipid droplets (189) and has been reported as the major lipid droplet breakdown mechanism in mouse embryo fibroblasts (174) and rat stellate cells (193). Moreover, in conjunction with lipophagy, cytoplasmic lipases such as ATGL play a role in lipid droplet breakdown in hepatocytes which can be inhibited by HILPDA (194). Although lipophagy provides a quicker and more significant release of lipids, cytoplasmic lipase-mediated lipid release has tighter regulation. Therefore, HILPDA- and PLIN2-mediated inhibition of lipases and lipophagy respectively provides increased control of hepatic lipid release. Cytoplasmic lipases have also been noted as important elements in the biology of many cancers. Indeed, monoglyceride lipase activity has been observed to

be increased in highly aggressive forms of melanoma and ovarian and prostate cancer (195,196). Moreover, cytoplasmic lipases have been established as an important lipid droplet breakdown mechanism in cervical cancer (197) and have been suggested to be involved in many others.

1.4.7.3. Autophagy and lipase-mediated lipid droplet breakdown are interlinked

As was observed with the lipid droplet production mechanisms, these pathways are interlinked and mutually contribute to the degradative outcome (Figure 1.11.). Indeed, the activity and regulation of lipophagy and ATGL are heavily interlinked in lipid droplet breakdown in hepatocytes (198) while the PNPLA5 lipase was required for optimal autophagy initiation in HeLa cancer cells (199).

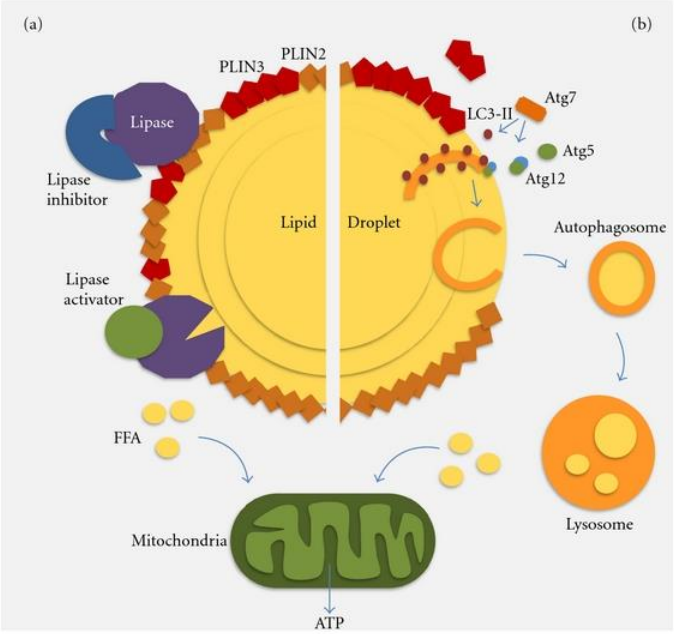

Figure 1.11. Proposed routes of lipid droplet breakdown. Lipid droplet breakdown is predominantly reported to occur through cytoplasmic lipases (left) and lipophagy (right). Image from Singh et al. (294)

1.4.8. Summary of lipid droplet metabolic mechanisms

Lipid droplet production and breakdown mechanisms can vary between cell types and species; however, several of these pathways are particularly prevalent in cancer. Lipid droplet production is predominantly reliant upon exogenous lipid uptake, *de novo* fatty acid synthesis or a combination of the two. In contrast, lipid droplet breakdown is predominantly performed through the actions of autophagy and cytoplasmic lipases which provide dual regulation over cellular lipid content and breakdown. Therefore, any experimental investigation attempting to underpin core lipid droplet metabolic mechanisms must consider the activity of these processes.

1.4.9. The roles of lipid droplets

Lipids droplets can be used for many purposes through both their physical presence and the release of the lipids they contain. Lipids are required for four primary processes; energy production, membrane synthesis, lipid signalling and protein modification which may all be impacted by lipid droplet metabolism.

1.4.9.1. The role of lipid droplets in energy production

The long hydrocarbon chains of fatty acids can be catabolised to provide a major source of energy through mitochondrial β-oxidation (200) (Figure 1.12.). Cytoplasmic free fatty acids are activated with a CoA molecule to facilitate mitochondrial transfer by the carnitine cycle. The acyltransferase CPT1 esterifies the activated fatty acid to a carnitine molecule, producing acylcarnitine, which can then be transported across the mitochondrial membrane by the mitochondrial transporter SLC25A20. The

carnitine is then removed by another acyltransferase, CPT2, and the fatty acid can undergo the cyclical reaction of fatty acid β-oxidation. Each fatty acid undergoes cycles of dehydrogenation, hydration, dehydrogenation and thiolation to repeatedly shorten the fatty acid chain by two carbon subunits. This produces acetyl CoA which can enter the TCA cycle and $FADH_2$ and NADH for oxidative phosphorylation.

Despite the higher energy production of β-oxidation, cancer cells frequently rely upon glycolysis due to reaction speed and efficacy in the absence of oxygen. Nevertheless, β-oxidation has been observed as an important energy production pathway in several cancers (201) including ovarian (150), prostate (85), colon (202) and breast cancer (203,204). Similarly, leukaemic cells can sequester in adipose tissues to fuel β-oxidation with adipocyte-derived lipids (205) whilst lung cancer cells upregulate CPT1C and β-oxidation to promote xenograft tumour growth (206). Perhaps unsurprisingly lipid droplets can be the major supply of lipids for mitochondrial β-oxidation in many healthy and cancerous cell types. Rambold et al. (174) and Nguyen et al. (175) found that, in mouse embryo fibroblasts, lipid droplets were predominantly broken down to fuel mitochondrial β-oxidation and prevent lipotoxicity. This was reliant upon good mitochondrial function and fusion. Interestingly, the lipid droplet-associated protein PLIN5 is involved in the recruitment of mitochondria to lipid droplets and the prevention of lipotoxic stress (207,208). Similarly, lipid droplets have been observed to re-localise to mitochondria for β-oxidation along microtubules in response to nutrient scarcity (135) whilst inhibition of mitochondrial β-oxidation in hepatocytes resulted in lipid accumulation (209). Lipid droplets were further observed to fuel mitochondrial β-oxidation in triple negative breast cancer (92) whilst colon cancer cells subverted surrounding adipose tissue to supply fatty acids for lipid droplets prior to β-oxidation (149). It is therefore clear that,

in addition to their many other roles, lipid droplets retain their importance as energy stores in healthy and cancerous cells.

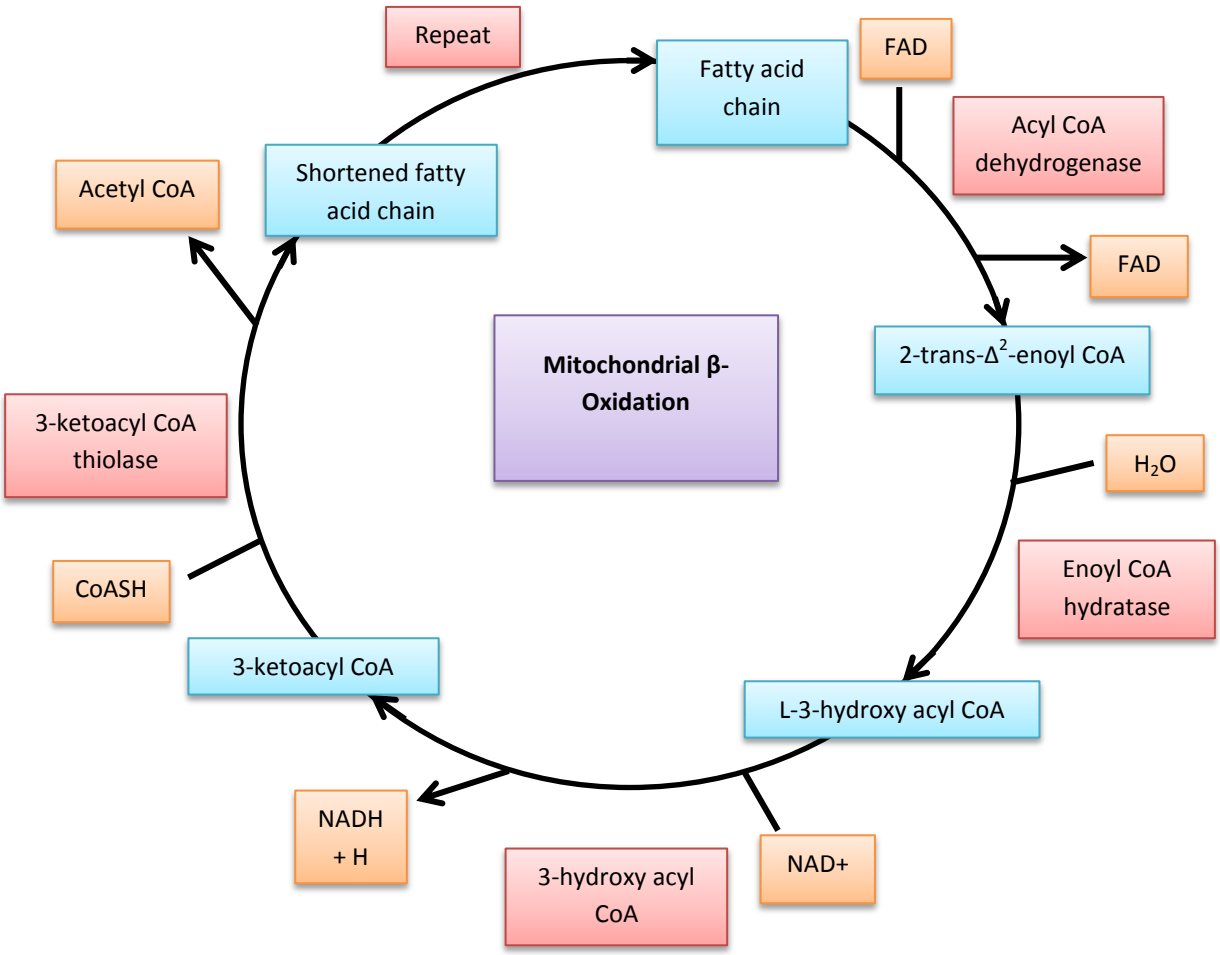

Figure 1.12. The mitochondrial β-oxidation pathway. Fatty acid chains are converted into acetyl CoA for energy production through cycles of β-oxidation in the mitochondria. Each cycle removes one acetyl CoA and shortens the fatty acid chain by two carbon units.

1.4.9.2. The role of lipid droplets in membrane synthesis

Lipid droplets also provide a store of precursors for the synthesis of cell and organelle membranes. Membranes are composed of amphipathic phospholipids such as phosphatidylcholine, phosphatidylethanolamine and phosphatidylserine, of which phosphatidylcholine is the most common and important and phosphatidylserine the least. The basic subunit of phospholipids is phosphatidic acid

which is composed of diacylglycerol with a phosphate group occupying the final fatty acid chain site. This phosphate group can be conjugated to choline, ethanolamine or serine to produce the different classes of phospholipids (Figure 1.13.) and convey specialised functions. Choline kinase (CKA and B) and ethanolamine kinase (ETNK1) catalyse the initial reactions of phospholipid synthesis and generate phosphocholine or phosphoethanolamine respectively. These molecules are then conjugated to diacylglycerol by cholinephosphotransferases (CEPT1 and CHPT1) to produce phospholipids. Alternatively, conjugated phosphocholine and phosphoethanolamine can be exchanged for phosphoserine by phosphatidylserine synthase 1 and 2 (PTDSS1 and 2) respectively to produce phosphatidylserine.

Abnormal choline metabolism is one of the most common and consistent observations in cancer due to its clear requirements during increased proliferation (210,211). Indeed, phosphatidylcholine was the most common phospholipid in breast cancer cells (212), concurrent with increased choline metabolism and CHPT1 expression (213). Moreover, pharmacological choline kinase inhibition prevented xenograft tumour growth (214) whilst siRNA down regulation of choline kinase decreased breast cancer cell line proliferation (215). Interestingly, this siRNA was also observed to increase lipid droplet accumulation suggesting that they may provide a source for phospholipid synthesis in these cells. Similarly, exogenous fatty acids, known to be incorporated into lipid droplets, can be used preferentially for membrane synthesis (216) further suggesting lipid droplet involvement. However, the literature connecting lipid droplets and membrane synthesis has remained limited due to the difficulty of investigating this process.

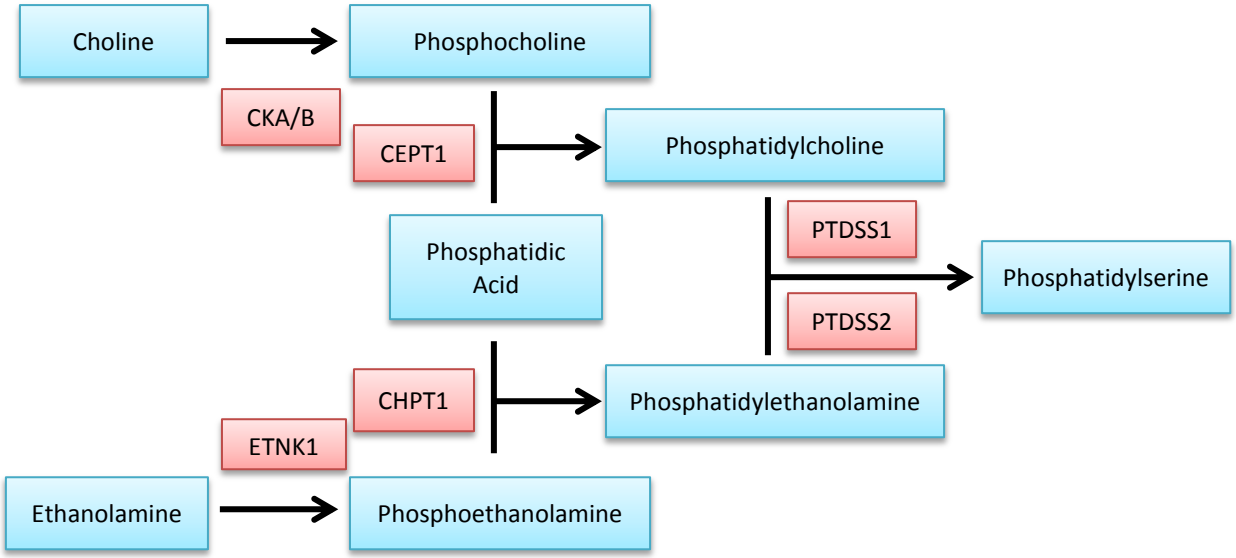

Figure 1.13.Phospholipid synthesis pathways. Phosphocholine and phosphoethanolamine are synthesised by CKA/B and ETNK1 respectively. These are then conjugated to phosphatidic acid by CEPT1 and CHPT1 to produce phosphatidylcholine and phosphatidylethanolamine respectively. Phosphatidylserine can then be produced from phosphatidylchoine or posphatidylethanolamine by PTDSS1 and 2 respectively.

1.4.9.3. The role of lipid droplets in signalling

Lipid signalling molecules such as sphingosine-1-phosphate, diacyglycerol, IP3 and PIP3 are key signalling molecules and represent an important function of lipid metabolism (217,218). Indeed, sphingosine-1-phosphate and lysophosphatidic acid can modulate inflammation, cell migration and survival (219,220). Moreover, sphingosine-1-phosphate can be derived from lipid droplets and its bioactive signalling has been linked to cancer (221,222).

1.4.9.4. The role of lipid droplets in cellular stress

One of the key functions of lipid droplets is the maintenance of cellular homeostasis and the prevention of cellular stress. The upregulated macromolecule synthesis in cancer causes increased ER stress. Interestingly, it has been suggested that lipid

droplets associate with the proteasome (223) and may positively regulate its activity through surface protein interactions, decreasing ER stress (224). Similarly, lipid droplets are thought to protect against oxidative damage. Hypoxia and mitochondrial β-oxidation are major sources of reactive oxygen species (ROS) (225) which can damage many cellular components, particularly unsaturated fatty acids. Bailey et al. (226) observed that lipid droplets protected against ROS-induced oxidative damage in *Drosophila* glial cells by providing a storage site for vulnerable polyunsaturated fatty acids. Similarly, Bensaad et al. (123) observed that lipid droplets could provide protection from re-oxygenation-induced ROS in several human cancer cell lines. Therefore, lipid droplets provide a storage site for the sequestration of vulnerable cellular components to decrease oxidative stress and aid in survival, providing clear benefits to cancer biology.

Excessive free fatty acids storage above the lipotoxic threshold induces lipotoxicity and cell death. Indeed, inhibition of triglyceride synthesis with TriascinC was observed to cause free fatty acid accumulation and apoptosis (138). Lipid droplets can therefore act as a buffering system, providing controlled regulation of intracellular lipid content and a robust lipid storage site (175). Moreover, lipid droplets can prevent cell stress through the sequestration of misfolded proteins (227,228) further demonstrating their importance as a stress resistance mechanism.

1.4.9.5. The role of lipid droplets in drug resistance

Lipid metabolism and lipid droplets have been suggested as important factors in drug resistance, a vital aspect of cancer biology. The altered membrane saturation observed with increased *de novo* fatty acid synthesis decreased chemotherapeutic

drug uptake (229) whilst increased FASN expression has been demonstrated as an important indicator of gemcitabine and radiation resistance in pancreatic cancer (230). Moreover, FASN protein levels were observed to correlate with cetuximab and bevacizumab efficacy both *in vitro* and *in vivo* in colorectal cancers (231), although the mechanism remains unclear. The characteristic increase in lipid droplet accumulation in apoptosis indicates a role for lipid droplets in drug response through either promoting or hindering cell death. In prostate and breast cancer cells, lipid droplet accumulation was increased in response to hormone drug treatment (151,232). Similarly, a vascular EGFR2 tyrosine kinase inhibitor promoted apoptosis and increased lipid droplet accumulation in GBM cell lines (233). Pan et al. (234) also observed that cisplatin treatment increased lipid droplet number and unsaturated fatty acid content in a medulloblastoma cell line further supporting increased lipid droplets as a response to drug treatment. However, although lipid droplets may increase during the cell death process, it has also been suggested that they represent a drug resistance response. Montopoli et al. (235) observed increased lipid droplets in cisplatin resistant ovarian cancer cells whilst Zietkowski et al. (236) noted a similar phenotype in paclitaxel resistant cervical cancer cell lines. Moreover, highly drug resistant colorectal cancer stem cells are often observed to have increased levels of lipid droplets, which correlates with the cancer stem cell marker CD133 (237). However, the underlying mechanism, linking lipid droplets to treatment resistance and response, remains unclear. One proposed mechanism for lipid droplet-induced drug resistance is through sequestration. As with misfolded protein and excess lipid, lipid droplets provide a nontoxic storage site for lipophilic drugs that may decrease their efficacy. Verbrugge et al. (238) observed that activation of an aminopeptidase inhibitor pro-drug was prevented through lipid

droplet sequestration in acute myeloid leukaemia cells. Similarly, Schlaepfer et al. (239) found high concentrations of docetaxel in the lipid droplets of a drug resistant breast cancer cell line, further suggesting that the role of lipid droplets in drug resistance may provide a therapeutic target. However, the metabolic influence of lipid droplets is also an important consideration regarding cell viability under cytotoxic stress and must also be further investigated.

1.4.9.6. Summary of the roles of lipid droplets

Lipid droplets have therefore been shown to interact with multiple cellular processes and organelles, as well as playing a role in the response to potentially cytotoxic stressors in a number of physiological and pathophysiological processes. However, they remain poorly understood, and more work is required to understand how they perform many of their suggested functions.

1.4.10. The role of lipid droplets in gliomas

As has been discussed, lipid droplets are important components of tumour metabolism in many different types of cancer. However, we chose to investigate lipid droplet metabolism in gliomas as, although lipid droplets have been strongly associated with several of the key clinical features of gliomas, the literature investigating the underlying biological pathways has remained limited.

Lipid droplet accumulation is increased throughout tumour progression and is associated with poor survival, providing a potential biomarker of clinical grade and prognosis (94,240,241). Moreover, the relative ease of performing MRS in the brain,

compared with other regions of the body, makes the *in vivo* measurement of lipid droplets as metabolic biomarkers clinically viable (242). The speed of treatment response detection may also be improved through the association of lipid droplets and cell death pathways (98,242,243) whilst hypoxia-induced lipid droplets are thought to be influential in the highly hypoxic and necrotic GBM cores (94,98).

Although these features are currently aiding clinical diagnosis, further utilisation and targeting of lipid droplets is severely limited by the incomplete understanding of glioma lipid droplet metabolism. Lipid droplet production in gliomas has been reported to occur through the uptake of exogenous lipids; however, this was only observed in hypoxia and the role of *de novo* fatty acid synthesis remains controversial (123,162). Similarly, glioma lipid droplet breakdown is yet to be investigated and the relative importance of pathways such as autophagy and cytoplasmic lipases remains to be explored. Lipid droplet metabolism varies between cancers and therefore greater understanding of glioma-specific lipid droplet pathways may clarify clinical observations and present therapeutic opportunities. Indeed, the poor prognosis of high grade gliomas and ineffective novel therapeutics clearly indicates a requirement for an altered clinical approach. It has been suggested that the manipulation of lipid droplet metabolism may improve the efficacy of current therapies; however, progress has again remained limited. Disruption of lipid droplet metabolic pathways such as the FABPs can impair GBM xenograft growth (123) whilst curcumin and temozolomide co-treatment may act synergistically but only with the support of autophagy inhibition (244). Therefore, improved understanding of glioma-specific lipid droplet metabolism may further improve glioma therapeutic options and aid in the development of clinical diagnostic tools.

1.5. Summary

In the majority of cancers, prognosis has consistently improved throughout the modern era. However, glioma survival remains largely unchanged due to cancer severity and the lack of efficacious therapeutic options. Improved understanding of tumour metabolism has highlighted many areas of potential interest, including lipid droplets. Although lipid droplets show clear associations with many clinical features of gliomas, past attempts to harness them to improve current therapies have been hindered by insufficient understanding of the glioma-specific lipid droplet metabolism. We therefore sought to investigate the importance of lipid droplet metabolic pathways across the glioma tumour grades and clarify the relative involvement of these pathways using GBM cell lines. Moreover, we aimed to pharmacologically manipulate these pathways to improve current therapeutic options *in vitro* and suggest how this may be clinically applicable.

1.6 Project Hypotheses

- Lipid droplet metabolism-associated genes are interlinked markers of survival and tumour progression
    - Gene expression is associated with prognostic indication in a grade-specific manner
    - “Grade 3-like” gene expression predicts poor prognosis grade 2 tumours
    - Gene expression correlates with other prognostic markers but is not limited to a tumour subset
- Lipid droplet metabolism is governed by select metabolic pathways
    - Exogenous lipid uptake, ATGL activity and autophagy are important lipid droplet metabolic pathways
    - *De novo* fatty acid synthesis does not have a major role in lipid droplet metabolism
    - Hypoxia and starvation alter lipid droplet metabolism
    - Lipid droplet flux is maintained during inhibition of a key metabolic pathway through compensation with alternative pathways
    - Lipid droplet metabolic pathways provide protection from oxidative stress
- Cytotoxic treatment efficacy is improved through interruption of lipid droplet flux
    - Temozolomide and irradiation cytotoxicity are improved through inhibition of lipid droplet breakdown
    - Cytotoxicity is improved through inhibition of metabolic pathways involved in lipid droplet production

Chapter 2

Materials and methods

2.1. Methods used in Chapter 3

2.1.1. The Cancer Genome Atlas (TCGA) tumour cohort

Genomic and clinical data was downloaded from the TCGA cBioPortal download data function (245,246) on the 3rd October 2016. The Brain Lower Grade Glioma (TCGA, Provisional) and Glioblastoma (TCGA, Cell 2013) cohorts were selected from the CNS/Brain tumour classification group; Brain Lower Grade Glioma cohort (n=530) and Glioblastoma cohort (n=580). The clinical data assigned to each cohort was downloaded and data regarding sample ID, neoplasm histologic grade, overall survival (months) and overall survival status were retained. A further overall survival status column was created where “deceased” was designated ‘1’ and “living” was designated ‘0’. The corresponding genomic data was downloaded for each cohort using the following parameters. Genomic Profile: mRNA expression data (RNA Seq V2 RSEM). Patient/Case Set: Tumour Samples with mRNA data (RNA Seq V2); Brain Lower Grade Glioma cohort (n=530) and Glioblastoma cohort (n=154). Gene Set: User defined list (Table 3.1.). Microsoft Excel was used to sort and match the clinical and genomic data according to Sample ID. Tumours without corresponding genomic data or clinical data were removed. The data sets generated from the Brain Lower Grade Glioma and Glioblastoma cohorts were renamed the combined grade 2 and 3 glioma cohort and the glioblastoma grade 4 cohort respectively. In the case of the combined grade 2 and 3 glioma cohort this data set was split further into two data sets: grade 2 (n=256) and grade 3 (n=270).

2.1.2. Survival analysis and Kaplan-Meier generation

Microsoft Excel was used to sort the data set by gene expression for each gene and find the median and mean gene expression. Median gene expression was used to separate the high and low gene expression groups. However, in the case of predicting “grade 3-like” tumours in the grade 2 cohort, the grade 3 mean gene expression was applied to the grade 2 cohort to separate high and low gene expression groups. GraphPad Prism 7.0 was used to produce Kaplan-Meier survival curves of all genes in the gene set. Overall survival (months) and overall survival status data for the high and low gene expression groups was entered into the data table. GraphPad Prism was used to generate a survival analysis for each survival curve including both Log-rank/Mantel-Cox (MC) and Gehan-Breslow-Wilcoxon (GBW) statistical tests. *$p<0.05$, **$p<0.01$, ***$p<0.001$, ****$p<0.0001$. The MC statistical test is the standard statistical test in the analysis of survival curves. It assumes that deaths per time remains constant at all time points, providing better analysis of the overall survival curve. In contrast, the GBW statistical test better analyses more deaths at early time points. Cancer can be a chronic disease dictating the need to analyse survival at all time points; however, particularly in GBM, survival can be very short and it is important to also investigate earlier changes in survival. Therefore, both statistical analysis methods were included.

2.1.3. Gene expression Boxplot generation.

Gene expression values for each gene, separated by clinical grade, were analysed using GraphPad Prism 7.0 to generate boxplots. The “box” was set to display the median gene expression and upper and lower quartiles and the error bars were set

to minimum and maximum values. ROUT outlier removal was performed to remove definitive outliers (Q=0.1%). mRNA data is non parametric and therefore the Kruskal-Wallis statistical test with a Dunn's post-hoc correction was selected to analyse this data. *p<0.05, **p<0.01, ***p<0.001, ****p<0.0001.

The IDH1 gene expression boxplots were generated from tumours in the combined grade 2 and 3 glioma cohort with known IDH1 mutational status. IDH1 wildtype (n=34), IDH1 mutant (n=91). An unpaired two-tailed t-test statistical test was performed in all cases; *p<0.05, **p<0.01, ***p<0.001, ****p<0.0001.

2.1.4. Gene expression correlation analysis

The combined grade 2 and 3 glioma cohort gene expression values were compared between genes. The expression values were plotted for each tumour on an XY scatter graph using GraphPad Prism 7.0. Spearman's rank correlation analysis was performed on each gene pair to generate r-values. Spearman's rank was selected over Pearson's correlation analysis as it is less susceptible to outliers within the data set. A positive or negative r-value denotes a positive or negative correlation respectively. The closer the r-value is to 1 or -1 the stronger the correlation whilst 0 signifies no correlation.

2.1.5. Correlation heat map

The r-values generated in the above correlation analysis were visualised in a histogram plotted using the corrplot package in the "R" statistical software. Green

and red denote positive and negative correlations respectively. The script is described in Appendix 7.1.

The significance of the correlations was assessed using the Hmisc package of “R”. The script is described in Appendix 7.1.

The p-values were copied into Microsoft Excel and assessed for significance using a Bonferroni correction to generate an adjusted p-value (q). q=p/n =0.05/135 =0.00037 (p=p-value, n=number of tests) (Appendix 7.1. and 7.2.). Those correlations which reached significance were plotted on the heat map as red or green crosses dependent upon the correlation.

Tables of the Spearman’s rank r-value and adjusted p-values can be found in Appendix 7.2.

2.1.6. Cluster analysis

A cluster analysis was performed on “R” using the gene expression data from the combined grade 2 and 3 glioma cohort. The gene expression of every tumour was first normalised to a percentage of the maximum gene expression of each gene. Green and red denote 100% and 0% of the maximum gene expression respectively. The script is described in Appendix 7.3.

2.1.7. TCGA cBioPortal query function

Using the TCGA cBioPortal query function the Brain Lower Grade Glioma (TCGA, Provisional) or Glioblastoma (TCGA, Cell 2013) cohorts were selected with the

following parameters: Genomic Profile: mRNA Expression z-scores (RNA Seq V2 RSEM), z-score threshold ± 2.0. Patient/Case Set: Tumour Samples with mRNA data. Gene Set: User-defined list. The gene list was varied dependent upon the parameter being investigated. (Table 2.1.) The co-occurrence and correlation investigations gene lists included all genes selected for further investigation in initial survival analysis. The combined survival analysis gene lists were separated into poor and good prognostic markers.

Co-occurrence/mutual exclusivity	PLIN1, PLIN2, PLIN3, PLIN4, PNPLA2, PNPLA3, PNPLA4, CD36, HILPDA, ACACA, FASN, MAP1LC3A, CEPT1, CPT2, ETNK1, PTDSS1, SLC25A20
Gene correlation	PLIN1, PLIN2, PLIN3, PLIN4, PNPLA2, PNPLA3, PNPLA4, CD36, HILPDA, ACACA, FASN, MAP1LC3A, CEPT1, CPT2, ETNK1, PTDSS1, SLC25A20
Combined survival analysis	PLIN2, PLIN3, PNPLA2, CD36, HILPDA, MAP1LC3A, ETNK1, PTDSS1 (CEPT1, CPT2) or PLIN1, PLIN4, PNPLA3, PNPLA4, ACACA, FASN, SLC25A20
Table 2.1. Gene lists for TCGA cBioPortal investigations.	

The “Co-occurrence and mutual exclusivity” tab was used to further investigate correlations in gene expression in both cohorts. The significance of each tendency towards co-occurrence or mutual exclusivity was assessed by the TCGA query function using the Fisher Exact test, $p<0.05$. Print screens were taken of the results of this test.

The “Plots” tab was used to assess gene expression correlations in the Glioblastoma (TCGA, Cell 2013) cohort. The expression values were plotted for each tumour on

an XY scatter graph and a Spearman's rank test was performed by the TCGA query function.

The TCGA query function was used to assess the effect of multiple gene alterations on survival in the Brain Lower Grade Glioma (TCGA, Provisional) cohort. CEPT1 and CPT2 were not included in the gene list for the multiple gene alterations query as they were associated with predominantly down-regulation genetic alterations (Figures 2.1. and 3.8.A.). Each data set was split into two groups: cases with alterations in query genes and cases without alterations in query genes. Cases with alterations in query genes were defined as any containing an up- or down-regulation in mRNA expression, as defined by the z-score threshold. A log-rank MC survival analysis was performed to assess significance. $p<0.05$. The process was repeated using the Glioblastoma (TCGA, Cell 2013) cohort.

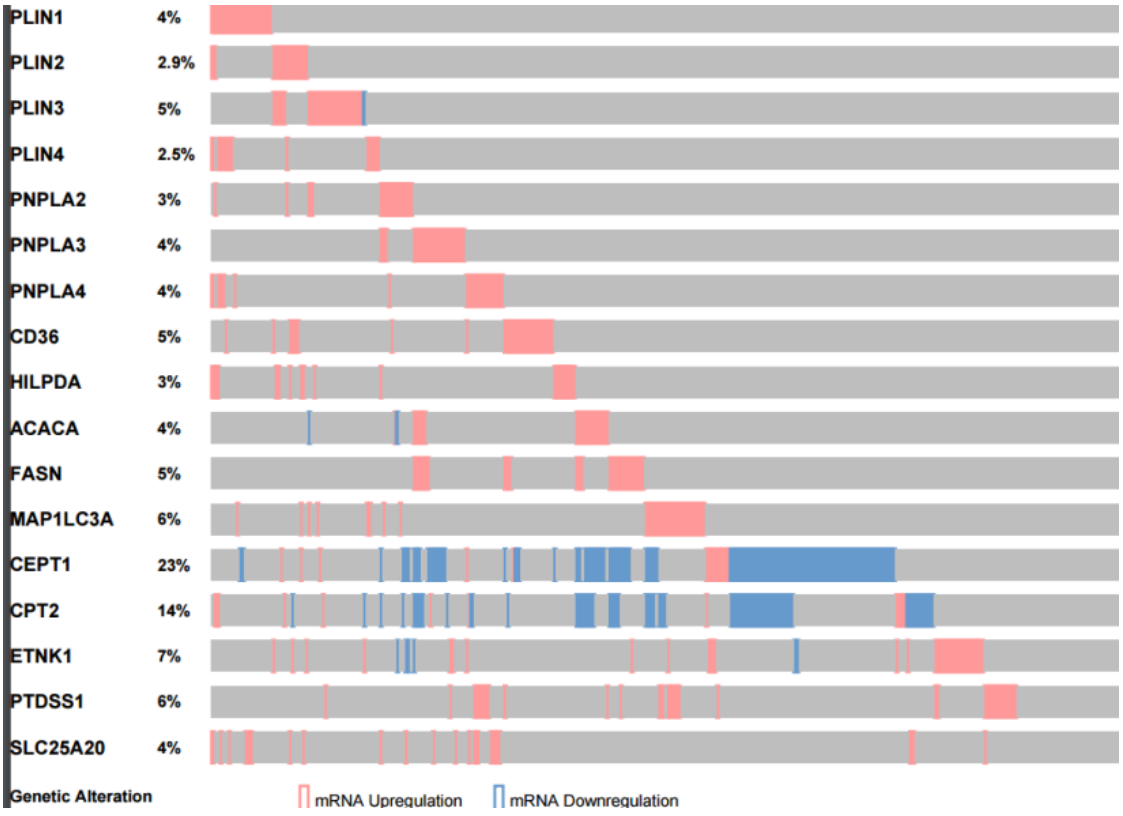

Figure 2.1. Representative oncoprint tab demonstrating mRNA up-regulation (red) and down-regulation (blue) alterations. Not all "no alteration" cases are shown here.

2.2. Methods used in Chapter 4

2.2.1. Cell lines

The T98G, U343 and U87 immortalised human GBM cell lines were obtained from the ATCC. The U87.1 and U87.2 cell lines were developed from the U87 cell line. Cells were cultured in high glucose Dulbecco's Modified Eagle's Medium (DMEM) containing 2mM glutamine (Sigma, D5796) and supplemented with 10% foetal bovine serum (FBS) (Hyclone, 10270). Cells were detached from culture dishes with a 1x phosphate buffered saline (PBS) (Hyclone, SH30258.02) wash followed by 0.05% Trypsin (Gibco, 15400-054) incubation.

Cells were incubated at standard culture conditions of 37^{o}C and 5% CO_2 and regularly tested for mycoplasma infection using the EZ-PCR Mycoplasma detection kit (Geneflow, 20-700).

2.2.2. Short Tandem Repeat (STR) profile analysis

Genomic DNA was extracted from the U87.1 and U87.2 cell lines using the PureLink Genomic DNA Mini extraction kit (ThermoFisher, K182001). The standard protocol included within the kit was followed:

Cells were harvested with 0.05% Trypsin and re-suspended in 200 µL PBS. 20 µL protein kinase A and 20 µL RNase A were added to each sample and vortexed before incubation for 2 minutes at room temperature. 200 µL PureLink Genomic Lysis/Binding Buffer was added to each sample and vortexed to obtain a homogenous solution. Samples were incubated at 55^{o}C for 10 minutes. 200 µL of 100% ethanol was added to each lysate and vortexed for 5 minutes to obtain a

homogenous solution. Lysate was transferred to a PureLink spin column and centrifuged at 10,000 G for 1 minute. Samples were washed with 500 µL Wash Buffer 1 and centrifuged at 10,000 G for 1 minute. The samples were washed again with 500 uL Wash Buffer 2 and centrifuged at maximum speed for 3 minutes. Genomic DNA was eluted by adding 50 µL of PureLink Genomic Elution Buffer, incubating for 1 minute at room temperature and centrifuging at maximum speed for 1 minute. Genomic DNA concentration and purity was checked with a ND-1000 nanodrop.

Extracted genomic DNA was sent to Eurofins, Germany to determine genetic characteristics through PCR-single-locus-technology. 21 independent PCR-systems were investigated with the Promega PowerPlex 21 PCR kit (Promega).

2.2.3. mRNA extraction

mRNA was extracted in triplicate from the U87, U87.1 and U87.2 cell lines using the RNeasy Mini kit (Qiagen, 74104). The standard protocol, including an on-column DNase digestion (Qiagen, 79254), was followed:

Cells were lysed with 350 µL Buffer RLT, scraped and collected. 350 µL of 70% ethanol was added to each sample and mixed well by pipetting. Samples were transferred to RNeasy Mini spin columns and centrifuged for 15 seconds at 8000 G. 350µL Buffer RW1 was added to each column and centrifuged for 15 seconds at 8000 G. 80µL DNase 1 incubation mix (10 µL DNase 1 and 70 µL Buffer RDD) was added to each column and incubated at room temperature for 15 minutes. 350 µL Buffer RW1 was added to each column and centrifuged for 15 seconds at 8000 G.

500 µL Buffer RPE was added to each column and centrifuged for 15 seconds at 8000 G. 500 µL Buffer RPE was added to each column and centrifuged for 2 minutes at 8000 G. 40 µL RNase-free water was added to each column and centrifuged for 1 minute at 8000 G to elute the RNA. Extracted RNA concentration and quality was assessed with a ND-1000 nanodrop.

2.2.4. RNA sequencing (RNAseq)

mRNA exome paired ends sequencing was performed by Genomics Birmingham, run by Dr Andrew Beggs. RNA quality was very high with RNA integrity number scores over 9.7 (7+ considered high quality). Fastq files were provided through the BaseSpace portal (Illumina).

2.2.5. RNAseq data analysis

Fastq files were downloaded from BaseSpace using the BaseSpace downloader and uploaded to Galaxy using the FileZilla FTP transfer program. RNAseq analysis was performed using the Galaxy platform. All analysis used the reference genome "human hg38" and the annotated reference genome "gencode v25.gtf".

FASTQC was run on all files to assess sequencing read quality. All files were found to have high quality transcripts. An example quality control read out is shown in Figure 2.2.

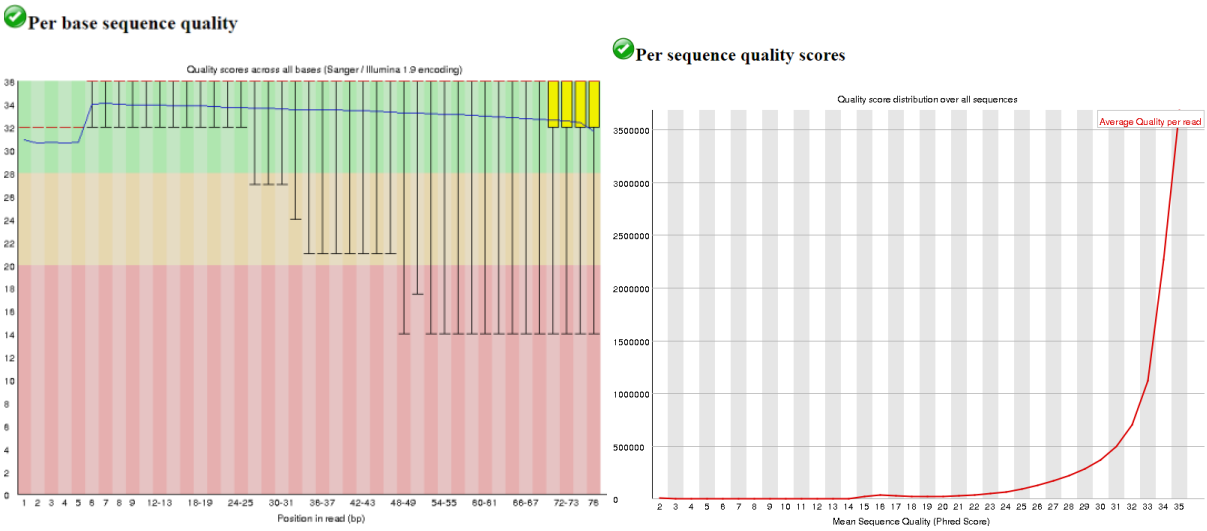

Figure 2.2. Example quality control readout of RNA sequencing data. Short and long transcripts were high quality (left). There was no evidence of transcript degradation into shorter transcript fragments (right).

Forward and reverse fragments for each read lane were aligned to the reference genome, hg38, using Hisat. This generated BAM and BAM index files. In each sample the 4 BAM files, one per read lane, were merged using BAMtools merge to generate a single BAM and BAM index file per sample for subsequent analysis.

Integrative Genomic Viewer (IGV) was used to view the transcripts aligned to the reference genome. In IGV single nucleotide polymorphisms (SNPs) can be found as well as gene deletions and truncations.

Gene expression was quantified using Stringtie transcript assembly and quantification to provide quantification of the expression of over 58,000 annotated genes (including protein coding genes, isoforms, microRNAs and pseudogenes). Gene expression was normalised using the Fragments Per Kilobase of transcript per Million mapped reads (FPKM) method.

Differences in gene expression between samples were compared using CuffDiff. The significance cut-off was set using an adjusted p-value (q). Differentially expressed genes were entered into the DAVID analysis tool and compared to known human biochemical pathways.

2.2.6. De-lipidated serum media preparation

FBS was incubated with 10 mg/mL activated charcoal (Sigma, C9157) for 3 hours at 37^{o}C. The solution was then filtered with a 2 µm filter and syringe. The filtered serum was used to supplement high glucose DMEM containing 2 mM glutamine with 10% de-lipidated FBS.

2.2.7. Hypoxic incubation

To achieve hypoxia cells were incubated in the Don Whitley H35 Hypoxystation which was maintained at 0.3% O_2, 5% CO_2, balance N_2, 37^{o}C and 75% humidity. This condition is referred to as hypoxia henceforth.

2.2.8. Cell treatments

The treatment conditions used in all experiments are summarised in Table 2.2. All treatments were optimised with literature sources and dose response curves (data not shown). Control samples were treated with dimethyl sulfoxide (DMSO) where appropriate.

Drugs/Treatments	Concentration	Incubation time	Product information
De-lipidated serum	10% FBS in DMEM	72 hours	N/A
Atglistatin	30 µM	8 hours	Generon, B3021
Bis-2-(5-phenylacetamido-1,3,4-thiadiazol-2-yl)ethyl sulphide (BPTES)	10 µM	4 hours	Sigma, SML0601
Orlistat	100 µM	4 hours	Sigma, O4139
Simvastatin	1 µM	24 hours	Sigma, S6196
Chloroquine	25 µM	8 hours	Sigma, C6628
3-MA	5 mM	8 hours	Sigma, M9281
siAtg5	100 nM	48 hours	Dharmacon, L-004374-00-0005
Dimethyloxalylglycine (DMOG)	1 mM	16 hours	Sigma, D3695
H_2O_2	100 µM	60 minutes	Sigma, 31642
Cisplatin	100 µM	60 minutes	Sigma, C2210000

Table 2.2. Cell treatments and corresponding dose and incubation period.

2.2.9. Defining alterations in lipid droplet burden

Alterations in the amount of lipid droplet contained within a cell can stem from altered lipid droplet number or size. However, overall alterations in the amount of lipid droplet within the cells have been assessed in this work, as opposed to lipid droplet number or diameter. Therefore, the lipid droplet burden of the cell, assessed qualitatively by confocal microscopy or quantitatively by flow cytometry, is referred to henceforth as “lipid droplet quantity” or “LDQ”.

2.2.10. Confocal Microscopy

2.2.10.1. Nile red lipid droplet standard staining protocol

Cells were plated on sterile glass coverslips and allowed to settle at 37^{o}C, 5% CO_2. Drug treatments or media changes were carried out for the specified time if applicable (Table 2.2.). In experiments investigating starvation conditions the media was changed to Hank's balanced salt solution (HBSS; Sigma, 55037C). Following treatment, cell fixation was performed using 4% paraformaldehyde (Sigma, F1365) in 1x PBS for 20 minutes. Wells were washed briefly 3 times with 1x PBS. Cells were stained with 3 µg/mL nile red (Sigma, T8787) in 1x PBS for 10 minutes in the dark. Wells were washed 5 times with 1x PBS. Cells were stained with 1 drop/mL DAPI (Molecular Probes, R37606) for 10 minutes in the dark. Wells were washed 3 times with 1x PBS and 1 time with dH_2O. Coverslips were inverted and mounted onto microscopy slides using mounting media (Vectorlabs, H-1400). Bubbles were pressed out and the coverslip affixed with nail varnish. Slides were stored at -20^{o}C until analysed.

Confocal microscopy was carried out on a Zeiss 510 Meta-confocal at 40x magnification, pinhole 100µM (Microscopy and Imaging Services, University of Birmingham).

Nile red is highly lipophilic and accumulates within hydrophobic regions such as cell membranes and lipid droplets. Due to its solvatochromic character, the excitation and emission wavelengths shift according to the polarity of its environment. Therefore, the fluorescence shifts from red in cell membranes to green in the more hydrophobic, less polar centre of a lipid droplet. Legend in Table 2.3.

Colour	Dye	Cellular structure
Blue	DAPI	Nucleus
Green	Nile red	Lipid droplet
Red	Nile red (non-droplet staining)	Cellular membrane/lipid structure

Table 2.3. Nile red confocal microscopy legend.

Qualitative analysis was performed by a single observer. Staining across each slide was examined and 3 representative fields (containing approximately 10-20 cells) were selected for image capture. The green signal intensity was compared visually to the number of DAPI stained nuclei in each field to qualitatively assess changes in LDQ between slides.

2.2.10.2. C16 and C11 BODIPY standard staining protocols.

Cells were plated on sterile glass coverslips and allowed to settle at 37^{o}C, 5% CO_2 before incubation at 21% or 0.3% O_2 overnight. The media was removed and the cells were washed with 1x PBS. Cells were incubated with 1 µM C16 BODIPY (Invitrogen, D3821) in DMEM or HBSS for 30 minutes at 37^{o}C. Cell treatments were carried out if applicable (Table 2.2.). Cells were washed once with 1x PBS and fixed with 4% paraformaldehyde in 1x PBS for 20 minutes. Cells were washed 3 times with 1x PBS and stained with 1 drop/mL DAPI for 10 minutes in the dark. Cells were mounted and affixed on microscope slides as per the nile red lipid droplet standard stain protocol.

Confocal microscopy was carried out on a Zeiss 510 Meta-confocal at 40x magnification, pinhole 100µM (Microscopy and Imaging Services, University of Birmingham).

C11 BODIPY (Invitrogen, D3861) staining followed the same protocol as C16 BODIPY. The fluorescence emission of this dye changes from ~590nm to ~510nm (red to green) following oxidation of the polyunsaturated lipid groups indicating oxidative damage.

2.2.11. Nile red lipid droplet quantification standard flow cytometry protocol

2.2.11.1. Sample preparation

Cells were plated and allowed to settle at 37^{o}C, 5% CO_2 before incubation at 21% or 0.3% O_2 overnight. Drug treatments or media changes were carried out for the specified time if applicable (Table 2.2.). In experiments investigating starvation conditions the media was changed to HBSS. Following treatment, cells were washed once with 1x PBS and detached from the plate with 0.05% Trypsin. Trypsin activity was neutralised with media collected post-treatment. Cells were centrifuged at 350 G for 5 minutes at 4^{o}C and the supernatant removed. Cells were washed with 1x PBS and centrifuged at 350 G for 5 minutes at 4^{o}C and the supernatant removed. Cells were fixed with 4% paraformaldehyde in 1x PBS for 20 minutes before centrifugation at 350 G for 5 minutes at 4^{o}C and removal of the supernatant. The above PBS wash step was repeated. Cells were stained with 1.5 µM nile red for 10 minutes before centrifugation at 350 G for 5 minutes at 4^{o}C and removal of the supernatant. The above PBS wash step was repeated. Cells were re-suspended in 300 µL 1x PBS and stored at 4^{o}C until analysed.

2.2.11.2. Data collection

Flow cytometry analysis was performed on the LSR-Fortessa X-20 flow cytometer. Forward scatter (FSC), side scatter (SSC), FITC (530 nm wavelength) and PE (575 nm wavelength) signal intensities were measured (laser wavelengths set according to manufacturer's instructions). The FITC laser was selected to measure the green signal intensity, representative of lipid droplet staining. The PE laser was selected to measure the red signal intensity, representative of lipid droplets and membrane lipid staining. FITC and PE laser intensities were set so the signal intensity of the unstained control sample was below 10^2 (Figure 2.3.). 10000 events were collected on FACSDiva.

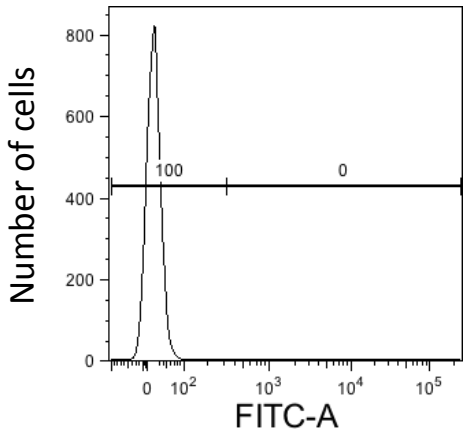

Figure 2.3. Example unstained control population histogram for flow cytometry.

2.2.11.3. Data analysis

Data analysis was performed on the FlowJo software. FITC signal intensity was analysed as it provides a more accurate measurement of lipid droplet specific staining (247). Data was converted to FITC signal intensity histograms (Figure 2.3.). The signal intensity gate was set at 50% of the population in the 21% or 0.3% O_2 DMSO control and applied to all other samples (Figure 2.4.). The percentage of the

population with a higher signal intensity than the median signal intensity of the control was used to measure changes in signal intensity. A percentage increase in this population represents an increased population FITC signal intensity, increased green nile red stain and therefore increased LDQ. A percentage decrease in this population therefore represents decreased LDQ. The percentage changes were graphed with GraphPad Prism 7.0. The data was analysed using unpaired t-tests; *p<0.05, **p<0.01, ***p<0.001, ****p<0.0001.

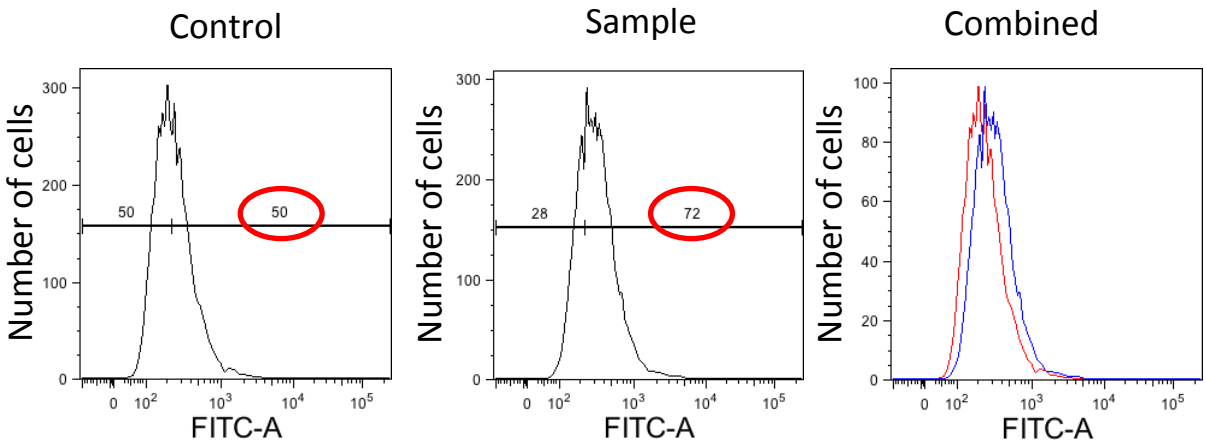

Figure 2.4. Gating used to generate nile red flow cytometry data. Gate set at 50% of the control population. The percentage change in the population with FITC signal intensity above this gate was measured and used for statistical analysis. In this case, LDQ is increased by 22%.

2.2.12. High resolution magic angle spinning (HRMAS) nuclear magnetic resonance (NMR) spectroscopy

2.2.12.1. Sample preparation

Cells were plated and grown until near confluence in 21% O_2. Three 15 cm^3 plates were required for each sample. Plates were transferred to 0.3% O_2 16 hours prior to collection or remained at 21% O_2. Cells were treated with DMSO, 30 µM atglistatin or 25 µM chloroquine for 8 hours. Media was removed and cells were washed 3 times with 10 mL ice cold high quality 1x PBS (Sigma, D8537). Cells were scraped into

1mL ice cold high quality 1x PBS, collected into one vial per sample and centrifuged at full speed for 1 minute. The supernatant was removed and the remaining cell pellet was snap frozen in liquid nitrogen. Samples were stored at -80^{o}C until analysed.

2.2.12.2. Data collection

Samples were defrosted and run on the Bruker 500 Mz spectrometer with a HRMAS probe. 45 µL of sample was transferred to a 50 µL rotor. 5 µL of 1 mM TMSP was added as a reference of chemical shift. Rotor speed was set at 4880 hz and the sample kept at 4^{o}C to maintain sample integrity. A NOESY sequence was run on each sample (256 scans). A CPMG sequence was also run on each sample to assist in metabolite assignment.

2.2.12.3. Data analysis

Data was imported to Mestrenova for metabolite and lipid peak assignment. Spectra were phase corrected and the baseline was set using the automatic Whittaker Smoother method. The TMSP peak was set as the reference peak at 0 ppm. Metabolites were assigned using the line fitting and peak picking tools (Table 2.4.). The peak picking tool was adjusted to measure broader peaks when assigning lipid peaks (Table 2.5.). Metabolite and lipid concentrations were quantified using the qNMR plug-in.

Metabolite	Chemical shift (PPM)	Proton number
Isoleucine	1.01	3
Valine	1.04	3
Lactate	1.33	3
Alanine	1.47	3
Glutamate	2.35	2
Succinate	2.41	4
Glutamine	2.45	2
Glutathione	2.55	2
Hypotaurine	2.65	2
Aspartate	2.82	2
Creatine	3.03	3
Choline	3.20/1	9
Phosphoethanolamine	3.21/3.22	2
Phosphocholine	3.22/23	9
Glycerophosphocholine	3.23	9
Taurine	3.42	2
Glycine	3.56	2

Table 2.4. Metabolite peaks for HRMAS assignment.

Lipid group	Nomenclature	Chemical shift (ppm)	Proton number
CH3	Methyl	0.9	3
CH2	Methylene	1.3	2
CH2CH2CO	Ketene methylene	1.6	2
CH2CH=CH	Methylene	2.0	2
CH2COO-	Carboxylic methylene	2.3	2
=CHCH2CH=	Diene methylene	2.8	2
CH=	Terminal alkene	5.3	1

Table 2.5. Lipid peaks for HRMAS assignment.

Metabolite and lipid concentrations were exported to Microsoft Excel and normalised to total metabolite concentration for each sample. Data was analysed in GraphPad Prism 7.0 using unpaired t-tests; *p<0.05, **p<0.01, ***p<0.001, ****p<0.0001.

Total saturated and unsaturated lipid group concentrations were analysed as a percentage of the total lipid concentration for each sample.

2.2.13. Protein knockdown

Atg5 protein knockdown was carried out with the Smartpool ONTARGET-Plus siAtg5 and the lipofectamine 2000 transfection reagent (Invitrogen, 11668-027) (Table 2.6.). A non-targeting siRNA (siNT) was transfected as a positive control.

Cells were plated and allowed to settle at 37^{o}C, 5% CO_2 before incubation at 21% O_2 overnight. 5 µM siRNA in Optimem (Gibco, 31985-047) was mixed with 6 µL/well lipofectamine for 20 minutes at room temperature to form complexes. 1600 µL fresh media was added to each well. 400 µL of the siRNA complexes was added to each well in a dropwise fashion to achieve a final concentration of 100 nM. Cells were lysed at 24, 48 and 72 hours after transfection.

Reagent	Concentration	Product number
siAtg5	100 nM	Dharmacon, L-004374-00-0005
siNT	100 nM	Dharmacon, D-001810-10-05
Lipofectamine	6 µL/well	Invitrogen, 11668-027

Table 2.6. Summary of reagents used in siRNA transfection.

2.2.14. Western blot

Cells were lysed and scraped in 100 µL 1x laemmli buffer (reducing, denaturing: Sigma, S3401). Cell lysates were boiled for 10 minutes at 100^{o}C. Lysates were separated by their approximate molecular weight by loading them onto a 10% polyacrylamide gel under reducing, denaturing conditions and subjecting them to a constant potential difference of 120 V. The gel was “dry” transferred to a nitrocellulose membrane using the Invitrogen iBlot. Membranes were blocked in 5%

milk (Marvel) in PBS-T (0.05% Tween) for 30 minutes. Membranes were washed with PBS-T for 30 minutes and incubated on a rocker with the primary antibody (Table 2.6.) in 5% milk in PBS-T at 4^{o}C overnight. Antibody was removed and membranes were washed in PBS-T for 30 minutes. Membranes were incubated with the appropriate HRP-linked secondary antibody (Table 2.7.) in 5% milk in PBS-T for 1 hour at room temperature. Antibody was removed and membranes were washed in PBS-T for 30 minutes. EZ-ECL (Biological Industries, 20-500-120) substrate was added to membranes and blots were developed.

Primary/Secondary	Antibody	Species	Concentration	Product number
Primary	Anti-Atg5	Rabbit	1:500	Cell Signalling, D5F5U
	Anti-Actin	Mouse	1:2000	Sigma, A4700
Secondary	Anti-Rabbit-HRP	Goat	1:4000	Cell Signalling, 7074S
	Anti-Mouse-HRP	Horse	1:4000	Cell Signalling, 7076S

Table 2.7. Summary of the antibodies used for western blotting.

2.2.15. Western blot densitometry

Western blot band density was analysed to further assess protein knockdown. Developed blots were scanned and imported into imageJ. The density of the Atg5 band for each sample was normalised to the density of the corresponding Actin band and plotted in GraphPad Prism 7.0.

2.2.16. Growth Curves

Cells were plated and allowed to settle at 37^{o}C, 5% CO_2 before incubation at 21% or 0.3% O_2. Cells were detached with 0.05% Trypsin, neutralised in DMEM and stained with trypan blue (Sigma, T8154). Cell number was assessed with duplicate cell counts at 24, 48, 72, 96 and 144 hours. Cell number was normalised to the 24 hour cell count. Proliferation was measured as fold increase in cell number. An unpaired t-test was performed using the 21% O_2 and 0.3% O_2 cell counts at 144 hours; *p<0.05, **p<0.01, ***p<0.001, ****p<0.0001.

2.3. Methods used in Chapter 5

2.3.1. Sulforhodamine B (SRB) proliferation assay

Cells were plated in triplicate and allowed to settle at 37^{o}C, 5% CO_2. The plates for hypoxic incubation were transferred to 0.3% O_2. Cells were treated with 10 µM chloroquine or dH_2O for 24 hours. This dose was selected to increase LDQ with minimal effect on proliferation based upon flow cytometry and dose response assays. Plates undergoing non-hypoxic pre-treatment were moved to 0.3% O_2 and incubated for a further 2 hours. Cells were treated with 100 µM temozolomide (Sigma, T2577) or DMSO. U87, T98G and U87.2 cell lines were incubated with temozolomide for 24, 48 and 72 hours respectively. The dose and incubation time were determined by dose response assays. Cells were fixed with 20% trichloroacetic acid (Sigma, T6399) at 4^{o}C for 30 minutes. Plates were washed 3 times with dH_2O and left to dry. Fixed cells were stained with 0.4% Sulforhodamine B (SRB) (Sigma, T0699) at room temperature for 10 minutes. Plates were washed 4 times with 1% acetic acid (Sigma, 45740) and left to dry. The stain was dissolved with 50 mM Tris buffer pH8.8 and transferred to a 96-well plate. Plates were analysed using a FLUOstar OMEGA plate reader with a 495 nm absorbance scan. The triplicate results were averaged and the data normalised to the DMSO control for each experiment. The data was analysed using a one way ANOVA with a Tukey post-hoc test; *$p<0.05$, **$p<0.01$, ***$p<0.001$, ****$p<0.0001$.

The atglistatin pre-treatment experiment followed this protocol with two alterations:

Cells were treated with 30µM atglistatin instead of chloroquine. All three cell lines were treated with 100µM temozolomide for 48 hours.

2.3.2. AnnexinV/PI cell death assay

2.3.2.1. Sample preparation

Cells were plated and allowed to settle at 37^{o}C, 5% CO_2 before incubation at 21% or 0.3% O_2. Cells were treated with 10 µM chloroquine or dH_2O for 24 hours followed by 100 µM temozolomide or DMSO for a further 72 hours. Dose and incubation time were selected as discussed in section 2.3.1. 100 µL H_2O_2 (30% w/w: Sigma, H1009) was added to the single stain and positive control samples for the final 2 hours to ensure cell death. Following treatment, cells were washed once with 1x PBS and detached from the plate with 0.05% Trypsin. Trypsin activity was neutralised with media collected post-treatment. Cells were incubated in media for 20 minutes before centrifugation at 350 G for 5 minutes and the supernatant removed. Cells were re-suspended in 500 µl 1x AnnexinV Binding Buffer (BD, 556454) before incubation with 5 µL AnnexinV-FITC (BD, 556419) and 1 µL 1:1000 PI (Life Technologies, V13242) for 10 minutes.

The chloroquine pre-treatment with irradiation experiment followed this protocol with two alterations:

Cells were pre-treated with 10µM chloroquine for 2 hours. Cells were then irradiated with 40 Gy radiation (IBL437C Caesium-137 Source Irradiator) and incubated for 24 hours before collection for analysis.

2.3.2.2. Data collection

Flow cytometry analysis was performed on the LSRFortessa X-20 flow cytometer. Forward scatter (FSC), side scatter (SSC), FITC (530 nm wavelength) and PE (575

nm wavelength) signal intensities were measured. The FITC and PE lasers were selected to measure the AnnexinV-FITC and PI signal intensities respectively. FITC and PE laser intensities were set so the signal intensity of the unstained control sample was below 10^3. Cross channel bleeding was checked through single stain control samples treated with AnnexinV-FITC or PI only (Figure 2.5.). Stain strength was assessed using a positive control sample. 10000 events were collected on FACSDiva.

2.3.2.3. Data analysis

Data analysis was performed on the FlowJo software. FITC signal intensity was plotted against PE signal intensity. AnnexinV-FITC and PI gates were set using the DMSO-treated control population at approximately 90% viability (Figure 2.6.). The viable cell population is representative of the percentage of AnnexinV-FITC and PI negative cells. Increased AnnexinV-FITC staining indicates cells in the early stages of apoptosis. Increased AnnexinV-FITC and PI staining indicates cells in the late stages of apoptosis. Increased PI staining indicates cells which have finished apoptosis or are undergoing necrosis. The viable cell population was used to assess changes in cell viability between samples. The data was analysed using a one way ANOVA with a Tukey post-hoc test; *$p<0.05$, **$p<0.01$, ***$p<0.001$, ****$p<0.0001$.

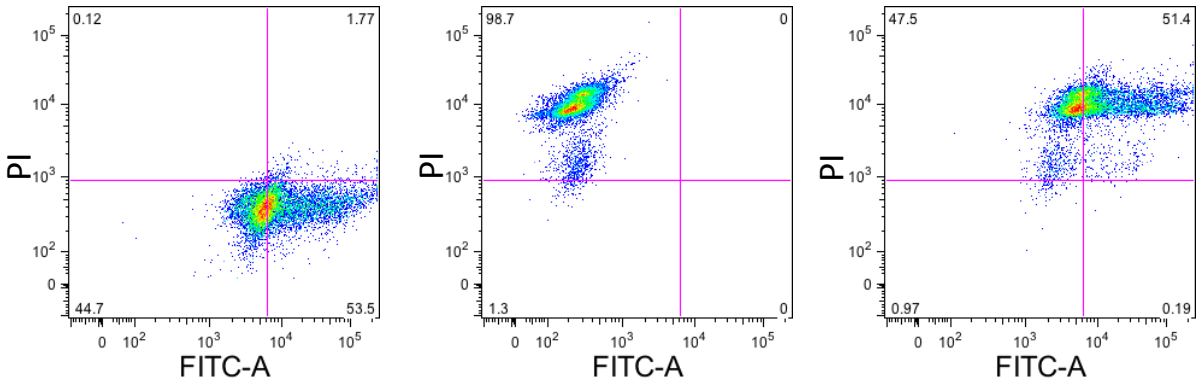

Figure 2.5. Example single and double stain controls for the AnnexinV-FITC/PI cell death assay. AnnexinV-FITC single stain control, PI single stain control, AnnexinV-FITC and PI double stain positive control (left to right).

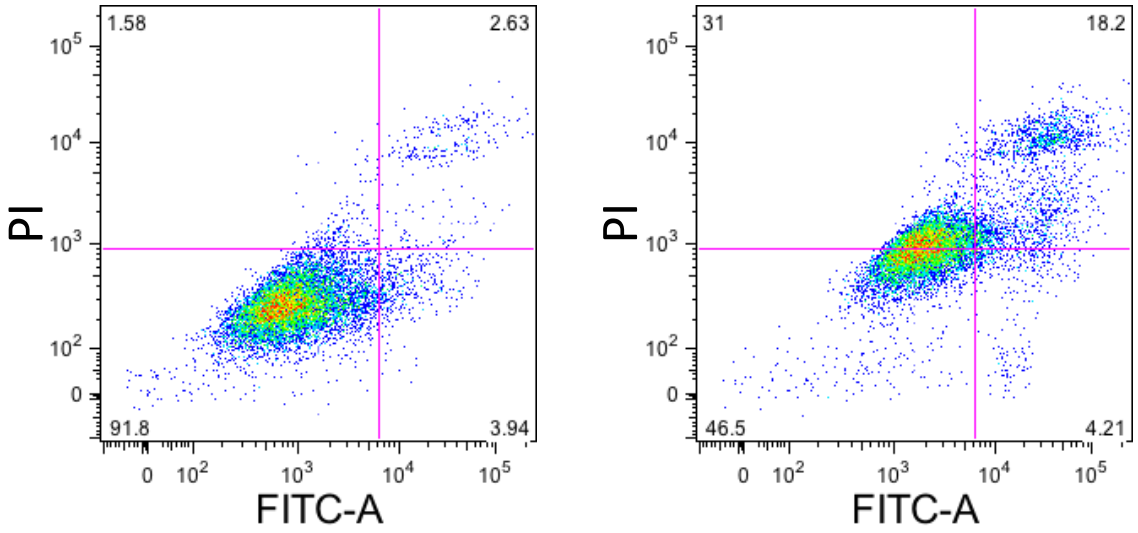

Figure 2.6. Untreated control (left) and drug treated sample (right) from AnnexinV-FITC/PI cell death assay. The viable cell population was represented by the lower left quadrant (AnnexinV-FITC and PI negative) and gated at approximately 90% viability. The viable cell percentage was used to assess changes in cell viability between samples.

Chapter 3

The importance of lipid droplet related genes in the prognosis of high grade gliomas

3.1. Introduction

Despite clear differences in severity, grade 2, 3 and 4 gliomas are intrinsically linked and share many characteristics. Proliferation, invasion, infiltration and aggressiveness are common features of all three glioma types and increase dramatically with tumour grade (9). The process of tumour progression therefore presents a significant challenge in glioma treatment as tumour severity and drug resistance increases.

Interestingly, distinct and characteristic genetic alterations frequently occur in gliomas as tumours progress through the clinical grades. IDH and TP53 mutations occur in 80% of grade 2 and 3 gliomas (29) and in 83% of secondary GBM (55). Moreover, these mutations appear to universally occur in a defined order wherein IDH mutations precede mutations of TP53 and subsequent GBM-associated genetic alterations (35,36). The frequency of these mutations in an established order suggests that they may be fundamentally linked to the tumour progression process. In contrast, primary GBM is believed to occur spontaneously at grade 4 without prior progression from lower grades and is associated with IDH and TP53 mutation in only 5% of cases (55). However, the tumour progression process remains unclear as the biological mechanisms are yet to be explored. Mutations in IDH affect the cellular metabolic and epigenetic profile and can promote tumorigenic genetic instability (30,34) whilst TP53 mutation and loss is well-established as a tumorigenic alteration (41,42). Paradoxically, IDH mutant tumours are also associated with an improved prognosis, possibly attributable to increased therapeutic sensitivity (37). Nevertheless, hypotheses regarding how these genetic alterations may influence a route to glioma tumour progression are based predominantly upon a general increased predisposition to mutation. Moreover, the spontaneous occurrence of

primary GBM at grade 4 suggests that there are other important aspects of glioma biology which produce high grade gliomas. Therefore, it is not unreasonable to hypothesise that these areas of glioma biology also impact tumour progression and produce high grade gliomas.

Lipid droplet metabolism represents an important component in the metabolism of many types of cancer (248) including gliomas (123,249) and influences many aspects of tumorigenesis. Moreover, lipid droplet accumulation is increased with clinical grade (94,240) and indicates prognosis (94,241) suggesting that the importance of lipid droplets alters with increased tumour grade. As such, lipid droplets and their associated metabolic pathways may be altered in response to tumour progression or may even influence the tumour progression process. In this case representative genes would be expressed differentially according to tumour grade and may represent prognostic biomarkers. Lipid droplet-associated metabolic pathways such as exogenous lipid uptake (123,152) and autophagy (152,184,185,188) have been suggested to be important in many cancers and, if associated with lipid droplets across the clinical grades, may indicate aspects of the underlying biological metabolism of tumour progression.

In this chapter we investigate the importance of genes that control and modulate the metabolism of lipid droplets and their associated metabolic pathways with regards to survival and tumour progression.

3.2. Results

3.2.1. The selection of genes for investigation

A list of genes representative of pathways such as; autophagy, lipase-mediated degradation, exogenous lipid uptake and *de novo* fatty acid synthesis which have known effects on lipid droplet metabolism in other cancers and cell types was created (Table 3.1.). Similarly, lipid droplet-associated proteins were selected as they have clear importance in lipid droplet biology whilst lipid utilising pathways were selected for possible post-lipid droplet roles. Many gene paralogs were also included to assess the effect of similar pathways with the expectation many would be later excluded. This list was not exhaustive and many other genes could have been included, but the aim was to create a clear and structured gene list for improved clarity in our analysis.

Biological Process	Gene	Name	Function
Lipid droplet-associated proteins	Plin1	Perilipin 1	Lipid droplet-associated protein
	Plin2	Adipophillin	Lipid droplet-associated protein
	Plin3	TIP47	Lipid droplet-associated protein
	Plin4	Perilipin 4	Lipid droplet-associated protein
	HILPDA	Hypoxia Inducible Lipid Droplet-Associated	Hypoxia-associated lipid droplet protein

Lipases	PNPLA1	Patatin-Like Phospholipase Domain-Containing Protein 1	Uncharacterised
	PNPLA2	Adipose triglyceride lipase	Removal of the first fatty acid from triacylglycerols
	PNPLA3	Adiponutrin	Triacylglycerol lipase
	PNPLA4	Patatin-Like Phospholipase Domain-Containing Protein 4	Triacylglycerol lipase
	PNPLA5	Patatin-Like Phospholipase Domain-Containing Protein 5	Inhibits transacylation
	PNPLA6	Neuropathy target esterase	Phospholipase responsible for the conversion of phosphatidylcholine to glycerophosphocholine
	PNPLA7	Patatin-Like Phospholipase Domain-Containing Protein 7	Uncharacterised
	PNPLA8	Intracellular Membrane-Associated Calcium-Independent Phospholipase A2 Gamma	Phospholipase that cleaves fatty acids from membrane phospholipids
	LIPE	Hormone-sensitive lipase	Removal of the second fatty acid from triacylglycerol
	LPL	Lipoprotein lipase	Lipoprotein and triacylglycerol degradation
Lipid uptake	CD36	CD36 (fatty acid translocase)	Exogenous lipid uptake transporter
Autophagy	MAP1LC3 A, B	Light-chain 3 autophagy protein	Autophagy vital proteins
	ATG2A, 2B, 3, 4A, 4B, 4C, 4D, 5, 7, 9A, 9B, 10, 12, 13, 15,	Autophagy proteins	Autophagy vital proteins

	16L1, 16L2		
De novo lipid synthesis	ACACA	Acetyl-CoA carboxylase	Converts acetyl CoA to malonyl CoA. Rate limiting step in fatty acid synthesis
	FASN	Fatty acid synthase	Vital to fatty acid synthesis
	GLS	Glutaminase	Converts glutamine to glutamate
	ACSL1, 3, 4, 5, 6	Long-chain fatty-acid-coenzyme A ligase family	Important to lipid biosynthesis
	ACSS2	Acetyl-Coenzyme A synthetase 2	Production of acetyl CoA from acetate
	DGAT1	Diacylglycerol O-Acyltransferase 1	Conversion of diacylglycerol to triacylglycerol
Phospholipid production	CEPT1	Choline/Ethanolamine Phosphotransferase 1	Production of phosphatidylcholine and phosphatidylethanolamine
	CHPT1	Cholinephosphotransferase 1	Production of phosphatidylcholine
	ETNK1	Ethanolamine kinase 1	Phosphatidylethanolamine synthesis
	PTDSS1, 2	Phosphatidylserine synthase	Synthesis of phosphatidylserine
	CHKA, B	Choline kinase/ethanolamine kinase	Phosphatidylcholine and phosphatidylethanolamine synthesis
Mitochondrial fatty acid transport	CPT1A, B	Carnitine palmitoyltransferase 1A and B	Transport of fatty acids across outer mitochondrial membrane
	CPT2	Carnitine palmitoyltransferase 2	Transport of fatty acids across the inner mitochondrial membrane

	CRAT	Carnitine Acetyl transferase	Catalyses the addition of carnitine to fatty acids for transport into mitochondria
	SLC25A20	Carnitine/Acylcarnitine Transolcase	Mediation of transport of acylcarnitines into the mitochondrial matrix
Cholesterol metabolism	LIPA	Sterol esterase	Breakdown of cholesteryl esters
	LDLR	Low density lipoprotein lipase receptor	Uptake of cholesterol

Table 3.1. Genes selected for investigation in initial survival analysis. Gene names are matched with the encoded protein, the protein function and the associated biological process.

3.2.2. Expression of lipid droplet-associated proteins and genes in key metabolic pathways is associated with survival in grade 2 and 3 gliomas

Using the selected genes we sought to investigate the effect of high or low gene expression on survival in the combined grade 2 and 3 glioma cohort using Kaplan-Meier survival analysis. The genes could be separated into three groups: those for which high expression correlated with poor survival, those for which high expression correlated with good survival and those where there was no association with survival (Figure 3.1.A, 3.1.B and 3.1.C respectively, Table 3.2.). The first group consisted predominantly of lipid droplet-associated proteins, autophagy and phospholipid synthesis genes. In contrast, the second group consisted of predominantly *de novo* fatty acid synthesis genes. The genes composing these two groups were selected for further investigation due to significant separation of survival curves. However, there were several exclusions: the ACSL and ATG genes were excluded from further investigation despite significant survival separation due to conflicting results from the

different gene paralogs (data not shown). In both cases, an alternative gene was used to represent each pathway; *de novo* fatty acid synthesis could be represented by FASN and ACACA whereas autophagy could be represented by MAP1LC3A. These genes better represent the metabolic pathways and avoid the confounding variables introduced by the gene paralogues, wherein each paralogue can have multiple associations with other pathways. The majority of genes with no significant difference between the high and low gene expression curves were excluded from this list with the exception of CD36, PLIN4 and CPT2. CD36 remains of interest as high gene expression indicated both poor and good survival over time (Figure 3.1.C) whereas PLIN4 was included because of a clear role in lipid droplet biology. CPT2 was included as the p-value approached significance (Table 3.2.). The final list of genes for further investigation is reported in Table 3.2. The separation of significantly different survival curves according to gene expression indicates that many of these pathways may be important aspects of grade 2 and 3 glioma biology.

We further investigated gene expression across several histological classifications. We observed no association between histological classification, such as astrocytoma or oligoastrocytoma, and survival association in our gene set (data not shown) indicating that these pathways are important in grade 2 and 3 tumours regardless of glioma sub-classification.

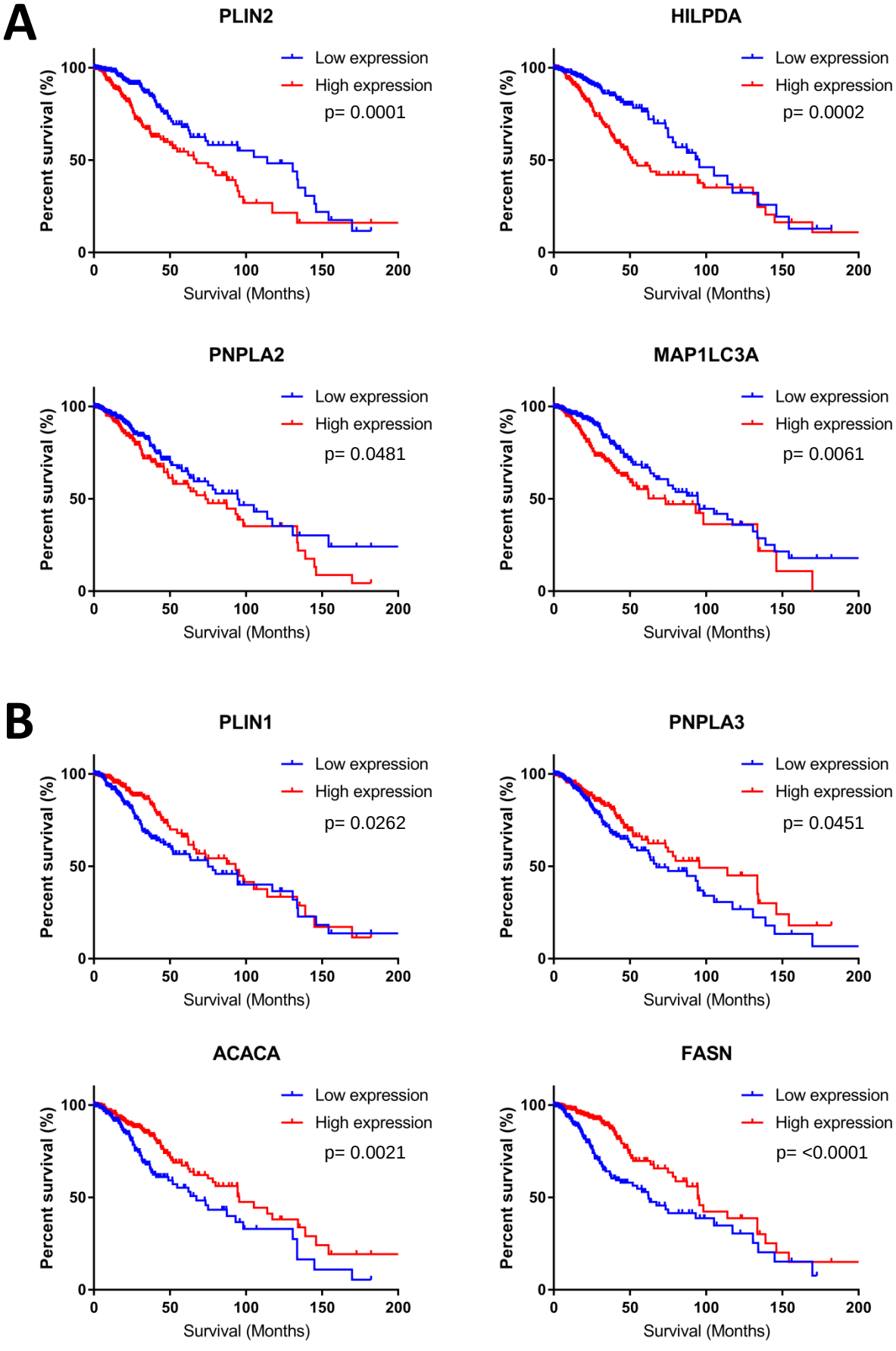
A
PLIN2
Low expression
High expression
p= 0.0001
Percent survival (%)
Survival (Months)
HILPDA
p= 0.0002
PNPLA2
p= 0.0481
MAP1LC3A
p= 0.0061
B
PLIN1
p= 0.0262
PNPLA3
p= 0.0451
ACACA
p= 0.0021
FASN
p= <0.0001

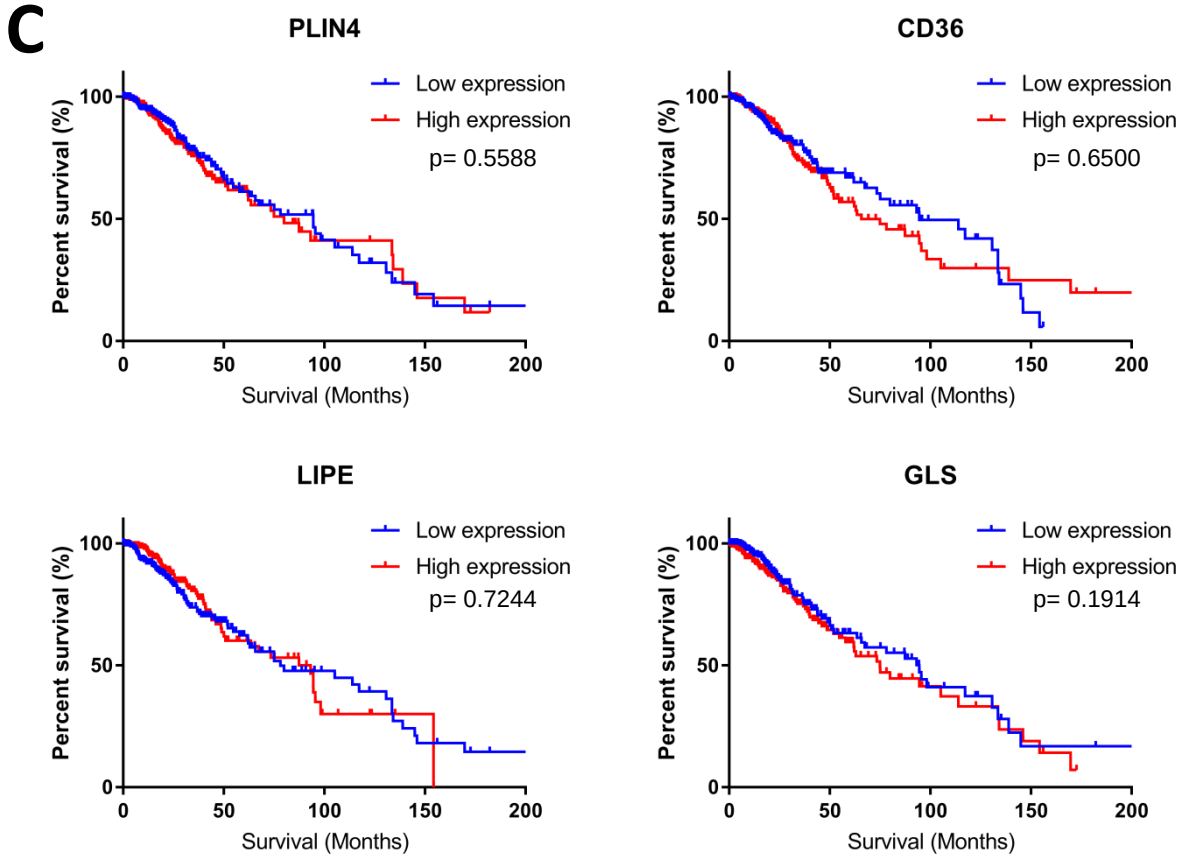

Figure 3.1. Expression of lipid droplet-associated genes was associated with survival in grade 2 and 3 gliomas. Representative Kaplan-Meier survival curves of the combined grade 2 and 3 glioma cohort. n=527. A) Representative graphs of genes where high gene expression was associated with worse survival. PLIN2 (lipid droplet-associated protein), HILPDA (hypoxia associated lipid droplet-associated protein) PNPLA2 (adipose triglyceride lipase [ATGL]), MAP1LC3A (autophagy vital protein). B) Representative graphs of genes where high gene expression was associated with better survival. PLIN1 (lipid droplet-associated protein), PNPLA3 (lipase), ACACA (acetyl-CoA carboxylase), FASN (fatty acid synthase). C) Representative graphs of genes where gene expression was not associated with survival. PLIN1 (lipid droplet-associated protein), CD36 (fatty acid uptake transporter), LIPE (hormone sensitive lipase), GLS (glutaminase). Log-rank (Mantel-Cox) and Gehan-Breslow-Wilcoxon statistical tests were performed in all cases; *p<0.05, **p<0.01, ***p<0.001, ****p<0.0001.

Gene	MC p-value	GBW p-value
High gene expression was associated with poor survival		
PLIN2	0.0001	<0.0001
PLIN3	0.0126	0.0203
PNPLA2	0.0481	0.0683
PNPLA4	0.0002	<0.0001
HILPDA	0.0002	<0.0001
MAP1LC3A	0.0061	0.0012
CEPT1	<0.0001	<0.0001
ETNK1	0.0242	0.2992
PTDSS1	0.0278	0.0017
SLC25A20	0.003	0.0001
High gene expression was associated with good survival		
PLIN1	0.0262	0.0022
PNPLA3	0.0451	0.1227
ACACA	0.0021	0.0049
FASN	<0.0001	<0.0001
Survival was independent of gene expression		
PLIN4	0.5588	0.3979
CD36	0.6500	0.8824
CPT2	0.059	0.1709

Table 3.2. Gene expression correlates with survival in grade 2 and 3 gliomas. Summary of data in Figure 3.1. and Appendix 7.4.

3.2.3. The prognostic value of gene expression varies between grade 2 and grade 3 gliomas

Tumour progression through clinical grades reflects the altered gene expression and metabolic pathway activity of the cell in response to new challenges. We further investigated the separation of survival curves by gene expression at grade 2 and 3 separately using the gene list established in section 3.2.2. There was a significant difference between the survival curves according to median PLIN3 expression in grade 2 tumours only (Figure 3.2.A, Table 3.3.), whereas a significant difference between the survival curves was observed in grade 3 tumours in several genes representing multiple pathways (Figure 3.2.B, Table 3.3.). In contrast, there was a significant difference between the survival curves separated by median CEPT1 and ACACA expression in both the individual grade 2 and grade 3 tumour cohorts (Figure3.2.C, Table 3.3.). Survival curves could not be separated in either grade 2 or 3 tumours for several genes which had significantly different survival curves according to median gene expression in the combined grade 2 and 3 cohort (Figure 3.2.D, Table 3.3.). However, the separation of survival curves according to high and low expression of PNPLA2, CPT2 and ETNK1 almost reached significance (Table 3.3.) whilst PLIN4 and CD36 expression did not separate survival curves in the original combined grade 2 and 3 cohort (Figure 3.1.C). As expected, the indication of poor or good survival according to high gene expression frequently mirrored the prognostic indications observed in the combined grade 2 and 3 glioma cohort. The significantly different survival curves at each clinical grade indicate that the importance of these genes is altered across the stages of tumour development, implying different roles throughout tumour progression.

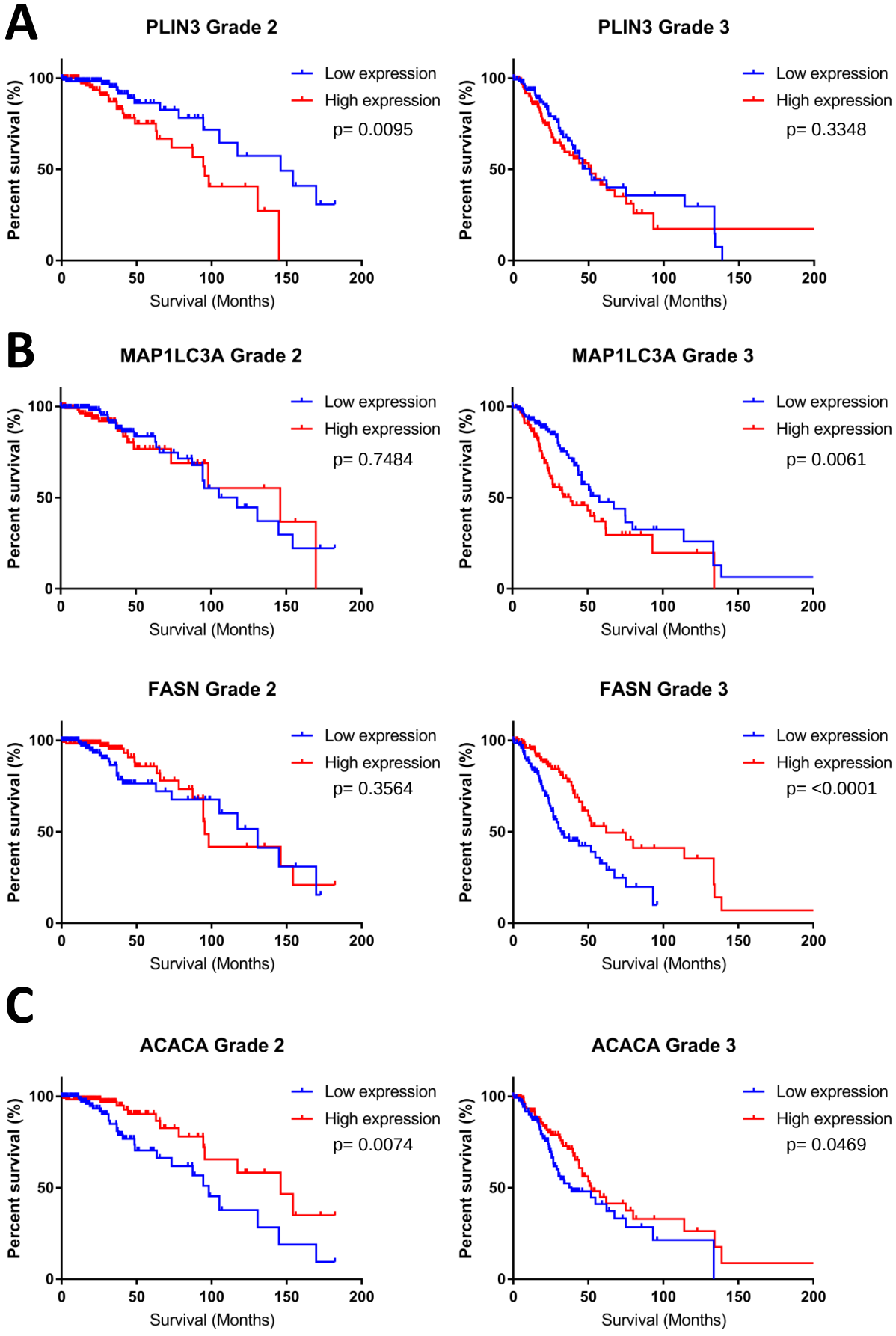
A
PLIN3 Grade 2
Low expression
High expression
p= 0.0095
Percent survival (%)
Survival (Months)
PLIN3 Grade 3
Low expression
High expression
p= 0.3348
Percent survival (%)
Survival (Months)
B
MAP1LC3A Grade 2
Low expression
High expression
p= 0.7484
Percent survival (%)
Survival (Months)
MAP1LC3A Grade 3
Low expression
High expression
p= 0.0061
Percent survival (%)
Survival (Months)
FASN Grade 2
Low expression
High expression
p= 0.3564
Percent survival (%)
Survival (Months)
FASN Grade 3
Low expression
High expression
p= <0.0001
Percent survival (%)
Survival (Months)
C
ACACA Grade 2
Low expression
High expression
p= 0.0074
Percent survival (%)
Survival (Months)
ACACA Grade 3
Low expression
High expression
p= 0.0469
Percent survival (%)
Survival (Months)

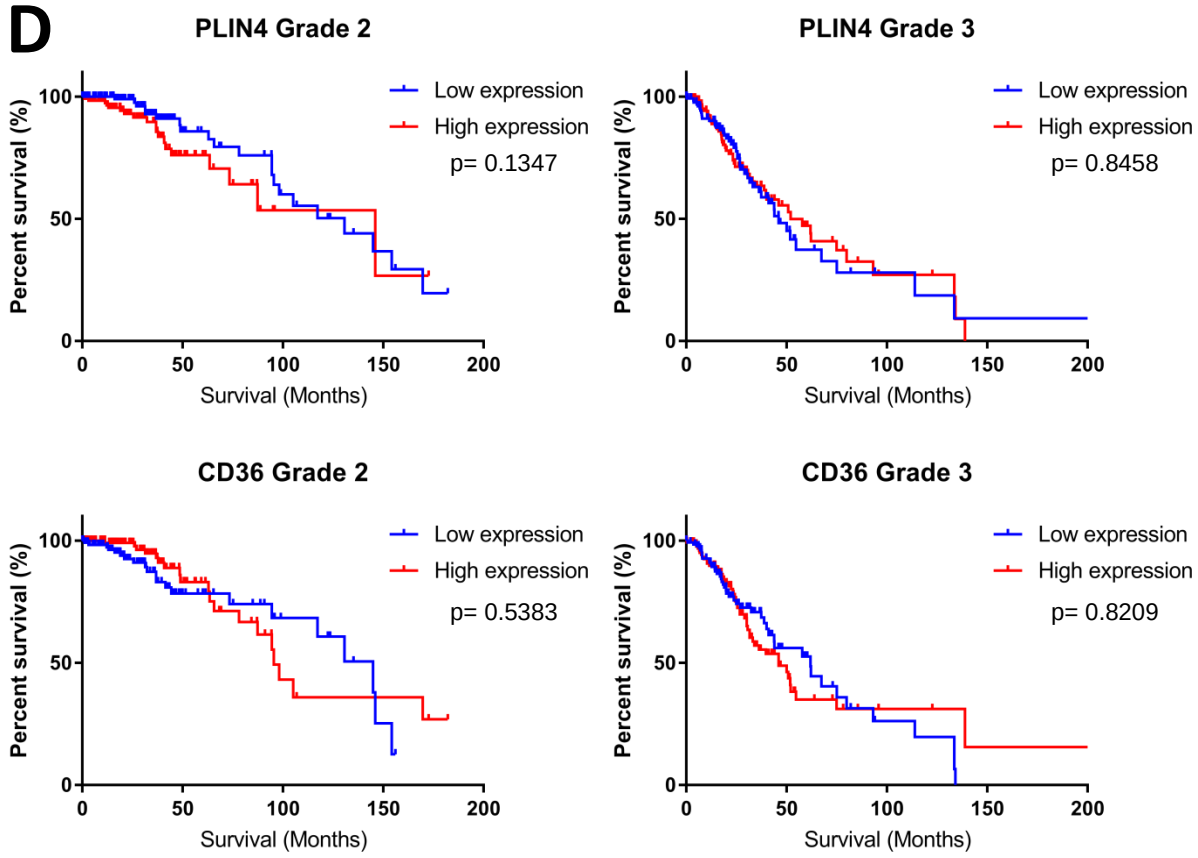

Figure 3.2. The association of gene expression with survival is grade dependent. Representative Kaplan-Meier survival curves of the combined grade 2 and 3 glioma cohort split into a grade 2 and a grade 3 glioma cohort. Grade 2 n=256, Grade 3 n=270. A) Representative graphs of a gene where survival curves were significantly separated according to median gene expression in grade 2 tumours. PLIN3 (lipid droplet-associated protein). B) Representative graphs of genes where survival curves were significantly separated according to median gene expression in grade 3 tumours. MAP1LC3A (autophagy vital protein), FASN (fatty acid synthase). C) Representative graphs of genes where survival curves were significantly separated according to median gene expression in grade 2 and 3 tumours. ACACA (acetyl-CoA carboxylase). D) Representative graphs of genes which did not separate survival curves according to median gene expression in either tumour grade. PLIN4 (lipid droplet-associated protein), CD36 (fatty acid uptake transporter). Log-rank (Mantel-Cox) and Gehan-Breslow-Wilcoxon statistical tests were performed in all cases; *p<0.05, **p<0.01, ***p<0.001, ****p<0.0001.

Gene	Grade 2		Grade 3	
	MC p-value	GBW p-value	MC p-value	GBW p-value
Grade 2 Separation				
PLIN3	0.0095	0.0667	0.3348	0.1444
Grade 3 Separation				
PLIN1	0.1754	0.3772	0.0035	0.0015
PLIN2	0.3027	0.4237	0.0163	0.0039
PNPLA4	0.2556	0.2229	0.0001	0.0004
FASN	0.3564	0.0955	<0.0001	0.0001
MAP1LC3A	0.7484	0.9335	0.0061	0.0024
PTDSS1	0.7460	0.4336	0.0350	0.0154
SLC25A20	0.0819	0.1154	0.0036	0.0002
Grade 2 and 3 Separation				
CEPT1	0.0216	0.1197	0.0003	0.0026
ACACA	0.0074	0.0248	0.0469	0.0760
No Grade Separation				
PLIN4	0.1347	0.0369	0.8458	0.9741
PNPLA2^{+}	0.0608	0.0996	0.4220	0.2324
PNPLA3	0.1214	0.3364	0.6870	0.5776
CD36	0.5383	0.1009	0.8209	0.7139
HILPDA	0.3069	0.1795	0.1632	0.0920
CPT2^{+}	0.0502	0.2453	0.7174	0.5424
ETNK1^{+}	0.3861	0.8695	0.0521	0.4209

Table 3.3. The prognostic value of gene expression is altered across tumour grades. Summary of data in Figure 3.2. and Appendix 7.5. $^{+}$ gene expression may associate with survival (p-value approaching significance)

3.2.4. Gene expression is not a prognostic marker for the majority of genes in grade 4 gliomas

As gene expression was a prognostic marker in grade 2 and 3 tumours, we sought to investigate the effect of gene expression on survival in the glioblastoma grade 4 cohort. Poor survival was observed in tumours with a high expression of MAP1LC3A or SLC25A20 only (Figure 3.3, Table 3.4). Although PNPLA2 and CEPT1 approached significance, the survival curves are too steep, due to the low survival time of glioblastoma, and no separation was observed. This suggests that either expression of these genes is no longer important at grade 4 or that expression is similar in all glioblastoma tumours.

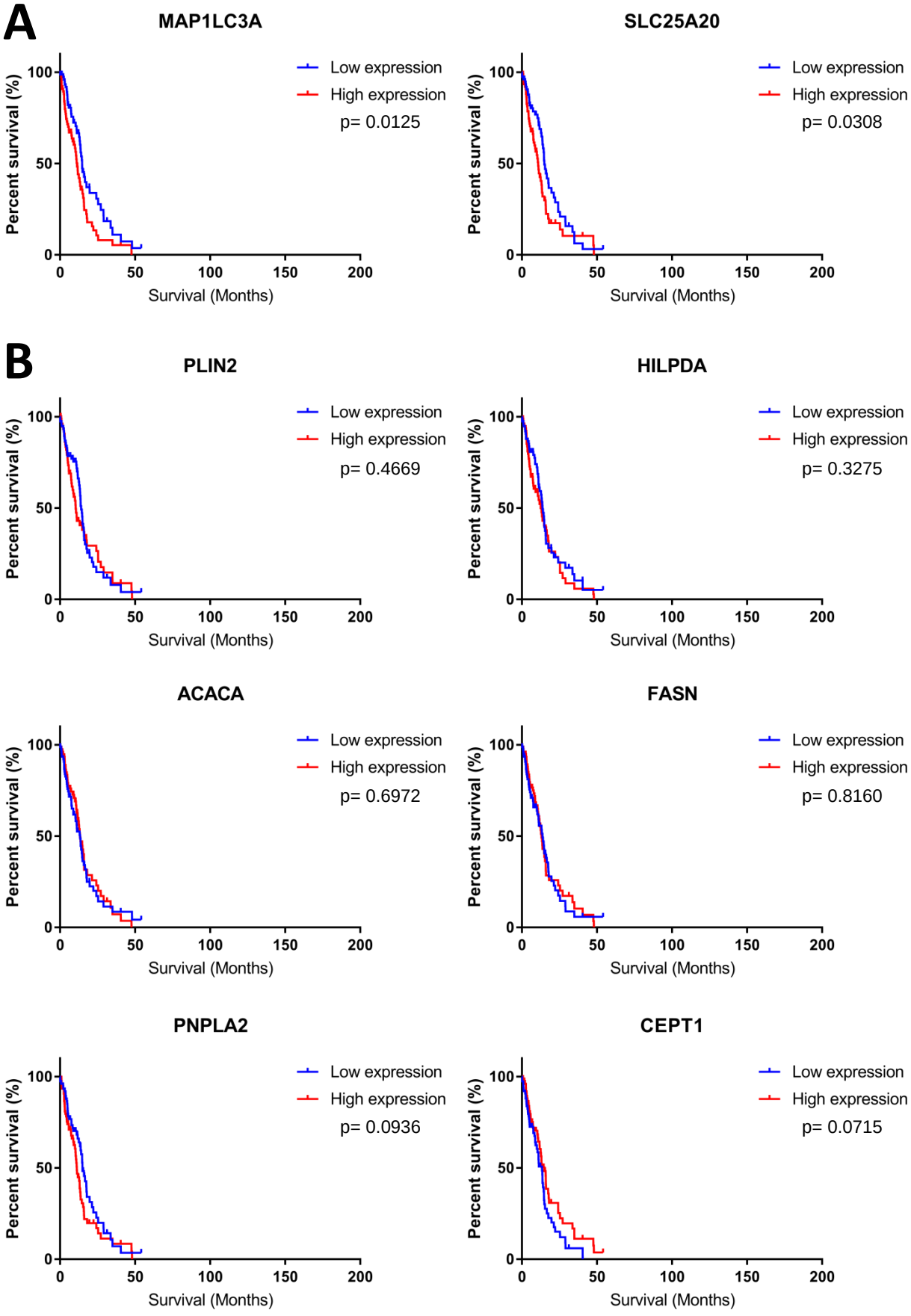
A
MAP1LC3A
Low expression
High expression
p= 0.0125
Percent survival (%)
Survival (Months)
SLC25A20
Low expression
High expression
p= 0.0308
Percent survival (%)
Survival (Months)
B
PLIN2
Low expression
High expression
p= 0.4669
Percent survival (%)
Survival (Months)
HILPDA
Low expression
High expression
p= 0.3275
Percent survival (%)
Survival (Months)
ACACA
Low expression
High expression
p= 0.6972
Percent survival (%)
Survival (Months)
FASN
Low expression
High expression
p= 0.8160
Percent survival (%)
Survival (Months)
PNPLA2
Low expression
High expression
p= 0.0936
Percent survival (%)
Survival (Months)
CEPT1
Low expression
High expression
p= 0.0715
Percent survival (%)
Survival (Months)

Figure 3.3. Gene expression does not associate with survival in grade 4 gliomas for the majority of genes. Representative Kaplan-Meier survival curves of the glioblastoma grade 4 cohort. n=151. A) Representative graphs of genes which separated survival curves by median gene expression in grade 4 tumours. MAP1LC3A (autophagy vital protein), SLC25A20 (mitochondrial fatty acid transporter). B) Representative graphs of genes which did not separate survival curves by median gene expression in grade 4 tumours. PLIN2 (lipid droplet-associated protein), HILPDA (hypoxia associated lipid droplet-associated protein), ACACA (acetyl-CoA carboxylase), FASN (fatty acid synthase), PNPLA2 (adipose triglyceride lipase [ATGL]), CEPT1 (phosphatidylcholine/phosphatidylethanolamine synthesis). Log-rank (Mantel-Cox) and Gehan-Breslow-Wilcoxon statistical tests were performed in all cases; *p<0.05, **p<0.01, ***p<0.001, ****p<0.0001.

Gene	MC p-value	GBW p-value
Expression is indicative of survival		
MAP1LC3A	0.0125	0.0123
SLC25A20	0.0308	0.0108
Survival is independent of expression		
PLIN1	0.4058	0.1408
PLIN2	0.4669	0.1826
PLIN3	0.5326	0.2168
PLIN4	0.1123	0.1067
PNPLA2	0.0936	0.0667
PNPLA3	0.8586	0.9001
PNPLA4	0.1987	0.2737
CD36	0.9108	0.8175
HILPDA	0.3275	0.2430
ACACA	0.6972	0.3787
FASN	0.8160	0.6188
CEPT1	0.0715	0.1807
CPT2	0.9655	0.8749
ETNK1	0.1396	0.1410
PTDSS1	0.8689	>0.9999

Table 3.4. Gene expression does not associate with survival at grade 4 for the majority of gliomas. Summary of data in Figure 3.3. and Appendix 7.6.

3.2.5. Gene expression alters with clinical grade indicating the importance of these pathways in grade 4 glioma biology

The lack of prognostic significance in grade 4 tumours suggests that expression of many of these genes could reach an “end-point” in grade 4 tumours. To assess this we compared gene expression across grade 2, 3 and 4 gliomas. Expression of genes representing several pathways such as autophagy, ATGL-mediated lipolysis, lipid uptake and phospholipid synthesis was increased at grade 3 and 4 or grade 4 alone (Figure 3.4.A. and 3.4.B, Table 3.5.). Interestingly, we observed above that high expression of many of these genes was associated with poor survival in grade 2, 3 or 4 tumours. In contrast, the expression of several *de novo* fatty acid synthesis genes and the lipid droplet-associated protein genes PLIN1 and PLIN4 was decreased in grade 3, grade 4 or both grade 3 and 4 tumours (Figures 3.4.A. and 3.4.B, Table 3.5.). Interestingly, for the majority of genes, expression was most different at grade 4 whereas expression was frequently similar at grade 2 and 3. This matches the clinical presentation of gliomas and indicates clearly that expression of these genes remains an important factor in grade 4 tumours.

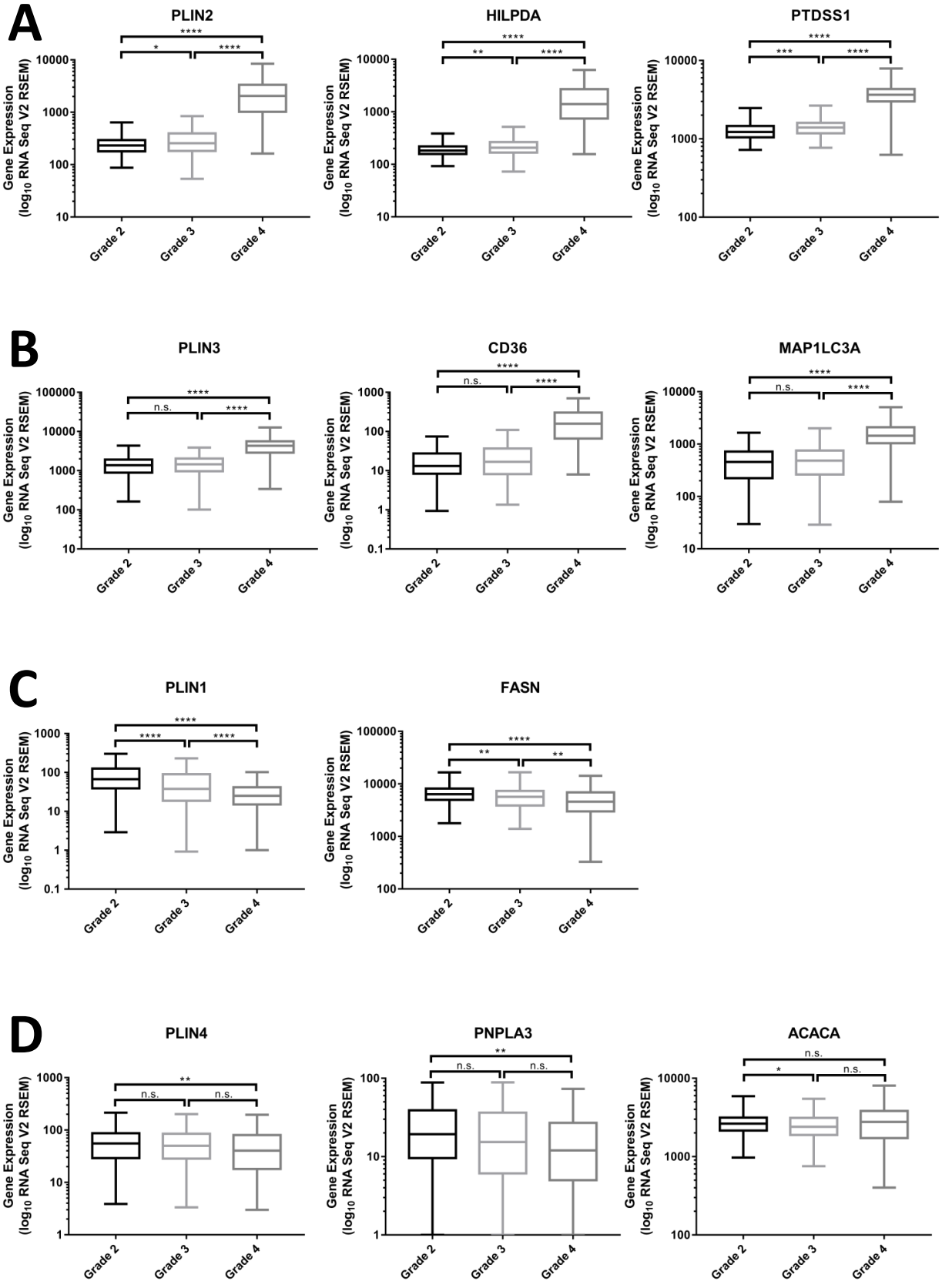
A
PLIN2
HILPDA
PTDSS1
B
PLIN3
CD36
MAP1LC3A
C
PLIN1
FASN
D
PLIN4
PNPLA3
ACACA
Gene Expression (log10 RNA Seq V2 RSEM)
Grade 2
Grade 3
Grade 4
n.s.

Figure 3.4. Gene expression alters with clinical grade. Representative Boxplots showing the range of gene expression in grade 2, 3 and 4 gliomas. Data produced from the combined grade 2 and 3 glioma cohort and grade 4 glioma cohorts. Grade 2 n=256, Grade 3 n=270, Grade 4 n=151. A) Representative Boxplots of genes for which gene expression was increased at higher clinical grades. PLIN2 (lipid droplet-associated protein), HILPDA (hypoxia associated lipid droplet-associated protein), PTDSS1 (phosphatidylserine synthesis). B) Representative Boxplots of genes for which gene expression was increased in grade 4 tumours only. PLIN3 (lipid droplet-associated protein), CD36 (fatty acid uptake transporter), MAP1LC3A (autophagy vital protein). C) Representative Boxplots of genes for which gene expression was decreased at grade 3 and 4. PLIN1 (lipid droplet-associated protein), FASN (fatty acid synthase). D) Representative Boxplots of genes for which gene expression was decreased in grade 3 or 4 only. ROUT outlier removal was performed for each gene to remove definitive outliers (Q=0.1%). Resulting data sets were analysed with using a Kruskal-Wallis statistical test with a Dunn's post-hoc correction; *p<0.05, **p<0.01, ***p<0.001, ****p<0.0001.

Gene expression increased at grade 3 and 4	Gene expression decreased at grade 3 and 4
PLIN2	PLIN1
HILPDA	FASN
PTDSS1	**Gene expression only decreased in grade 4**
Gene expression only increased in grade 4	PLIN4
PLIN3	PNPLA3
PNPLA2	**Gene expression only decreased in grade 3**
PNPLA4	ACACA
CD36	
MAP1LC3A	
CEPT1	
CPT2	
ETNK1	
SLC25A20	

Table 3.5. Gene expression alters across clinical grades. Summary of data in figure 3.4. and Appendix 7.7.

3.2.6. “Grade 3 like” gene expression in grade 2 gliomas characterises a poor prognostic group of tumours suggesting a role in tumour progression

If alterations in gene expression across clinical grades can indicate worse survival due to tumour progression then it may be possible to detect lower grade tumours with a higher probability of progression. We sought to investigate this by defining high and low gene expression in the grade 2 cohort with the grade 3 mean gene expression. High or low gene expression was determined to be “grade 3 like” using our previous survival analysis and gene expression data (Section 3.2.1 to 3.2.5). Genes such as PLIN3 and PNPLA2 have indicated an association between high expression and poor survival and were increased in higher clinical grades. Therefore, in these cases grade 2 tumours with higher gene expression than the grade 3 mean were determined to be “grade 3 like” and therefore associated with the lower survival and higher probability of tumour progression observed with grade 3 tumours. Conversely, genes such as ACACA and FASN previously indicated an association between high expression and good survival and had decreased expression in higher grade tumours. Therefore, tumours with expression of these genes below the grade 3 mean were determined to be “grade 3 like”. “Grade 3 like” gene expression separated significantly different survival curves in several genes suggesting poor prognosis grade 2 tumours can be predicted (Figure 3.5.A, Table 3.6.). Moreover, in the case of PLIN2, HILPDA and MAP1LC3A, the small number of “grade 3 like” tumours indicated that gene expression resembles grade 3 tumours in very few grade 2 tumours, providing evidence regarding a role for these genes in later tumour grades (Figure 3.5.B). Therefore, gene expression can indicate a poor survival set of grade 2 tumours based upon their similarity to a higher clinical grade. Indeed, these data draw interesting parallels with the changes in IDH1 and TP53

mutation observed during tumour progression. In summary, grade 2 tumours with a worse prognosis have an increased chance of progression and recurrence and therefore, combined with our previous data, this suggests that these genes may alter across clinical grades and that understanding of these alterations may allow the prediction of tumour progression.

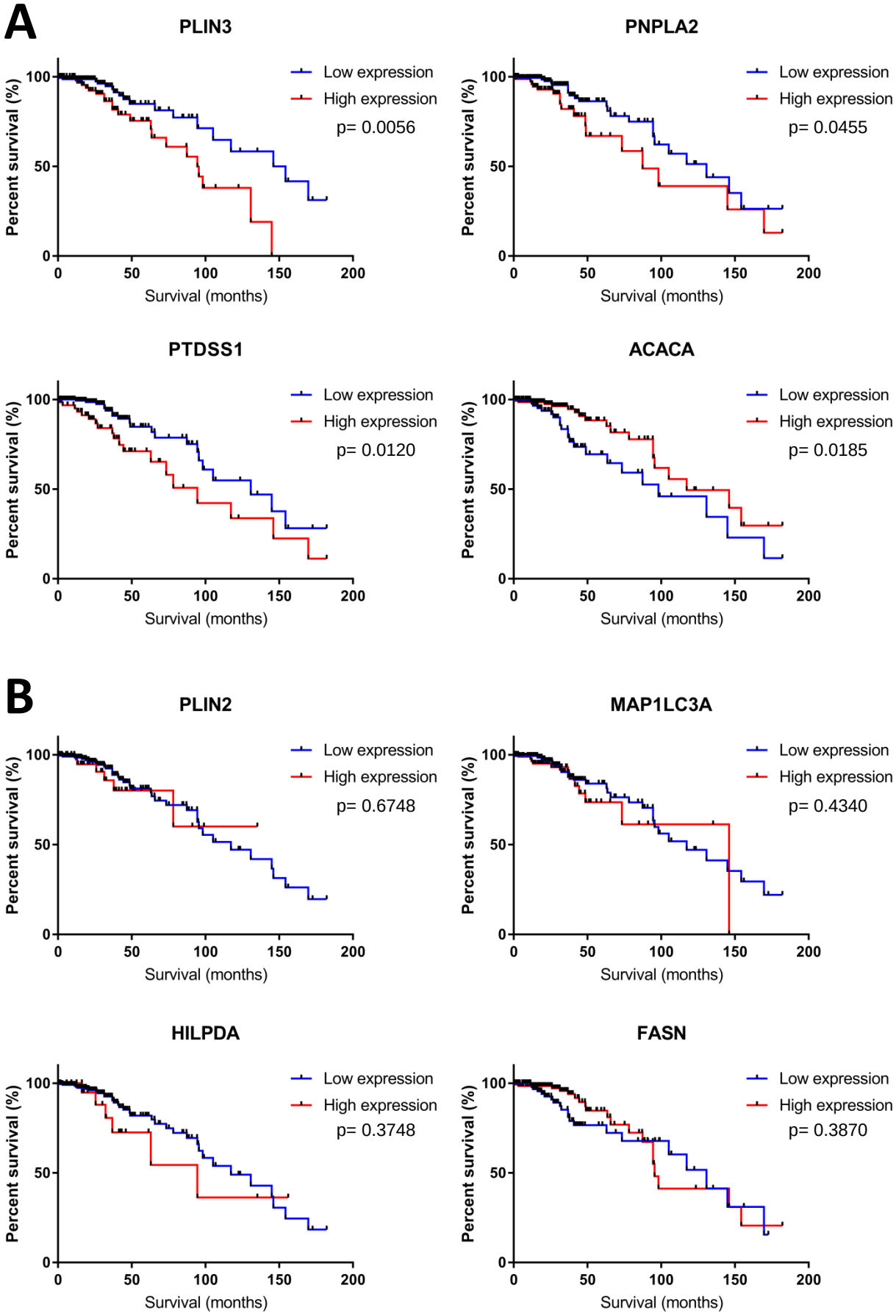
A
PLIN3
Low expression
High expression
p= 0.0056
Percent survival (%)
Survival (months)
PNPLA2
Low expression
High expression
p= 0.0455
Percent survival (%)
Survival (months)
PTDSS1
Low expression
High expression
p= 0.0120
Percent survival (%)
Survival (months)
ACACA
Low expression
High expression
p= 0.0185
Percent survival (%)
Survival (months)
B
PLIN2
Low expression
High expression
p= 0.6748
Percent survival (%)
Survival (months)
MAP1LC3A
Low expression
High expression
p= 0.4340
Percent survival (%)
Survival (months)
HILPDA
Low expression
High expression
p= 0.3748
Percent survival (%)
Survival (months)
FASN
Low expression
High expression
p= 0.3870
Percent survival (%)
Survival (months)

Figure 3.5. "Grade 3 like" expression of several genes is associated with poor survival in grade 2 gliomas. Representative Kaplan-Meier survival curves of the grade 2 glioma cohort. High/Low gene expression was determined by grade 3 mean gene expression. n=256. A) Representative graphs of genes which separated survival curves according to grade 3 mean gene expression. PLIN3 (lipid droplet-associated protein), PNPLA2 (adipose triglyceride lipase [ATGL]), PTDSS1 (phosphatidylserine synthesis), ACACA (acetyl-CoA carboxylase). B) Representative graphs of genes which did not separate survival curves according to grade 3 mean gene expression. PLIN2 (lipid droplet-associated protein), MAP1LC3A (autophagy vital protein), HILPDA (hypoxia associated lipid droplet-associated protein), FASN (fatty acid synthase). Log-rank (Mantel-Cox) and Gehan-Breslow-Wilcoxon statistical tests were performed in all cases; *p<0.05, **p<0.01, ***p<0.001, ****p<0.0001.

Gene	MC p-value	GBW p-value
“Grade 3 like” gene expression is associated with survival in grade 2 tumours		
PLIN3	0.0056	0.0483
PLIN4	0.0013	0.0064
PNPLA2	0.0455	0.0164
PNPLA4	0.0240	0.0529
ACACA	0.0185	0.0182
CPT2	0.0109	0.0519
PTDSS1	0.0120	0.0008
“Grade 3 like” gene expression is not associated with survival in grade 2 tumours		
PLIN1	0.3013	0.3696
PLIN2	0.6748	0.4051
PNPLA3	0.0512	0.2389
CD36	0.4188	0.9142
HILPDA	0.3748	0.2569
FASN	0.3870	0.0807
MAP1LC3A	0.4340	0.3621
CEPT1	0.1633	0.3087
ETNK1	0.1507	0.2667
SLC25A20	0.1180	0.0603

Table 3.6. “Grade 3 like” expression of several genes was associated with poor survival. Summary of data in Figure 3.5. and Appendix 7.8.

3.2.7. IDH1 mutation is associated with expression of selected genes

IDH1 mutations are known to result in alterations in glioma metabolism and are linked to tumorigenesis and we sought to investigate an association with the expression of genes in our selected gene set. Several of the genes we investigated were noted to have increased expression in either the IDH wildtype (WT) or mutant (MUT) tumours (Figure 3.6, Table 3.7.). Many of the genes we have associated with poor survival in our glioma cohorts had increased gene expression in IDH1 WT tumours (Figure 3.6.A), also known to have poor survival (250,251). In contrast, only the genes associated with *de novo* fatty acid synthesis had increased expression in the IDH1 MUT tumours (Figure 3.6.B). Interestingly, IDH1 MUT tumours are known to have a better survival (250,251) and we observed the tumours with high ACACA and FASN expression tended to result in better overall survival. Notably, few tumours in the combined grade 2 and 3 glioma cohort had a known IDH1 mutational status and this may limit the strength of these findings. Nevertheless, this data raises the possibility of an interesting association between lipid droplet-associated pathways and IDH1 mutational status as independent markers of tumour severity and patient survival.

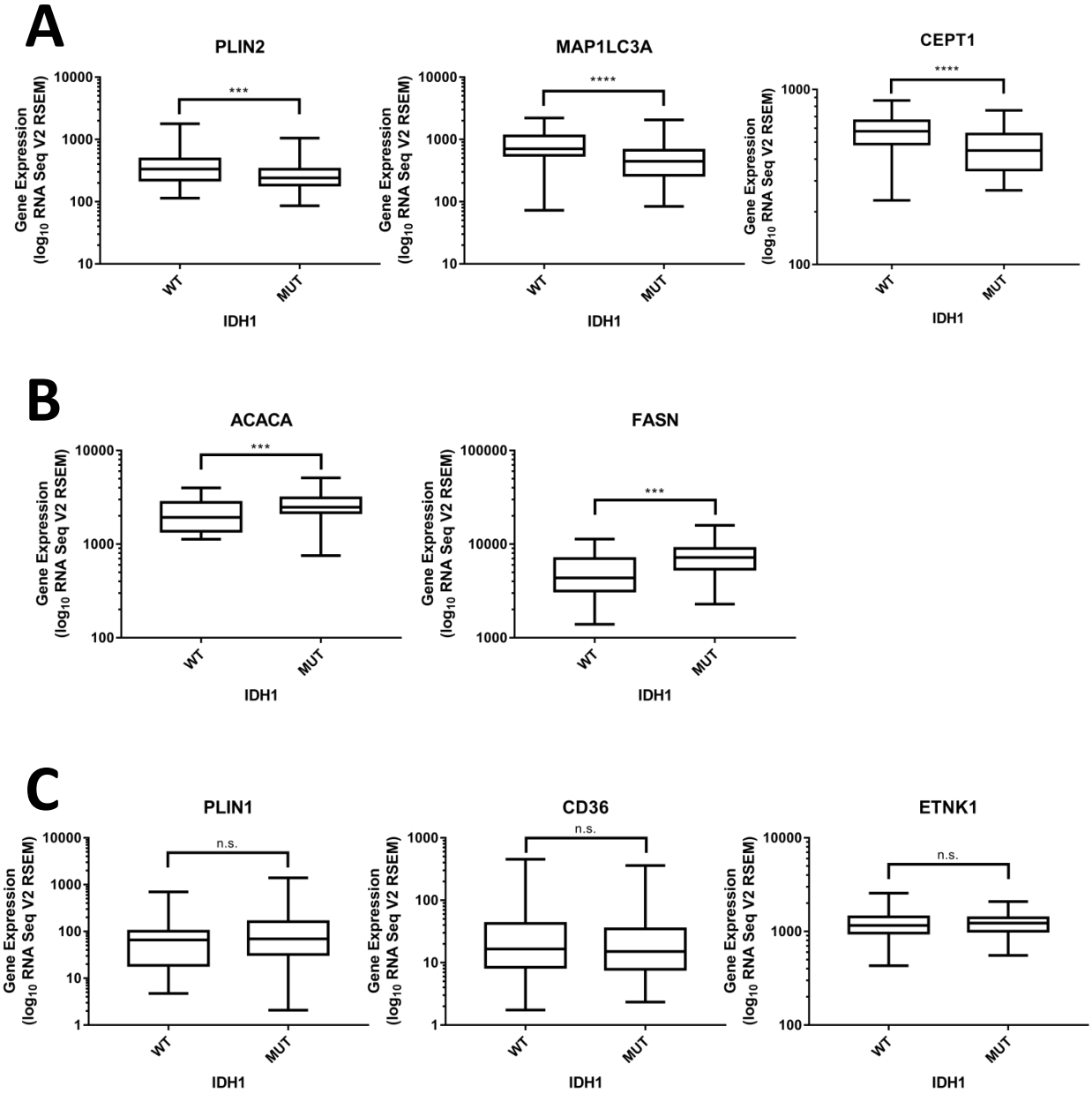

Figure 3.6. IDH1 mutational status is associated with the expression of selected genes. Representative Boxplots comparing the gene expression of IDH1 wild-type (WT) and mutant (MUT) tumours in the combined grade 2 and 3 glioma cohort. Known IDH mutational status was required for inclusion. IDH1 WT n=34, IDH1 MUT n=91. A) Representative Boxplots of genes with increased gene expression in IDH1 WT tumours. PLIN2 (lipid droplet-associated protein), MAP1LC3A (autophagy vital protein), CEPT1 (phosphatidylcholine/phosphatidylethanolamine synthesis). B) Representative Boxplots of genes with increased gene expression in IDH1 MUT tumours. ACACA (acetyl-CoA carboxylase), FASN (fatty acid synthase). C) Representative Boxplots of genes with no significant difference in IDH1 WT or MUT tumour gene expression. PLIN1 (lipid droplet-associated protein), CD36 (fatty acid uptake transporter), ETNK1 (phosphatidylethanolamine synthesis). Unpaired two-tailed t-test statistical tests were performed in all cases; *p<0.05, **p<0.01, ***p<0.001, ****p<0.0001.

Gene	p-value
Higher gene expression in IDH1 WT tumours	
PLIN2	0.0005
PLIN3	0.0064
PLIN4	0.0236
PNPLA2	0.0090
PNPLA4	<0.0001
HILPDA	0.0060
MAP1LC3A	<0.0001
CEPT1	<0.0001
CPT2	0.0365
PTDSS1	0.0003
SLC25A20	<0.0001
Higher gene expression in IDH1 MUT tumours	
ACACA	0.0007
FASN	0.0001
Gene expression is independent of IDH1 mutational status	
PLIN1	0.2968
PNPLA3	0.3094
CD36	0.1688
ETNK1	0.9849

Table 3.7. Expression of several genes associates with IDH1 mutational status. Summary of data in Figure 3.6. and Appendix 7.9.

3.2.8. Significant correlations are found between genes with prognostic indications

We sought to explore whether the genes investigated in the previous sections are independently or co-ordinately expressed. Specifically we investigated whether genes are independent biomarkers as a prelude to determining gene combinations as prognostic markers. We also explored whether genes of prognostic value define specific tumour sub-groups or rather are altered continuously throughout tumour progression. Spearman's rank correlation analysis was used to highlight the correlation between the expression of many genes (Figure 3.7.A.). This was visualised using a heat map (Figure 3.7.B.) which displayed significant correlations between genes associated with better survival or genes associated with worse survival. Negative correlations were observed in gene expression between genes associated with different survival outcomes. This indicates that these genes do not act as independent biomarkers and suggests that the represented pathways are linked by a shared attribute such as an association with lipid droplet metabolism. Moreover, the tumours were not observed to cluster by cluster analysis indicating that these tumours do not form specific sub-groups defined by the expression of these genes (Figure 3.7.C.). Many significant correlations observed in Figure 3.7.B. were also found to be significant using the TCGA cBioPortal query function (Figure 3.7.D.), further supporting the gene correlations. Notably, alterations in CEPT1 and CPT2 expression co-occurred with several genes; however, as CEPT1 and CPT2 were predominantly detected as mRNA down-regulation, this is in fact mutual exclusivity. The TCGA cBioPortal query function was also used to assess these correlations in the grade 4 glioblastoma cohort (Figure 3.7.E.). Although far fewer correlations were present in this data set, PLIN2 and HILPDA alterations and ACACA and FASN alterations were observed to co-occur indicating their importance.

Therefore, gene expression appears to alter across grade 2 and 3 tumours in a continuous manner as opposed to defining separate tumour sub-groups and further suggests an association with tumour progression

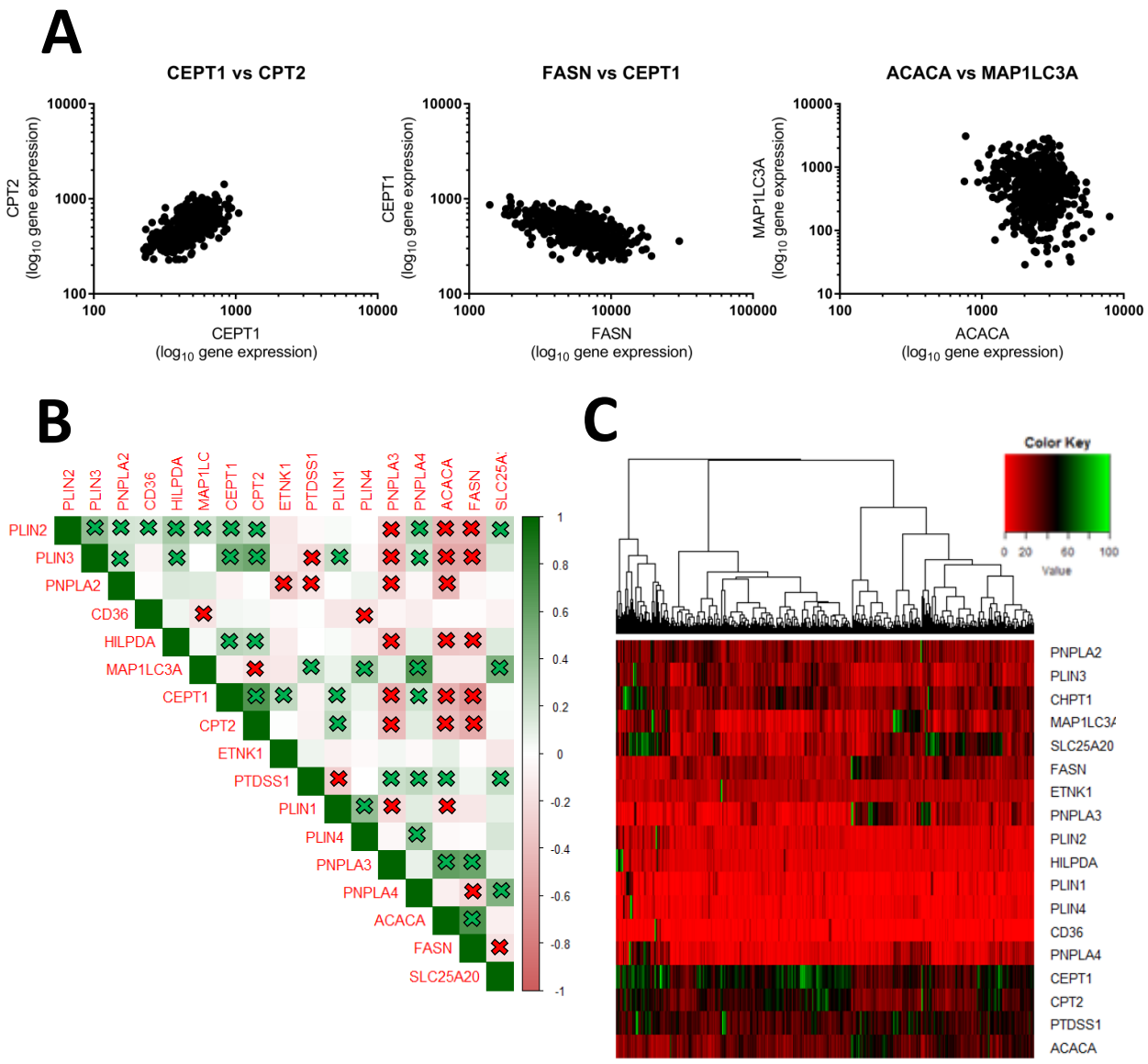

D

The query contains **72** gene pairs with mutually exclusive alterations (**4** significant), and **64** gene pairs with co-occurrent alterations (**27** significant).

Mutual exclusivity ☐ Co-occurrence ☑ Significant pairs Search Gene

Gene A	Gene B	p-Value	Log Odds Ratio	Association
PLIN1	PLIN4	<0.001	>3	Tendency towards co-occurrence Significant
PLIN1	PNPLA4	<0.001	2.269	Tendency towards co-occurrence Significant
PLIN1	SLC25A20	<0.001	2.445	Tendency towards co-occurrence Significant
PLIN2	PLIN3	<0.001	2.465	Tendency towards co-occurrence Significant
PLIN2	HILPDA	<0.001	>3	Tendency towards co-occurrence Significant
PLIN4	PNPLA4	<0.001	2.633	Tendency towards co-occurrence Significant
PNPLA3	ACACA	<0.001	2.269	Tendency towards co-occurrence Significant
PNPLA3	FASN	<0.001	2.267	Tendency towards co-occurrence Significant
PNPLA4	PTDSS1	<0.001	2.037	Tendency towards co-occurrence Significant
PNPLA4	SLC25A20	<0.001	>3	Tendency towards co-occurrence Significant
ACACA	FASN	<0.001	2.962	Tendency towards co-occurrence Significant
ACACA	CEPT1	<0.001	1.945	Tendency towards co-occurrence Significant
ACACA	CPT2	<0.001	2.178	Tendency towards co-occurrence Significant
FASN	CEPT1	<0.001	1.743	Tendency towards co-occurrence Significant
FASN	CPT2	<0.001	1.905	Tendency towards co-occurrence Significant
CEPT1	CPT2	<0.001	2.029	Tendency towards co-occurrence Significant
MAP1LC3A	PTDSS1	0.001	1.714	Tendency towards co-occurrence Significant
PLIN2	CD36	0.004	2.098	Tendency towards co-occurrence Significant
PNPLA3	CEPT1	0.004	1.298	Tendency towards co-occurrence Significant
HILPDA	SLC25A20	0.005	2.059	Tendency towards co-occurrence Significant
PLIN4	SLC25A20	0.014	2.062	Tendency towards co-occurrence Significant
PNPLA2	ACACA	0.019	1.909	Tendency towards co-occurrence Significant
PLIN2	SLC25A20	0.020	1.876	Tendency towards co-occurrence Significant
PNPLA3	CPT2	0.022	1.140	Tendency towards co-occurrence Significant
PNPLA2	PNPLA3	0.024	1.794	Tendency towards co-occurrence Significant
PLIN1	HILPDA	0.034	1.647	Tendency towards co-occurrence Significant
PLIN2	PLIN4	0.049	1.953	Tendency towards co-occurrence Significant

Showing 1 to 27 of 27 entries (filtered from 136 total entries)

The query contains **72** gene pairs with mutually exclusive alterations (**4** significant), and **64** gene pairs with co-occurrent alterations (**27** significant).

Mutual exclusivity ☑ Co-occurrence ☐ Significant pairs Search Gene

Gene A	Gene B	p-Value	Log Odds Ratio	Association
PLIN4	CEPT1	0.034	<-3	Tendency towards mutual exclusivity Significant
CEPT1	PTDSS1	0.036	-1.125	Tendency towards mutual exclusivity Significant
PNPLA4	CEPT1	0.038	-1.755	Tendency towards mutual exclusivity Significant
PLIN3	CEPT1	0.042	-1.300	Tendency towards mutual exclusivity Significant

Showing 1 to 4 of 4 entries (filtered from 136 total entries)

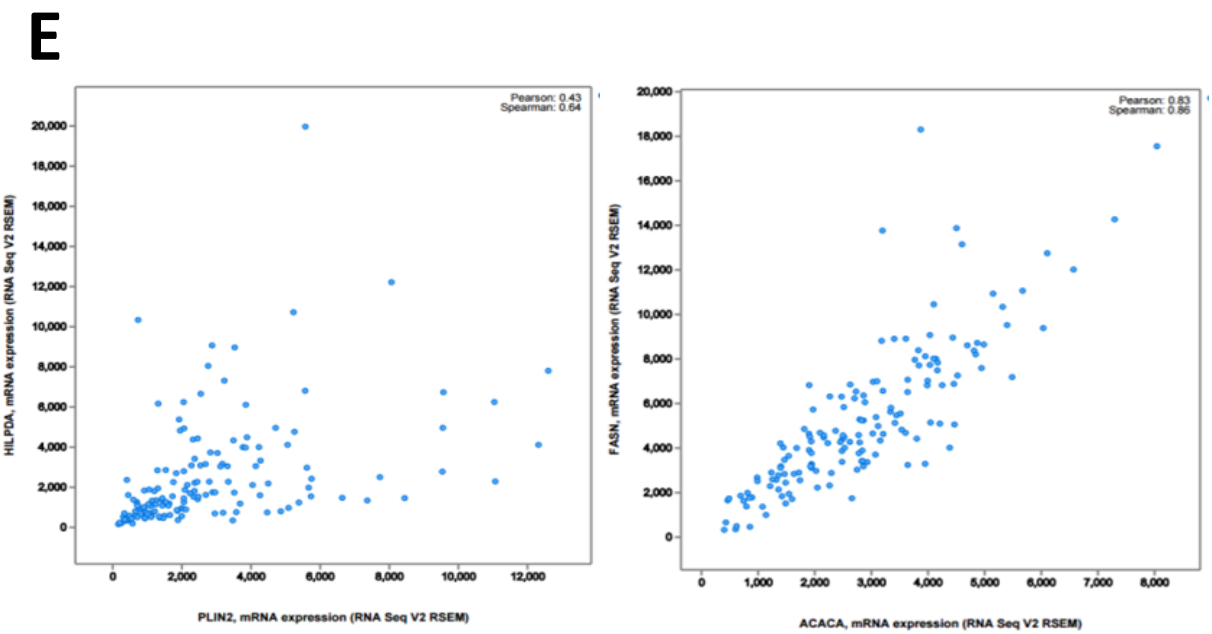

Figure 3.7. The expression of prognostic genes correlates but tumours do not form clusters by gene expression. A) Representative correlation scatter plots of gene expression in the combined grade 2 and 3 glioma cohort. Graphs represent positive, negative and no correlation (left to right). Spearman's correlation analysis was used to assess correlation strength [r]. B) A heat map of gene expression correlation shows correlations between genes predictive of survival. Genes predictive of poor survival: PLIN2 to PTDSS1. Genes predictive of good survival: PLIN1 to FASN. Green to red colour change represents positive to negative correlations [r]. X icons mark significant correlations; A Bonferroni correction was applied to generate adjusted p-value $p<0.00037$, n=135. r-values and p-values can be found in Appendix 7.2. C) Cluster analysis of gene expression indicated that these genes do not form distinct groups. Gene expression normalised to percentage of the maximum gene expression for each gene. D) Correlation analysis performed on the combined grade 2 and 3 glioma cohort using the TCGA cBioPortal query function supported many of the correlations identified in the above heat map (Figure 3.7.B). $p<0.05$. E) Correlation scatter plots of gene expression in the grade 4 glioblastoma cohort using the TCGA cBioPortal query function supported some correlations observed in the combined grade 2 and 3 glioma cohort. PLIN2 and HILPDA (left), ACACA and FASN (right).

3.2.9. Combined gene sets show higher levels of prognostic prediction in grade 4 gliomas

As previously observed it is difficult to associate gene expression with survival in grade 4 tumours. We therefore sought to investigate the expression of combinations of genes as prognostic markers in these tumours instead. Genes were separated into two gene sets: those associated with poor survival and increased expression in higher grade tumours and those associated with good survival and decreased expression in higher grade tumours. In contrast, with the rest of the gene set, CEPT1 and CPT2 mRNA was predominantly down-regulated and were therefore excluded from this analysis (Figure 3.8.A). These two gene sets separated significantly different survival curves in the combined grade 2 and 3 glioma cohort. Tumours with mRNA up-regulation of genes in the poor survival gene set were associated with a significantly worse survival compared to those without (Figure 3.8.A). Interestingly, mRNA up-regulation of this poor survival gene set was also able to separate survival curves in the grade 4 glioblastoma cohort (Figure 3.8.B) implicating these genes as biomarkers of poor prognosis. Similarly, mRNA up-regulation of the good survival gene set also separated survival curves in the grade 4 glioblastoma cohort (Figure 3.8.C.) suggesting these genes may be biomarkers of good prognosis. However, this separation of the survival curves in grade 4 tumours was not significant due to the low number of cases detected with mRNA up-regulation compared to the control group. Nevertheless, it has always been difficult to separate survival curves at grade 4 and therefore it is encouraging that the p-values are close to significance. Despite difficulties separating survival curves in grade 4 tumours with univariate analysis, we observe here that combinations of correlated genes can improve survival curve separation and prognostic prediction.

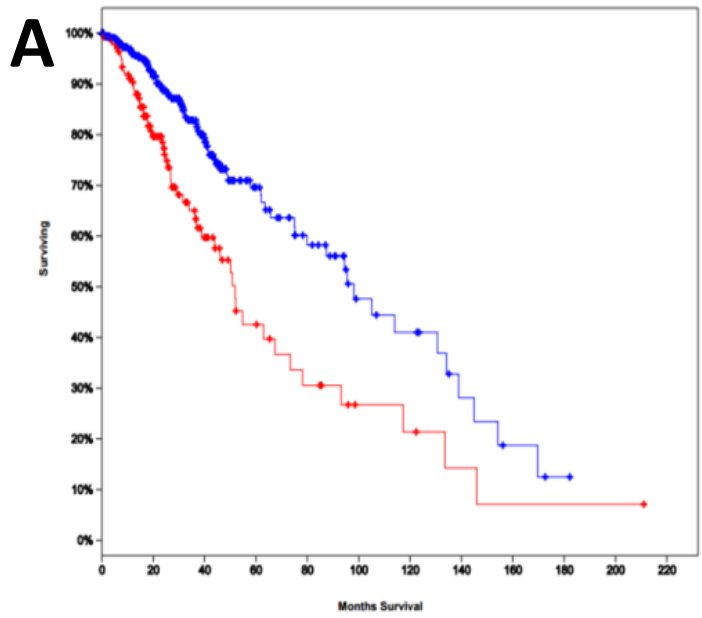

-- Cases with Alterations in Query Genes

-- Cases without Alterations in Query Genes

Log-rank Test p-value 3.229e-5

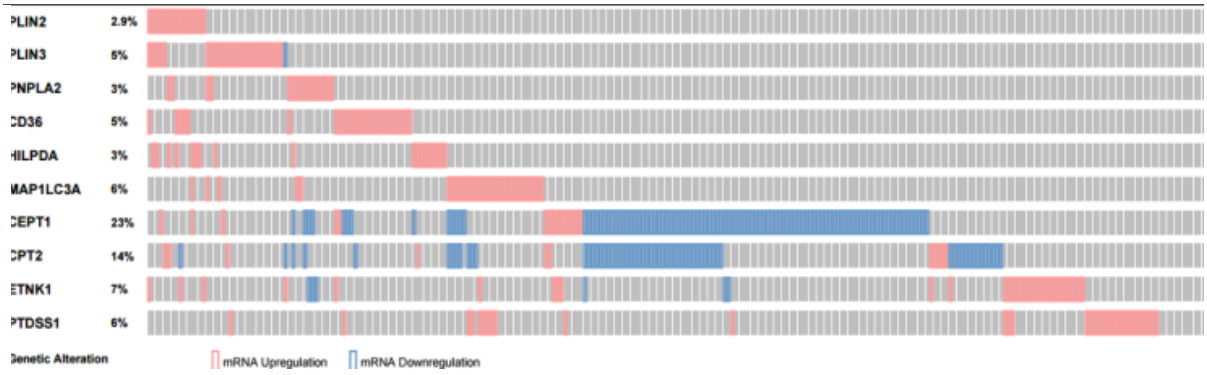

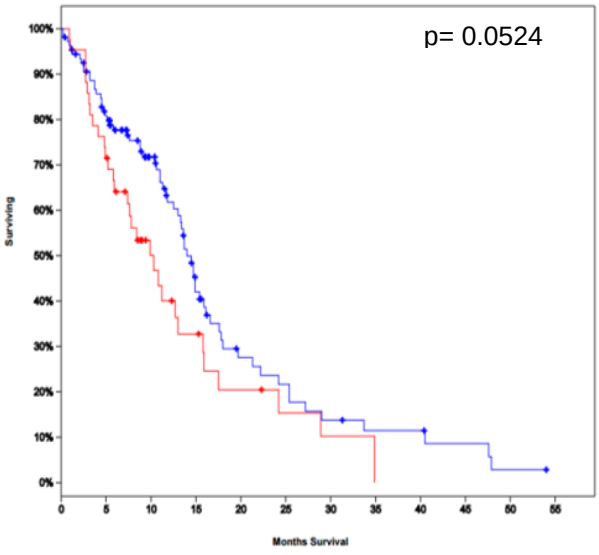

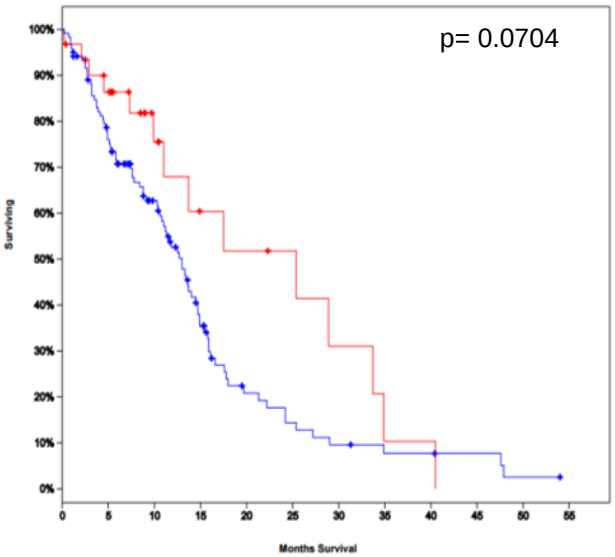

-- Cases with Alterations in Query Genes

-- Cases without Alterations in Query Genes

Figure 3.8. Analysis of combined gene alterations can improve prognostic prediction. A) Representative Kaplan-Meier survival curves of the combined grade 2 and 3 glioma cohort. The combined analysis of genes individually predictive of a worse survival also associated mRNA upregulation with poor survival in a multivariate analysis. n=527. B) Representative Kaplan-Meier survival curves of the grade 4 glioblastoma cohort. Expression of genes associated with poor prognosis in grade 2 and 3 tumours had improved prognostic value in grade 4 tumours through multivariate analysis and associated with poor survival. The p-value did not reach significance due to the small number of tumours with mRNA upregulation alterations. n=151. C) Representative Kaplan-Meier survival curves of the grade 4 glioblastoma cohort. Expression of genes associated with good prognosis in grade 2 and 3 tumours had improved prognostic value in grade 4 tumours through multivariate analysis and associated with good survival. The p-value did not reach significance due to the small number of tumours with mRNA upregulation alterations. n=151. Genes analysed: A) and B); PLIN2, PLIN3, PNPLA2, CD36, HILPDA, MAP1LC3A, ETNK1, PTDSS1. CEPT1 and CPT2 were excluded from this analysis as the query function recognised predominantly mRNA down-regulation alterations. C); PLIN1, PLIN4, PNPLA3, PNPLA4, ACACA, FASN, SLC25A20. Survival curve analysis was performed in all cases using the TCGA cBioPortal query function; statistical analysis performed using the log-rank test.

3.3. Discussion

3.3.1. Introduction

Lipid droplets are an important area of tumour metabolism in many cancers, including gliomas, where they are clinically associated with poor survival and higher tumour grade (94,240,241). However, despite characterisation of lipid droplet metabolism in other tumours, the glioma-specific lipid droplet metabolic pathways remain poorly characterised. Through survival and correlation analysis of clinical tumour data, we identified possible pathways involved in glioma lipid droplet metabolism which could be biologically investigated. Moreover, tumour progression presents a major challenge in glioma management and we therefore investigated changes in gene expression across clinical grades, uncovering possible associations with the tumour progression pathway.

3.3.2. Gene expression of key metabolic pathways and lipid droplet-associated proteins is associated with survival in the combined grade 2 and 3 glioma cohort

The separation of the gene list into three groups indicated a number of genes with possible effects on survival in grade 2 and 3 gliomas and provided an initial indication of which genes may be pro- or anti-survival (Figure 3.1.). The association of the lipid droplet-associated proteins PLIN2 and PLIN3 with poor survival tumours suggests that increased lipid droplet presence is a negative indicator of survival. Indeed, this is supported by Wilson et al. (241) who observed that increased presence of lipid droplets was a negative indicator of survival *in vivo*. Hypoxia is also an established marker of poor prognosis (252,253) and is known to increase lipid

droplet accumulation (123). Therefore, the association of HILPDA with poor survival tumours further suggests that increased lipid droplet presence in conjunction with hypoxia is an indicator of poor survival. Interestingly, autophagy and the lipase ATGL were also associated with poor prognosis and both have established roles in lipid droplet metabolism (179,194). Although autophagy also has pro- and anti-survival effects (170,171) which may obscure its contribution to survival in grade 2 and 3 gliomas, it has a well-established role in lipid droplet breakdown in many cell types (152,179,184,185,188). Similarly, several genes involved in phospholipid synthesis, a possible fate for lipid droplet derived lipids, were also associated with poor survival suggesting an association between lipid droplets and membrane synthesis in gliomas. However, these enzymes are also vital to proliferation and the impact of increased expression may be independent of lipid droplets.

In contrast, high expression of several genes linked to lipid droplet metabolism was associated with good survival in grade 2 and 3 gliomas (Figure 3.1.). High expression of the lipid droplet-associated protein PLIN1 was associated with tumours with a better survival and, in contrast with PLIN2 and PLIN3, is thought to promote lipid droplet breakdown by cytoplasmic lipases (115). Moreover, *de novo* fatty acid synthesis is known be involved in lipid droplet metabolism (136,164) and be associated with poor survival (156,157) in other tumours, yet expression of ACACA and FASN, which are vital in *de novo* fatty acid synthesis, was associated with a better survival in grade 2 and 3 gliomas. Similarly, expression of PNPLA3, which encodes an alternative lipase (254), was also associated with good survival. This suggests that different metabolic pathways, for example a preference for autophagy and ATGL as opposed to *de novo* lipogenesis, may influence the tumour phenotype and prognosis. Indeed, the importance of the expression of these genes in glioma

biology and survival endorses the further investigation of the represented pathways in lipid droplet metabolism using biological models.

Notably, several genes representing other important metabolic pathways were not associated with survival in grade 2 or 3 gliomas (Figure 3.1.) including the metabolism of cholesterol, a known component of lipid droplets (255). Genes encoding lipases responsible for the subsequent steps of lipolysis post-ATGL were also not associated with survival further highlighting PNPLA2 specifically as a gene of interest. The majority of genes in this final group, with the exception of a CD36, PLIN4 and CPT2, were excluded from the analysis to focus on genes with more significant associations to glioma survival. CD36 expression was associated with both poor and good survival dependent upon survival time indicating prognostic prediction may be altered in long term survivors. This is of particular interest as patient survival was monitored for up to 16.5 years, far longer than standard glioma studies in which CD36 would have been associated with poor survival. Moreover, uptake of exogenous serum lipids is an important pathway in lipid droplet metabolism in many cancers (123,152), justifying its inclusion for further analysis. In summary the survival analysis of grade 2 and 3 gliomas generated an edited list of genes, representative of several metabolic pathways, which may impact glioma lipid droplet metabolism and survival.

3.3.3. The prognostic value of gene expression varies between grade 2 and 3 gliomas

As tumours progress from grade 2 to 3 the requirements for continued growth and survival change and therefore gene expression is altered correspondingly. In the

separated grade 2 and 3 cohorts several genes were associated with survival (Figure 3.2.) and mirrored the prognostic prediction observed in the combined data set. However, expression of several genes such as PNPLA3 and HILPDA was not associated with survival in grade 2 or 3 tumours, despite prior association with survival in the combined grade 2 and 3 cohort. This suggests key differences in the biological importance of gene expression between grades 2 and 3. Nevertheless, the increased number of tumours in the combined cohort provides further statistical power in the significant separation of survival curves.

The altered expression of numerous genes between grade 2 and 3 tumours suggests the expression of these pathways may be altered in response to the different metabolic and survival requirements of each clinical grade. Moreover, it is possible that altered expression of these pathways at each clinical grade may influence the tumour progression process, rather than be a response to tumour progression. Nevertheless, lipid droplets have been associated with multiple tumour grades (94,240,241) suggesting that, although expression of each gene and pathway may change, lipid droplet metabolism remains fundamental in glioma biology.

3.3.4. Gene expression cannot separate significantly different survival curves in grade 4 gliomas for the majority of the investigated genes

In contrast to grade 2 and 3 tumours, gene expression within the defined gene set provided significant biomarkers of survival at grade 4 in very few genes (Figure 3.3.). Separation of survival curves is particularly uncommon in grade 4 gliomas due to their steep nature, emphasising the importance of any distinguishing genes. Notably, MAP1LC3A is a vital protein in autophagy, which is frequently investigated in GBM

(172), and was associated with poor survival at grade 3 and 4 implying increased importance in higher grade tumours. Similarly, expression of the phospholipid synthesis gene CEPT1 was significantly associated with survival in grade 2 and 3 tumours and neared significance in grade 4 tumours. Phospholipid synthesis is an important component of proliferation and expression of these genes can be expected to impact glioma biology across tumour grades.

However, expression was not associated with survival in the majority of investigated genes in grade 4 tumours despite previous association with survival in grade 2 and 3 tumours. This could be due to these genes having decreased importance in grade 4 tumours, due to significant metabolic alterations, or differences between the combined grade 2 and 3 tumour cohort and the grade 4 tumour cohort. The grade 4 cohort was comprised predominantly of primary GBMs whereas grade 2 and 3 tumours are believed to precede secondary GBM and share several key mutations and characteristics. This important variable between the two cohorts could influence whether gene expression is associated with survival across all three grades. Alternatively, the loss of prognostic indication from gene expression at grade 4 could provide further evidence regarding an association of gene expression with tumour progression. GBM is the final stage of tumour progression and therefore gene expression would no longer separate survival curves by the probability of progression. If these genes become statistically less significant in survival in grade 4 tumours or represent the difference between primary and secondary GBM then gene expression should not alter sequentially between grade 2, 3 and 4 tumours. In contrast, if these genes are associated with the tumour progression process then expression should be further altered in grade 4 tumours.

3.3.5. Gene expression alters with clinical grade indicating the importance of these pathways in grade 4 glioma biology despite not being associated with survival

In many cases gene expression was altered sequentially across tumour grades with the greatest difference frequently observed at grade 4 (Figure 3.4.), matching the clinical presentation of grade 4 tumours. As discussed in section 3.3.4, this provides evidence that these genes continue to be important at grade 4 and may be associated with glioma progression from low to high grade. Interestingly, when combined with the survival data, genes associated with poor survival had an increased expression in higher grade tumours with an inverse relationship observed in genes associated with good survival. For example high expression of the autophagy gene MAP1LC3A was associated with poor survival in grade 3 and 4 tumours and expression was significantly increased in grade 4 tumours. Therefore, tumours with high MAP1LC3A expression resemble higher grade tumours in aspects of molecular phenotype, perhaps suggestive of a more severe phenotype with worse prognosis. Conversely, high expression of the *de novo* fatty acid synthesis enzyme FASN was associated with good survival in grade 2 and 3 tumours and had decreased expression in higher grade tumours. This suggests that tumours with high FASN expression maintain aspects of a lower grade phenotype with a better prognosis. Alterations in the expression of these genes may be associated with the process of tumour progression as cells adapt to the increased metabolic demand, microenvironment and altered phenotypes of higher clinical grades. Moreover, gene expression may indicate tumour aggressiveness within each grade and therefore understanding the pattern of gene expression may predict tumour severity or the probability of tumour progression.

3.3.6. Expression of genes known to be involved in lipid droplet metabolism is important in gliomas across clinical grades and is associated with survival in grade 2 and 3 gliomas

Importantly the genes investigated represent key metabolic pathways and proteins that could represent essential changes in tumour biology, influencing the tumour phenotype. Several genes representing lipid droplet proteins, autophagy proteins, ATGL, phospholipid synthesis enzymes and mitochondrial lipid uptake transporters were associated with poor survival and higher grade tumours (Figures 3.1. to 3.4.). Indeed, in a study using immunohistochemistry, Kohe et al. (240) noted that the lipid droplet-associated protein adipophilin, encoded by PLIN2, was increased in higher grade gliomas. We have also demonstrated an association between genes encoding the lipid droplet-associated protein perilipin 1, the PNPLA3 lipase and key *de novo* fatty acid synthesis enzymes with lower grade tumours and good survival (Figures 3.1. to 3.4.). Therefore, we suggest that tumour lipid metabolism is altered as tumours progress from grade 2 to 4 and that gene expression may indicate prognosis and tumour progression. Increased *de novo* fatty acid synthesis may therefore indicate a lower grade tumour phenotype or that increased activity of this pathway has tumour suppressive activity in high grade gliomas. In contrast, increased lipid droplet presence, autophagy and ATGL activity may indicate an increased probability of progression and a higher grade tumour phenotype. Therefore, the metabolic pathways that predominate may drive progression and aggressiveness across the glioma grades and indicate important metabolic requirements for high grade glioma. Moreover, these genes were selected in relation to lipid droplet metabolism and may indicate the glioma-specific lipid droplet metabolic pathways, requiring further biological investigation.

3.3.7. “Grade 3 like” gene expression in grade 2 gliomas characterises a poor prognostic group suggesting an association with tumour progression

The role of the investigated genes across tumour grades also presents an opportunity to better understand the process of tumour progression from lower clinical grades. Therapy efficacy is significantly improved in low tumour grades and the aggressiveness of treatment regimens can be altered depending upon the chance of progression making this a valuable clinical tool. We therefore aimed to use these genes to predict “grade 3 like” tumours in the grade 2 cohort with a worse prognosis and therefore a higher chance of progression (Figure 3.5.). The increased expression of genes representing pathways, such as lipid droplets and ATGL in “grade 3 like” tumours associated with poor survival and correlated with the previous survival analysis. Conversely, expression of genes representing pathways such as *de novo* fatty acid synthesis was low in the “grade 3 like” tumours and was associated with poor survival, further correlating with the previous survival analysis. Therefore, the poor survival, higher grade phenotype of a “grade 3 like” gene expression profile in grade 2 tumours is characterised by increased expression of genes representing lipid droplets and ATGL and decreased expression of genes representing *de novo* fatty acid synthesis. Moreover, poor survival tumours have a higher probability of progression and therefore the expression profile of “grade 3 like” tumours combined with our previous survival analysis suggests an association with tumour progression.

As expected, not all genes predict a “grade 3 like” survival phenotype. However, several of these genes predominantly associate with survival in grade 3 and 4 tumours suggesting that these may be a later event in the process of tumour progression and emphasising the importance of appropriate gene selection. Indeed,

the separation of survival curves using PLIN2, HILPDA and MAP1LC3A expression was limited by the small number of tumours with “grade 3 like” expression indicating a large difference in gene expression between grade 2 and 3 tumours. Further prediction of grade 3 tumours with a “grade 4 like” phenotype could indicate the importance of this gene set in each tumour grade and the overall biological significance of alterations in expression. However, prediction of progression from grade 3 to 4 was impractical due to the large difference between grade 3 and 4 gene expression observed in many genes.

Moreover, these data represent the gene expression of different tumours across clinical grades. Assessing follow-up data from each tumour as gene expression is altered during progression to higher grades could clarify the difference between grade-specific phenotypes and the process of tumour progression. However, these data are difficult to obtain and may be skewed by the effects of increasingly aggressive therapies used in higher grade tumours. We therefore suggest that selected gene expression can offer useful insight into the progression of tumours between tumour grades.

Although this investigation is limited to gene expression, the pathways represented by these tumours provide an indication of the core tumour biology and may influence the tumour progression process. The biological changes underlying the altered gene expression remain to be understood. However, through this we may better predict patient survival and tumour progression and adapt treatment regimens appropriately.

3.3.8. IDH1 mutation is linked to expression of selected genes

Mutations in genes such as IDH1 and TP53 have become established biomarkers in several glioma sub-groups (9). Although no association between gene expression and TP53 mutation was observed in this study, the prognostic indication of genes such as PLIN2, MAP1LC3A, ACACA and FASN correlated with the prognostic indication and mutational status of IDH1 (Figure 3.6.). IDH1 mutation can significantly alter cell metabolism, although a mechanistic link to lipid droplets is not known. Notably, several genes with significant prognostic value in our survival analysis remain unaffected by IDH1 mutational status suggesting that other factors are involved. Indeed, the interlinked nature of cellular metabolism may mean that the impact of changes in a given metabolic pathway affect the activity of other metabolic pathways, such as those represented by these genes. Therefore, the association of several of these genes with IDH1 mutational status requires further investigation but may not indicate a mechanistic link to lipid droplets.

Interestingly, this association with IDH1 mutational status further supports the importance of these genes across all glioma grades. As discussed in Section 3.3.4, it could be suggested that gene expression did not associate with survival in grade 4 tumours as this cohort is comprised predominantly of primary GBM tumours whereas grade 2 and 3 gliomas are more associated with secondary GBM. However, in this case, gene expression would be associated with IDH1 mutant tumours whereas expression of many genes was instead associated with IDH1 wildtype tumours suggesting that these genes are relevant to all GBMs.

3.3.9. Significant correlations are found between genes with prognostic indications

The ability to predict survival and tumour progression at different tumour grades presents an important clinical opportunity, but requires further investigation. Genes can act independently as individual biomarkers or be interlinked and correlated. They can also define delineated groups of tumours containing characteristic genetic alterations synergistically affecting tumorigenesis and tumour progression. The positive correlation of genes associated with similar prognostic indications and the negative correlation between these two groups suggests these genes are not independent biomarkers and are, instead, interlinked by a shared attribute (Figure 3.7.). Indeed, these genes were selected due to possible associations with lipid droplet metabolism and correlate with lipid droplet-associated proteins. Whilst the involvement of the pathways represented by these genes in lipid droplet metabolism could be tested with pathway analysis software, investigation using biological models would provide more definitive proof.

Many cancer types can be classified into clear groups and sub-groups defined by the expression of characteristic genes and mutations and often present a specific phenotype such as decreased survival. However, these gliomas could not be classified into sub-groups defined by expression of these genes, as observed in the cluster analysis (Figure 3.7.). Therefore, we suggest that alterations in these genes represent an important part of glioma biology in all cases and that expression is altered in a continuous process as tumours grow and progress. Moreover, through proper understanding of these alterations, gene expression may predict the tumour severity and progression at a given time point.

The gene expression correlations were supported using the TCGA cBioPortal query function which further highlighted several important genetic alterations (Figure 3.7.). Alterations in PLIN2 co-occurred with alterations in PLIN3, HILPDA and CD36 supporting the importance of lipid droplet-associated proteins and linking them to fatty acid uptake. Similarly, the co-occurrence of mRNA alterations in ACACA and FASN suggests their importance in gliomas is due to the activity of the *de novo* fatty acid synthesis pathway. Additionally the co-occurrence of MAP1LC3A and PTDSS1 links autophagy with membrane production, although the reason for the co-occurrence of alterations in PLIN1, PLIN4, PNPLA4 and SLC25A20 is currently unclear.

Although this multivariate analysis did not support all significant alterations observed through the Spearman's rank analysis, the TCGA cBioPortal query function is more conservative. An mRNA z-score cut-off was used to determine tumours with mRNA upregulation as opposed to consideration of the whole tumour population with Spearman's rank correlation analysis. Therefore, correlations observed through both methodologies have increased validity.

Notably, associations in gene expression correlate with the prognostic indications of the univariate survival analysis and several of these correlations were also observed in the grade 4 tumour cohort (Figure 3.7.), further supporting the validity of these findings and the importance of these pathways in glioma biology. Therefore, the expression of genes with prognostic importance in grade 2, 3 and 4 gliomas may represent important and interlinked stages in adaptation through tumour progression and could represent a diagnostic opportunity.

3.3.10. Combined gene sets show higher levels of prognostic prediction in grade 4 gliomas

Despite no separation of survival curves for many genes in grade 4 tumours through univariate analysis, the correlated gene sets improved prognostic prediction (Figure 3.8.). Although the survival curves did not significantly separate, this may be due to the low number of cases classified as having mRNA up-regulation by the mRNA z-score cut-off. However, a lower cut-off could not be used as this identified an increased number of contradictory mRNA down-regulation alterations. Therefore, these gene sets require further testing on alternative data sets. The separation of survival curves remains difficult in grade 4 gliomas and, whilst multivariate expression of these genes is unlikely to offer a clinical prognostic tool or alter the current glioblastoma treatment regimens, it further advocates investigation into the biological significance of these pathways.

3.3.11. Summary

We have defined a list of genes associated with survival in grade 2, 3 and 4 gliomas. The prognostic value of these genes varies between tumour grades and indicates that gene expression may be altered in response to higher clinical grade and tumour aggressiveness. Moreover, we suggest that gene expression is important in tumour progression and can predict poor survival “grade 3 like” tumours in a grade 2 tumour cohort. The correlation of gene expression in genes with similar prognostic indications suggests that altered gene expression is not limited to a tumour sub-group but occurs across all gliomas throughout progression. Indeed, the represented pathways can improve prognostic prediction in grade 4 tumours. We further suggest

that the pathways, represented by gene expression, are involved in or altered by the tumour progression process and that we may predict progression through understanding the changing involvement of these pathways in gliomas across the tumour grades. Although this hypothesis is limited as it does not follow-up gene expression after tumour progression, the consistent association of gene expression with survival and tumour grade suggests a possible role in tumours undergoing progression. Therefore, whilst this area requires greater investigation, the possibility of progression prediction represents an interesting clinical opportunity.

Expression of specific genes was associated with indicators of poor or good prognosis repeatedly throughout univariate and multivariate analysis. Genes representing adipophillin, TIP47, ATGL, autophagy and phospholipid synthesis were consistently associated with poor survival, high grade and progression indicating that these proteins are important in glioma tumour biology and constitute possible therapeutic targets. In contrast, genes representing perilipin 1, the PNPLA3 lipase and *de novo* fatty acid synthesis enzymes were associated with good survival, low tumour grade and less progressive tumours indicating a possible shift in metabolism as tumours progress. The correlations between these pathways may suggest a common feature such as a unifying area of metabolism. Indeed, these pathways are known to be important in lipid droplet metabolism (136,152,179,184-188,197) in many other cancers and lipid droplets have clear importance in glioma biology across tumour grades (240). However, lipid droplet metabolism remains poorly understood in gliomas and therefore these pathways and proteins form the basis for further biological investigation.

Chapter 4

Metabolic pathways in GBM lipid droplet metabolism

4.1. Introduction

Lipid droplets are important aspects in many cancers and increased levels are associated with clinical features such as poor survival and clinical grade (94,240,241). However, the underlying metabolic pathways in gliomas remain poorly understood. In many cancers, lipid droplet production occurs through increased uptake of exogenous lipids, *de novo* fatty acid synthesis or a combination of both pathways (123,136,152) whilst lipid droplet breakdown occurs through the combined or independent action of autophagy or cytoplasmic lipases (152,184-188,197). Increased lipid droplet uptake has been suggested to affect hypoxic lipid droplet production in gliomas (123), although the roles of *de novo* fatty acid synthesis, autophagy and cytoplasmic lipases in glioma lipid droplet metabolism are yet to be fully explored. In Chapter 3 we demonstrated that expression of exogenous lipid uptake, autophagy and cytoplasmic lipase genes was associated with poor prognosis and was an important aspect of glioma biology at higher clinical grades. Given this evidence, it is important to investigate the roles of lipid droplets in the biology of gliomas and try to establish mechanistic links between these intracellular organelles and the malignant phenotypes observed in GBM.

Choice of cell model is, as always, important, as most cell lines represent grade 4 tumours due to the difficulty in growing cells derived from lower grade tumours. Cell lines from GBM are therefore used for the majority of studies into glioma biology, and are used in this investigation.

In this chapter we investigate lipid droplet metabolism using GBM cell lines. Through confocal microscopy, flow cytometry and NMR-based methods we explore the

metabolic pathways involved in lipid droplet production and breakdown and indicate possible applications for lipid droplets in GBM.

4.2. Results

4.2.1. Uptake of exogenous serum lipids is important in normoxic lipid droplet production.

Exogenous serum provides an abundant source of lipids and fatty acids which can be imported via membrane transport proteins (146,147). Activated charcoal was used to produce a de-lipidated serum to culture cells in the absence of this lipid source. The LDQ of cells grown in standard or de-lipidated serum was assessed over 5 GBM cell lines using confocal microscopy and flow cytometry. Qualitative analysis of confocal microscopy images revealed that incubation in de-lipidated serum decreased LDQ in the T98G and U87.1 cell lines (Figure 4.1.A.). This was supported by a negative percentage shift in the population FITC signal intensity in all 5 cell lines when incubated in de-lipidated serum (Figure 4.1.B). Therefore, lipid droplet production is decreased in the absence of the exogenous serum lipid pool. Moreover, exogenous C16 BODIPY, an extracellular fatty acid, was observed within lipid droplets (Figure 4.1.C.). This demonstrated the presence of an exogenously supplied fatty acid in lipid droplets and further supports exogenous serum lipids as an important source in lipid droplet production.

A

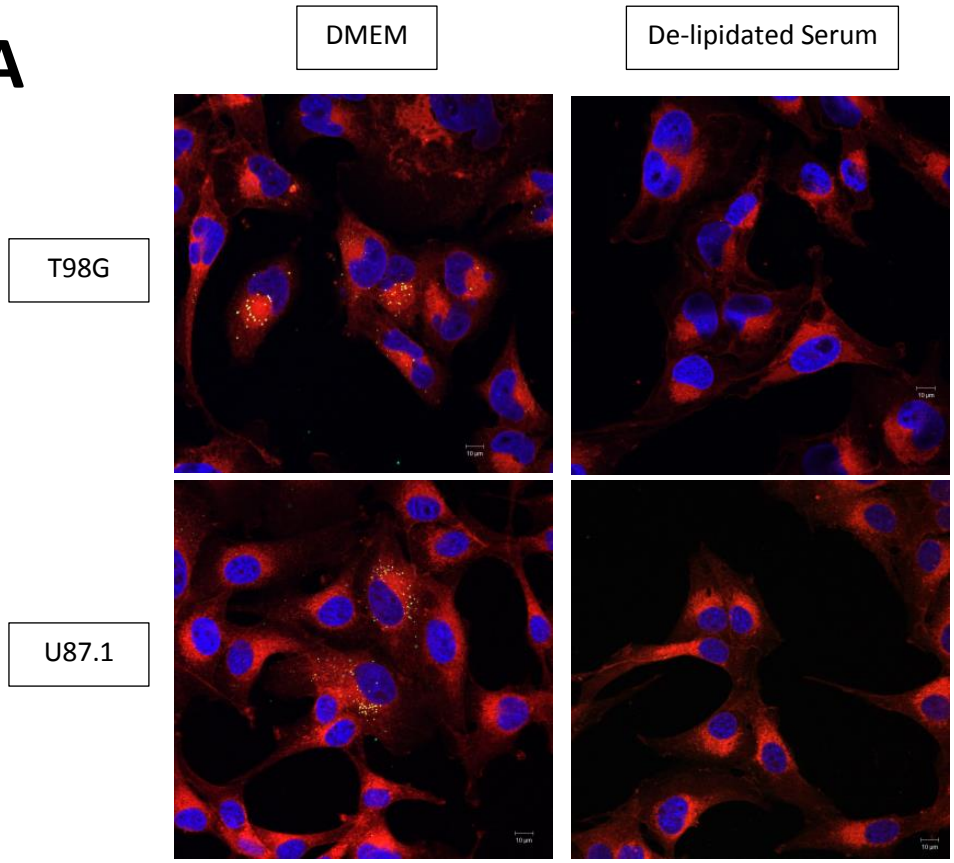
DMEM
De-lipidated Serum
T98G
U87.1

B

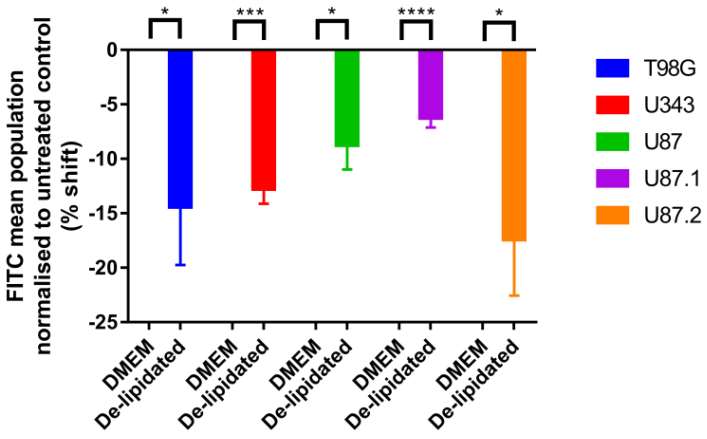
FITC mean population normalised to untreated control (% shift)
0
-5
-10
-15
-20
-25
*
***
*
****
*
DMEM
De-lipidated
T98G
U343
U87
U87.1
U87.2

C

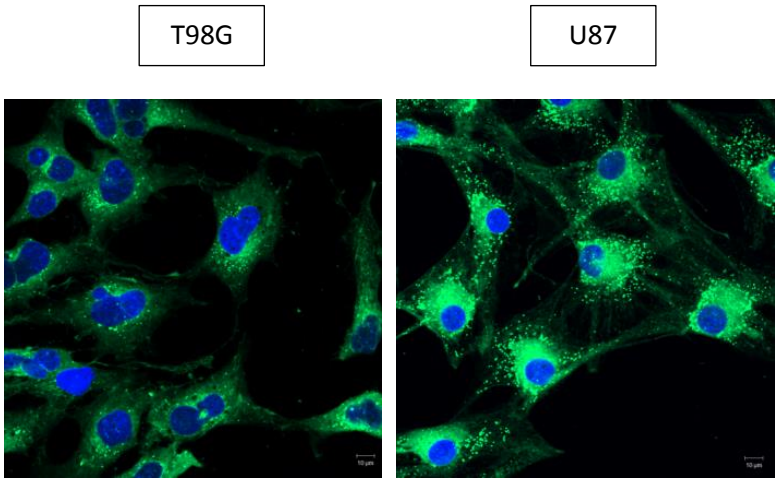
T98G
U87

Figure 4.1. Uptake of exogenous serum lipids is important in lipid droplet production in normoxia. A) Confocal microscopy of nile red stained T98G and U87.1 cells incubated in DMEM or de-lipidated serum media in normoxia for 72 hours. Incubation in de-lipidated serum decreased LDQ. B) LDQ was decreased in cells incubated in de-lipidated serum, as observed by flow cytometry, in all five cell lines. Data shown as mean ±SEM, representative of several independent experiments (U343, U87, U87.2 n=3; T98G, U87.1 n=4), analysed with an unpaired t-test; *p<0.05, **p<0.01, ***p<0.001, ****p<0.0001. C) Confocal microscopy images of T98G and U87 cells incubated with C16 BODIPY for 30 minutes prior to 8 hours HBSS incubation. C16 BODIPY was observed within lipid droplets.

4.2.2. ATGL may impact lipid droplet production through cell membrane unsaturated fatty acid release.

ATGL is the rate-limiting lipase in the hydrolysis of fatty acids from TAGs (189) and has been previously implicated in lipid droplet metabolism in other cell types (174,194). Confocal microscopy and flow cytometry were used to investigate the effect of the competitive and selective ATGL inhibitor atglistatin on LDQ across the 5 cell lines. Following atglistatin treatment LDQ was observed to be decreased in the U87 and U87.2 cell lines (Figure 4.2.A). This was further supported in all 5 cell lines by a negative percentage shift in the FITC signal intensity following atglistatin treatment (Figure 4.2.C.), suggesting a common role for ATGL in lipid droplet production. Moreover, the atglistatin-induced decrease in LDQ was enhanced in HBSS as observed with confocal microscopy and flow cytometry (Figure 4.2.B. and 4.2.D. respectively) reflecting flexibility in the activity of ATGL in response to metabolic need.

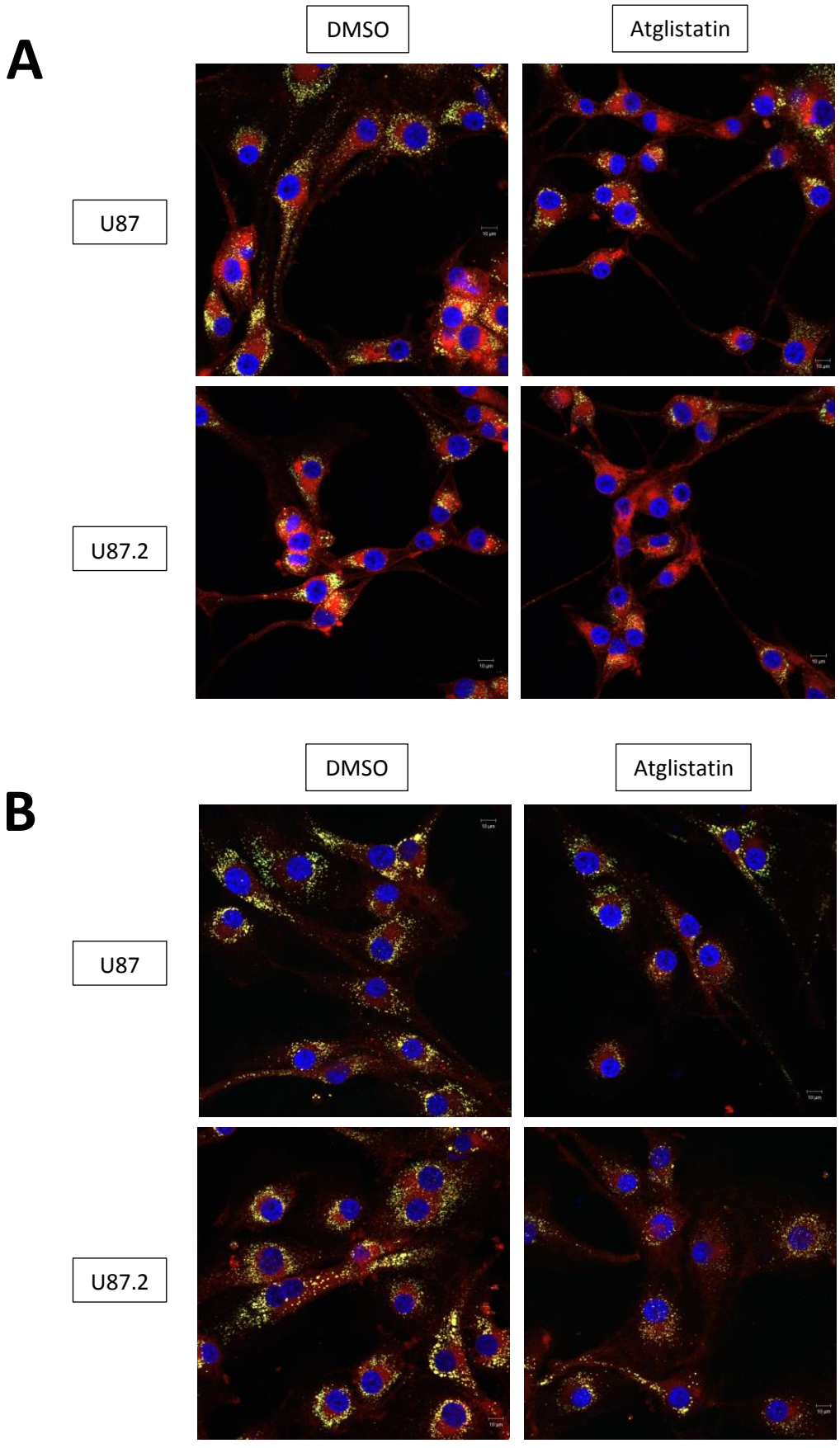
A
DMSO
Atglistatin
U87
U87.2
B
DMSO
Atglistatin
U87
U87.2

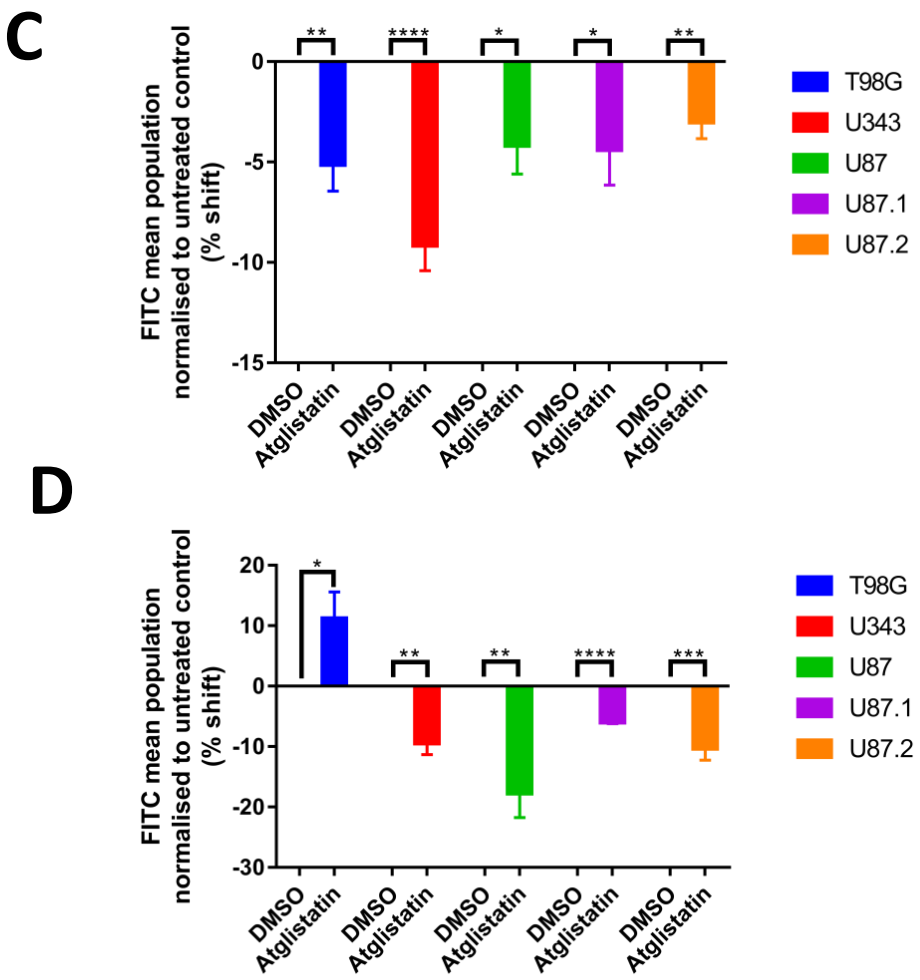

Figure 4.2. ATGL plays a role in lipid droplet production in fed and starvation conditions. A) Confocal microscopy of nile red stained U87 and U87.2 cells incubated with DMSO or atglistatin for 8 hours in DMEM. Atglistatin treatment decreased LDQ. B) Confocal microscopy of nile red stained U87 and U87.2 cells incubated with DMSO or atglistatin for 8 hours in HBSS. Atglistatin treatment in HBSS enhanced the observed decrease in LDQ. C) and D) Flow cytometry quantification of the decrease in LDQ observed with atglistatin treatment in DMEM (C) and HBSS (D) across all five nile red stained cell lines with the exception of T98G in HBSS. Data shown as mean ±SEM, representative of several independent experiments (T98G n=3; U343, U87.1 n=4; U87, U87.2 n=5), analysed with an unpaired t-test; *p<0.05, **p<0.01, ***p<0.001, ****p<0.0001.

ATGL is known to localise at the cell membrane as well as lipid droplets (189) and associate with proteins important to lipid droplet production such as FABPs (192). Therefore, a role in the release of fatty acids from the cell membrane for transport to

lipid droplets was investigated using fluorescent labelled fatty acids and NMR HRMAS. Atglistatin treated cells had an increased accumulation of the C16 BODIPY saturated fatty acid in their membranes in both normoxia and hypoxia compared to DMSO controls (Figure 4.3.A.), implicating ATGL in the metabolism of saturated lipids at the cell membrane. No change in membrane staining was detected with the C11 BODIPY unsaturated fatty acid; however, observation of this effect is limited by the lower stain intensity of C11 BODIPY and the oxidation-induced colour change observed in hypoxia (Figure 4.3.B.). Notably, the concentration of unsaturated fatty acid groups in lipid droplets was decreased in atglistatin treated cells when assessed by HRMAS NMR (Figure 4.3.C.). This was accompanied by a slight increase in the concentration of saturated lipid groups (Figure 4.3.D). This trend suggests ATGL activity can alter the concentration of unsaturated lipids in lipid droplets. However, statistical significance was not achieved, most likely due to challenges in accurately quantifying the lipid peaks, which were at low levels. The proportion of saturated and unsaturated lipid groups in lipid droplets represented as a percentage of total lipid concentration indicated that unsaturated lipid groups decreased in lipid droplets following atglistatin treatment in the U87 cell line (Figure 4.3.E.). The decreased unsaturated lipid group concentration in the atglistatin treated samples was mainly due to the decreased CH2CH=CH concentration as shown in the example HRMAS spectra (Figure 4.3.F.). Taken together, this data further supports a role for ATGL in altering the concentration of unsaturated lipids in lipid droplets, potentially through the release of unsaturated fatty acids from the cell membrane.

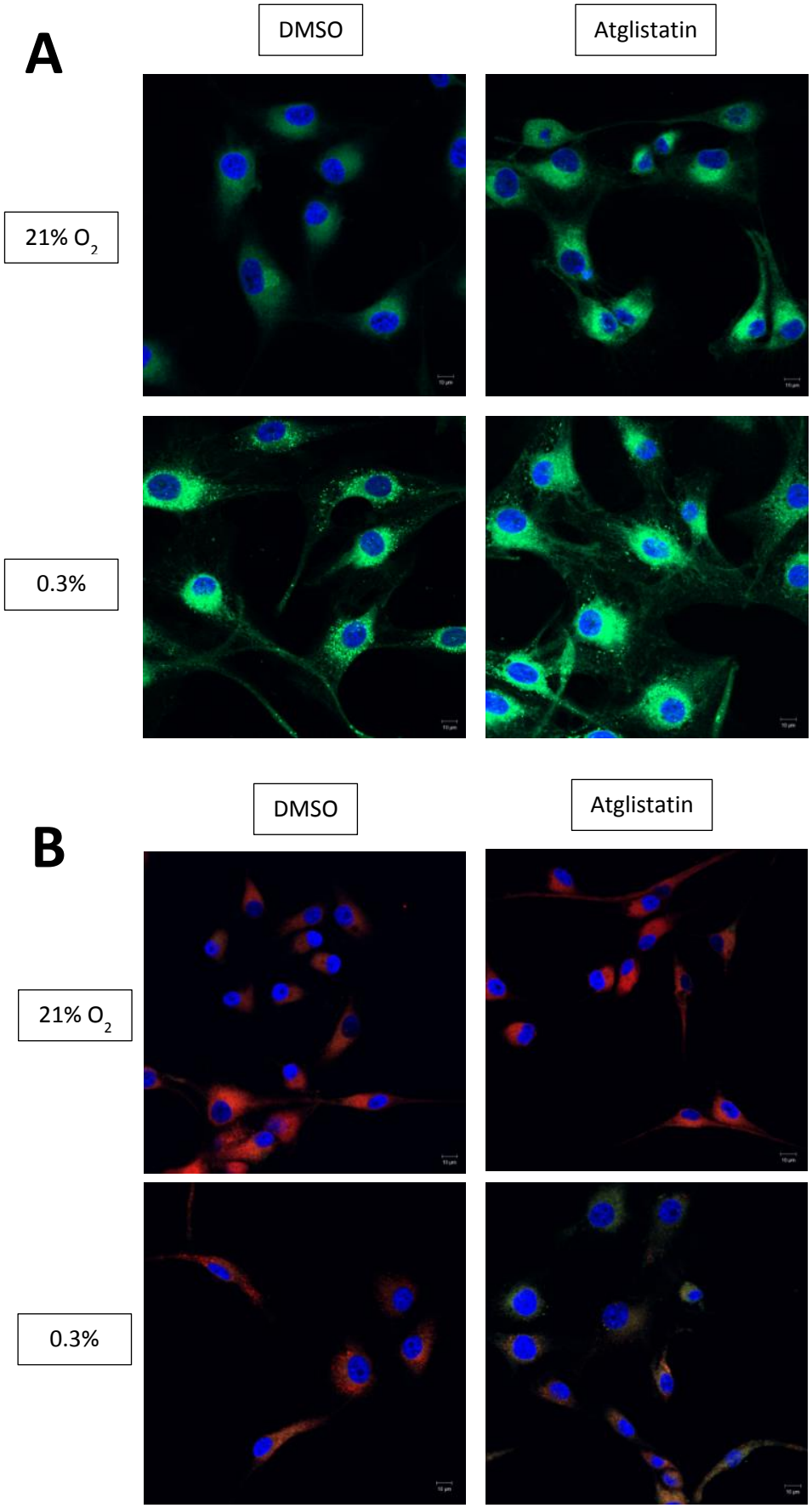
A
DMSO
Atglistatin
21% O2
0.3%
B
DMSO
Atglistatin
21% O2
0.3%

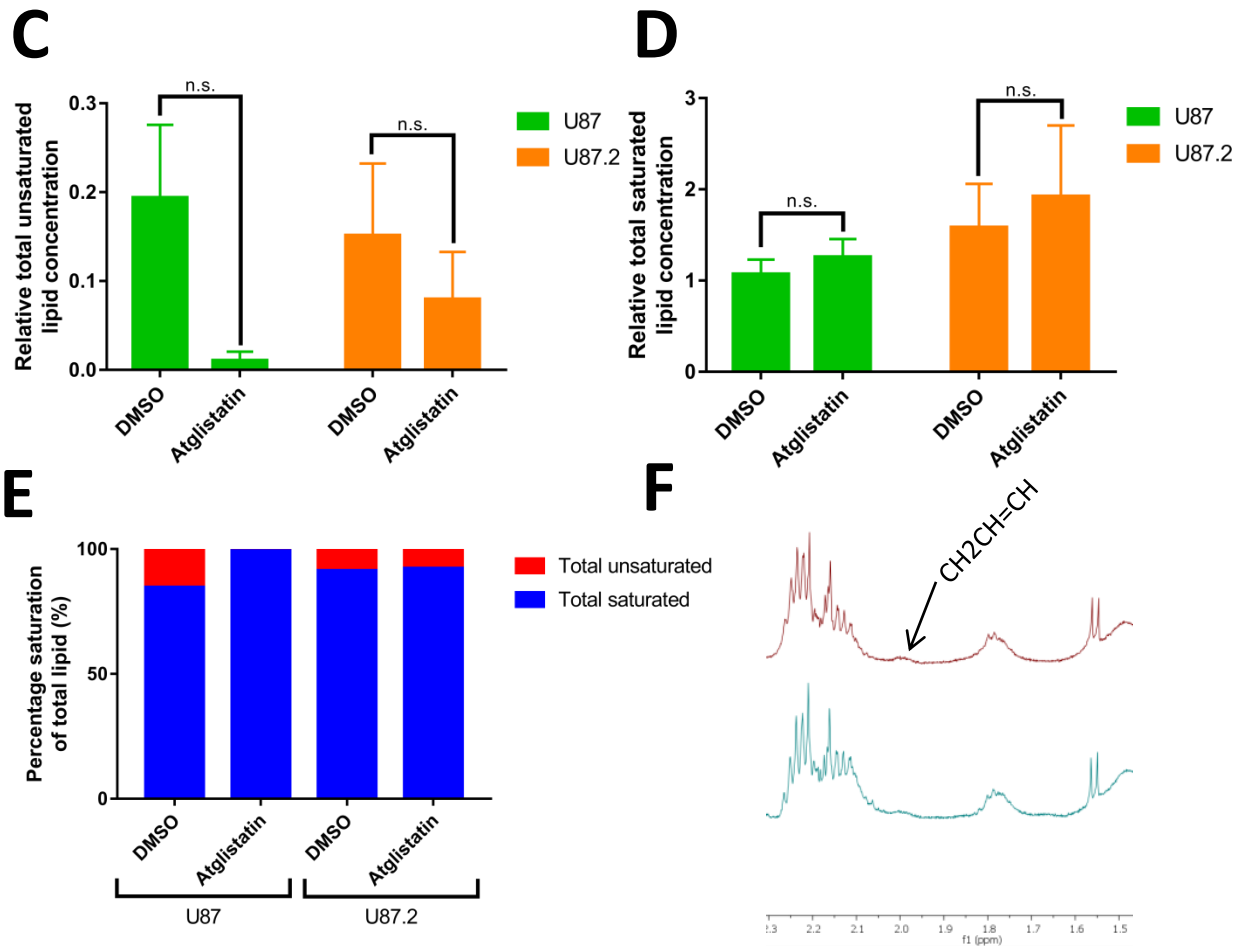

Figure 4.3. ATGL may be important in the release of fatty acids, particularly unsaturated fatty acids, from the membrane for transport to lipid droplets. A) Confocal microscopy images of U87 cells incubated with C16 BODIPY prior to 30 minute atglistatin treatment in HBSS. Atglistatin treated cells had an increased accumulation of C16 BODIPY in their membranes in both oxygen concentrations compared to the DMSO-treated controls. B) Confocal microscopy images of U87 cells incubated with C11 BODIPY prior to 60 minute atglistatin treatment in HBSS. There was no visible difference in C11 BODIPY membrane accumulation with atglistatin treatment in normoxia. The lipid oxidation-induced colour change observed in hypoxic atglistatin-treated cells further hindered visualisation of potential lipid accumulation. C) and D) Total unsaturated (C) and saturated (D) mobile lipid groups in U87 and U87.2 cells treated with DMSO or atglistatin for 8 hours, as measured by HRMAS NMR. Atglistatin decreased the quantity of unsaturated fatty acid groups and increased the saturated fatty acid groups in both U87 and U87.2 cells. Due to high variability in HRMAS lipid peak assignment, significance could not be reached within this sample size (n=3); n.s. p>0.05. Lipid group concentrations were normalised to the total metabolite concentration of each sample. E) Representation of saturated and unsaturated lipid group concentrations as a proportion of total lipid group concentration in U87 and U87.2 cells. Atglistatin treatment decreased the proportion of total lipid which is unsaturated in the U87 cell line but not the U87.2 cell line. F) Representative HRMAS spectra demonstrating the decreased CH2CH=CH unsaturated lipid group peak size in the atglistatin (bottom) treated cells compared to DMSO (top) treated cells. Spectra includes only the 1.5 – 2.3 ppm region of the spectra.

4.2.3. *De novo* fatty acid synthesis may impact lipid droplet production; however, pharmacological inhibition may induce cell stress, confounding the effect.

De novo synthesis of fatty acids can provide a dynamic source for the production of lipid droplets (136,164,165). The importance of *de novo* fatty acid synthesis in lipid droplet production was investigated with BPTES, a selective GLS1 inhibitor, and orlistat, a non-selective FASN inhibitor. Analysis of confocal microscopy images suggested that there was no effect from either drug on LDQ (Figure 4.4.A.), although changes were observed when assessed using flow cytometry (Figure 4.4.B.). BPTES treatment decreased the FITC signal intensity in the U87 cell line suggesting glutamine may be a pre-cursor for lipid droplet production. However, BPTES treatment increased the FITC signal intensity in the T98G cell line emphasising the effect of cellular stress upon LDQ. As this was only observed in one cell line, this suggests that the glutamine contribution to lipid droplets may be dependent on the genetic background. Orlistat treatment increased the FITC signal intensity observed in both cell lines. However, orlistat has previously been suggested to have off-target effects, suggesting that this effect could be induced through a non-FASN mechanism.

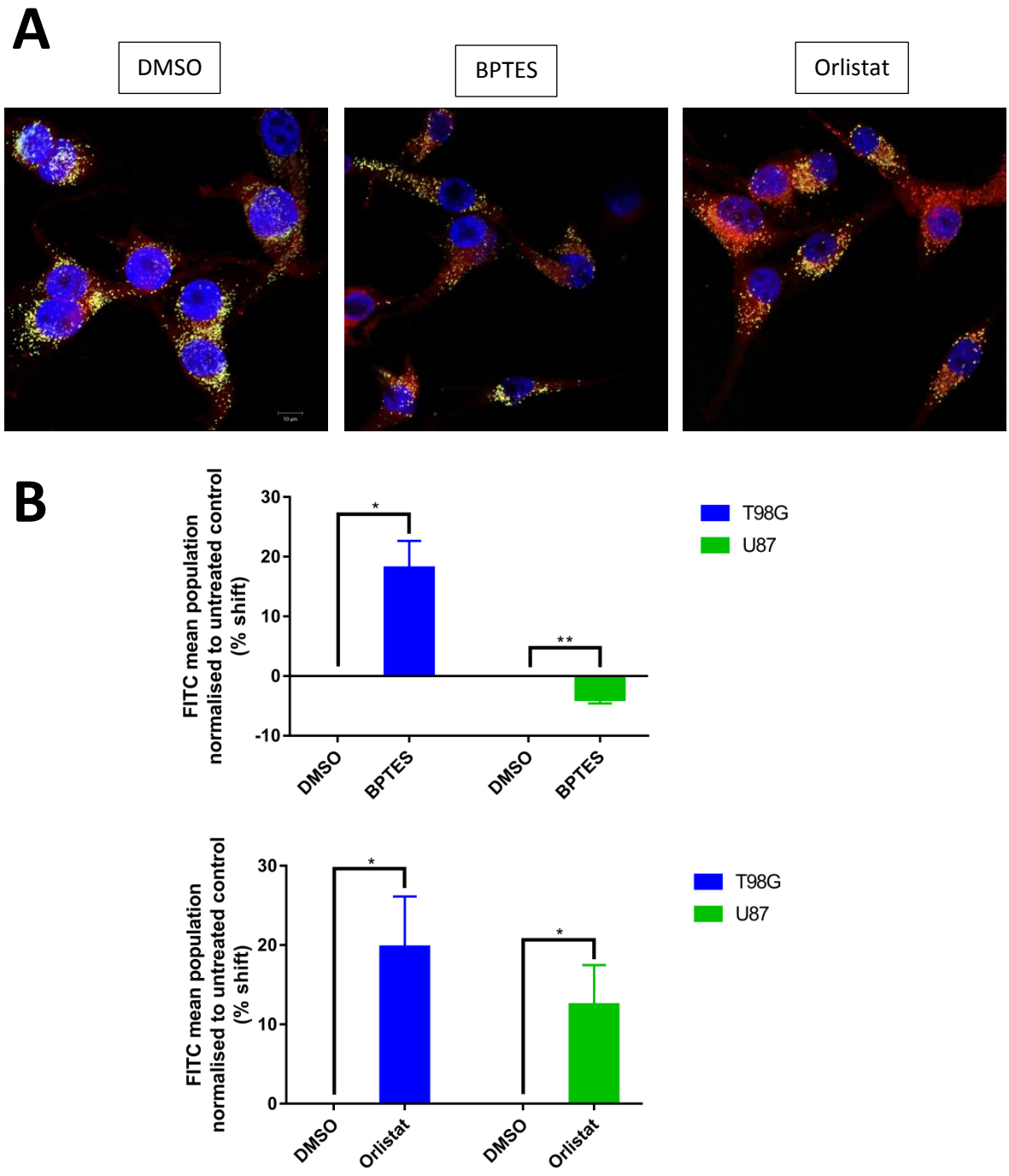

Figure 4.4. Pharmacological targeting of *de novo* fatty acid synthesis has an unclear impact on lipid droplets and may induce cell stress. A) Confocal microscopy images of nile red stained U87.1 cells incubated with DMSO, BPTES or orlistat for 4 hours in normoxia. BPTES and orlistat had no effect on LDQ. B) Flow cytometry quantification of the decreased LDQ following BPTES treatment in the U87 cell line. In contrast, orlistat treatment increased LDQ. Both drug treatments increased LDQ in the T98G cell line. Data shown as mean ±SEM, representative of several independent experiments (T98G, U87 n=3), analysed with an unpaired t-test; *p<0.05, **p<0.01, ***p<0.001, ****p<0.0001.

4.2.4. Inhibition of cholesterol synthesis did not have a major effect on LDQ by confocal microscopy.

Cholesterol is an important component of lipid droplets (255) and therefore the effect of simvastatin, a HMG-CoA reductase inhibitor, on LDQ was investigated. Analysis of confocal microscopy images indicated that inhibition of cholesterol synthesis may increase LDQ in the T98G, U87 and U87.1 cell lines, although this effect was very small and variable (Figure 4.5.). These data suggest that there is not a major role for cholesterol synthesis in lipid droplet metabolism in our system. Therefore, this was not further investigated with flow cytometry.

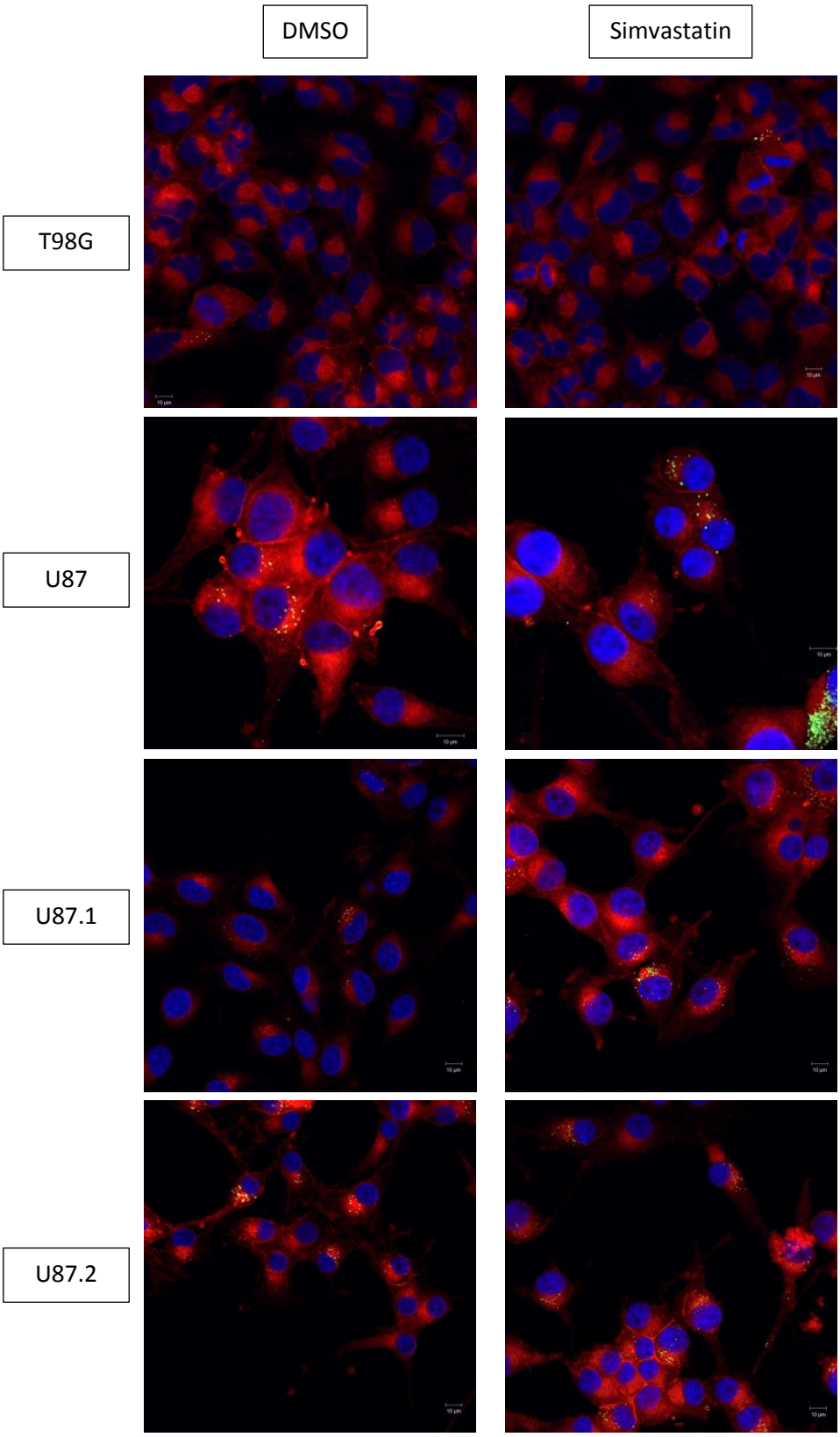

Figure 4.5. Cholesterol synthesis does not have a major role in lipid droplet metabolism. Confocal microscopy images of nile red stained T98G, U87, U87.1 and U87.2 cells incubated with DMSO or simvastatin for 24 hours in normoxia. Simvastatin treatment increased LDQ in the T98G, U87 and U87.1 cell lines. There is no clear effect in the U87.2 cell line.

4.2.5. Lipid droplets are broken down by lipid droplet-specific autophagy.

Autophagy is an important mechanism by which cellular components, including lipid droplets, can be broken down (178,179). LDQ was assessed following autophagy inhibition across 5 cell lines using confocal microscopy and flow cytometry. An increase in LDQ was observed through analysis of confocal images of cells treated with chloroquine, a late stage autophagy inhibitor (Figure 4.6.A.). This was supported by flow cytometry wherein chloroquine treatment increased the FITC signal intensity, representing increased LDQ, in all 5 cell lines (Figure 4.6.B.). This suggests that autophagy inhibition prevents lipid droplet breakdown and causes lipid droplet accumulation. An early stage autophagy inhibitor, 3-methyladenine (3-MA), also increased LDQ, observed through both confocal microscopy and flow cytometry (Figures 4.6.C. and 4.6.D.). Moreover, 3-MA increased the accumulation of C16 BODIPY within lipid droplets in the T98G and U87 cell lines, as assessed through confocal microscopy, further implicating autophagy in lipid droplet breakdown (Figure 4.7.A.). The role of off-target drug effects and cell-stress induced lipid droplet alterations were tested using targeted siRNA knockdown of the vital autophagy protein Atg5. siAtg5 increased LDQ compared to the non-targeted control in both the U87 and U87.2 cell lines confirming that autophagy inhibition is responsible for the accumulation of lipid droplets (Figure 4.7.B.). Knockdown of the Atg5 protein was confirmed via western blot (Figure 4.7.C.), further analysed with densitometry (Figure 4.7.D.). This indicated 48 hours as the optimal incubation period for protein knockdown.

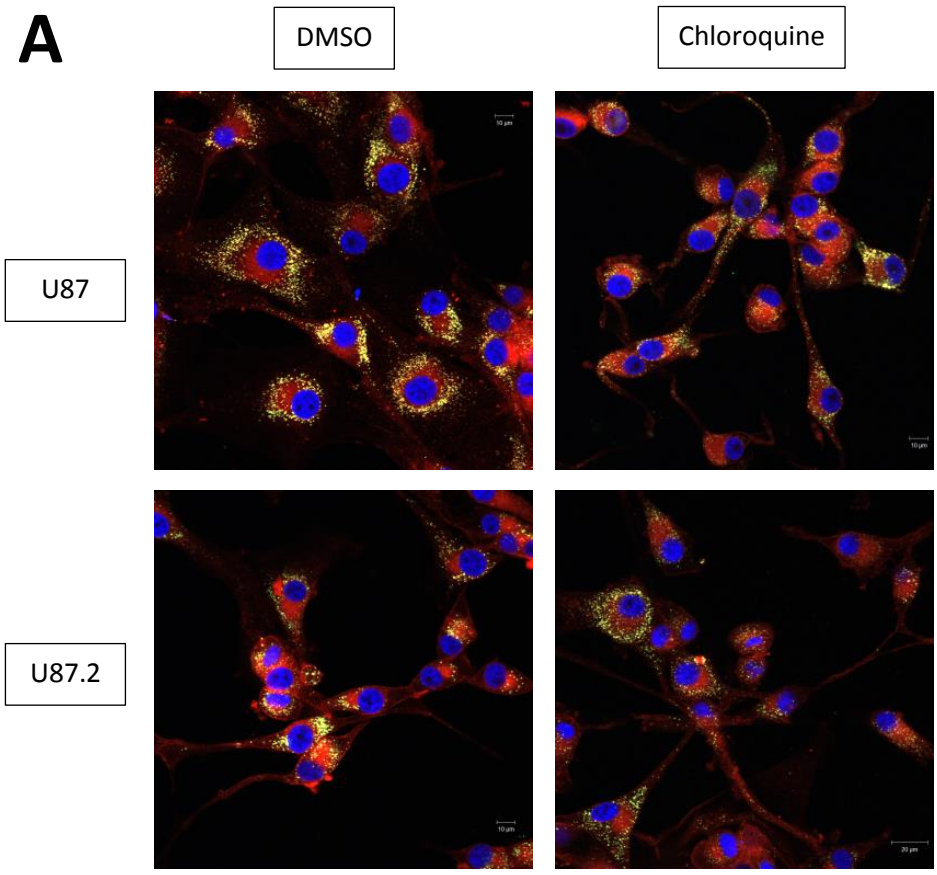
A
DMSO
Chloroquine
U87
U87.2

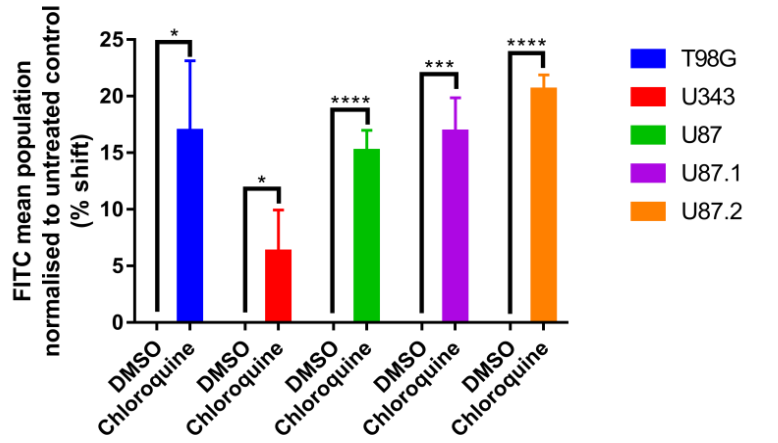
B
FITC mean population normalised to untreated control (% shift)
25
20
15
10
5
0
*
*
****
***
****
DMSO
Chloroquine
T98G
U343
U87
U87.1
U87.2

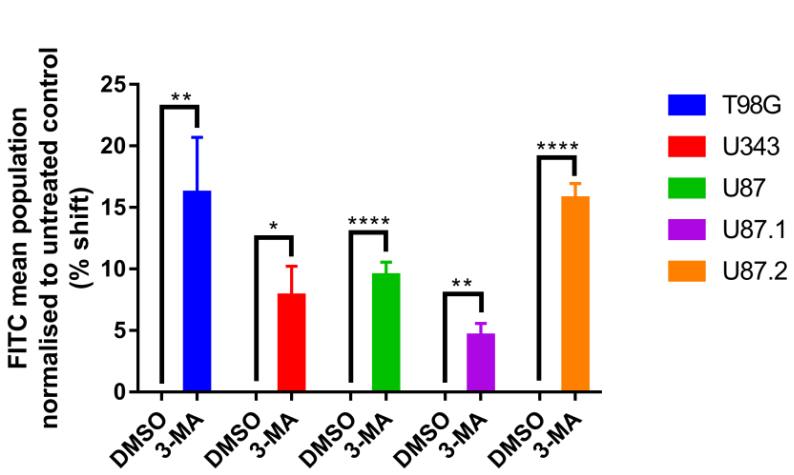
C
FITC mean population normalised to untreated control (% shift)
25
20
15
10
5
0
**
*
****
**
****
DMSO
3-MA
T98G
U343
U87
U87.1
U87.2

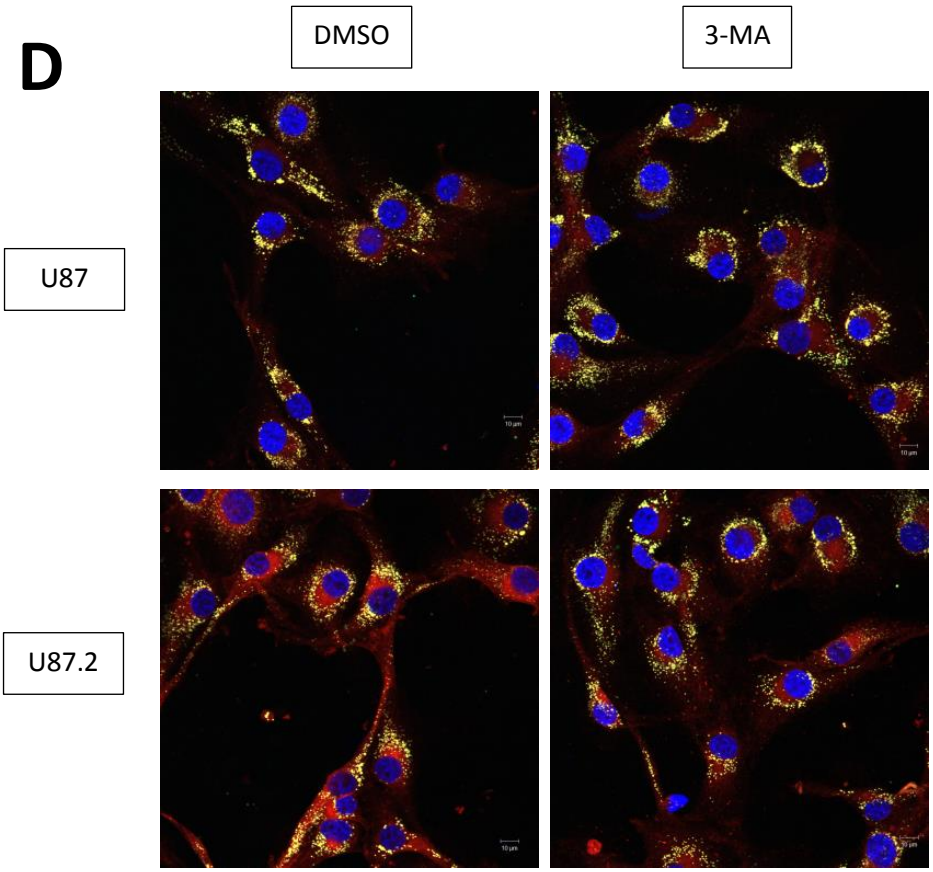

Figure 4.6. A**utophagy inhibition prevents lipid droplet breakdown and causes accumulation.** A) Confocal microscopy of nile red stained U87 and U87.2 cells incubated with DMSO or chloroquine for 8 hours in DMEM. Chloroquine treatment increased LDQ. B) and C) Flow cytometry quantification of the increased LDQ observed with chloroquine treatment in DMEM (B) and 3-MA treatment in HBSS (C) across all five nile red stained cell lines. Data shown as mean ±SEM, representative of several independent experiments (U343 n=3; U87.2 n=4; T98G, U87, U87.1 n=5), analysed with an unpaired t-test; *p<0.05, **p<0.01, ***p<0.001, ****p<0.0001. D) Confocal microscopy of nile red stained U87 and U87.2 cells incubated with DMSO or 3-MA for 8 hours in HBSS. 3-MA treatment in HBSS increased LDQ, supporting Figure 4.6.C.

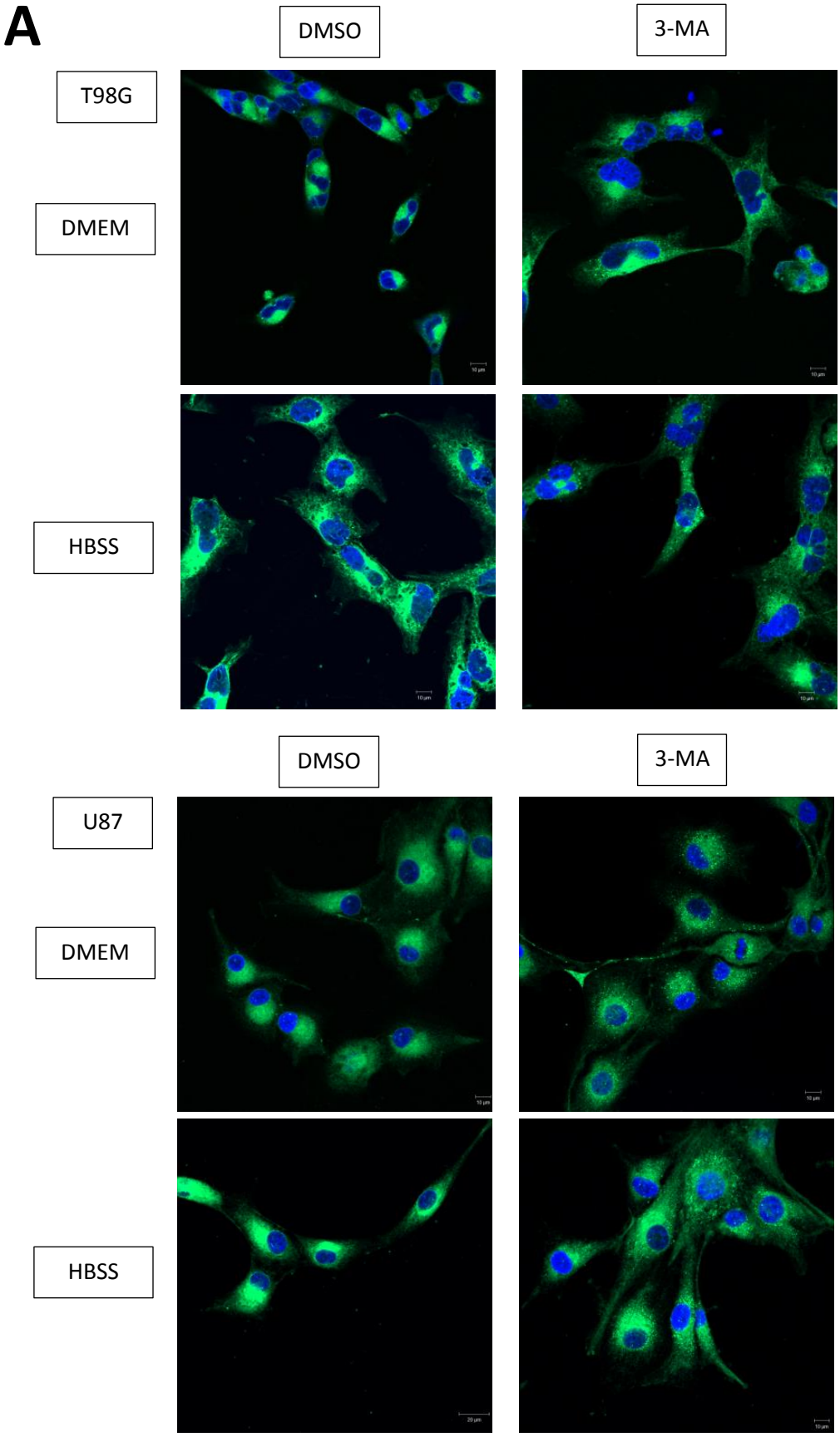
A
DMSO
3-MA
T98G
DMEM
HBSS
DMSO
3-MA
U87
DMEM
HBSS

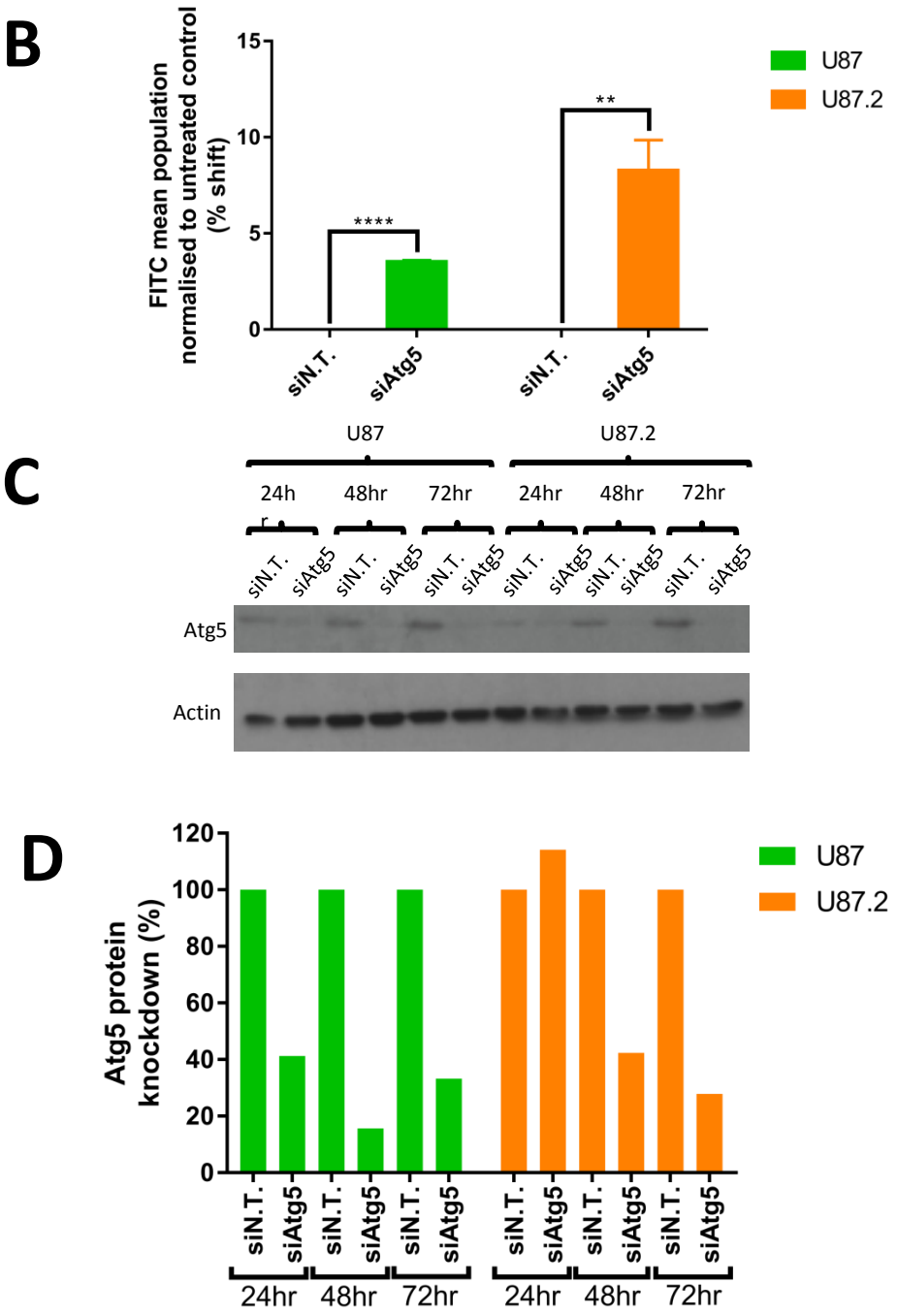

Figure 4.7. **Autophagy is important in the metabolic regulation of lipid droplets.** A) Confocal microscopy of T98G and U87 cells incubated with C16 BODIPY prior to 8 hour treatment with 3-MA in either DMEM or HBSS. 3-MA treatment increased LDQ and the accumulation of C16 BODIPY within them. B) Flow cytometry of nile red stained U87 and U87.2 cell lines treated with siN.T. and siAtg5 for 48 hours. siAtg5 increased LDQ in both cell lines compared to the non-targeting control. Data shown as mean ±SEM, representative of several independent experiments (U87 n=2; U87.2 n=4), analysed with an unpaired t-test; *p<0.05, **p<0.01, ***p<0.001, ****p<0.0001. C) Protein knockdown was confirmed with western blot. U87 and U87.2 cells treated with siN.T. or siAtg5 for 24, 48 and 72 hours. D) Densitometry analysis of western blot (C) confirmed knockdown (%) of Atg5 protein. Normalised to siN.T. control. Raw densitometry data in Appendix 7.12.

4.2.6. LDQ is increased in hypoxia and in response to HIF1α stabilisation.

Hypoxia induces global changes in cellular metabolism (256) and is known to increase lipid droplet accumulation (123). Indeed, LDQ was increased in hypoxic conditions in the T98G, U87, U87.1 and U87.2 cell lines, as observed by confocal microscopy (Figure 4.8.A.). This was supported by a positive shift in the FITC signal intensity of cells incubated at 0.3% O_2 as measured by flow cytometry in all 5 cell lines (Figure 4.8.B.). Hypoxic incubation also increased the total lipid concentration detected by HRMAS NMR in the U87 and U87.2 cell lines (Figure 4.8.C.).

Low oxygen concentrations result in the stabilisation of the HIF protein which is responsible for many of the downstream effects of hypoxia (256). DMOG, an alpha-ketoglutarate-like inhibitor of the prolyl hydroxylase enzymes, stabilises HIF1α regardless of oxygen concentration, allowing the HIF1α-specific effects of hypoxia to be mimicked in normoxic conditions (257). LDQ in the U87 and U87.2 cell lines was observed to be increased in DMOG treated cells in normoxic and hypoxic conditions compared to DMSO controls (Figure 4.9.A.). Flow cytometry supported the evidence suggesting that DMOG induced an increase in LDQ in normoxic and hypoxic conditions (Figure 4.9.B.). Indeed, normoxic DMOG treatment increased the FITC signal intensity more than hypoxia alone, a result likely attributable to the increased stabilisation of HIF1α by DMOG (257). This is supported by other studies showing that the hypoxia induces an increased LDQ through HIF1α (123).

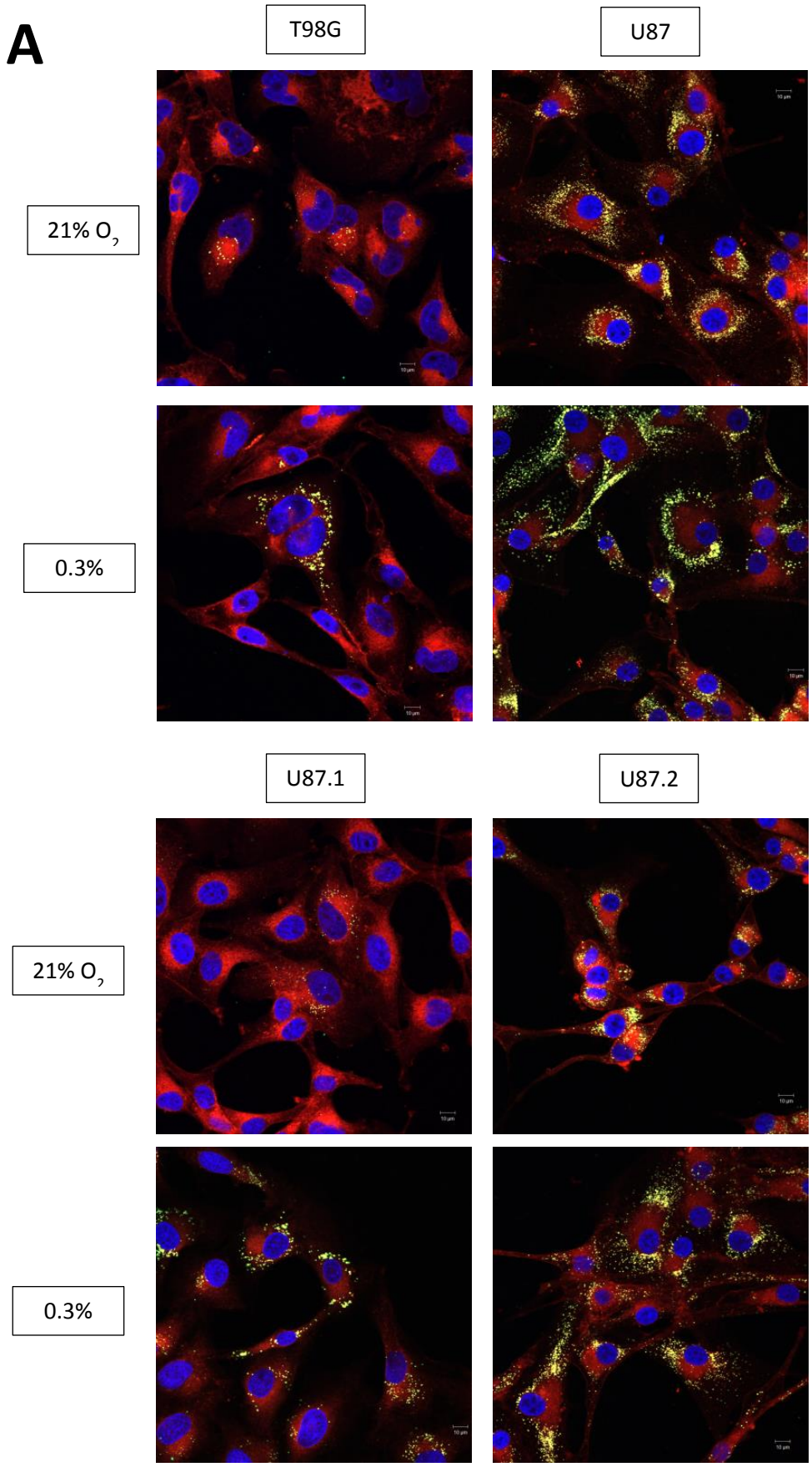
A
T98G
U87
21% O2
0.3%
U87.1
U87.2
21% O2
0.3%

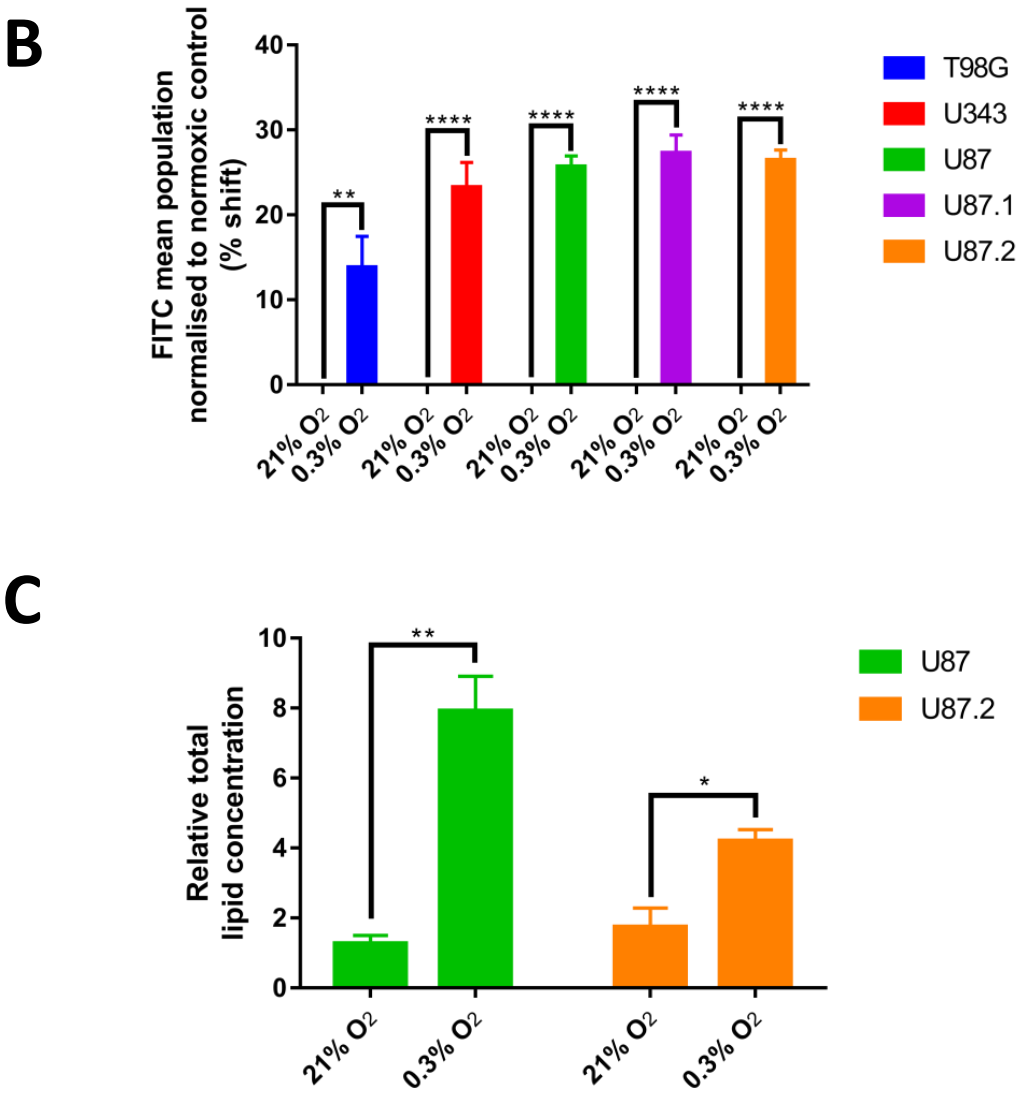

Figure 4.8. Hypoxia increased LDQ. A) Confocal microscopy of nile red stained T98G, U87, U87.1 and U87.2 cells incubated in 21% or 0.3% O_2 for 16 hours. Hypoxia increased LDQ within the four cell lines. B) Flow cytometric quantification of the increased LDQ observed with hypoxic incubation across all five nile red stained cell lines. Data shown as mean ±SEM, representative of several independent experiments (U87.2 n=4; T98G, U87, U87.1 n=5; U343 n=6), analysed with an unpaired t-test; *p<0.05, **p<0.01, ***p<0.001, ****p<0.0001. C) Relative total lipid concentration in U87 and U87.2 cells incubated in 21% or 0.3% O_2 for 24 hours as measured by HRMAS NMR. The relative total lipid concentration was increased in hypoxia in both cell lines. Data shown as mean ±SEM, representative of three independent experiments analysed with an unpaired t-test; *p<0.05, **p<0.01, ***p<0.001, ****p<0.0001. Total lipid concentrations were normalised to the total metabolite concentration of each sample.

A

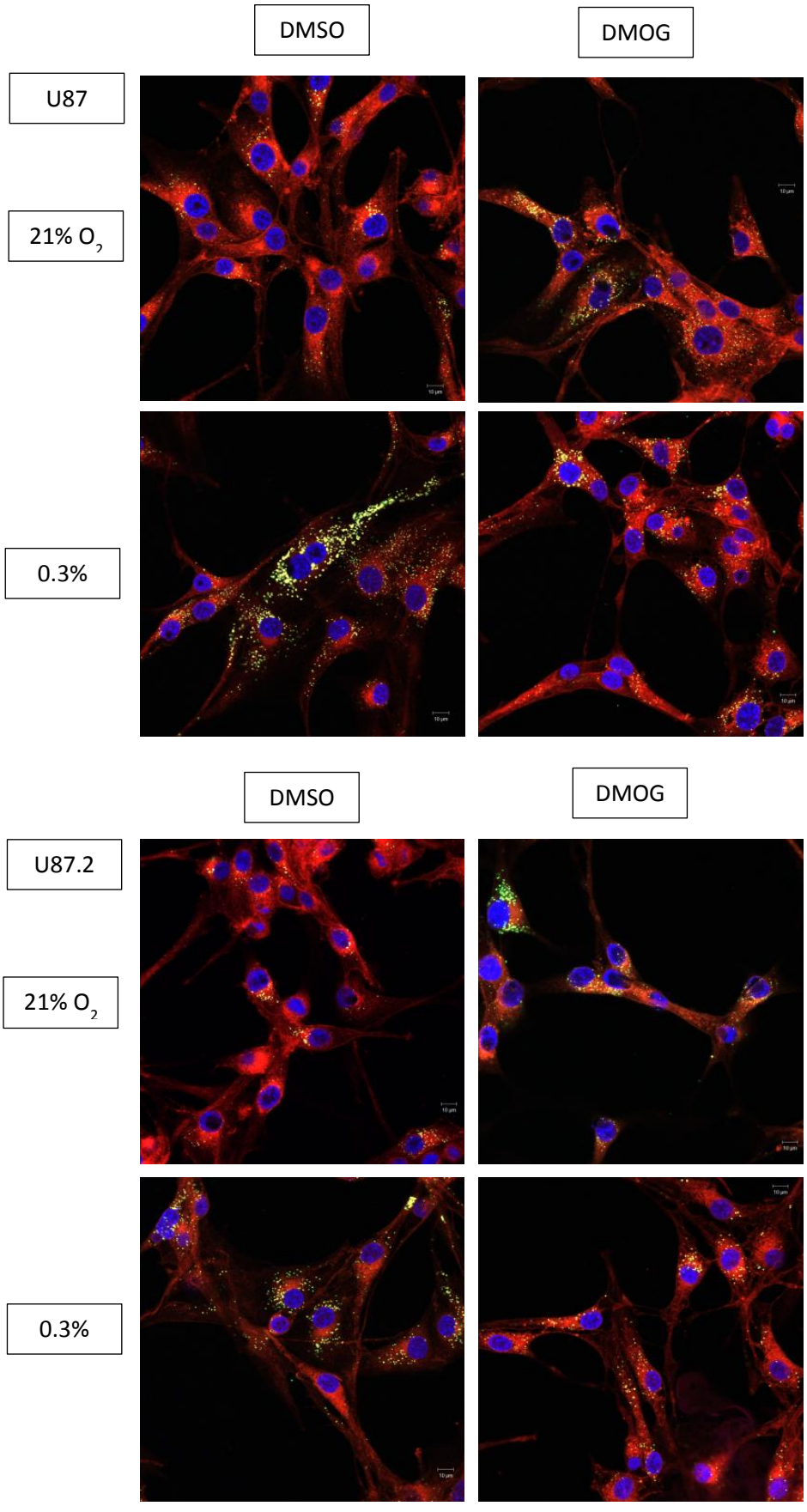

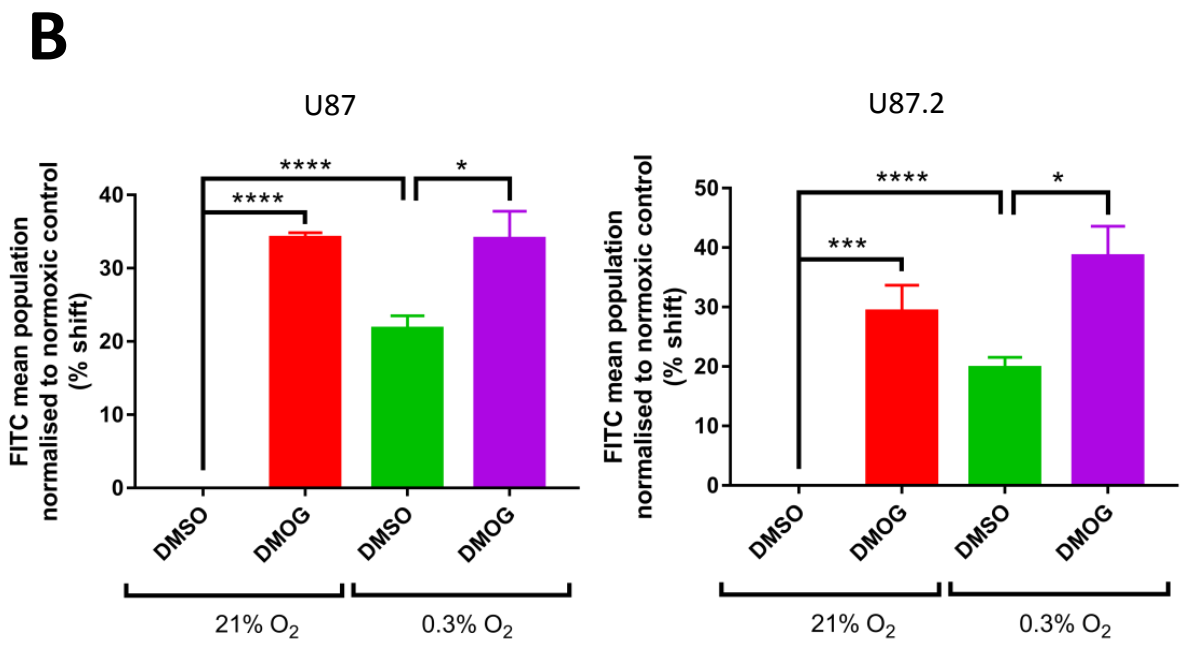

Figure 4.9. HIF-1a stabilisation can increase LDQ at 21% and 0.3% O_2. A) Confocal microscopy of nile red stained U87 and U87.2 cells incubated in 21% or 0.3% O_2 for 16 hours with DMSO or DMOG. DMOG treatment increased LDQ further than hypoxia alone in both cell lines. B) Flow cytometric quantification of the DMOG-induced increase in LDQ observed in both the U87 and U87.2 cell lines. Data shown as mean ±SEM, representative of several independent experiments (n=5), analysed with an unpaired t-test; *p<0.05, **p<0.01, ***p<0.001, ****p<0.0001.

4.2.7. The uptake of exogenous serum lipids is important in lipid droplet production in hypoxia as well as normoxia.

The exogenous lipid pool was an important factor in lipid droplet production in normoxia and was therefore investigated further in hypoxia. Confocal microscopy images of cells grown in de-lipidated serum media in hypoxia indicated that removal of the exogenous lipid droplet pool decreased LDQ (Figure 4.10.A). Concurrently growth in de-lipidated serum in hypoxia decreased the FITC signal intensity in the U343 and U87 cell lines, as assessed by flow cytometry (Figure 4.10.B.). This further supports the use of the exogenous lipid pool to produce lipid droplets. The T98G, U87.1 and U87.2 cell lines did not reach significance, but all three cell lines demonstrate a trend toward decreased LDQ when grown in de-lipidated serum media. This suggests that compensation from other mechanisms may also be important in hypoxic lipid droplet production in these cell lines. Moreover, hypoxia increased the uptake of C16 BODIPY in the T98G and U87 cell lines whilst C11 BODIPY uptake was increased only slightly (Figure 4.11.A. and 4.11.B.). The increased uptake of fatty acids such as C16 and C11 could contribute to the increased LDQ observed in hypoxia.

A

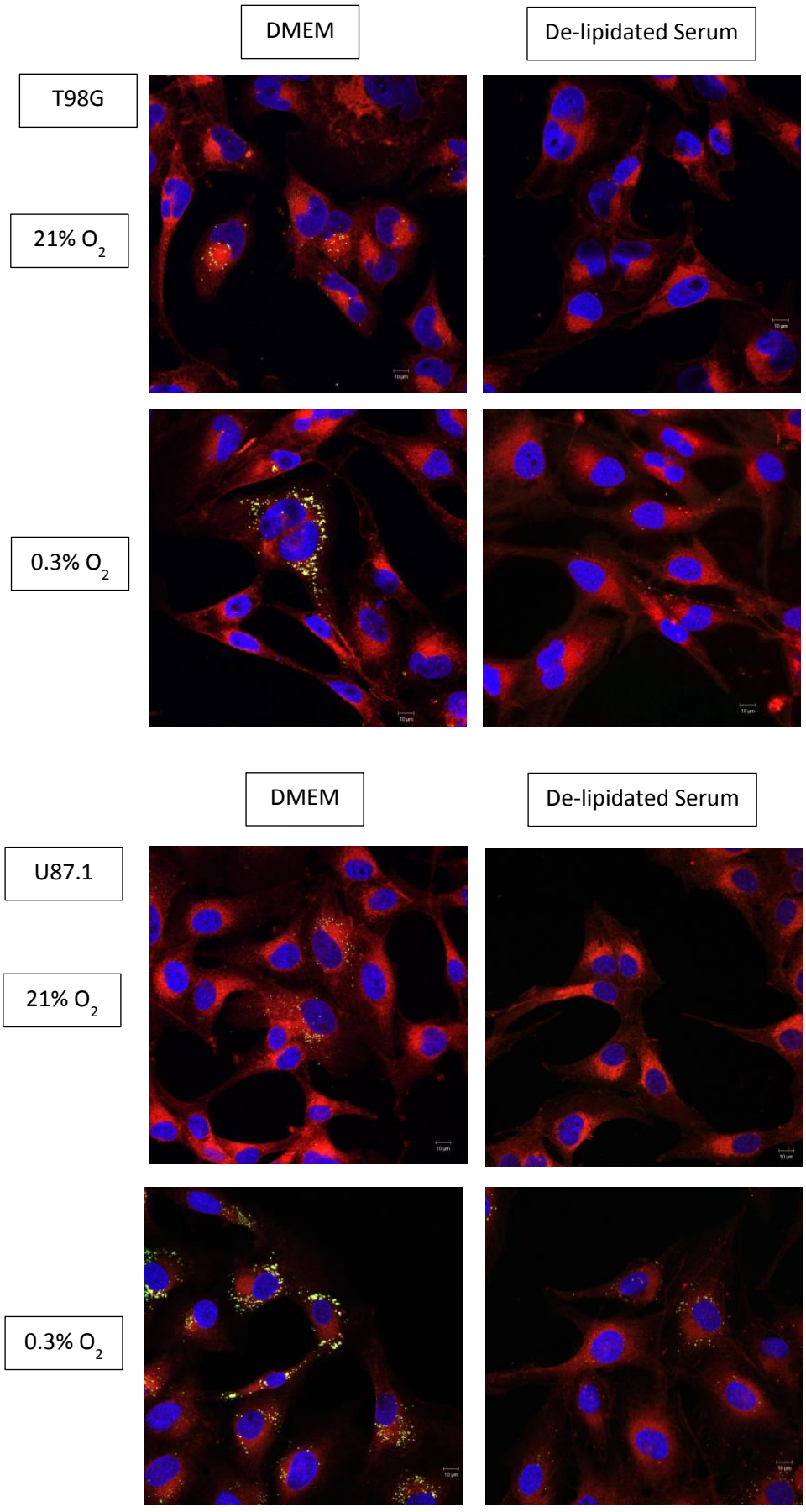
DMEM
De-lipidated Serum
T98G
21% O2
0.3% O2
DMEM
De-lipidated Serum
U87.1
21% O2
0.3% O2

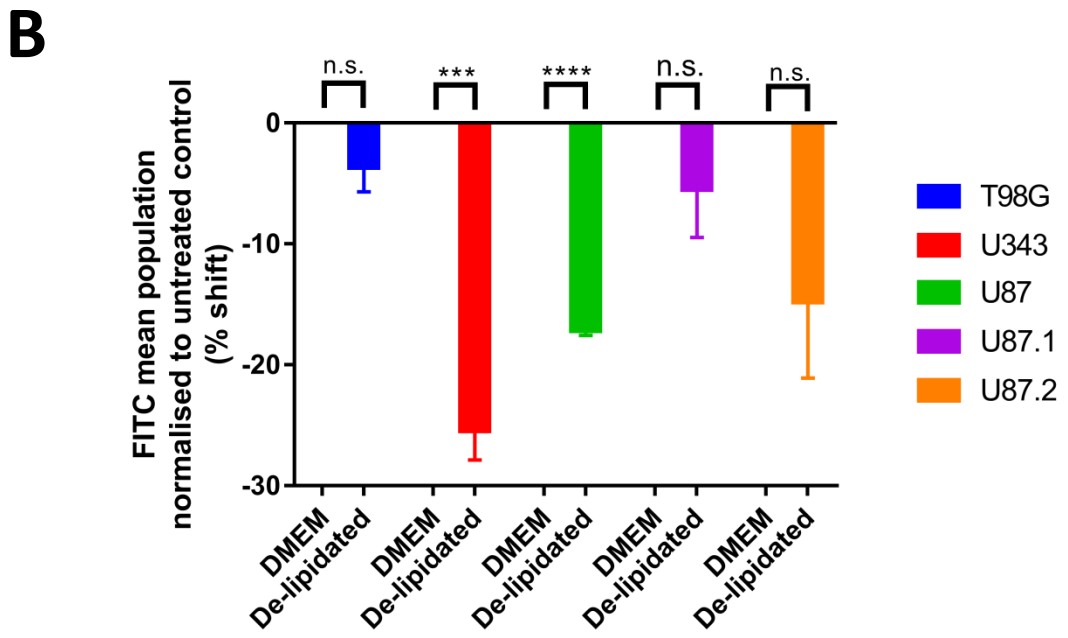

Figure 4.10. Uptake of exogenous serum lipids is important in lipid droplet production in hypoxia. A) Confocal microscopy of nile red stained T98G and U87.1 cells incubated in 21% or 0.3% O_2 for 72 hours with DMEM or de-lipidated serum media. Incubation in de-lipidated serum media decreased the LDQ of both cell lines in normoxia and hypoxia. Normoxic images are taken from Figure 4.1.A. B) Flow cytometric quantification of the decrease in LDQ observed with incubation in de-lipidated serum in hypoxia across all five nile red stained cell lines. Due to large error bars the T98G, U87.1 and U87.2 cell lines did not reach significance. Data shown as mean ±SEM, representative of several independent experiments (U343, U87, U87.2 n=3; T98G, U87.1 n=4), analysed with an unpaired t-test; *p<0.05, **p<0.01, ***p<0.001, ****p<0.0001.

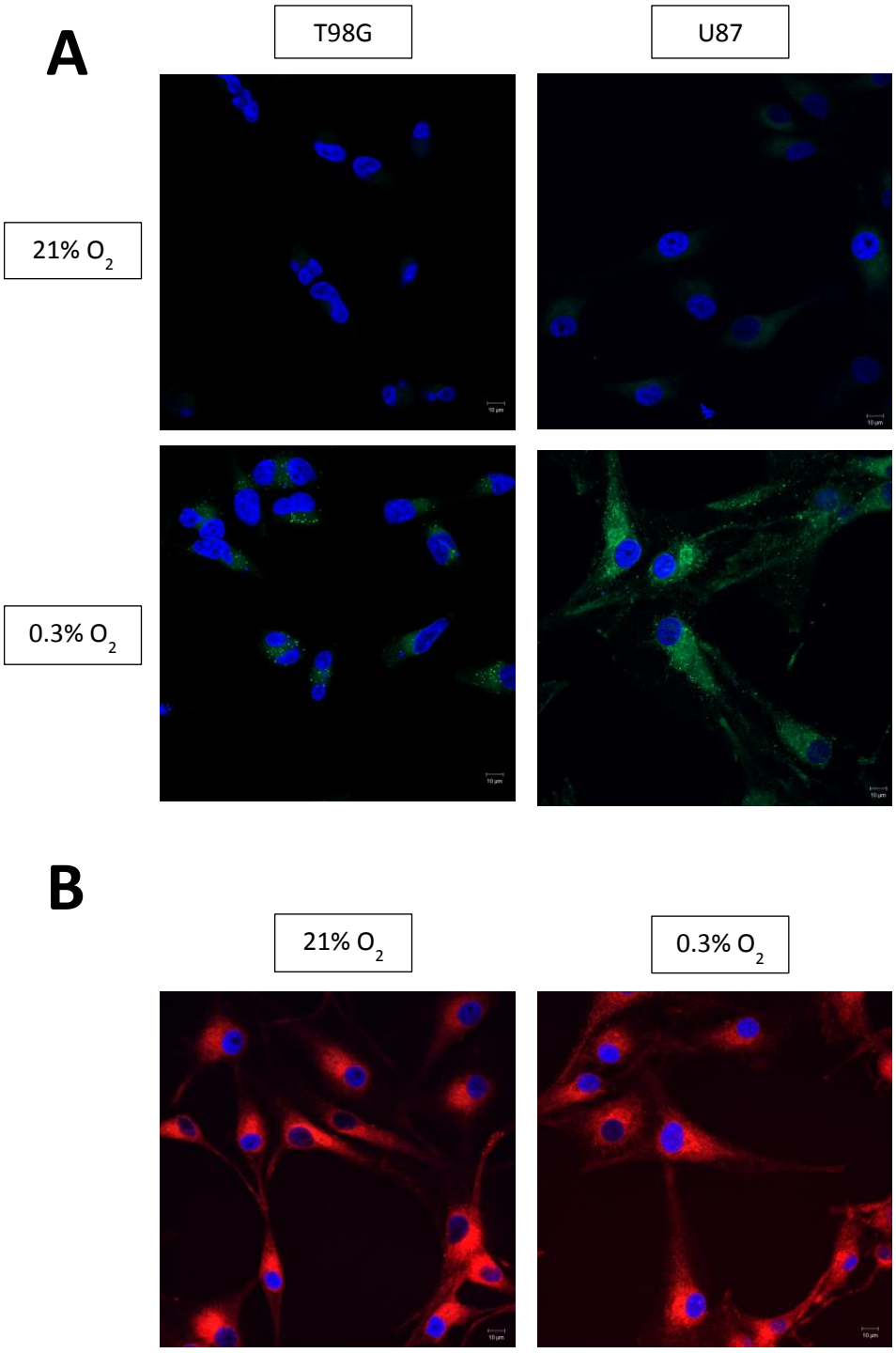

Figure 4.11. Hypoxia increases the uptake of exogenous serum lipids. A) Confocal microscopy of T98G and U87 cells incubated with C16 BODIPY after 16 hours incubation in 21% or 0.3% O_2. The uptake of C16 BODIPY was increased in both cell lines at 0.3% O_2. B) Confocal microscopy of U87 cells incubated with C11 BODIPY after 16 hours incubation in 21% or 0.3% O_2. The uptake of C11 BODIPY was increased to a lesser extent in hypoxic conditions.

4.2.8. ATGL activity affects LDQ in hypoxia in a cell line-specific manner.

Our data suggests that ATGL inhibition with atglistatin decreases LDQ in normoxia, potentially through preventing the release of fatty acids from cell membranes. In hypoxia, a decrease in LDQ following atglistatin treatment was observed with confocal microscopy in the U87.2 cell line (Figure 4.12.A.). In contrast, no effect on LDQ following atglistatin treatment was observed in the U87 cell line. In support of this, flow cytometry indicated cell line-specific differences in LDQ following treatment of hypoxic cells with atglistatin (Figure 4.12.B.). There was no significant difference in the FITC signal intensity following atglistatin treatment in the T98G, U87 and U87.1 cell lines and a small decrease in the FITC signal intensity in the U343 cell line. However, LDQ was considerably decreased in the U87.2 cell line indicating a key difference in the metabolic regulation of hypoxic lipid droplet metabolism between the cell lines. Moreover, cell specific differences may reflect the natural heterogeneity of GBM tumours.

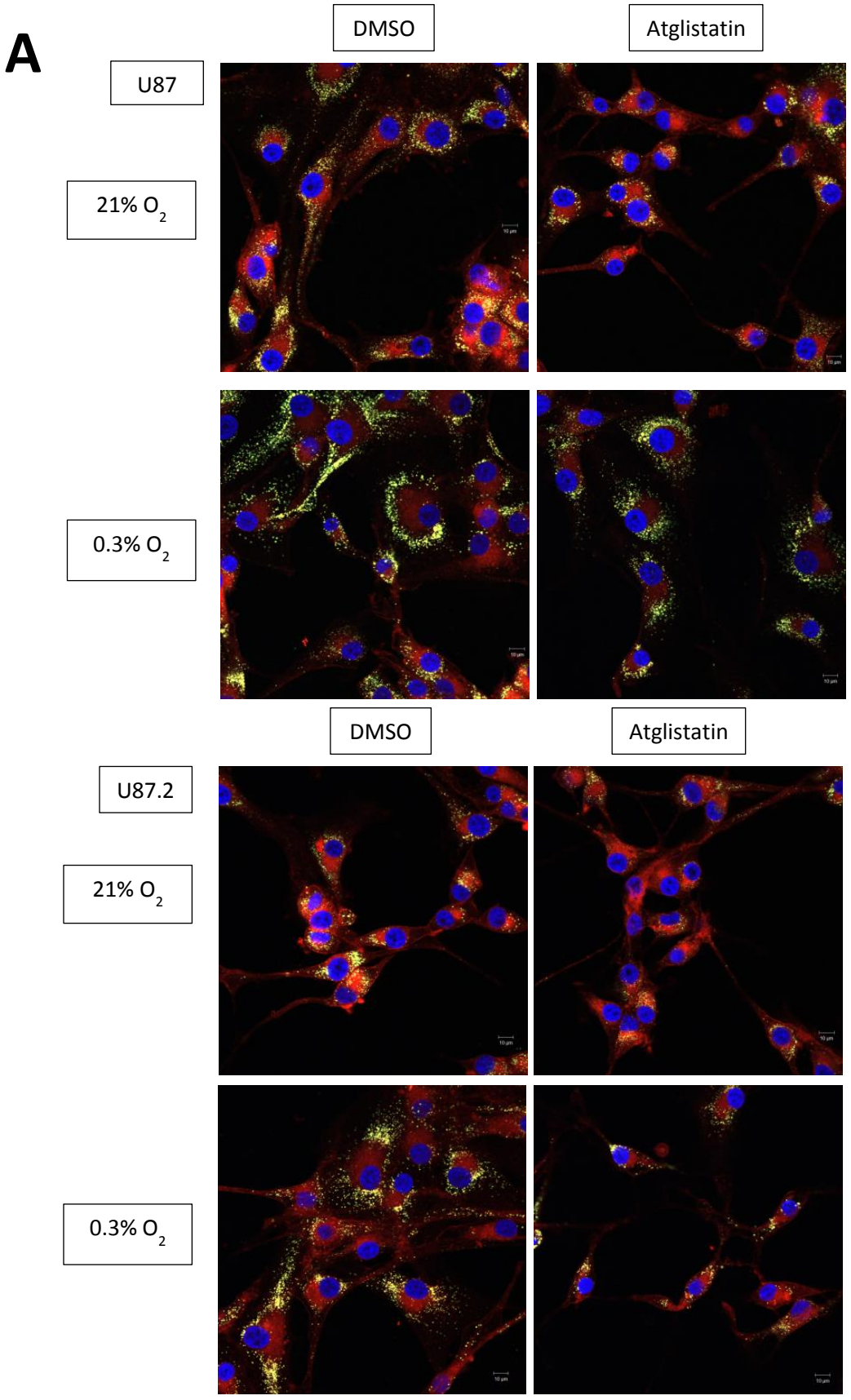
A
DMSO
Atglistatin
U87
21% O2
0.3% O2
DMSO
Atglistatin
U87.2
21% O2
0.3% O2

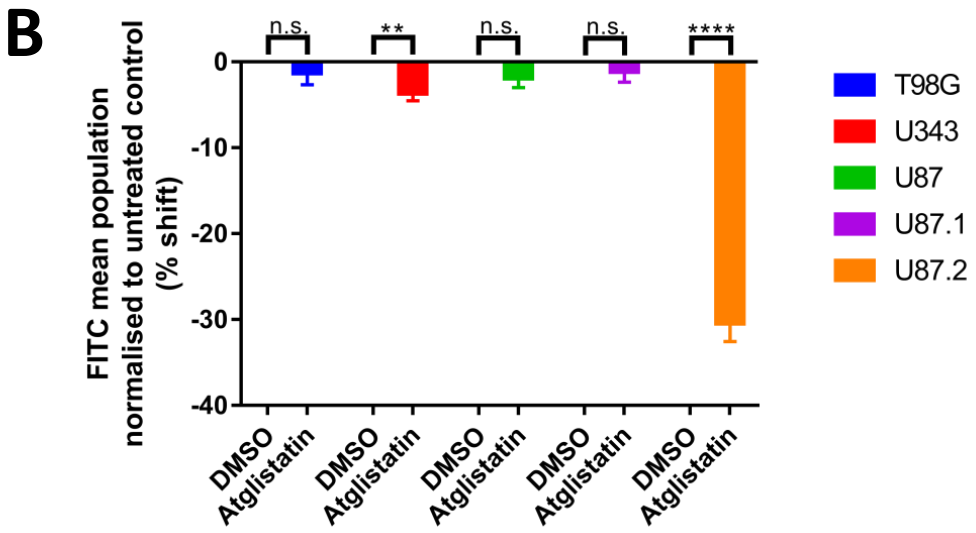

Figure 4.12. ATGL has a cell line dependent role in lipid droplet production in hypoxia. A) Confocal microscopy of nile red stained U87 and U87.2 cells treated with DMSO or atglistatin at 21% or 0.3% O_2. Atglistatin treatment decreased LDQ in both cell lines in normoxia but there was no clear change in hypoxia. Normoxic images are taken from Figure 4.2.A. B) Flow cytometric quantification of the effect of atglistatin treatment in hypoxia across all five nile red stained cell lines. Atglistatin did not significantly affect LDQ in the T98G, U87 and U87.1 cell lines. There was a small decrease in LDQ in the U343 cell line and a much larger decrease observed in the U87.2 cell line. Data shown as mean ±SEM, representative of several independent experiments (U87.1, U87.2 n=3; U87 n=4; T98G, U343 n=5), analysed with an unpaired t-test; *p<0.05, **p<0.01, ***p<0.001, ****p<0.0001.

4.2.9. The role of *de novo* fatty acid synthesis in lipid droplet production in hypoxia requires further exploration.

Our data suggested that *de novo* fatty acid synthesis may impact lipid droplet production in normoxia, although the induction of a cell stress response confounded the results. Following treatment with BPTES and orlistat in hypoxia no change in LDQ was observed through analysis of confocal microscopy images (Figure 4.13.A.). In addition, BPTES did not significantly alter the FITC signal intensity of the T98G and U87 cell lines (Figure 4.13.B.). As observed in normoxia, orlistat increased LDQ in the T98G and U87 cell lines, as assessed by flow cytometry. This is likely attributable to the induction of cell stress by a non-FASN orlistat effect. Therefore, the importance of *de novo* fatty acid synthesis in lipid droplet production requires further investigation in hypoxia as well as normoxia.

The role of cholesterol synthesis was not further investigated in hypoxia due to the minor role in lipid droplet metabolism observed in normoxia.

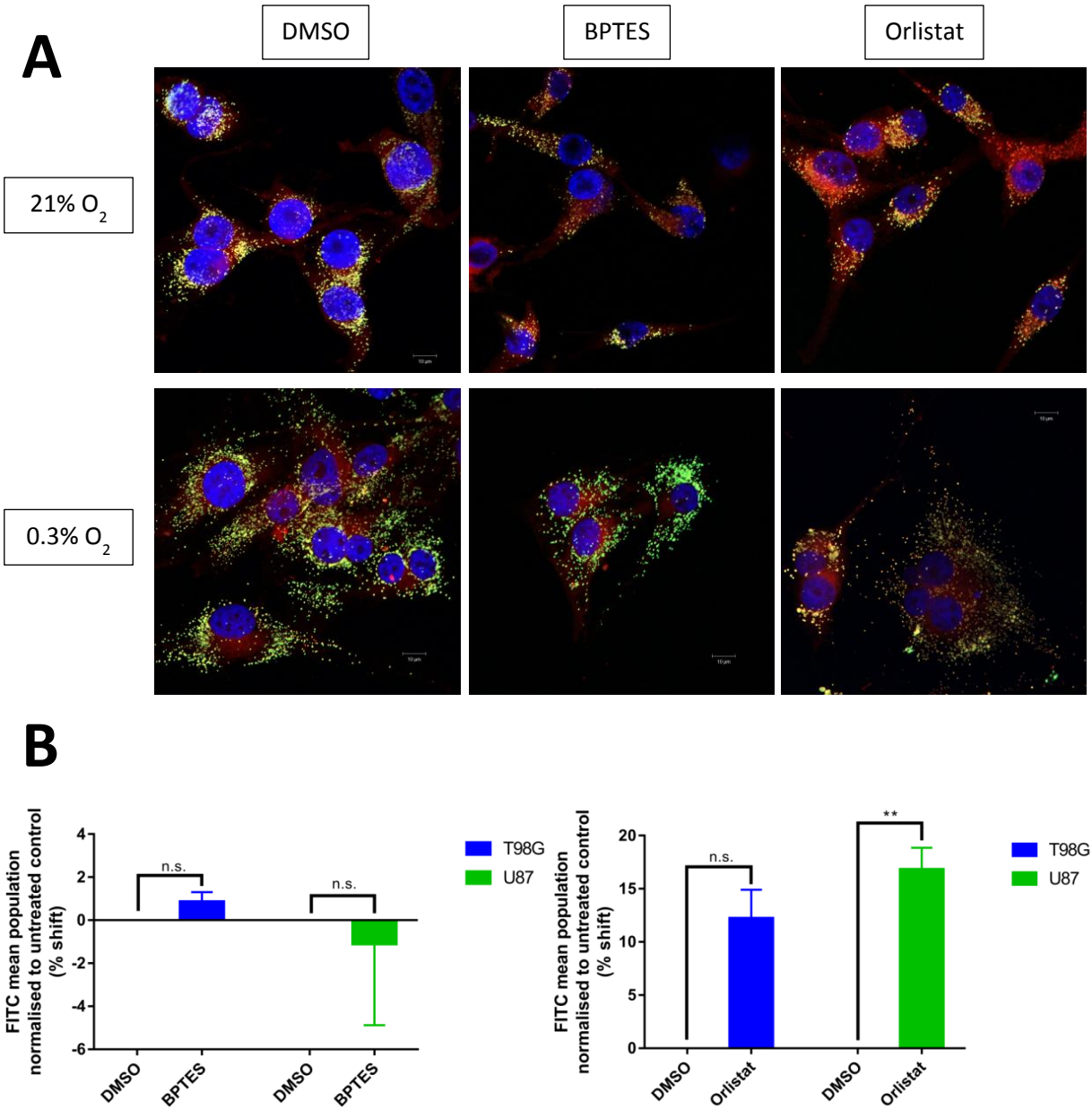

Figure 4.13. The role of *de novo* fatty acid synthesis in lipid droplet production in hypoxia requires further investigation. A) Confocal microscopy of nile red stained U87.1 cells treated with DMSO, BPTES or orlistat at 21% or 0.3% O_2. There was no clear change in LDQ in hypoxia with either treatment. Hypoxic cells treated with orlistat contain highly stained lipid structures which may be membrane blebs. Normoxic images are taken from Figure 4.4.A. B) Flow cytometric quantification of the effect of BPTES and orlistat treatment in hypoxia in the nile red stained T98G and U87 cell lines. BPTES did not significantly decrease LDQ. Orlistat significantly increased LDQ in the U87 cell line. Data shown as mean ±SEM, representative of several independent experiments (T98G BPTES n=2; T98G Orlistat, U87 BPTES and Orlistat n=3), analysed with an unpaired t-test; *p<0.05, **p<0.01, ***p<0.001, ****p<0.0001.

4.2.10. The effect of autophagy inhibition on LDQ in hypoxia is cell line dependent.

In normoxia, we observed that lipid droplets were broken down through autophagy and therefore the effect of autophagy inhibition in hypoxia was investigated using confocal microscopy and flow cytometry. Analysis of confocal microscopy images did not suggest alterations in LDQ following chloroquine treatment in hypoxia in the U87 and U87.2 cell lines (Figure 4.14.A.). In contrast, flow cytometry indicated that chloroquine has cell line-specific effects on LDQ (Figure 4.14.B.). The FITC signal intensity was increased in chloroquine treated cells in the T98G and U87 cell lines indicating decreased lipid droplet breakdown and increased accumulation. In contrast, chloroquine decreased the FITC signal intensity of the U343, U87.1 and U87.2 cell lines suggesting that autophagy inhibition paradoxically decreases lipid droplet accumulation in these cell lines.

A

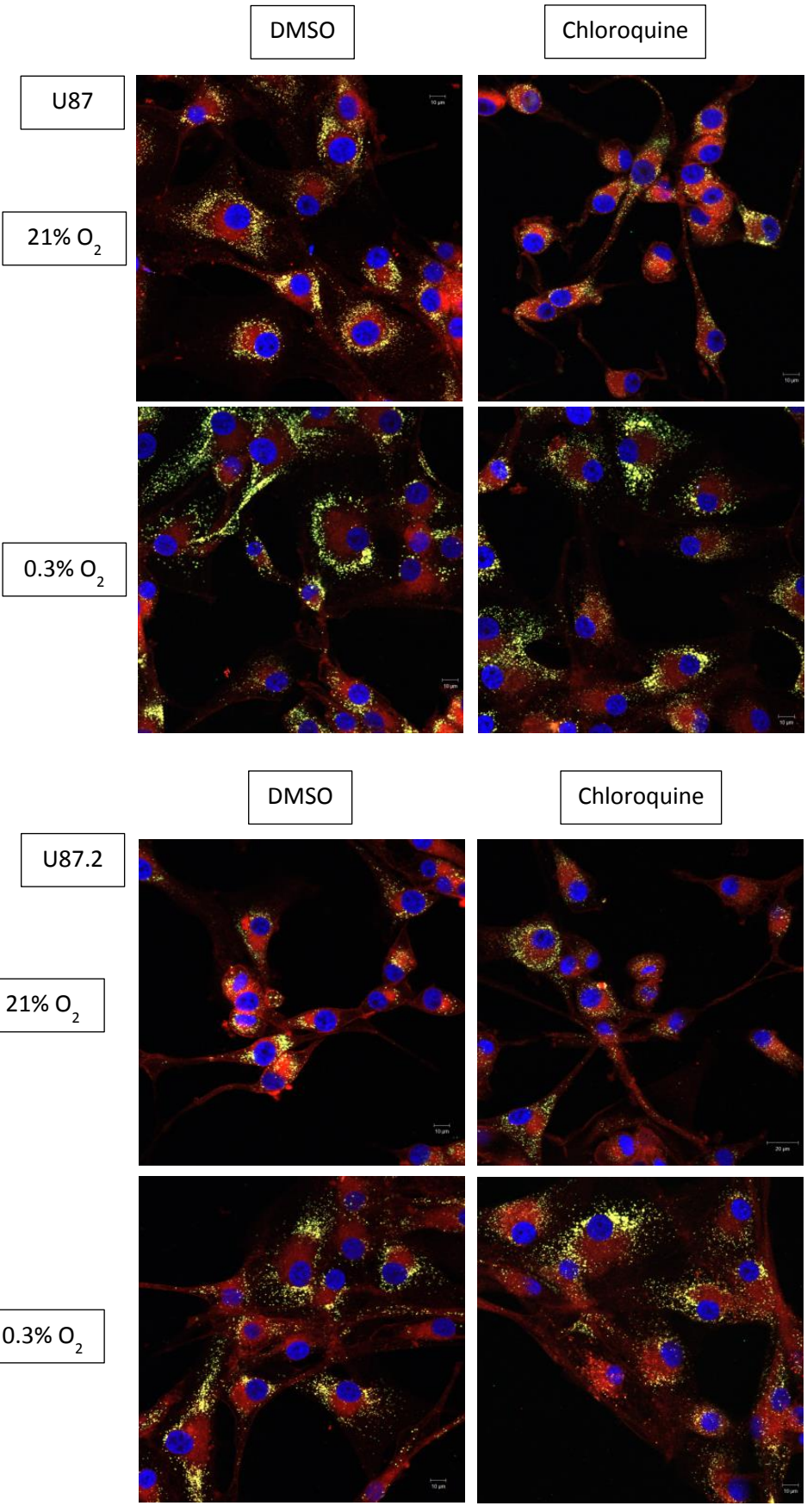
DMSO
Chloroquine
U87
21% O_2
0.3% O_2
DMSO
Chloroquine
U87.2
21% O_2
0.3% O_2

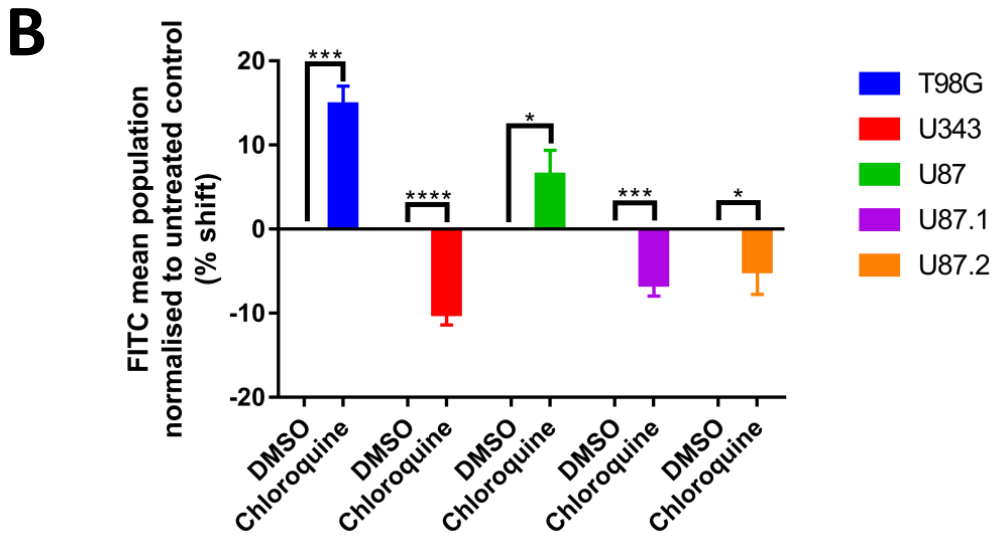

Figure 4.14. Autophagy impacts lipid droplet breakdown in a cell line dependent manner. A) Confocal microscopy of nile red stained U87 and U87.2 cells treated with DMSO or chloroquine at 21% or 0.3% O_2. Chloroquine treatment increased LDQ in the U87 cell line; however, the effect is not clear in the U87.2 cell line. Normoxic images are taken from Figure 4.6.A. B) Flow cytometric quantification of the effect of chloroquine treatment in hypoxia across all five nile red stained cell lines. Chloroquine increased LDQ in the T98G and U87 cell lines; however, it decreased LDQ in the U343, U87.1 and U87.2 cell lines. Data shown as mean ±SEM, representative of several independent experiments (U87, U87.1, U87.2 n=3; T98G n=5; U343 n=6), analysed with an unpaired t-test; *p<0.05, **p<0.01, ***p<0.001, ****p<0.0001.

4.2.11. Lipid droplets are in a state of flux subject to metabolic demand.

Starvation places a metabolic demand on the cell which can be sustained through lipid catabolism. HBSS was therefore used to mimic starvation conditions and its impact on fatty acid uptake and lipid droplets investigated using confocal microscopy. Incubation in HBSS increased the uptake and incorporation of C16 BODIPY into cell membranes and lipid droplets in the T98G and U87 cell lines (Figure 4.15.A.). This was observed in both normoxia and hypoxia. In conjunction with Figure 4.9, hypoxia increased the uptake of C16 BODIPY in the T98G and U87 cell lines in both DMEM and HBSS. Incubation in HBSS also increased the uptake of C11 BODIPY in the U87 cell line (Figure 4.15.B.). The intensity of fluorescent labelled fatty acid staining was increased in some cases to the extent that images in high uptake conditions are over exposed.

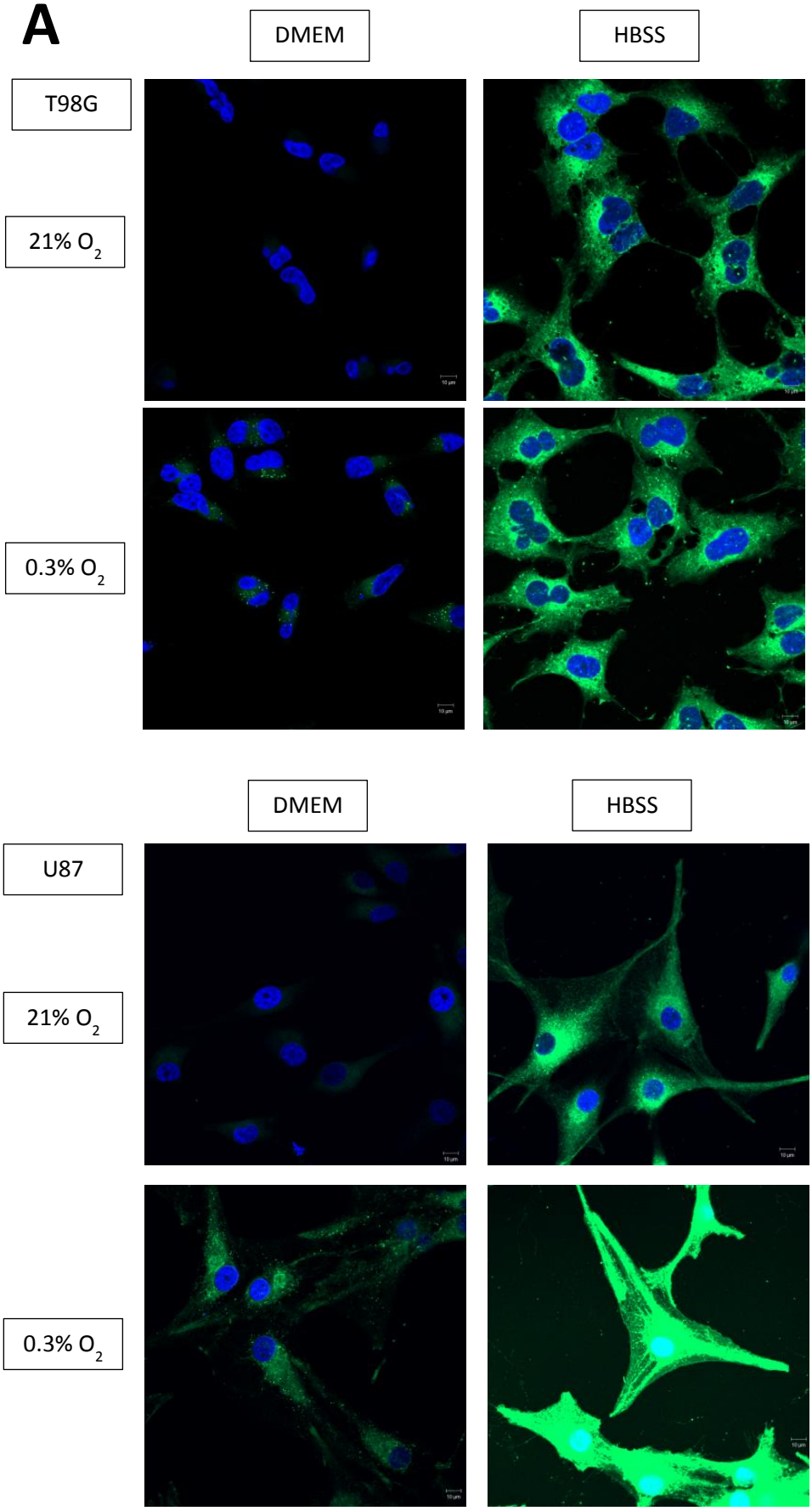
A
DMEM
HBSS
T98G
21% O2
0.3% O2
DMEM
HBSS
U87
21% O2
0.3% O2

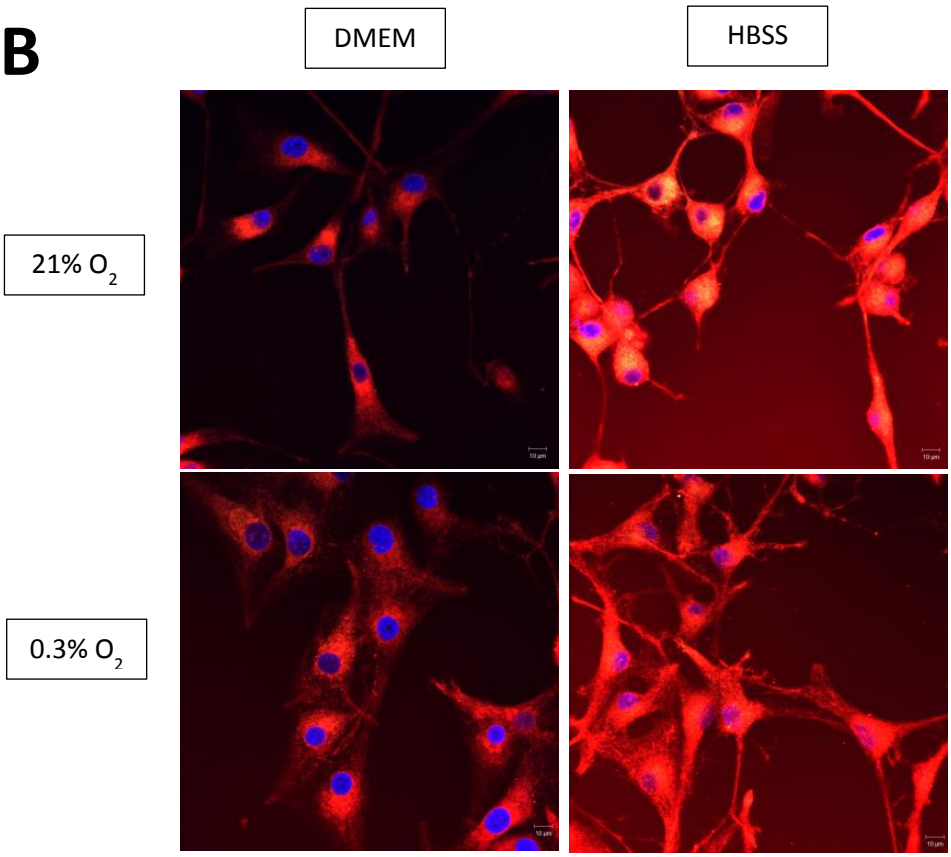

Figure 4.15. Starvation increases exogenous serum lipid uptake. A) Confocal microscopy images of T98G and U87 cells incubated with C16 BODIPY in DMEM or HBSS at 21% and 0.3% O_2. HBSS increased the uptake of C16 BODIPY compared to DMEM at 21% and 0.3% O_2 in both cell lines. Hypoxia also increased uptake of C16 BODIPY in DMEM and HBSS in both cell lines as previously shown in Figure 4.9. B) Confocal microscopy images of U87 cells incubated with C11 BODIPY in DMEM or HBSS at 21% and 0.3% O_2. HBSS increased the uptake of C11 BODIPY compared to DMEM in both 21% and 0.3% O_2.

As lipid uptake is altered in starvation conditions we hypothesised that the other mechanisms governing lipid droplet metabolism would also be altered. Atglistatin treatment in HBSS further decreased the FITC signal intensity of the U87 and U87.2 cell lines, but had no effect in the U343 and U87.1 cell lines (Figure 4.16.A.). In contrast, atglistatin treatment in HBSS increased the FITC signal intensity in the T98G cell line suggesting cell line-specific differences in the importance of ATGL in lipid droplet production under starvation conditions. Co-treatment with atglistatin and the autophagy inhibitor, 3-MA, in HBSS decreased the FITC signal intensity compared to the DMSO controls in the U343, U87 and U87.2 cell lines (Figure 4.16.B.). No significant differences were observed in the FITC signal intensity of the T98G and U87.1 cell lines. Interestingly, the FITC signal intensity following atglistatin and 3-MA co-treatment was decreased compared to 3-MA treatment alone in all 5 cell lines (Figure 4.16.C.). The extent of the decrease in LDQ varied between cell lines and defined whether LDQ was decreased compared to the DMSO control in Figure 4.16.B. This is further indication of cell line-specific differences in response to inhibition of lipid droplet metabolism pathways.

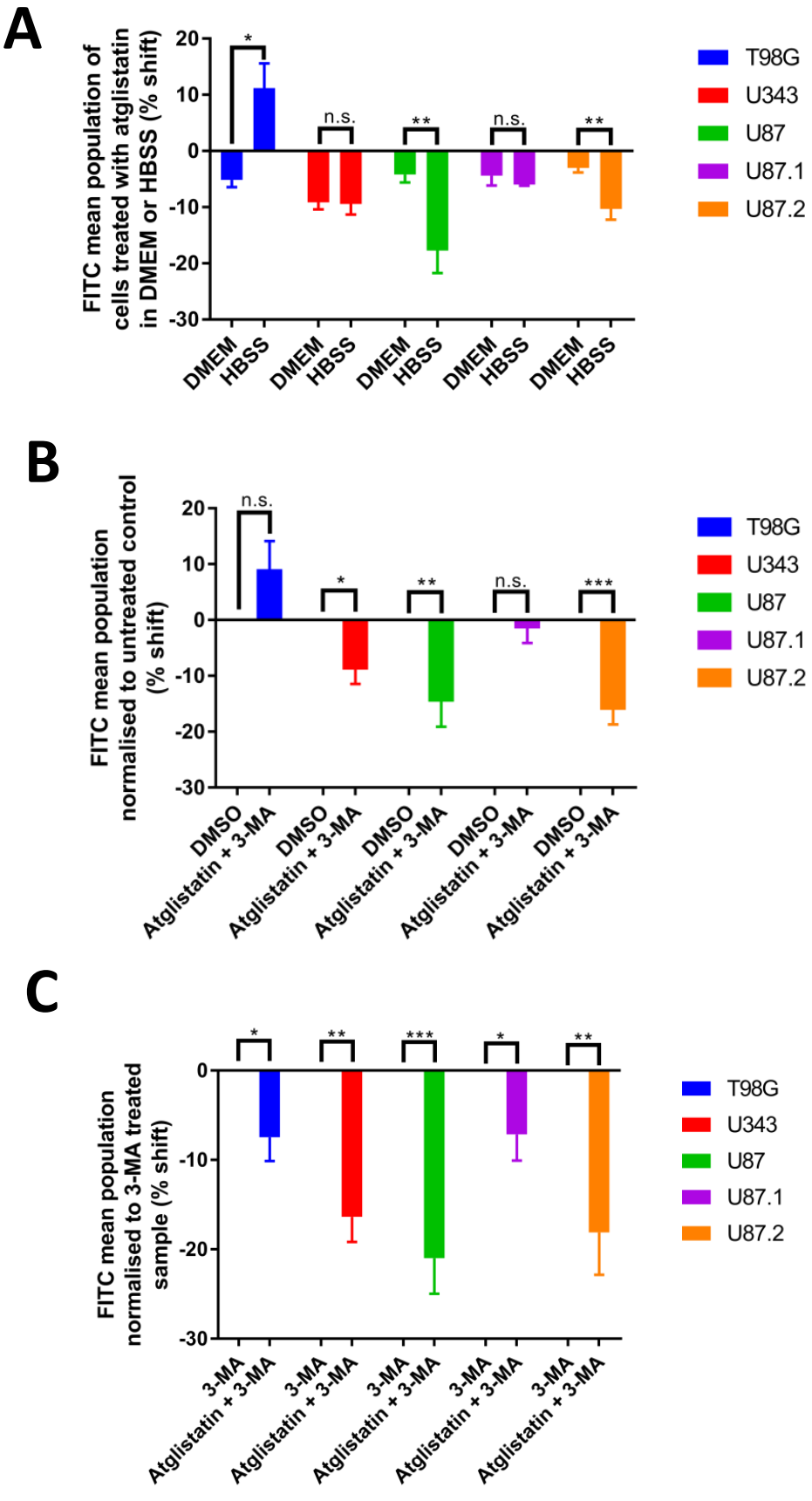
A
FITC mean population of cells treated with atglistatin in DMEM or HBSS (% shift)
20
10
0
-10
-20
-30
*
n.s.
**
n.s.
**
DMEM
HBSS
T98G
U343
U87
U87.1
U87.2
B
FITC mean population normalised to untreated control (% shift)
n.s.
*
**
n.s.
***
DMSO
Atglistatin + 3-MA
C
FITC mean population normalised to 3-MA treated sample (% shift)
*
**
***
*
**
3-MA
Atglistatin + 3-MA

Figure 4.16. Lipid droplets are in constant flux which is increased in starvation. A) Flow cytometry comparing the effect of atglistatin treatment in DMEM and HBSS in normoxia across all five nile red stained cell lines. The atglistatin treated FITC signal intensity in DMEM or HBSS was normalised to the DMSO control in DMEM or HBSS respectively. The resulting normalised population shifts in DMEM and HBSS induced by atglistatin treatment were plotted against each other. The atglistatin-induced decrease in LDQ was enhanced in HBSS in the U87 and U87.2 cell lines. This effect was not significant in the U343 and U87.1 cell lines and was reversed in the T98G cell line. Data shown as mean ±SEM, representative of several independent experiments (T98G n=3; U343, U87, U87.1, U87.2 n=4), analysed with an unpaired t-test; *p<0.05, **p<0.01, ***p<0.001, ****p<0.0001. B) Flow cytometry comparing the effect of atglistatin and 3-MA co-treatment with DMSO controls in normoxia across all five nile red stained cell lines. Atglistatin and 3-MA co-treatment decreased LDQ compared to the DMSO control in the U343, U87 and U87.2 cell lines. LDQ was unchanged in the U87.1 cell line and increased in the T98G cell line. The sample FITC signal intensity shift was normalised to the DMSO controls. Data shown as mean ±SEM, representative of several independent experiments (U87, U87.2 n=3; U343, U87.1 n=4; T98G n=5), analysed with an unpaired t-test; *p<0.05, **p<0.01, ***p<0.001, ****p<0.0001. C) Flow cytometry comparing the effect of 3-MA with 3-MA and atglistatin co-treatment in normoxia across all five nile red stained cell lines. 3-MA and atglistatin co-treatment decreased LDQ compared to the 3-MA treatment alone in all five cell lines. The 3-MA and atglistatin co-treatment sample population shift, according to FITC signal intensity, was normalised to each 3-MA treatment population. Data shown as mean ±SEM, representative of several independent experiments (U343 n=4; T98G, U87, U87.1 U87.2 n=5), analysed with an unpaired t-test; *p<0.05, **p<0.01, ***p<0.001, ****p<0.0001.

4.2.12. Lipid droplets are broken down for phospholipid membrane synthesis and fatty acid β-oxidation.

Two major lipid utilising pathways are energy production through mitochondrial β-oxidation and phospholipid synthesis for cell membranes (200,258). Confocal microscopy was used to investigate the fate of fatty acids originating from lipid droplets. In normoxic T98G and U87 cells under starvation conditions, C16 BODIPY was observed to accumulate in peri-nuclear regions that may be consistent with mitochondrial localisation (Figure 4.17.A.). This was not observed in hypoxia where C16 BODIPY was observed to instead accumulate in lipid droplets. Mitochondrial β-oxidation is decreased in hypoxia (259) and it is unsurprising that saturated fatty

acids are targeted to this pathway in normoxia only. C11 BODIPY was not observed to accumulate in this mitochondrial region in the U87 cell line suggesting that the C11 unsaturated fatty acid is primarily incorporated into cell membranes and lipid droplets. Inhibition of autophagy and lipid droplet breakdown with 3-MA increased the localisation of C16 BODIPY to lipid droplets and decreased its localisation in cell membranes in both normoxia and hypoxia (Figure 4.17.B.). This suggests that C16 BODIPY accumulates in lipid droplets prior to breakdown, conversion into phospholipids and subsequent incorporation in cell membranes. Inhibition of lipid droplet breakdown therefore would interrupt this pathway and prevent the integration of C16 BODIPY into the cell membrane.

4.2.13. Incubation in hypoxia decreases proliferation

Altered lipid droplet metabolism in hypoxia decreases β-oxidation energy production and membrane synthesis, impairing proliferation, although other mechanisms may be involved. Proliferation was assessed using cell growth curves across 144 hours. The proliferation of the T98G, U87, U87.1 and U87.2 cell lines was decreased upon incubation in hypoxia (Figure 4.18.).

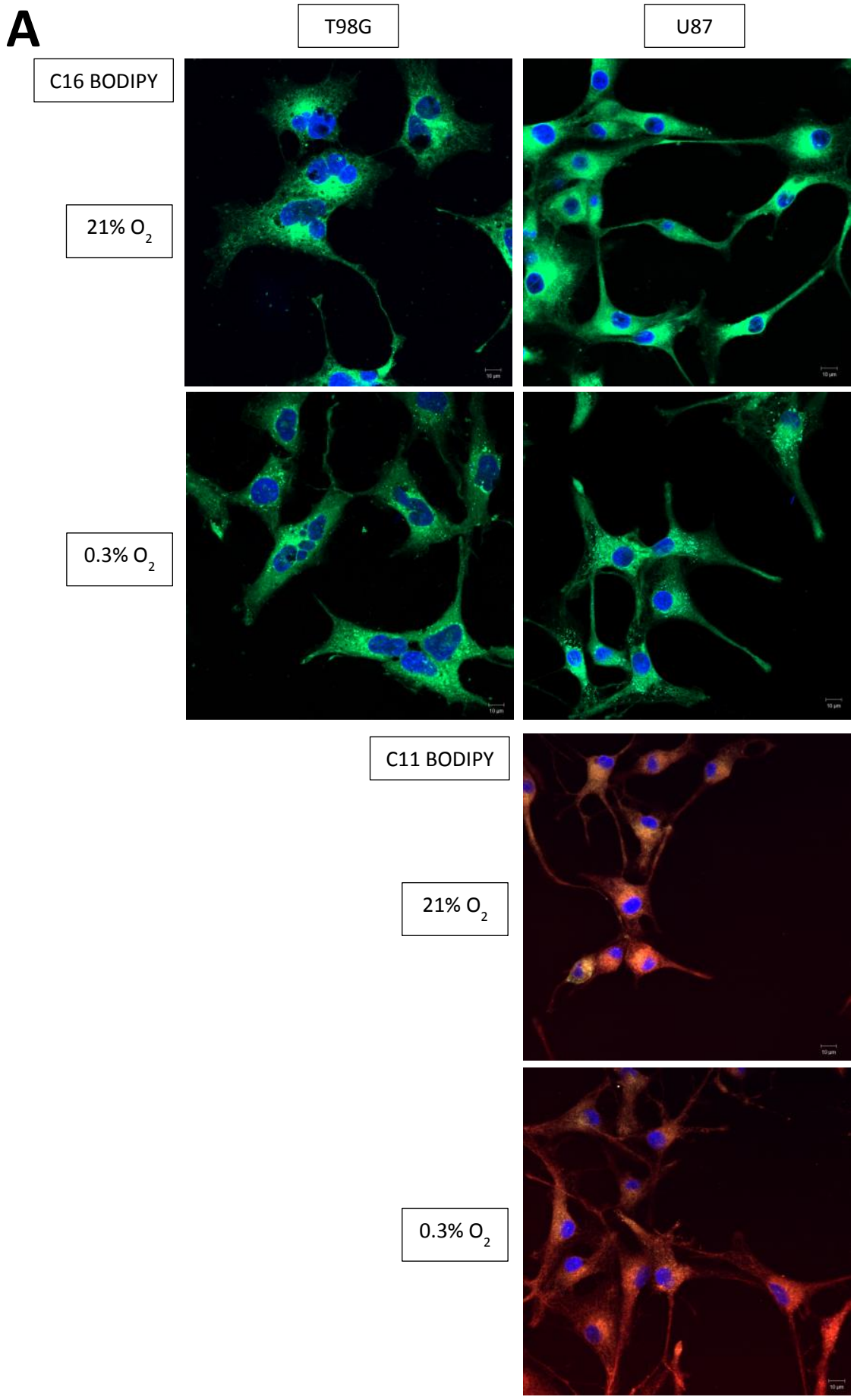
A
T98G
U87
C16 BODIPY
21% O2
0.3% O2
C11 BODIPY
21% O2
0.3% O2

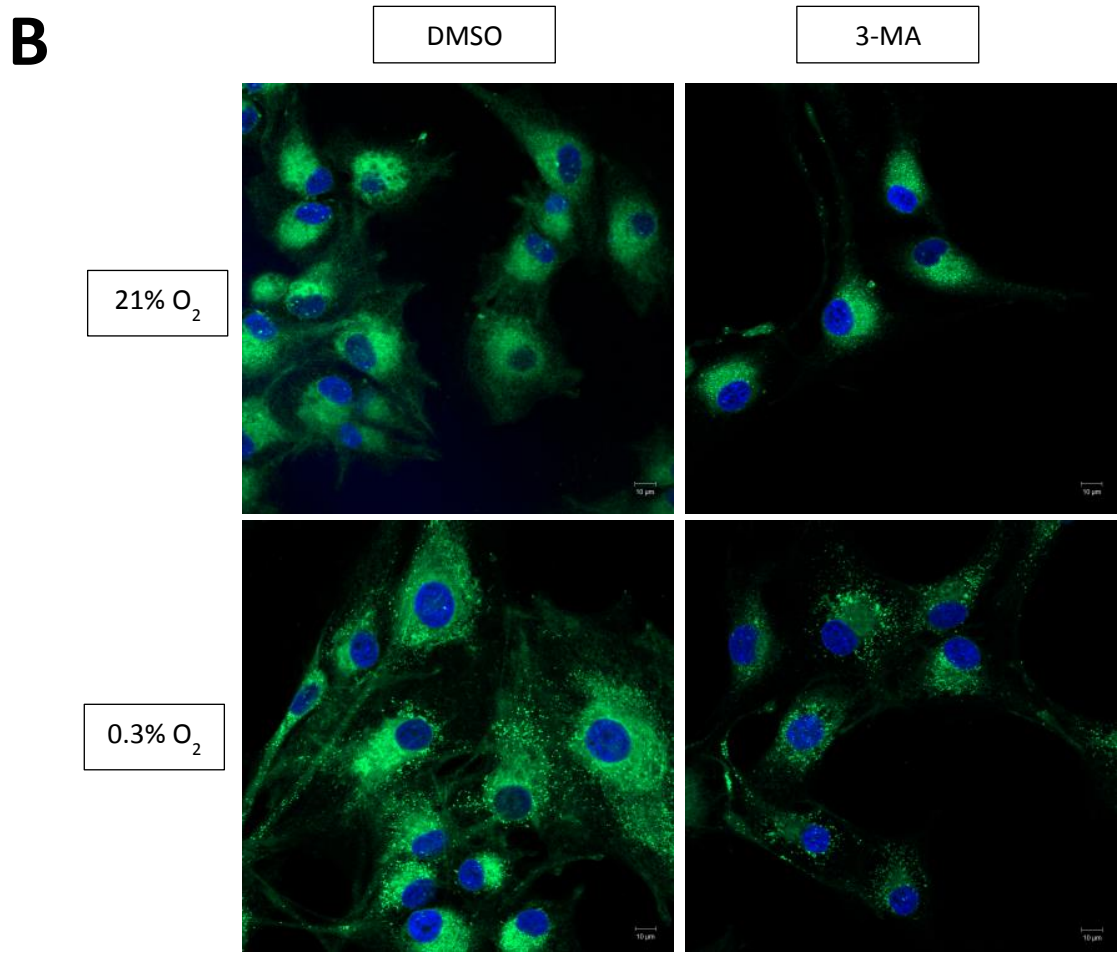

Figure 4.17. Lipid droplet lipids are used for β-oxidation and membrane synthesis. A) Confocal microscopy images of T98G and U87 cells incubated with C16 BODIPY and U87 cells incubated with C11 BODIPY in HBSS in 21% and 0.3% O_2. In normoxia C16 BODIPY accumulated in a peri-nuclear region that may be consistent with mitochondrial localisation whereas in hypoxia C16 BODIPY was localised to lipid droplets. C11 BODIPY did not accumulate in this region at 21% or 0.3% O_2. B) Confocal microscopy images of U87 cells incubated with C16 BODIPY prior to treatment with DMSO or 3-MA in DMEM at 21% and 0.3% O_2. 3-MA treatment increased the localisation of C16 BODIPY in lipid droplets and decreased localisation in cell membranes.

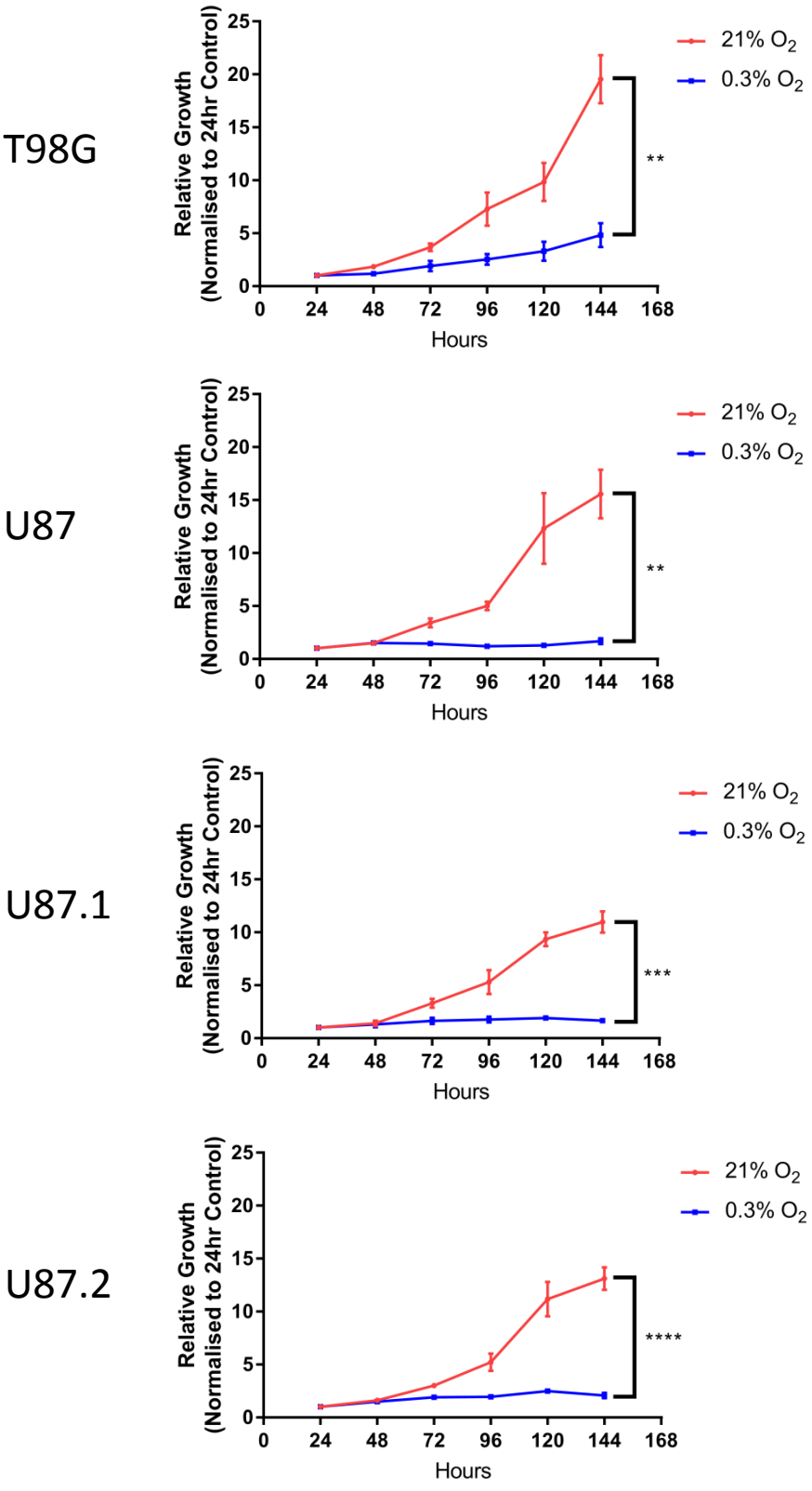

Figure 4.18. Hypoxia decreases proliferation. Cell count growth curves of T98G, U87, U87.1 and U87.2 cell lines at 21% and 0.3% O_2. Incubation in 0.3% O_2 significantly decreased the proliferation of all four cell lines compared to normoxia.

4.2.14 Lipid droplet saturation is altered in hypoxia.

The balance of saturated and unsaturated lipids within a lipid droplet can change in response to cellular processes and environmental pressures; however, the effect of hypoxia upon lipid droplet lipid saturation is unknown. Hypoxic incubation increased the relative concentration of both the total saturated and total unsaturated lipid groups detected by HRMAS NMR (Figure 4.19.A.). Importantly, the proportion of total unsaturated lipid was increased in hypoxic cells in both the U87 and U87.2 cell lines (Figure 4.19.B) suggesting a greater localisation of unsaturated lipids to lipid droplets in hypoxia. The hypoxia-induced increased saturated and unsaturated lipid peaks are shown in the example HRMAS spectra (Figure 4.19.C.). This change in saturation state may reflect a response to hypoxia-induced stress.

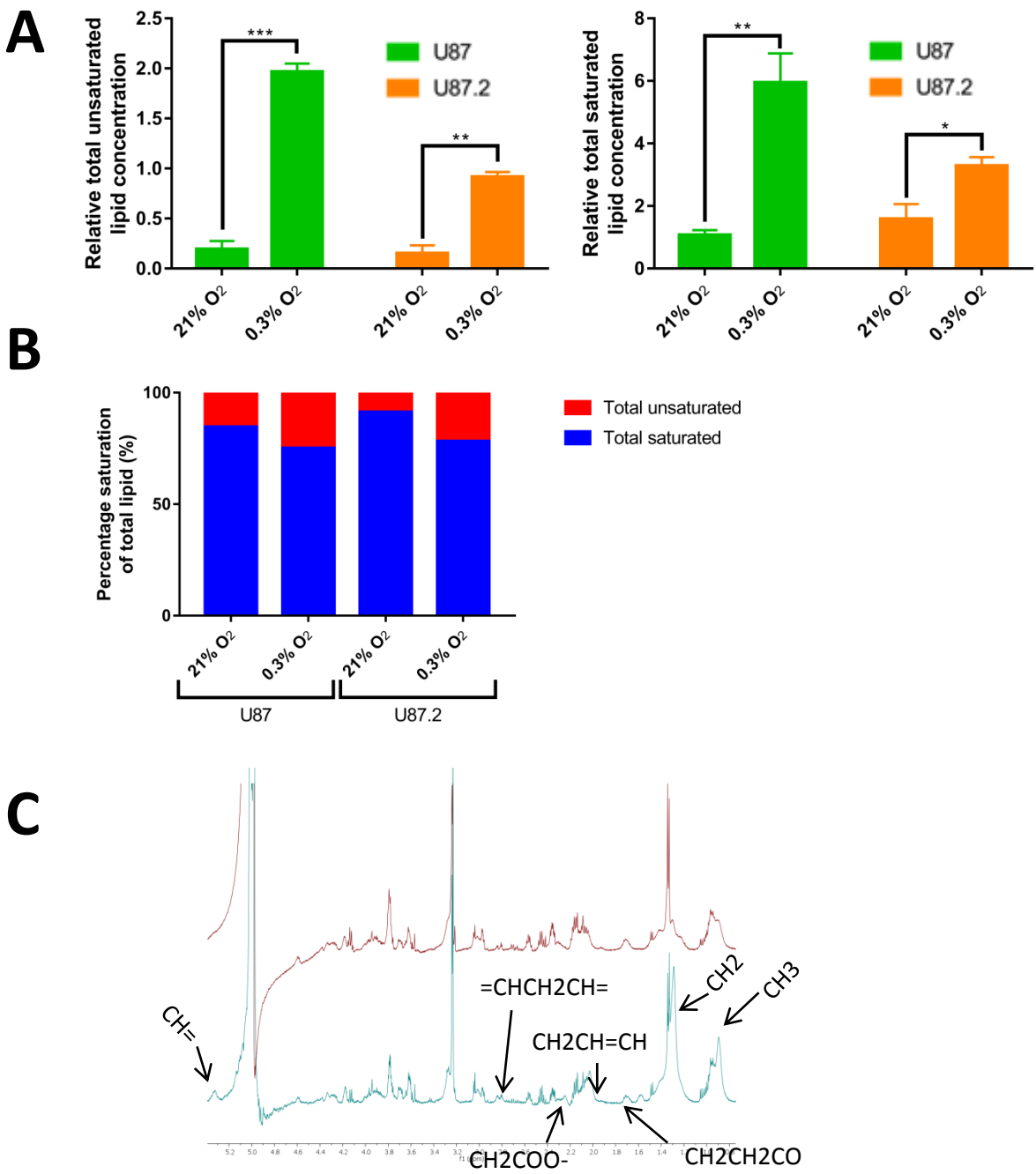

Figure 4.19. Hypoxia increases the amount of unsaturated lipid present in lipid droplets. A) Total unsaturated and saturated mobile lipid groups in U87 and U87.2 cells incubated at 21% or 0.3% O_2 for 24 hours, as measured by HRMAS NMR. Hypoxia increased the relative total unsaturated and total saturated lipid groups in both the U87 and U87.2 cell lines. Data shown as mean ±SEM, representative of several independent experiments (n=3); *p<0.05, **p<0.01, ***p<0.001, ****p<0.0001. Unsaturated and saturated lipid group concentrations were normalised to the total metabolite concentration of each sample. B) Representation of saturated and unsaturated lipid group concentrations as a proportion of total lipid group concentration in U87 and U87.2 cells. Hypoxia increased the proportion of total lipid which is unsaturated in both cell lines. C) Representative HRMAS spectra demonstrating the increased lipid concentration in hypoxia (bottom) compared to normoxia (top). The lipid groups are noted on the spectra (for nomenclature see Table 2.5).

4.2.15. ATGL activity protects unsaturated fatty acids from hypoxia-induced lipid oxidation.

C11 BODIPY undergoes a colour change from red to green upon oxidisation of its unsaturated carbon chain which can be caused by cellular oxidative stress. Confocal microscopy was used to observe the effect of atglistatin treatment on normoxic and hypoxic cells incubated with C11 BODIPY (Figure 4.20.). Hypoxia slightly increased the green C11 BODIPY stain intensity compared to the DMSO control. Hypoxia is known to increase ROS generation (225) and therefore increased oxidative damage is unsurprising. Interestingly, atglistatin treatment in hypoxia clearly increased the green C11 BODIPY stain intensity, representing a large increase in unsaturated fatty acid oxidative damage. Inhibition of ATGL activity could decrease the transport of unsaturated fatty acids to lipid droplets, preventing protective storage. Membrane unsaturated lipids are vulnerable to lipid oxidation and therefore increased damage would be observed. In contrast, atglistatin treatment in normoxia decreased the green C11 BODIPY signal intensity, indicating a different response to ATGL inhibition in the absence of oxidative stress, such as the upregulation of alternative anti-oxidant pathways.

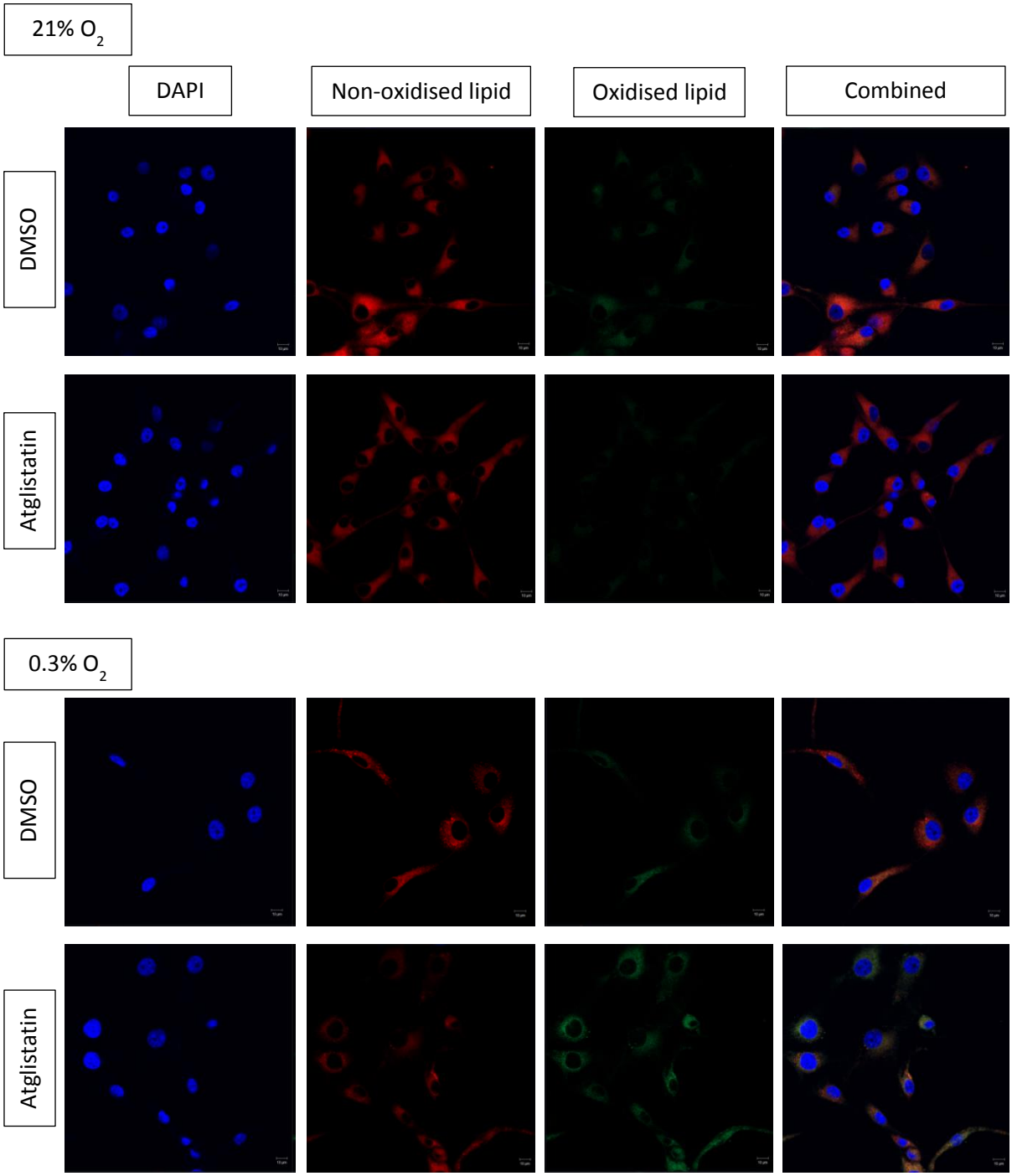

Figure 4.20. ATGL function is important to protect against ROS-induced lipid oxidation in hypoxia. Confocal microscopy images of U87 cells incubated with C11 BODIPY prior to 60 minute DMSO or atglistatin treatment. Atglistatin treatment increased the oxidation of C11 BODIPY in hypoxia resulting in a colour change of red to green, representative of increased lipid oxidation damage. There was a corresponding decrease in the non-oxidised C11 BODIPY in this sample. Atglistatin treatment decreased lipid oxidation damage in normoxia. There was no change in the non-oxidised C11 BODIPY in either normoxic sample or the hypoxic DMSO-treated sample. There was increased C11 BODIPY located in lipid droplets in the hypoxic DMSO-treated cells.

4.2.16. ATGL activity protects unsaturated fatty acids from ROS-induced lipid oxidation by H_2O_2 in normoxia.

The importance of ATGL in protecting unsaturated fatty acids from H_2O_2, a potent ROS, was investigated with confocal microscopy. Cells were incubated with C11 BODIPY prior to atglistatin, H_2O_2 or cisplatin treatment (Figure 4.21. and 4.22.). As seen in Figure 4.20, atglistatin treatment increased the green C11 BODIPY stain intensity in hypoxia reflecting increased oxidative damage. H_2O_2 increased the green C11 BODIPY stain intensity in normoxia and hypoxia, representing increased oxidation of the C11 unsaturated fatty acid. Interestingly, atglistatin and H_2O_2 co-treatment in normoxia further increased the green C11 BODIPY stain intensity suggesting that ATGL activity can protect unsaturated fatty acids against ROS generated by H_2O_2 treatment as well as hypoxia. Indeed, in hypoxia, the combination of H_2O_2 and hypoxia-induced ROS further increased lipid oxidation upon ATGL inhibition, represented by increased green C11 BODIPY stain intensity, reflecting increased oxidative damage.

In addition to damaging DNA the chemotherapeutic agent cisplatin is known to increase ROS generation (260). However, green C11 BODIPY stain intensity was decreased by cisplatin treatment alone and remained unchanged with atglistatin co-treatment. The numerous cytotoxic effects of cisplatin are a probable confounding variable in this result and the effect of cisplatin and atglistatin treatment on C11 BODIPY oxidation was not investigated in hypoxia.

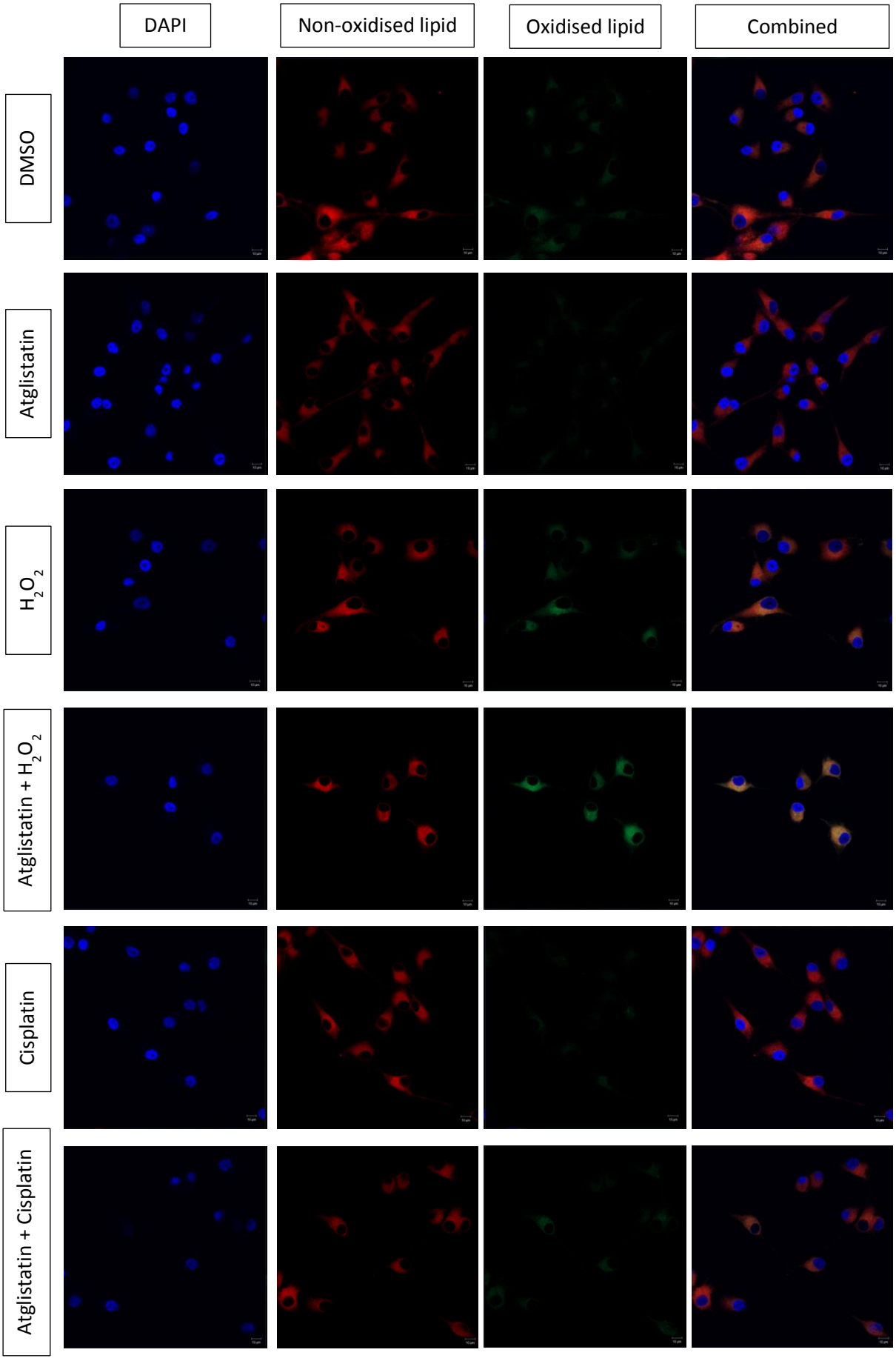
DAPI
Non-oxidised lipid
Oxidised lipid
Combined
DMSO
Atglistatin
H_2O_2
Atglistatin + H_2O_2
Cisplatin
Atglistatin + Cisplatin

Figure 4.21. ATGL function is important to protect against H_2O_2 ROS-induced lipid oxidation in normoxia. Confocal microscopy images of U87 cells incubated with C11 BODIPY prior to treatment with DMSO, atglistatin, H_2O_2, cisplatin, atglistatin with H_2O_2 or atglistatin with cisplatin in normoxia for 60 minutes. C11 BODIPY lipid oxidation was increased by H_2O_2 treatment and further increased by co-treatment with atglistatin and H_2O_2. Cisplatin and atglistatin co-treatment had no effect on C11 BODIPY lipid oxidation whereas cisplatin treatment alone decreased lipid oxidation.

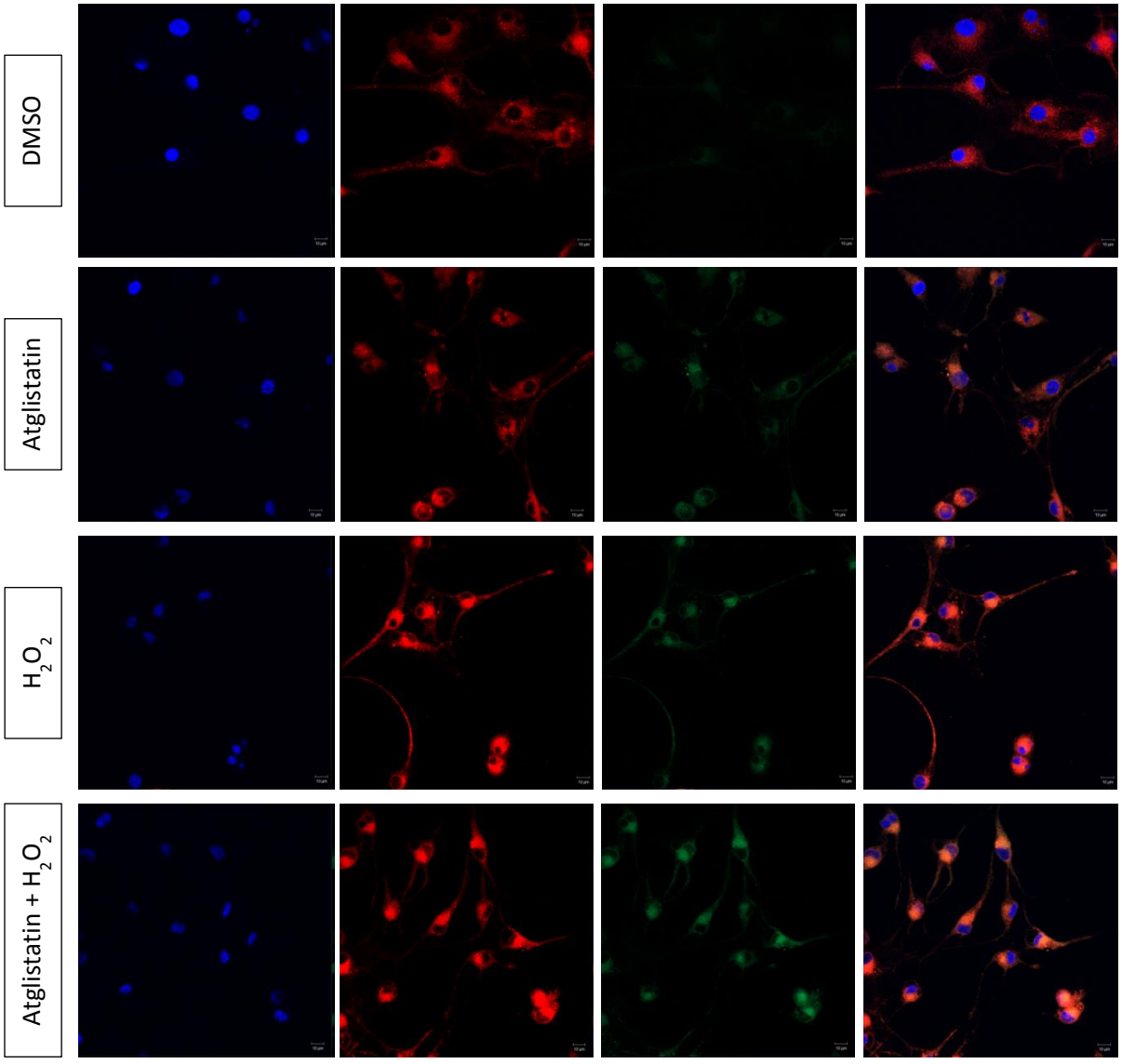

Figure 4.22. ATGL function is important to protect against H_2O_2 ROS-induced lipid oxidation in hypoxia. Confocal microscopy images of U87 cells incubated with C11 BODIPY prior to treatment with DMSO, atglistatin, H_2O_2 or atglistatin with H_2O_2 in hypoxia for 60 minutes. Atglistatin and H_2O_2 increased C11 BODIPY lipid oxidation compared to the DMSO-treated control. Co-treatment of atglistatin with H_2O_2 further increased C11 BODIPY lipid oxidation.

4.2.17. Genetic drift may be responsible for cell line specific differences

RNAseq analysis was performed upon the U87 clonal mutant cell lines during their characterisation. Gene abundance in key metabolic and cancer pathways was significantly altered between the U87.1 cell line and the other cell lines (Figure 4.23. and Table 4.1.), suggesting that this cell line has undergone significant genetic drift. In contrast, the U87 and U87.2 cell lines remained similar according to gene abundance. Nevertheless, these cell lines show clear differences throughout this chapter, most notably in hypoxia (Figures 4.12 and 4.14), suggesting these cell lines may differ through a key mutation. Indeed, this data suggests the genetic differences between the clonal mutants may be responsible for cell line-specific effects throughout this chapter.

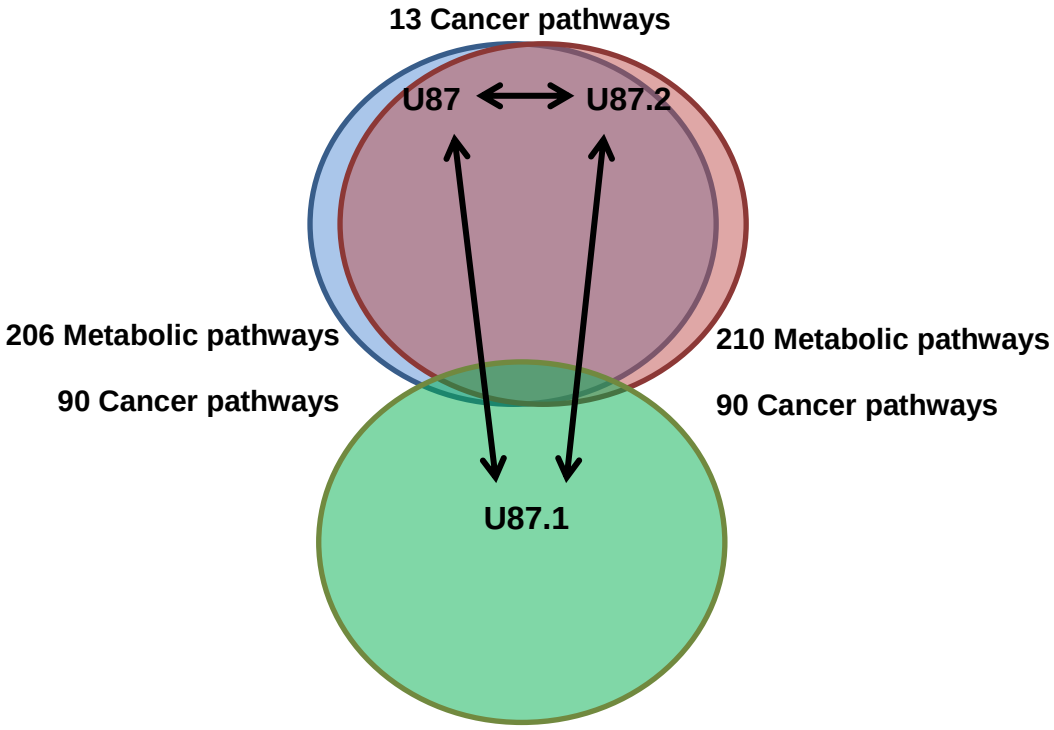

Figure 4.23. The U87.1 cell line shows clear separation from the remaining two cell lines which show distinct overlap. Representative visualisation of Table 4.1. Genes in key cancer and metabolic pathways have significant differences in gene abundance between the U87.1 and the other two cell lines. Conversely the U87 and U87.2 cell lines have similar gene abundance profiles.

Cell line comparison	Pathway name	Number of alterations
U87 and U87.1	Metabolic pathways	206
	Pathways in cancer	90
U87 and U87.2	Pathways in cancer	13
U87.1 and U87.2	Metabolic pathways	210
	Pathways in cancer	90

Table 4.1. Alterations in key pathways define clonal mutant cell lines. The U87.1 cell line clearly separates from the U87 and U87.2 cell lines. Table extracted from Appendix 7.11.

4.3. Discussion

4.3.1. Introduction

The pathways involved in lipid droplet metabolism have been partially characterised in a number of tissues and several cancers (248). Interestingly, whilst the involvement of each lipid droplet metabolic pathway is cell line-specific, several pathways including exogenous lipid uptake (123,152), *de novo* fatty acid synthesis (136,164,165), autophagy (174,179) and cytoplasmic lipases (174,196) are frequently observed to influence lipid droplet metabolism. However, despite characterisation in many cancers, lipid droplet metabolism remains poorly explored in gliomas. We therefore investigated and established the involvement of these metabolic pathways in GBM cell lines in both normoxic and hypoxic conditions.

4.3.2. The U87 clonal mutant cell lines

Animal models provide the most biologically relevant non-clinical model as implanted tumours will be exposed to many of the factors encountered in a human host such as the presence of other cell types, dietary nutrient supply and 3D structure. However, due to the high cost and ethical implications associated with these models, the majority of investigations are performed initially in cell lines. Cell lines provide a cheap, fast growing model to rapidly test perturbed cellular processes in pathological states; however, they are further removed from the clinical setting, increasing the chance of *in vitro* artefacts. Importantly, the intrinsic genetic instability of cancer cell lines ensures they are affected by genetic drift, wherein mutations accumulate over countless replication events, creating clonal mutant cell lines with an altered genetic

profile from the original line. These mutations are typically silent but can affect key cellular processes and identical cell lines can differ genetically between labs. Nevertheless, through genetic characterisation of serendipitous alterations in relevant genes, clonal mutant cell lines can become natural investigative resources and provide further insight into the mechanistic ‘wiring’ of near identical cells.

Through STR profile analysis and RNA sequencing we sought to investigate this phenomenon in the U87, U87.1 and U87.2 cell lines. STR profile analysis can characterise a genetic ‘barcode’ individual to each cell line, found to be identical between the three cell lines (Appendix 7.10). Therefore, the three cell lines derive from the same original parent line; the U87 adult GBM cell line available from the ATCC. RNA sequencing revealed a high number of significantly altered gene abundance values between the U87.1 and the two other cell lines including genes impacting on many important metabolic pathways (Appendix 7.11.). This indicates increased genetic drift and an earlier divergence from the parent cell line (Figure 4.24.). In contrast, the U87 and U87.2 cell lines have far fewer significant alterations in gene abundance indicating a more similar genetic profile. However, the contrasting response of these two cell lines to pharmacological manipulation, most notably in the case of atglistatin treatment in hypoxia (Figure 4.12.B.), rules out identical cell lines. Therefore, we propose that these cell lines are separated by currently unknown epigenetic alterations or a key metabolic mutation which may be revealed through further analysis of the RNA sequencing data. Despite being limited to gene abundance, the RNA sequencing data provides strong evidence that the U87, U87.1 and U87.2 cell lines are clonal mutants which may be vital tools in further understanding lipid droplet metabolism.

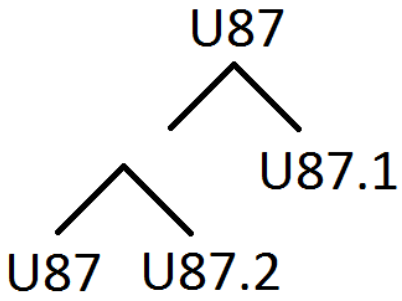

Figure 4.24. The proposed differentiation pathway of the U87 clonal mutant cell lines

The creation of these clonal mutant cell lines serves to further highlight the role genetic drift can play in altering the biological activity of a cell line. Whilst measures exist to minimise the impact of genetic drift, cell lines originating from different labs may still contain influential genetic alterations. Therefore it remains essential to characterise cell lines prior to publication and to support this data with similar cell lines and more physiologically relevant models.

This data also provides a strong explanation for the cell line-specific differences observed throughout this chapter. Importantly, the significant difference in response to atglistatin and chloroquine treatment in hypoxia between the U87 and U87.2 cell lines (Figures 4.12 and 4.14.), despite similar gene abundance values, suggests mutational status may be an important factor in determining lipid droplet metabolic pathway activity. In this case, the otherwise similar genetic profile of these clonal mutants may highlight the genes governing hypoxic lipid droplet metabolism. Future studies should therefore aim to utilise these cell lines to characterise critical regulatory genes, through associating altered responses to pharmaceutical manipulation of lipid droplet metabolic pathways with alterations in gene expression and mutation. Elucidating this genetic control could have far reaching implications in

understanding patient-specific biology as well as identifying target groups for any resulting lipid droplet-related therapeutic strategies. Indeed, considering the importance of hypoxia in lipid droplet metabolism and its prevalence in GBMs, this may prove vital to the full manipulation of lipid droplet metabolism.

Finally, through similar characterisation of the remaining 2 cell lines, a genetic profile data set could be created, allowing the investigation of cell-line specific differences in future studies of these 5 cell lines. As discussed for hypoxic lipid droplet metabolism in this study, the rapid identification of potential regulatory genes, followed-up with targeted gene silencing could prove a powerful investigative tool for future researchers.

4.3.3. Lipid droplet production in normoxia – Exogenous serum uptake

Activated charcoal is long established as a methodology for removing lipids from serum and other biological samples (261,262). Lipids are adsorped onto the porous surface of the charcoal which can then be filtered out. This produces lipid-free serum whilst preserving the many other important components of serum such as growth factors. Moreover, this step is performed prior to media supplementation preserving the media contents.

It has been reported in many cell types that lipid droplet production may rely upon the uptake of exogenous serum lipids (123,150,152). Indeed, in chapter 3 we observed a correlation between gene expression of the exogenous lipid uptake transporter CD36 and the lipid droplet-associated proteins adipophilin and TIP47 suggesting an important association between lipid droplets and exogenous lipid uptake. Interestingly, Bensaad et al. (123) reported that growth in de-lipidated serum

in normoxia resulted in increased accumulation of lipid droplets in the U87 cell line. However, in contrast to our experiment, they compared cells grown in media supplemented with 10% standard or 1% de-lipidated serum. The decreased supplementation will change the amount of metabolites and growth factors to which the cells are exposed, a factor known to alter LDQ (263,264). By maintaining supplementation at 10% we sought to avoid the introduction of this variable and potential cell stress responses. Using confocal microscopy and flow cytometry we demonstrated that, in the absence of the exogenous lipid pool, all 5 cell lines have a lower LDQ (Figure 4.1.). Moreover, C16 BODIPY, an exogenously supplied fatty acid, was taken up and incorporated into lipid droplets further supporting exogenous lipid uptake as a lipid droplet production mechanism (Figure 4.25.). Exogenous serum provides an excellent source of lipids for a rapidly proliferating cell as adequate access to blood vessels will ensure supply remains constant. However, in tumours such as GBM, increased cellularity and ineffective angiogenesis ensures blood supply is frequently insufficient and it is therefore unlikely that lipid droplet production would rely upon a single mechanism. Moreover, LDQ would therefore vary across the tumour, and this has been observed in *in vivo* MRS studies (94,265).

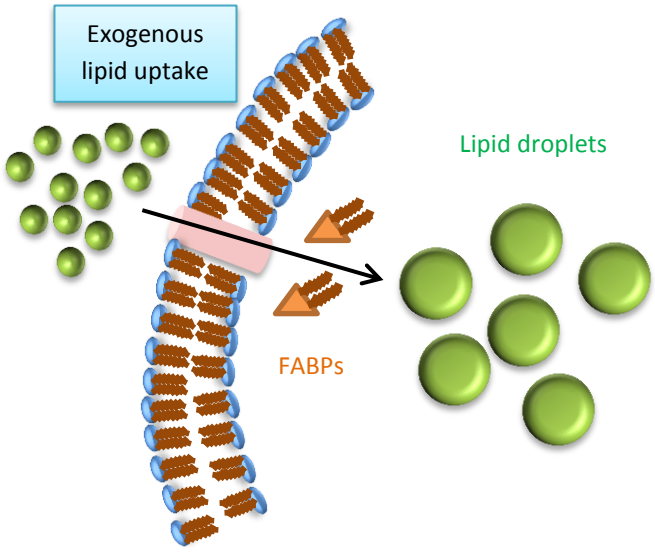

Figure 4.25. Exogenous lipid uptake is an important lipid droplet production pathway in normoxia. Fatty acid binding protein (FABP).

4.3.4. Lipid droplet production in normoxia – The role of ATGL

ATGL catalyses the rate-limiting step in the lipolysis of TAGs and has been reported in many cell types to have an important role in lipid droplet breakdown (174,194). Interestingly, we observed in chapter 3 that high expression of PNPLA2, the gene encoding ATGL, was associated with lipid droplet-associated genes and decreased survival, suggesting an important role in glioma lipid droplet metabolism and tumour viability. Atglistatin is a competitive ATGL inhibitor established to work *in vitro* and *in vivo* (266). Inhibition is selective for ATGL and has been reported to have no effect on hormone sensitive lipase, monoglyceride lipase, pancreatic lipase, lipoprotein lipase and other lysophospholipases. Although ATGL has previously been implicated in lipid droplet breakdown (174), we observed that ATGL inhibition decreased LDQ, suggesting a role for ATGL in lipid droplet production (Figure 4.2.). Interestingly, with the exception of the T98G cell line, this effect was enhanced in starvation conditions. As HBSS does not contain exogenous lipids, this enhanced decrease in LDQ is likely attributable to the combined effect of losing two lipid droplet sources simultaneously and emphasises the importance of these two pathways in lipid droplet metabolism.

As the primary role of ATGL is to facilitate the degradation of lipids, a role in lipid droplet production was unexpected. However, ATGL is known to be associated with cell membranes as well as lipid droplets (189). Hofer et al. (192) found that CGI-58, a potent activator of ATGL activity, interacts with fatty acid binding proteins (FABPs) including H-FABP, also known as FABP3. Bensaad et al. (123) established that FABP3 was critical to lipid droplet production through the shuttling of lipids in the U87 cell line. We therefore propose that ATGL functions at the cell membrane to release fatty acids which are subsequently transported to lipid droplets by FABPs

(Figure 4.26). Thus inhibition of ATGL activity with atglistatin would result in decreased lipid droplet production.

The effect of ATGL inhibition on unsaturated fatty acid release from cell membranes could not be confirmed using C11 BODIPY due to the weak signal intensity and oxidation-induced colour change in hypoxia (Figure 4.3.). However, inhibition of ATGL decreased the concentration of unsaturated fatty acids in lipid droplets suggesting that ATGL mediates the release of unsaturated fatty acids destined for lipid droplets. Similarly, the increase in cell membrane C16 BODIPY accumulation following atglistatin treatment further supports the release of fatty acids by ATGL at the cell membrane. However, saturated fatty acid concentration in lipid droplets was increased by ATGL inhibition suggesting that, although saturated fatty acids may be released from the cell membrane by ATGL, they are not destined for lipid droplets. Therefore, we suggest that ATGL can release both saturated and unsaturated fatty acids from the cell membrane but that the ATGL-mediated lipid shuttle is responsible for the specific transport of unsaturated fatty acids to lipid droplets (Figure 4.26). The reason for this lipid shuttle is discussed in section 4.3.14.

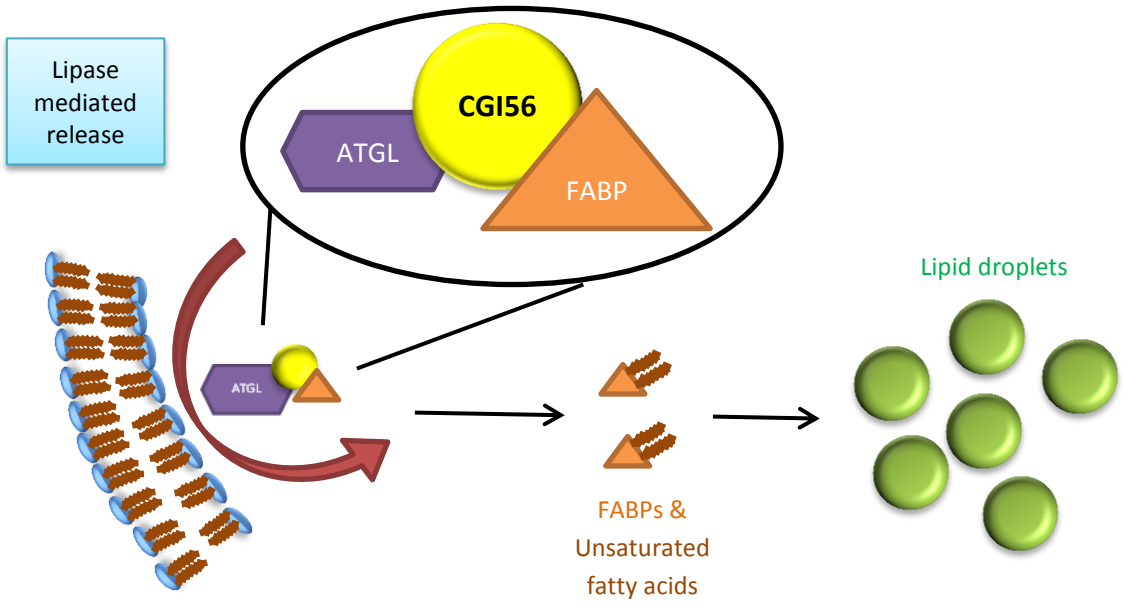

Figure 4.26. The ATGL-mediated unsaturated fatty acid shuttle. ATGL is activated by CGI58 and releases unsaturated fatty acids from the cell membrane which are transported to lipid droplets by FABPs. Fatty acid binding protein (FABP).

It is important to note that this work does not rule out an alternative source of unsaturated fatty acids which must be addressed in future experiments. Labelled unsaturated fatty acids should co-localise with FABPs in the cytoplasm as well as with ATGL, CGI58 and lipid droplets. Moreover, FABP knockdown should interrupt the lipid shuttle and result in a decreased lipid droplet unsaturated fatty acid concentration, although this may also impact other lipid droplet production mechanisms such as exogenous lipid uptake. Finally, alterations in lipid droplet saturation could be confirmed using mass spectrometry, providing greater insight into changes in the concentrations of specific fatty acids. Nevertheless, our data demonstrate an important role for ATGL in normoxic lipid droplet production.

4.3.5. Lipid droplet production in normoxia – *De novo* lipid synthesis

There is a growing body of evidence for the upregulation of enzymes involved in *de novo* fatty acid synthesis in many types of cancer (156,160,161) whilst lipid pre-cursors such as glucose and glutamine have been reported as a source of lipid droplets in several cell lines (136,164,165). BPTES is a non-competitive inhibitor of GLS1, inhibiting the conversion of glutamine to glutamate for entry into the TCA cycle. The contrasting effects of BPTES treatment on LDQ in the T98G and U87 cell lines (Figure 4.4.) suggest cell line-specific differences in the importance of this pathway. The data suggests a minor role for glutamine in lipid droplet production in the U87 cell line whereas alternative lipid droplet production pathways may be

upregulated in T98G cells or the cells may undergo a stress response. Interestingly, Bensaad et al. (123) reported that U87 GBM cells and MCF-7 breast cancer cells have an increased accumulation of lipid droplets in glutamine-free media in normoxia. However, GLS1 inhibition and the complete absence of glutamine in glutamine-free media may induce different cellular responses. Indeed, many cancers, including some gliomas, have been observed to be “glutamine addicted” (81,82), and this may account for these contrasting results.

The FASN inhibitor, orlistat, increased LDQ in both the T98G and U87 cell lines (Figure 4.4.); however, this may be due to a cell stress response as orlistat is known to affect several off-target proteins including metabolic enzymes and heat shock proteins (267). Therefore, it cannot be concluded that fatty acid synthesis has no role in lipid droplet production; however, it would appear unlikely that it has a significant role in these cell lines under normoxic conditions. A more selective FASN inhibitor such as C75 may provide further information in future studies.

Cholesterol constitutes an important component of lipid droplets and requires synthesis or uptake (255). We observed a small increase in LDQ in several of the cell lines upon inhibition of cholesterol synthesis with the HMG CoA reductase inhibitor, simvastatin (Figure 4.5.). A similar result was observed in embryonic kidney and pancreatic cancer cell lines wherein the authors propose compensatory upregulation of cholesterol uptake and fatty acid synthesis (268) whilst cholesterol uptake has been shown to be of vital importance in oestrogen receptor negative breast cancer (269). Although a similar compensatory upregulation of cholesterol uptake in these cell lines may be uncovered through further investigation, our data demonstrates that cholesterol synthesis is unlikely to have a major role in lipid droplet production in these cell lines.

The importance of *de novo* lipid synthesis precursors in many aspects of the cell metabolism hinders the interpretation of lipid droplet-specific effects. However, we observed in chapter 3 that increased expression of *de novo* fatty acid synthesis genes was associated with a better survival and lower clinical grades. Moreover, expression of these genes did not correlate with the expression of known lipid droplet markers such as the lipid droplet-associated proteins adipophilin and TIP47. This suggests that *de novo* fatty acid synthesis may not be of vital importance in lipid droplet metabolism, particularly in GBM cell lines. Therefore, whilst we can conclude that *de novo* lipid synthesis is important to the overall cell metabolism and may impact lipid droplet production in other cancers, we have been unable to characterise a major role for this pathway in glioma lipid droplet metabolism.

4.3.6. Lipid droplet breakdown in normoxia – Autophagy

The importance of autophagy in the production of lipid droplets has been noted in several cell types (174,175). However, its importance in the degradation of lipid droplets is also well established, most notably in hepatocytes (179). We chose to investigate this pathway, in the context of lipid droplet metabolism, using early and late stage autophagy inhibitors. 3-MA prevents autophagosome initiation through inhibition of type III phosphatidylinositol 3 kinases (270) whilst chloroquine inhibits late stage autophagy through the prevention of autophagosome-lysosome binding (271). By targeting different stages of autophagy we hoped to decrease the risk of off-target drug effects. Moreover, this could be further tested through siRNA knockdown of the vital autophagy protein Atg5. All three methods of autophagy inhibition resulted in increased LDQ (Figures 4.6. and 4.7.) strongly implicating

autophagy as a lipid droplet breakdown mechanism (Figure 4.27.). Moreover, autophagy inhibition caused the accumulation of C16 BODIPY in lipid droplets (Figure 4.7.) further demonstrating the inhibition of lipid droplet turnover. Interestingly, autophagy inhibition in HBSS continued to increase LDQ (Figure 4.6.), despite the absence of the exogenous serum lipid pool, suggesting that the loss of one lipid droplet production mechanism may be compensated for using alternative pathways. Taken together our data suggests that lipid droplet breakdown in GBM cell lines occurs through autophagy and that inhibition of this pathway can cause the accumulation of lipid droplets.

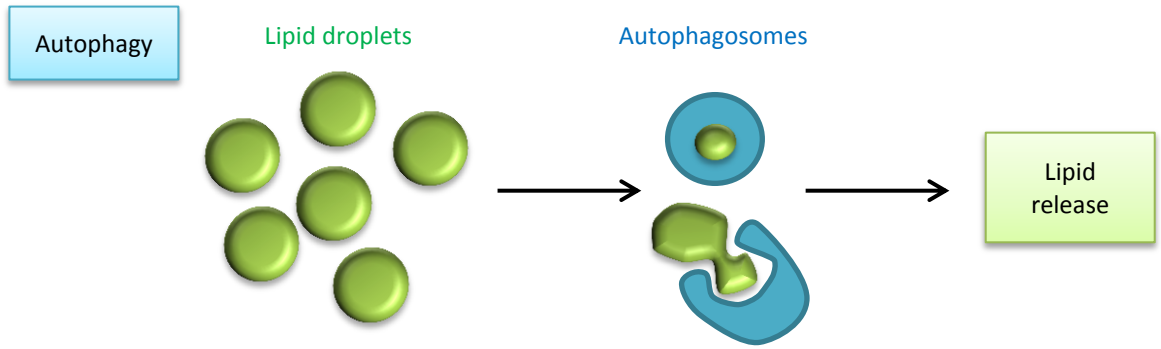

Figure 4.27. Lipid droplets are broken down by autophagy in these cell lines.

4.3.7. The role of hypoxia in lipid droplet metabolism

In line with the current literature (123), we found that hypoxia increased LDQ in a HIF1α-dependent manner in all 5 of our cell lines (Figures 4.8. and 4.9.), indicating this is a common feature of GBM. This was further supported by HRMAS NMR, providing an important link between *in vitro* studies of lipid droplet biology and *in vivo* MRS. This data also shows the increased effect of hypoxia upon total lipid concentration relative to metabolite concentration, further demonstrating the scale of increase in hypoxic lipid droplet metabolism and its clear importance. Moreover, this

dramatic increase may reflect a response to hypoxia-induced stress, as discussed further in section 4.3.14.

4.3.8. Lipid droplet production in hypoxia – Exogenous serum uptake

In chapter 3, we observed a correlation between lipid droplet-associated proteins including the hypoxic lipid droplet protein HIG2 and the lipid uptake transporter CD36, further suggesting lipid droplets may be associated with exogenous lipid uptake in hypoxia. Indeed, as exogenous lipid uptake contributed to lipid droplet production in normoxia, we investigated its role in the increased LDQ in hypoxia. Although significance was not reached in every cell line, a clear trend is demonstrated (Figure 4.10.), suggesting access to the exogenous lipid pool is important to maintaining lipid droplet production. Bensaad et al. (123) also reported a role for exogenous lipid uptake in hypoxic lipid droplet production in the U87 cell line although, as previously noted, this relied upon decreased supplementation as well as de-lipidation of serum. Interestingly, we observed a greater LDQ decrease in cells incubated in de-lipidated serum in hypoxia in the majority of the cell lines compared to the corresponding experiment in normoxia. This implies hypoxic lipid droplet breakdown continues in the absence of the exogenous lipid pool, depleting the increased hypoxic LDQ. Moreover, the increased uptake of the saturated C16 BODIPY fatty acid, and to a lesser extent the unsaturated C11 BODIPY fatty acid, in hypoxia (Figure 4.11.) suggest that increased uptake from this exogenous lipid pool may contribute to increased LDQ in hypoxia. Therefore, the uptake of exogenous serum lipids appears to be an important factor in lipid droplet production in hypoxia as well as normoxia.

4.3.9. Lipid droplet production in hypoxia – The role of ATGL

The role of ATGL in hypoxia is relatively unexplored, remaining limited to adipocytes in hypoxic exercise (272) and cardiac myocytes in ischaemia (273). Importantly a role for ATGL in hypoxic lipid droplet metabolism has not been investigated. The U343 cell line demonstrated a similar role for ATGL in lipid droplet production as in normoxia (Figure 4.12.). Similarly, this is supported by the non-significant trend observed in the T98G, U87 and U87.1 cell lines. The effect of ATGL inhibition in hypoxia may be smaller in these cell lines due to a compensatory increase in exogenous lipid uptake in hypoxia. In contrast, the significant decrease in LDQ in the U87.2 cell line could suggest that ATGL is the main lipid droplet production pathway in this cell line under hypoxic conditions, without which the cell cannot adequately compensate. Moreover, it could indicate increased importance for the shuttling of fatty acids to lipid droplets in hypoxia within this cell line. The different response of this cell line to ATGL inhibition emphasises the importance of understanding cell line-specific differences in lipid droplet metabolic pathway activity. Moreover, further comparison with the U87 clonal mutant may reveal genetic factors influencing ATGL activity in hypoxic lipid droplet metabolism.

4.3.10. Lipid droplet production in hypoxia – *De novo* synthesis

Hypoxia has been shown to induce a switch from pyruvate metabolism to reductive carboxylation as the major source of *de novo* fatty acid synthesis (31). Although Bensaad et al. (123) observed decreased labelled pyruvate incorporation in lipids in hypoxia in the U87 cell line, they found culturing U87 cells in glutamine-free media in hypoxia increased lipid droplet accumulation, suggesting glutamine was not used to

produce lipid droplets in this cell line. In conjunction with this, we found no clear role for GLS1 in lipid droplet production in hypoxia (Figure 4.13.). Moreover, inhibition of FASN in hypoxia with orlistat did not decrease LDQ; however, as previously discussed, we cannot discount off target effects. Nevertheless, the literature (123,155) strongly indicates *de novo* fatty acid synthesis does not have a major role in hypoxic lipid droplet metabolism in glioma cell lines, further supporting our data. This also supports the importance of other lipid droplet production mechanisms, such as increased exogenous lipid uptake.

Cholesterol synthesis was not further investigated in hypoxia due to the small LDQ effects observed in normoxia (Figure 4.5). Whilst the relationship between hypoxia, cholesterol synthesis and lipid droplets could be further investigated in future studies with drugs such as simvastatin, GBMs have been shown to downregulate cholesterol synthesis in favour of uptake (274). Taken together with the data regarding *de novo* fatty acid synthesis in GBMs and the small effect on LDQ in normoxia, this suggests a role in lipid droplet metabolism is likely to continue to be minor and was, therefore, not further investigated within this project.

4.3.11. Lipid droplet breakdown in hypoxia – Autophagy

We observed a clear role for autophagy as a lipid droplet breakdown mechanism in normoxia; however, its role in hypoxia is less clear. In the T98G and U87 cell lines autophagy inhibition caused lipid droplet accumulation (Figure 4.14.) suggesting a continued role in lipid droplet breakdown. In contrast, LDQ was decreased by autophagy inhibition in hypoxia in the U343, U87.1 and U87.2 cell lines. Decreased LDQ from autophagy inhibition could suggest that autophagy becomes a lipid droplet

production mechanism in hypoxia. Indeed, autophagy has been reported as an important mechanism for lipid droplet production in several cell types (174,175), although this would require significant metabolic alterations. Alternatively, a compensatory lipid droplet breakdown mechanism may catabolise lipid droplets in the absence of autophagy. Indeed, cytoplasmic lipases have been observed as lipid droplet breakdown mechanisms in several cancers (195-197) and are interlinked with the process of autophagy (198,199). An alternative lipid droplet breakdown pathway with increased lipid droplet clearance, activated by autophagy inhibition, may explain the decreased LDQ observed in these cell lines. Interestingly, increased LDQ is frequently associated with higher clinical grades (240,241) and hypoxia (94,123) implying that hypoxic lipid droplet accumulation must confer a survival benefit. Indeed, in chapter 3, high expression of autophagy proteins was associated with poor survival and correlated with high HILPDA expression. A compensatory pathway would be suppressed in favour of autophagy; however, excessive intracellular lipid accumulation induces lipotoxicity and therefore autophagy inhibition may necessitate the activation of this pathway. Nevertheless, establishing an alternative pathway in these cell lines for hypoxic lipid droplet breakdown requires further investigation.

4.3.12. Lipid droplet flux may be maintained during metabolic pathway inhibition through alternative pathway upregulation.

Starvation increases the metabolic demand placed upon cellular pathways to maintain energy production which can be achieved through upregulating the catabolism of cellular components including lipid droplets (174). Starvation

conditions can be mimicked using HBSS which contains no exogenous lipid pool or *de novo* fatty acid precursors. As expected, uptake of the C16 and C11 BODIPY fatty acids was increased in starvation conditions (Figure 4.15.) reflecting the importance of the exogenous lipid pool in the cell metabolism. Interestingly, despite increased metabolic demand, LDQ was at least partially maintained under starvation conditions suggesting compensation with alternative lipid droplet production mechanisms.

Starvation conditions increased the effect of atglistatin by decreasing LDQ (Figure 4.16.). Lipid droplets could be further depleted in this case by increased starvation-induced lipid droplet breakdown during impaired lipid droplet production. Alternatively, simultaneous loss of exogenous lipid uptake, ATGL activity and the exogenous *de novo* fatty acid synthesis pre-cursors may further impair lipid droplet production (Figure 4.28). Indeed, the increased LDQ in the T98G cell line may represent a stress response to the combined loss of these pathways.

If starvation increases the metabolic need for lipid droplet breakdown then flux may continue until lipid droplet depletion, despite impaired lipid droplet production (Figure 4.29). 3-MA inhibits autophagosome initiation and, until all pre-existing autophagosomes are exhausted, lipid droplet breakdown would continue. Upon depletion of this pool, alternative lipid droplet production mechanisms such as ATGL and *de novo* fatty acid synthesis may compensate for the loss of the exogenous lipid pool and replenish lipid droplet stores. This would result in lipid droplet accumulation (Figure 4.29), as seen with 3-MA treatment in HBSS in our cell lines (Figure 4.16). When ATGL activity is also inhibited through co-treatment with atglistatin and 3-MA there may be inadequate compensation for the loss the exogenous lipids and metabolites. Lipid droplets depleted prior to the inhibition of lipid droplet breakdown

with 3-MA may not be replenished due to impaired lipid droplet production. Therefore, LDQ would be decreased in response to 3-MA and atglistatin in comparison to 3-MA treatment alone (Figure 4.29), as observed in our cell lines (Figure 4.16.). The extent to which lipid droplets are depleted would rely upon the number of pre-existing autophagosomes and the ability of the cell to compensate using lipid synthesis from intracellular pre-cursors. Thus LDQ in atglistatin and 3-MA co-treated cells may be decreased to different extents in our cell lines.

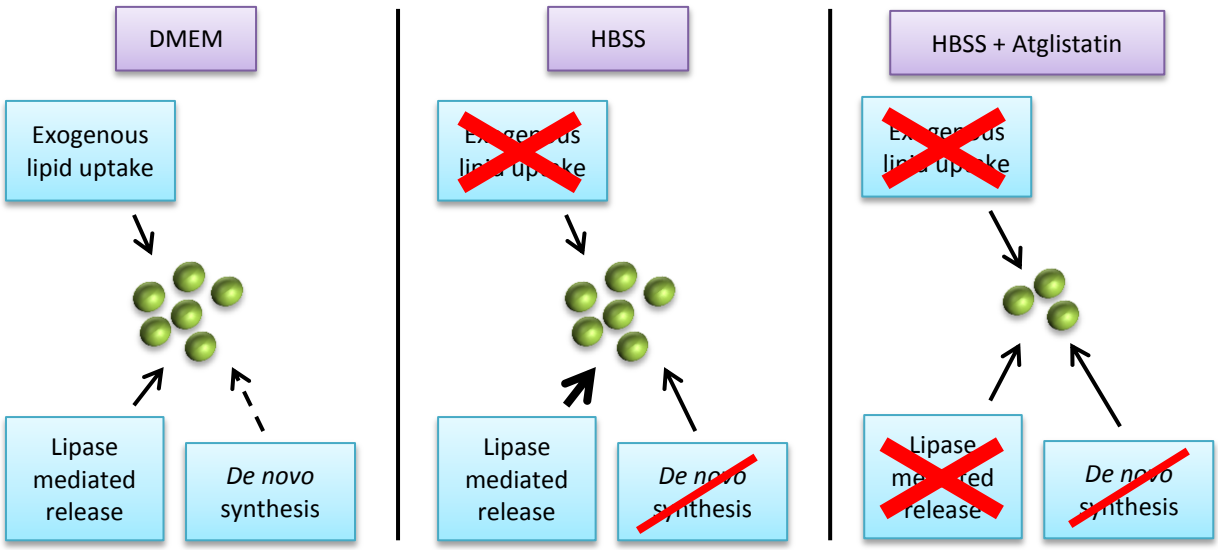

Figure 4.28. Compensatory activity of lipid droplet production pathways can maintain LDQ to an extent. DMEM: LDQ is maintained by exogenous lipid uptake and lipase mediated lipid release. *De novo* fatty acid synthesis does not play a major role. HBSS: No access to exogenous lipid pool or extracellular lipid pre-cursors in HBSS. Lipase mediated lipid release and *de novo* fatty acid synthesis from intracellular pre-cursors are increased to maintain LDQ. HBSS + Atglistatin: All three mechanism of lipid droplet production are unavailable or impaired and LDQ is decreased, increasing the effect of atglistatin. "X" denotes fully inhibited pathway, "/" denotes impaired pathway.

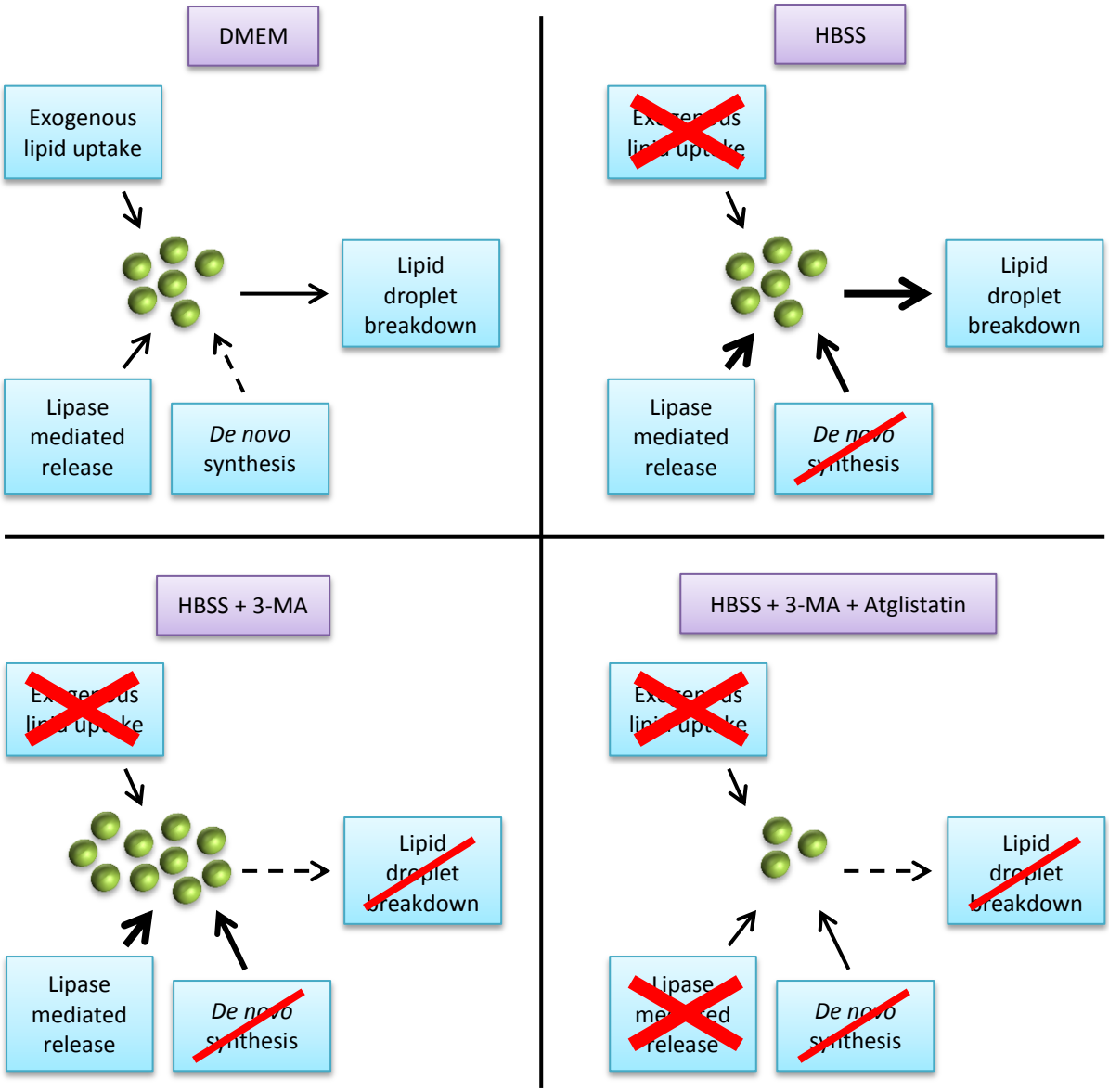

Figure 4.29. Lipid droplet metabolism is in constant flux. DMEM: Lipid droplet production occurs through exogenous lipid uptake and lipase-mediated lipid release. Lipid droplet breakdown occurs through autophagy. HBSS: Increased metabolic demand from starvation increases lipid droplet breakdown. LDQ is maintained by lipase-mediated lipid release and *de novo* synthesis from intracellular precursors. HBSS and 3-MA: Lipid droplet breakdown is halted once the pre-existing autophagosomes are exhausted. Lipids droplets are replenished by the two active production pathways and accumulate. HBSS + 3-MA + Atglistatin: The pre-existing autophagosomes, initiated prior to 3-MA treatment, catabolise lipid droplets due to the increased metabolic demand in starvation. The lipid droplet production pathways are impaired or halted and cannot sustain lipid droplet replenishment resulting in decreased LDQ. “X” denotes fully inhibited pathway, “/” denotes impaired pathway.

Compensatory pathway activation requires further investigation. However, this has proved difficult as pharmacological targeting of two pathways simultaneously frequently resulted in a cell stress response or cell death (data not shown). Future experiments should aim to remove the activity of one pathway whilst non-invasively monitoring the activity of others. For example *de novo* fatty acid synthesis could be monitored using ^{13}C labelled glucose and glutamine whilst inhibiting ATGL or lipid uptake. Alternatively, lipid uptake could be monitored with ^{13}C labelled fatty acid mass spectrometry by assessing changes in ^{13}C label accumulation in lipid droplets following inhibition of ATGL or *de novo* fatty acid synthesis. By targeting a single pathway, stress-induced lipid droplet changes may be avoided and pathway compensation may be better understood.

4.3.13. The fates of lipid droplets

The importance of maintaining lipid droplet metabolism is clear, although we are yet to understand why. Lipids can be used for four main functions; energy production, membrane phospholipid synthesis, lipid signalling rafts and protein modification. The lipid requirements of protein modification are too small to be the primary demand for lipid droplet metabolism, whilst the investigation of lipid signalling rafts requires far greater exploration than allowed within this investigation. We therefore chose to focus upon energy production and membrane phospholipid synthesis which are suggested outcomes of lipid droplet metabolism in other cell types (92,149,174).

C16 BODIPY was observed to accumulate in normoxia in a peri-nuclear region associated with mitochondrial localisation (Figure 4.17.), suggesting that C16 BODIPY may be transported to the mitochondria for β-oxidation. Indeed, C16

BODIPY does not localise to this region in hypoxia which is known to decrease mitochondrial β-oxidation (259). However, accumulating C16 BODIPY may also originate from non-lipid droplet sources and this requires further investigation. In contrast, C11 BODIPY did not accumulate in this peri-nuclear region suggesting that unsaturated fatty acids may not be used for β-oxidation to the same extent. Unsaturated fatty acid β-oxidation requires two additional enzymes and therefore saturated fatty acids may provide a more optimal lipid source for mitochondrial β-oxidation. Importantly C16 and C11 BODIPY differ by chain length as well as saturation. However, lipid metabolism is more dependent on saturation rather than chain length and therefore the altered metabolism of these two fatty acids is more likely attributable to saturation status.

This methodology remains limited as co-localisation of mitochondrial dyes is required to confirm that labelled fatty acid is present in mitochondria. Moreover, the fluorescent label interferes in the processing of these fatty acids and may alter their metabolism. Indeed, prolonged exposure to the C11 BODIPY fatty acid induced cell death (data not shown). In addition to co-localisation of mitochondria and lipid droplet derived lipids, alterations in respiration rate and mitochondrial β-oxidation enzyme activity following lipid droplet depletion could further support the role of lipid droplets as a mitochondrial energy source. This avoids altering lipid metabolism with fluorescent labels and provides a quantitative comparison of mitochondrial β-oxidation activity. Moreover, this can be combined with ^{13}C metabolic tracer studies (275) to better track the metabolism of lipid droplet derived lipids.

Lipid droplets also provide an excellent source of pre-assembled lipids for phospholipid synthesis. Upon the inhibition of lipid droplet breakdown C16 BODIPY was observed to accumulate in lipid droplets with decreased accumulation at the cell

membrane (Figure 4.17.). Inhibited lipid droplet breakdown could prevent the release of lipids from lipid droplet stores for the synthesis of membrane phospholipids. Indeed, in chapter 3, we observed correlations between expression of autophagy and phospholipid synthesis genes suggesting a link between lipid droplet breakdown and membrane synthesis. Alternatively, the inhibition of lipid droplet breakdown may induce a compensatory increase in ATGL activity, releasing labelled fatty acids from cell membranes and causing accumulation in lipid droplets. However, this appears less likely as earlier data suggested that ATGL-released saturated fatty acids may not be destined for storage in lipid droplets. Therefore, we suggest that lipid droplet-derived lipids are also used in membrane synthesis in these cell lines.

A role for lipid droplet-derived lipids in membrane synthesis could be further investigated through knockdown of phospholipid synthesis enzymes which may replicate the shift in C16 BODIPY accumulation from membranes to lipid droplets. However, the use of fluorescent labelled fatty acids has the same limitations as noted previously whilst lipid droplet-derived lipids remain difficult to track. Therefore, the impact of lipid droplet metabolism on membrane synthesis must also be confirmed using alternative methodologies in future investigations.

As discussed above, hypoxia can alter lipid droplet metabolism and was observed to decrease proliferation in several GBM cell lines (Figure 4.18.). Decreased phospholipid production would slow membrane synthesis whilst decreased β-oxidation would alter energy metabolism. Therefore, if increased lipid droplet accumulation in hypoxia is the result of decreased lipid droplet catabolism, proliferation may be suppressed through these proliferative pathways. However, this is speculative and requires further investigation.

We present preliminary data which suggests a possible role for lipid droplets as a lipid source for mitochondrial β-oxidation and membrane phospholipid synthesis in these cell lines (Figure 4.30). Whilst several reports in the literature support this theory (174,215), further in depth investigation is required.

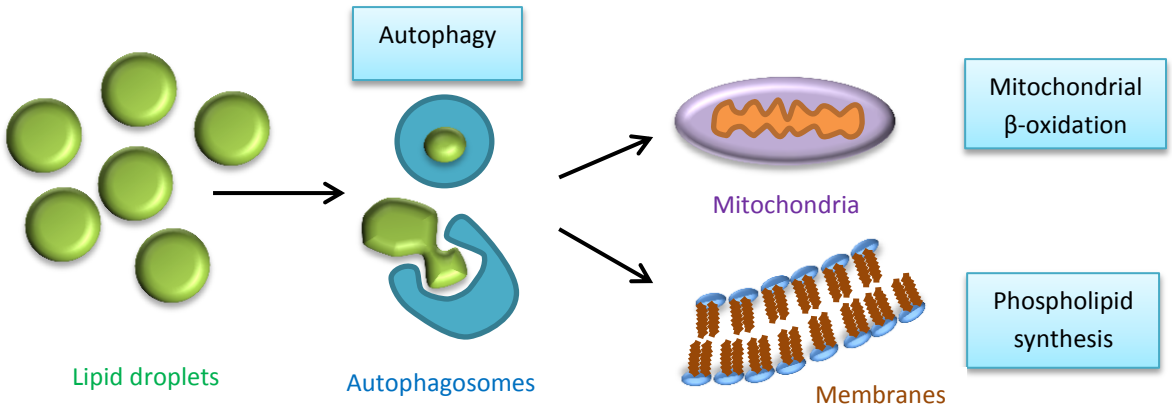

Figure 4.30. The fates of lipid droplet lipids. Lipid droplet lipids can be used for energy production through mitochondrial β-oxidation and the production of membranes through phospholipid synthesis.

4.3.14. Lipid shuttling is an important oxidative damage protection mechanism

We observed that the unsaturated fatty acid concentration was increased significantly in hypoxia (Figure 4.19). Interestingly, hypoxic cancer cells have been shown to acquire unsaturated fatty acids through increased uptake as opposed to *de novo* desaturase activity (168). Moreover, desaturase enzymes require oxygen, limiting their use in hypoxia (276). Therefore, it is likely that the unsaturated fatty acid concentration of lipid droplets is not changed by desaturase activity but by increased intra- and extra-cellular unsaturated fatty acid uptake, driven by an unknown factor.

ROS is a well-known source of oxidative damage and will readily oxidise unsaturated fatty acids. Hypoxia is known to increase the generation of ROS (225) and was

observed to increase C11 BODIPY unsaturated fatty acid oxidation (Figure 4.20.). ATGL inhibition in hypoxia further increased unsaturated fatty acid oxidation, specifically at cell membranes, suggesting a role for ATGL in preventing hypoxic oxidative damage. In combination with our previous findings regarding the role of ATGL in lipid droplet production (Figure 4.26.), we propose that unsaturated fatty acids are released from cell membranes by ATGL, transported by FABPs and sequestered in lipid droplets, thereby preventing oxidative damage (Figure 4.31). A similar mechanism was reported by Bailey et al. (226) in *Drosophila* glial cells. Using mass spectrometry, poly-unsaturated fatty acids were shown to increase in lipid droplets following exposure to oxidative stress with higher unsaturated fatty acid oxidation occurring at cell membranes compared to lipid droplets. The authors concluded that unsaturated fatty acids may be transported from cell membranes to lipid droplets to protect against ROS damage in the *Drosophila* model, supporting our proposed pathway in GBM.

H_2O_2 is a potent ROS and was used to further investigate this pathway. Similarly, to hypoxia, H_2O_2 treatment increased unsaturated fatty acid oxidative damage, which was further increased by simultaneous ATGL inhibition (Figure 4.21.). This was observed in normoxia and hypoxia suggesting that ATGL is important in the prevention of unsaturated fatty acid oxidation regardless of oxygen concentration. Interestingly, H_2O_2 treatment should induce an increase in the unsaturated fatty acid concentration of lipid droplets, as was observed with hypoxia, and investigation of this may provide further evidence to support this pathway.

The chemotherapeutic agent cisplatin is known to increase the concentration of poly-unsaturated fatty acids in lipid droplets (98) and can induce ROS as well as DNA damage (260). Therefore, we hypothesised that cisplatin, as with hypoxia and H_2O_2,

may induce the protective shuttling of unsaturated fatty acids to lipid droplets. Moreover, this may be inhibited by ATGL inhibition, increasing cell membrane fatty acid oxidation. However, cisplatin did not induce unsaturated fatty acid oxidation (Figure 4.21.) and we therefore did not test the effect of cisplatin and atglistatin co-treatment as we cannot confirm ROS induction. Moreover, cisplatin is associated with many mitochondrial effects as well as ROS induction which may confound these results.

It is unclear why ATGL inhibition in normoxia decreased unsaturated fatty acid oxidation as this would not be expected to alter the amount of oxidative stress to which the cell is exposed. Indeed, no change in lipid oxidation was expected and this requires further investigation. Nevertheless, the induction of lipid oxidation by H_2O_2 treatment in normoxia was increased by ATGL inhibition (Figure 4.21.) confirming that this pathway remains important in preventing oxidative damage under oxidative stress in normoxia.

Taken together our results suggest that the ATGL-mediated unsaturated fatty acid shuttle sequesters unsaturated fatty acids in lipid droplets in response to oxidative stress (Figure 4.31). This is supported by the literature (226) and highlights a potential new therapeutic target in GBM. Therefore, future experiments should aim to explore the impact of ATGL inhibition and oxidative damage on cell viability.

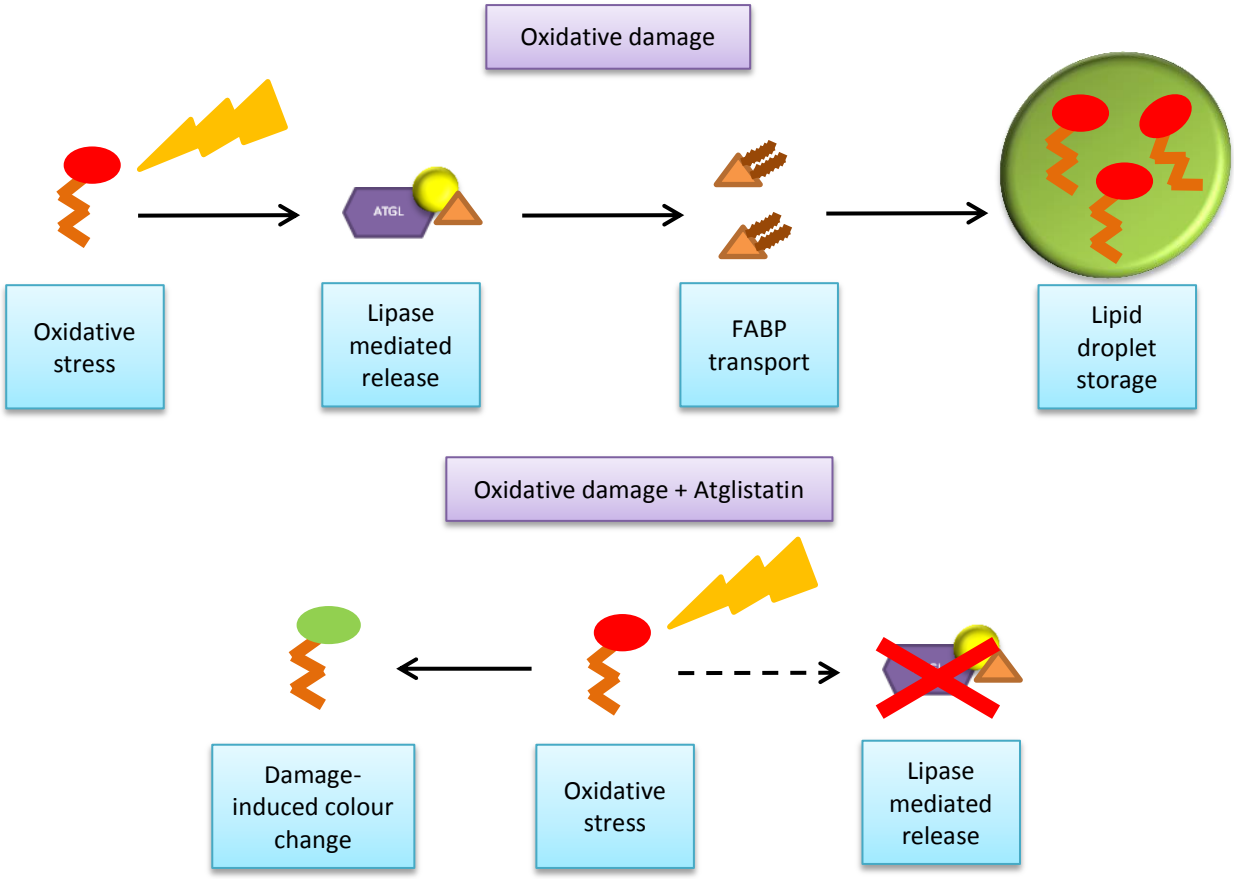

Figure 4.31. The ATGL-mediated unsaturated fatty acid shuttle protects cell membrane lipids from oxidative damage. Oxidative stress, such as the induction of ROS by hypoxia or H_2O_2, induces the movement of unsaturated fatty acids from vulnerable cell membranes to protective lipid droplets through the ATGL-mediated unsaturated fatty acid shuttle. However, atglistatin treatment inhibits this pathway resulting in oxidative lipid damage at the cell membranes. This causes the C11 BODIPY to undergo a red to green colour shift. Fatty acid binding protein (FABP).

4.3.15. Summary

In chapter 3 we highlighted the expression of many genes including those representing lipid droplets, exogenous lipid uptake, ATGL, phospholipid synthesis and mitochondrial lipid transporters as important aspects of glioma biology with significant association to survival. In this chapter, we have confirmed and defined the role of several of these pathways as important aspects of lipid droplet metabolism. Lipid droplets are produced by the uptake of exogenous lipids; however, there is also contribution from the ATGL-mediated release of fatty acids from the cell membrane. Interestingly, our data suggests that the loss of a single pathway may be compensated for through increased activity in alternative pathways. We further defined a role for autophagy in the breakdown of lipid droplets which may fuel mitochondrial β-oxidation and membrane phospholipid synthesis. Furthermore, these pathways are also involved in lipid droplet metabolism in hypoxia. However, the importance of each pathway appears cell line-specific. Finally, we suggest an ATGL-mediated unsaturated fatty acid shuttle for the sequestration of unsaturated fatty acids in lipid droplets to reduce oxidative damage.

Understanding lipid droplet metabolism provides greater insight into the overall metabolic profile of GBM tumours and may highlight potential therapeutic targets. Notably, the roles of autophagy in lipid droplet breakdown and of ATGL as a protective mechanism under oxidative stress may be of particular interest. Lipid droplets have been associated with treatment efficacy (234,238,239,277) and, through pharmacological targeting of lipid droplet metabolic pathways, they may be manipulated to improve the cytotoxicity of current therapies.

Chapter 5

Manipulating lipid droplets for therapeutic effect in high grade glioma cell lines

5.1. Introduction

Non-curative therapeutic options remain a major factor in the high mortality associated with gliomas, particularly at higher grades. Current treatment regimens are composed of three main factors: surgery, radiotherapy and chemotherapy. Surgical resection has the greatest clinical impact through removal of the bulk tumour mass. However, despite extensive resection, tumours frequently reoccur in peripheral post-operative areas due to infiltration (57). Adjuvant radiotherapy constitutes the second most important aspect of glioma therapy and causes cell death through direct DNA damage and ROS generation. However, through adaptation to the tumour microenvironment and several cellular mechanisms; including upregulated DNA repair enzymes and cancer stem cell intrinsic radio-resistance (58,62,63), radiation remains non-curative. Although recent interest has focussed on proton beam therapy, current research implies this may decrease side effects as opposed to improving survival (278,279). The final component of glioma treatment regimens is chemotherapy. In 2005, temozolomide became the major chemotherapeutic agent in glioma therapy and, in combination with surgery and radiotherapy, increased median survival (20,280). Temozolomide is an alkylating agent which predominantly methylates DNA at the O6 position on guanine, triggering apoptosis. However, the DNA repair enzyme MGMT removes this lesion and is frequently highly expressed in high grade gliomas, limiting temozolomide efficacy (65). As discussed in Chapter 1, novel therapeutics have resulted in limited improvements to treatment regimens and therefore new approaches are required.

Lipid droplets are an important component of tumour biology and may represent an interesting and relatively unexplored therapeutic target. Associated with apoptosis (138) and necrosis (94), they are increased in response to a number of cytotoxic

treatments in many cancers including GBM (98). Whilst it has been suggested that lipid droplets are part of the cell death process and are increased in response to cytotoxic insult, lipid droplets could instead form part of a drug resistance pathway, increased in the prevention of cell death. Indeed, lipid droplet accumulation was increased in a number of drug resistant cells (235-237). Moreover, several studies have suggested that lipid droplets influence drug resistance through sequestration of cytotoxic compounds. In acute myeloid leukaemia, an aminopeptidase inhibitor pro-drug was prevented from activation through lipid droplet sequestration (238) whilst docetaxel was observed within drug resistant breast cancer lipid droplets (239). Indeed, curcumin was observed to co-localise with lipid droplets in GBM, although this study remains limited by the shared fluorescence of both curcumin and the selected lipid droplet marker (277).

Conversely, the importance of lipid droplets in metabolism and proliferation could be significant. Lipid droplets provide increased metabolic plasticity and disruption of lipid droplet metabolism has been shown to decrease growth and survival in many cancer cell lines and xenografts (123,165). Through increased understanding of lipid droplet metabolic pathways, we may better appreciate the role lipid droplets play within cell death and drug resistance and facilitate the improvement of current therapies. In Chapter 4 we observed important roles for the uptake of exogenous lipids, ATGL and autophagy in lipid droplet metabolism suggesting manipulation of lipid droplet flux through subversion of these pathways may influence cell death and drug efficacy.

In this Chapter we investigate the effect of reducing lipid droplet flux through pharmacological inhibition of lipid droplet metabolic pathways with regards to temozolomide and radiation efficacy. Moreover, we assess the relevance of co-treatment in hypoxia and address its potential for clinical application.

5.2. Results

5.2.1. Chloroquine pre-treatment can increase temozolomide cytotoxicity in normoxia.

Based upon the role of autophagy in lipid droplet breakdown observed in Chapter 4, we sought to investigate the effect of the late-stage autophagy inhibitor chloroquine on the cytotoxicity of temozolomide. Pre-treatment with the autophagy inhibitor chloroquine decreased cell viability in temozolomide-treated cells compared to the DMSO-only and drug-only conditions at 21% O_2, as assessed by SRB proliferation assays (Figure 5.1.A.). This was observed in the T98G, U87 and U87.2 cell lines suggesting that manipulation of lipid droplet breakdown can influence temozolomide efficacy. Moreover, decreased cell viability in the chloroquine-only condition indicated sensitivity to autophagy inhibition whilst temozolomide cytotoxic activity was confirmed by decreased cell viability in the temozolomide-only condition. The temozolomide dose required to induce cytotoxicity is much higher than *in vivo* concentrations, as expected *in vitro*, reflecting the inherent resistance of these cell lines and GBM tumours. These findings were confirmed with AnnexinV-FITC/PI flow cytometry apoptosis assays (Figure 5.1.B.). Therefore, manipulation of lipid droplet metabolism using the autophagy inhibitor chloroquine may increase the cytotoxicity of temozolomide in normoxia.

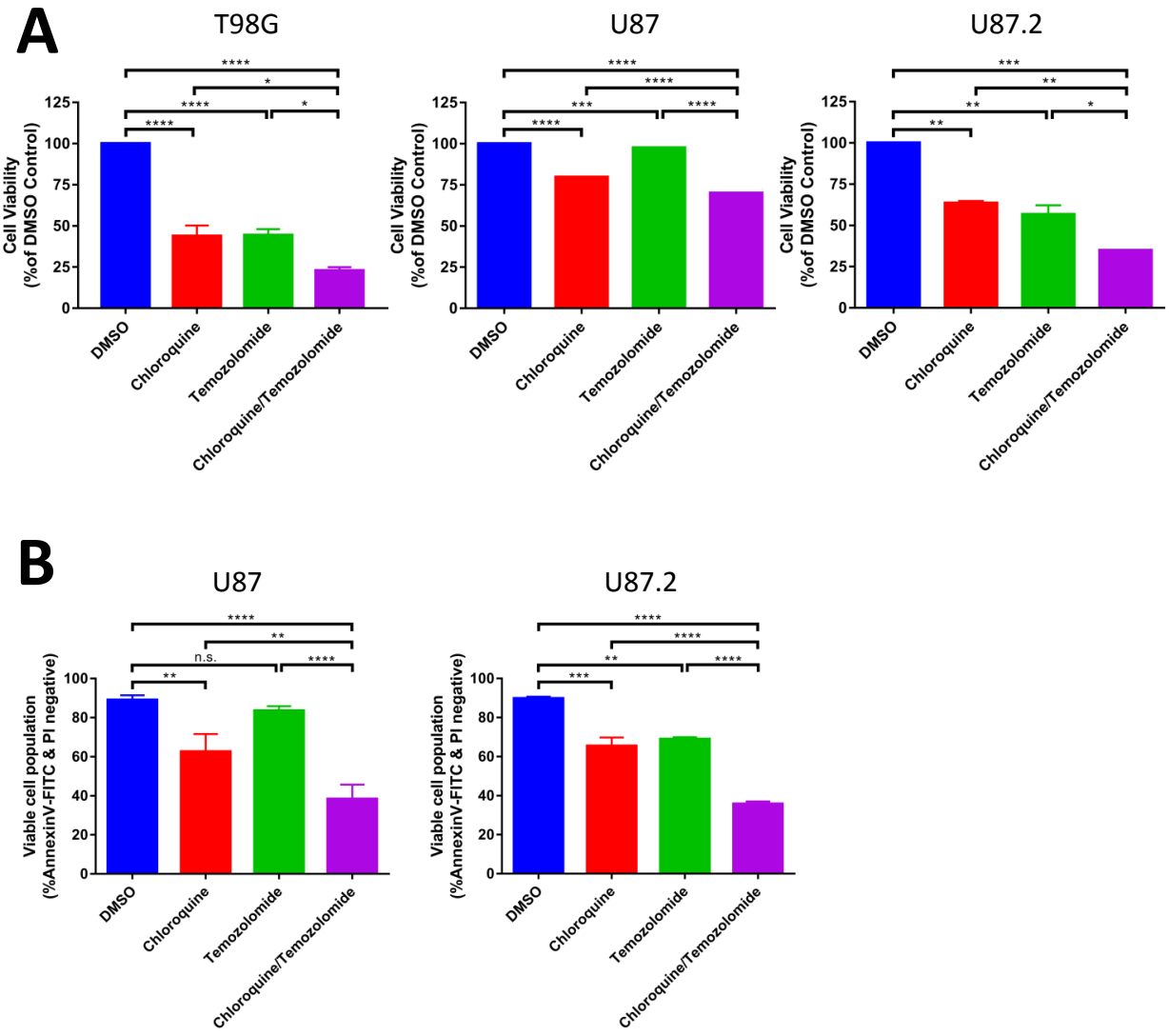

Figure 5.1. Chloroquine pre-treatment can increase the cytotoxicity of temozolomide in normoxia. A) SRB viability assays of T98G, U87 and U87.2 cells treated with DMSO, chloroquine, temozolomide or chloroquine and temozolomide at 21% O_2. Chloroquine pre-treatment 24 hours prior to temozolomide treatment decreased the cell viability of all three cell lines. Data shown as mean ±SEM representative of several independent experiments (U87, U87.2 n=2; T98G n=3), each composed of 3 technical replicates. B) Flow cytometric AnnexinV-FITC/PI cell death assay of U87 and U87.2 cells treated with DMSO, chloroquine, temozolomide or chloroquine and temozolomide at 21% O_2. Chloroquine pre-treatment prior to temozolomide treatment decreased the viability of the U87 and U87.2 cell line. Data shown as mean ±SEM representative of several independent experiments (U87, U87.2 n=3). Statistical analysis in (A) and (B) was performed using a one-way ANOVA with Tukey post-hoc test; *p<0.05, **p<0.01, ***p<0.001, ****p<0.0001.

Due to the hypoxia-induced alterations in lipid droplet metabolism observed in Chapter 4, we investigated the effect of chloroquine pre-treatment with temozolomide in hypoxia. In contrast to normoxia, the combination of temozolomide and chloroquine pre-treatment did not decrease cell viability at 0.3% O_2 compared to the drug-only conditions, as assessed via SRB proliferation assays (Figure 5.2.A.). Indeed, the cell viability in chloroquine and temozolomide-treated cells was observed to mirror the chloroquine-only condition suggesting that any effects observed in cells exposed to both chloroquine and temozolomide in hypoxia were attributable to chloroquine alone. Moreover, there was no effect on cell viability in the temozolomide-only condition further supporting this theory. Interestingly, cell viability in the chloroquine-only condition varied between cell lines. Chloroquine treatment decreased cell viability in the T98G cell line suggesting a high sensitivity to autophagy inhibition when compared to the other cell lines, in particular the U87.2 cell line. Moreover, chloroquine treatment increased the viability of the U87 cell line suggesting that autophagy inhibition may increase proliferation under some conditions or genetic backgrounds. AnnexinV-FITC/PI apoptosis assays confirmed that chloroquine pre-treatment with temozolomide does not further decrease cell viability in the U87.2 cell line in hypoxia (Figure 5.2.B.).

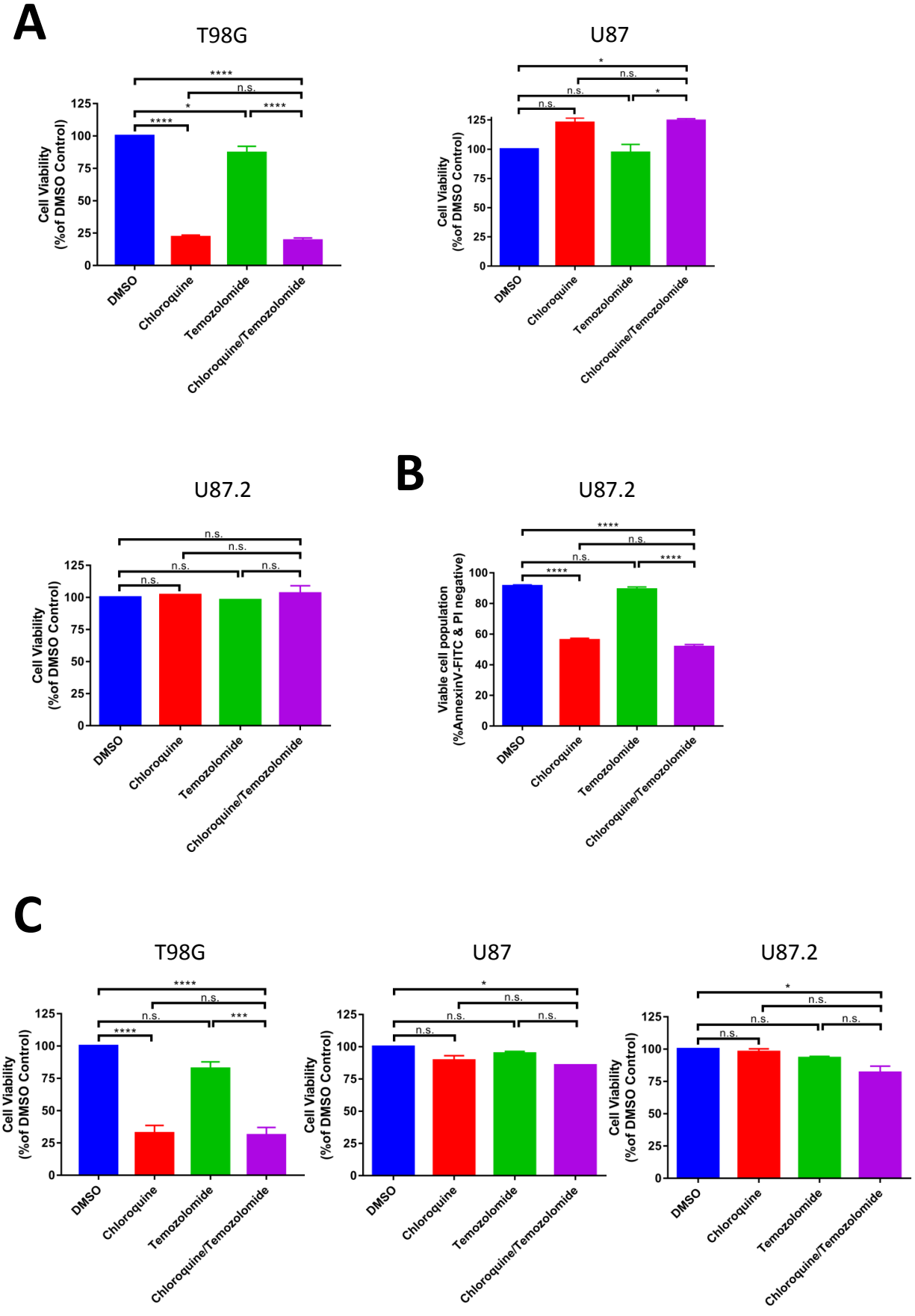
A
T98G
U87
Cell Viability (%of DMSO Control)
DMSO
Chloroquine
Temozolomide
Chloroquine/Temozolomide
B
U87.2
Viable cell population (%AnnexinV-FITC & PI negative)
C
T98G
U87
U87.2

Figure 5.2. Prior normoxic chloroquine pre-treatment may improve temozolomide cytotoxicity; however, hypoxic chloroquine pre-treatment does not. A) SRB viability assays of T98G, U87 and U87.2 cells treated with DMSO, chloroquine, temozolomide or chloroquine and temozolomide at 0.3% O_2. Chloroquine pre-treatment affected cell viability in a cell line dependent manner but did not improve the cytotoxicity of temozolomide. Data shown as mean ±SEM representative of several independent experiments (U87, U87.2 n=2; T98G n=3), each composed of 3 technical replicates. B) Flow cytometric AnnexinV-FITC/PI cell death assay of U87.2 cells treated with DMSO, chloroquine, temozolomide or chloroquine and temozolomide at 0.3% O_2. Chloroquine treatment decreased cell viability; however, pre-treatment did not improve temozolomide cytotoxicity. Data shown as mean ±SEM representative of several independent experiments (U87.2 n=3). C) SRB viability assays of T98G, U87 and U87.2 cells pre-treated with chloroquine for 24 hours at 21% O_2 prior to incubation in 0.3% O_2 and treatment with DMSO or temozolomide. Chloroquine pre-treatment partly restored the increased temozolomide cytotoxicity in the U87 and U87.2 cell lines; however, did not reach significance. Data shown as mean ±SEM representative of several independent experiments (U87, U87.2 n=2; T98G n=3), each composed of 3 technical replicates. Statistical analysis in (A), (B) and (C) was performed using a one-way ANOVA with Tukey post-hoc test; *p<0.05, **p<0.01, ***p<0.001, ****p<0.0001.

As lipid droplet metabolism is altered in hypoxia, we hypothesised that inhibition of lipid droplet flux may be required prior to hypoxia. Therefore, cells were incubated with chloroquine for 24 hours prior to hypoxic incubation and subsequent temozolomide treatment. There was a non-significant trend towards a decrease in cell viability following temozolomide treatment with prior normoxic chloroquine treatment in the U87 and U87.2 cell lines (Figure 5.2.C.). However, cell viability was decreased in cells pre-treated with chloroquine in normoxia (Figure 5.2.C.) compared to those pre-treated with chloroquine in hypoxia (Figure 5.2.A.), particularly in the U87 cell line. The T98G cell line was highly sensitive to hypoxic autophagy inhibition (Figure 5.2.C.), as observed in Figure 5.2.A, further supporting cell line-specific differences in chloroquine sensitivity. This data demonstrates that temozolomide efficacy is lost in hypoxia and cannot be rescued with hypoxic chloroquine pre-treatment. Whilst normoxic chloroquine pre-treatment comparatively improved temozolomide cytotoxicity, viability remained high, presenting a complicated challenge to improve drug efficacy through reduced lipid droplet flux in hypoxia.

5.2.2. Atglistatin-induced reduction of lipid droplet flux does not improve temozolomide cytotoxicity to the same extent as observed with chloroquine.

Using SRB proliferation assays, we investigated the impact of impairing a lipid droplet production pathway on temozolomide efficacy through ATGL inhibition. Treatment with the ATGL inhibitor atglistatin 24 hours prior to temozolomide treatment in the U87 and U343 cell lines significantly decreased cell viability compared to the DMSO condition suggesting a co-treatment effect (Figure 5.3.A). However, in contrast to chloroquine, atglistatin and temozolomide treatment had no significant effect on cell viability in normoxia compared to the drug-only conditions suggesting a smaller increase in cytotoxicity. This trend was not observed in the T98G cell line; however, cell viability was not decreased in the atglistatin-only condition in this cell line. As with chloroquine, cells were also treated with atglistatin for 24 hours in normoxia or hypoxia prior to temozolomide treatment in hypoxia. Both normoxic and hypoxic atglistatin pre-treatment had no significant effect on cell viability in any of the cell lines (Figures 5.3.B. and 5.3.C. respectively). Moreover, no effect on cell viability was observed in any of the drug-only conditions. Therefore, impairment of lipid droplet flux, through impairing lipid droplet production with atglistatin, may marginally improve temozolomide cytotoxicity in normoxia but has no effect on cell viability in hypoxia.

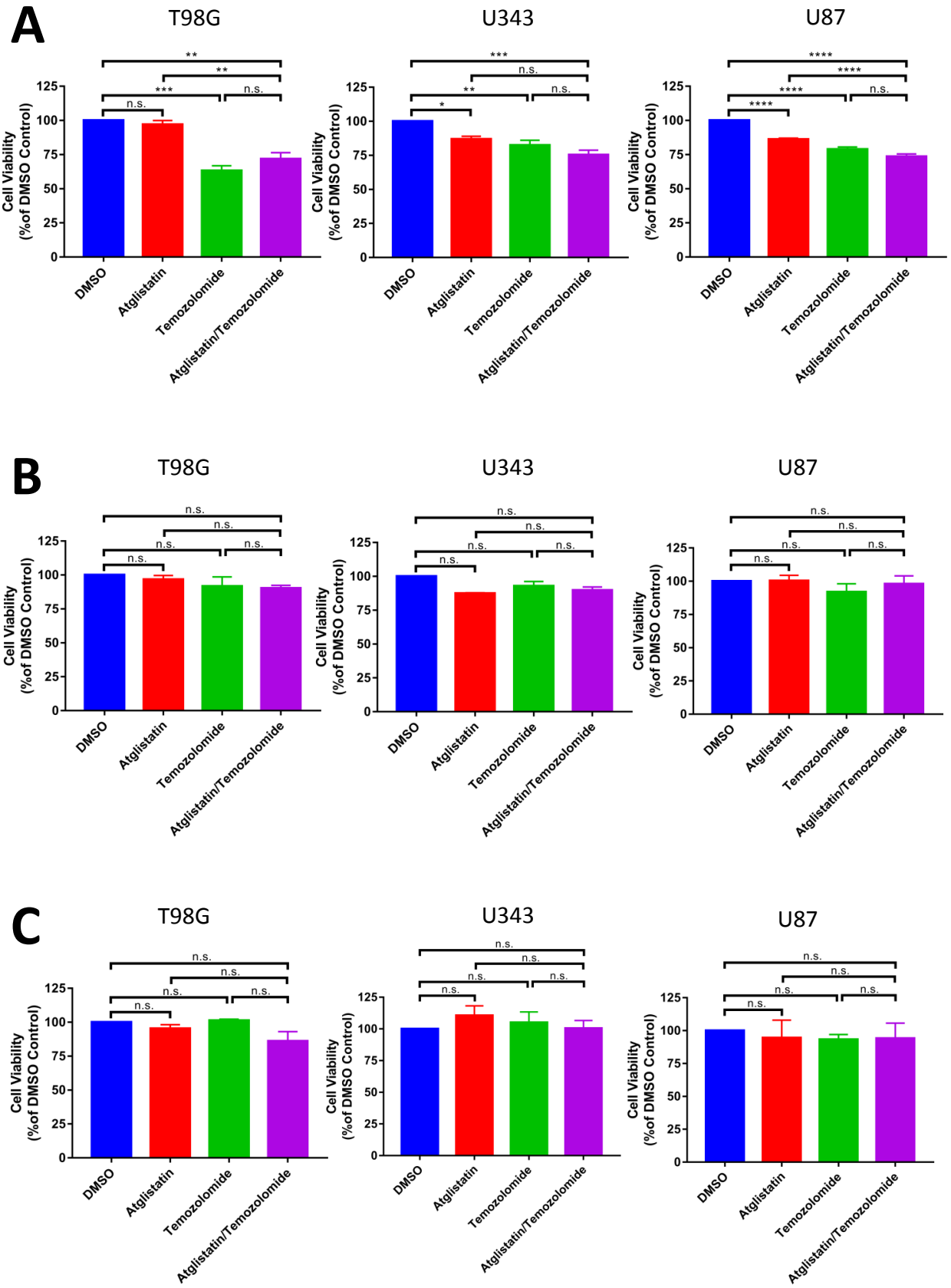
A
T98G
U343
U87
B
T98G
U343
U87
C
T98G
U343
U87
Cell Viability (%of DMSO Control)
0
25
50
75
100
125
n.s.
*
**
***
****
DMSO
Atglistatin
Temozolomide
Atglistatin/Temozolomide

Figure 5.3. Atglistatin pre-treatment did not improve temozolomide cytotoxicity to the same extent as chloroquine. SRB viability assays of T98G, U87 and U87.2 cells treated with DMSO, atglistatin, temozolomide or atglistatin and temozolomide. Cells were pre-treated for 24 hours with atglistatin prior to temozolomide or DMSO treatment. Cells were treated at 21% O_2 (A), at 21% O_2 for 24 hours prior to 0.3% O_2 (B) and at 0.3% O_2 (C). Atglistatin pre-treatment significantly increased temozolomide cytotoxicity compared to the DMSO-only condition in normoxia but not compared to the drug-only conditions. Cell line-specific co-treatment effects were also indicated. No significant differences were observed following hypoxic temozolomide treatment. Data shown as mean ±SEM representative of several independent experiments (T98G, U343 n=3; U87 n=4), each composed of 3 technical replicates. Statistical analysis in (A), (B) and (C) was performed using a one-way ANOVA with Tukey post-hoc test; *p<0.05, **p<0.01, ***p<0.001, ****p<0.0001.

5.2.3. Chloroquine can improve the cytotoxicity of irradiation in normoxia.

Radiotherapy is an integral part of GBM treatment regimens and therefore we investigated the impact of lipid droplet manipulation on irradiation treatment using AnnexinV-FITC flow cytometry apoptosis assays. Pre-treatment with chloroquine prior to irradiation decreased the viable cell population compared to the DMSO-only and treatment-only conditions in normoxia in the T98G and U87 cell lines (Figure 5.4.). Despite the high dosage of radiation, there was only a small decrease in the viable cell population in the irradiation-only condition representing the inherent radio-resistance of these cell lines. Due to logistical problems in maintaining hypoxic conditions during irradiation, the effect of chloroquine pre-treatment on irradiation cytotoxicity was only investigated in normoxia.

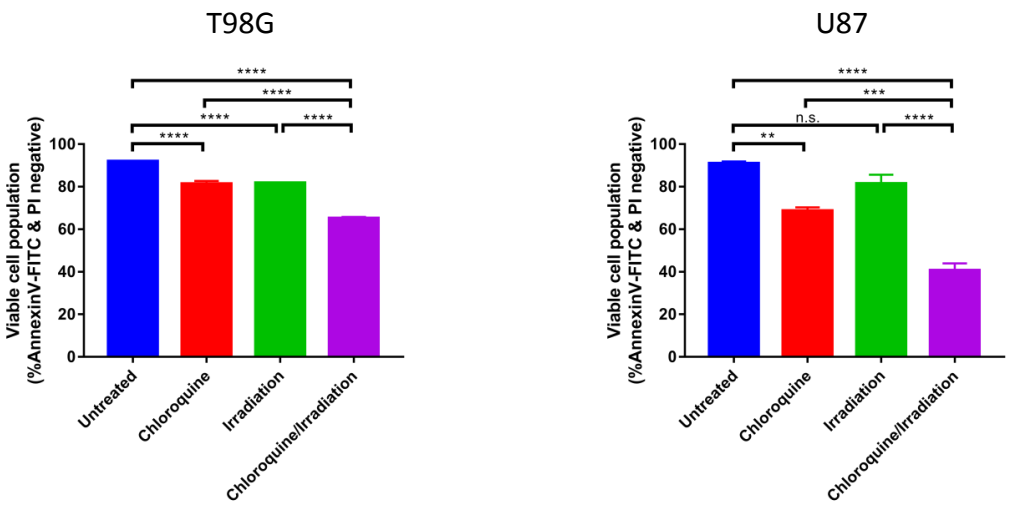

Figure 5.4. Chloroquine pre-treatment can improve the cytotoxicity of irradiation. Flow cytometric AnnexinV-FITC/PI cell death assay of T98G and U87 cells treated with DMSO, chloroquine, irradiation or chloroquine and irradiation at 21% O_2. Chloroquine pre-treatment prior to irradiation significantly decreased the viability of both cell lines. Data shown as mean ±SEM representative of several independent experiments (n=3). Statistical analysis was performed using a one-way ANOVA with Tukey post-hoc test; *p<0.05, **p<0.01, ***p<0.001, ****p<0.0001.

5.3. Discussion

5.3.1. Introduction

Lipid droplets have previously been suggested as an important consideration in GBM treatment due to potential roles in drug response, resistance and sequestration. Indeed, lipid droplets have become a target for manipulation to improve chemotherapy, an important component of GBM treatment regimens. Zhang et al. (277) attempted to deplete lipid droplets through phospholipase A2 inhibition and, despite several experimental issues, their data suggest that lipid droplet depletion may decrease sequestration of curcumin, improving cytotoxicity. However, whist Zhang et al. argue that lipid droplets influence cell viability through their physical presence; we propose that the cytotoxicity of chemotherapeutic agents may be improved through impairing lipid droplet flux. Impaired lipid droplet flux will affect downstream processes and impair the full utilisation of lipid droplets in aiding cell survival during cytotoxic stress. Indeed, lipid droplets were observed to provide a catabolic energy source to aid in survival during re-oxygenation-induced stress in prostate cancer cells (151) whilst inhibition of lipid droplet metabolic pathways decreased growth and survival during re-oxygenation-induced stress (123).

Lipid droplet flux can be disrupted through inhibition of the lipid droplet metabolic pathways observed in Chapter 4 and can result in decreased or increased LDQ depending upon the inhibition of lipid droplet production or breakdown respectively. If cell viability is influenced by effective lipid droplet flux then chemotherapeutic cytotoxicity may be improved in conditions of both high and low LDQ. This is distinct from the drug sequestration hypothesis suggested by Zhang et al. (277) which predicts that only decreased LDQ will increase cytotoxicity. We therefore sought to

investigate the effect of reduced lipid droplet flux on cell viability during cytotoxic insult through inhibiting lipid droplet metabolic pathways.

5.3.2. The impact of impairing lipid droplet breakdown on the cytotoxicity of the chemotherapeutic agent temozolomide

Autophagic lipid droplet breakdown was investigated because autophagy inhibition had the clearest effect upon lipid droplet metabolism in our earlier investigations. Moreover, lipid droplet production can be influenced by multiple pathways and displayed compensatory action from alternative pathways which could complicate the investigation. Autophagy inhibitors are established within the clinic and provide a good opportunity for high translational impact. Indeed, the autophagy inhibitor chloroquine is a commonly used anti-malarial drug with a high tolerability and could be swiftly implemented in clinical trials. Moreover, chloroquine was selected as opposed to 3-MA as less toxicity was induced following longer drug exposure (data not shown).

Chloroquine pre-treatment increased the cytotoxicity of the chemotherapeutic agent temozolomide in normoxia in our GBM cell lines (Figure 5.1.). This indicates that chloroquine pre-treatment may improve the efficacy of chemotherapeutic agents in normoxic GBM tumour cells. These cell lines displayed an intrinsic temozolomide resistance which is commonly observed in GBM tumours, emphasising the impact of improving temozolomide efficacy. Interestingly, autophagy inhibition halts lipid droplet breakdown and causes lipid droplet accumulation implying that the improved temozolomide cytotoxicity is due to increased lipid droplet presence or decreased lipid droplet flux. Previous studies (238,239,277) have suggested that lipid droplet

accumulation may hinder drug efficacy through drug sequestration. In this case, the induction of increased LDQ by autophagy inhibition would be expected to increase cell viability; however, we observe a contrasting effect. In addition to increasing LDQ, inhibition of lipid droplet breakdown impairs lipid droplet flux. If cell viability is affected by the impairment of effective lipid droplet flux then cytotoxicity would be increased by lipid droplet breakdown inhibition regardless of the increased LDQ. Therefore, we propose that autophagy inhibition improves temozolomide cytotoxicity through hindering lipid droplet flux.

As established in Chapter 4, lipid droplet metabolism is altered in hypoxia and it is therefore unsurprising that the effect of autophagy inhibition on temozolomide cytotoxicity was correspondingly altered in hypoxia (Figure 5.2.). GBM tumours contain highly hypoxic regions and therefore the lack of effect of chloroquine pre-treatment on temozolomide efficacy in hypoxia could present difficulties in clinical application. However, our data also suggests it may be possible to partially rescue temozolomide cytotoxicity in hypoxia with prior normoxic chloroquine pre-treatment (Figure 5.2.). Although cell viability is not significantly different to the DMSO-only condition following temozolomide and normoxic chloroquine pre-treatment, cell viability is clearly decreased compared to temozolomide and chloroquine pre-treatment in hypoxia. We can therefore conclude that the cytotoxicity of temozolomide in hypoxia is not increased by hypoxic chloroquine pre-treatment and suggest partial restoration of cytotoxicity in hypoxia through prior normoxic impairment of lipid droplet flux. However, these results could be attributable to alternative effects from autophagy inhibition or chloroquine treatment and require further investigation. Lipid droplet flux is altered in hypoxia and therefore improved understanding of altered hypoxic lipid droplet metabolism will better inform our

conclusions regarding co-treatment in hypoxia. Moreover, it may indicate additional therapeutic targets to further restore hypoxic temozolomide cytotoxicity.

Interestingly, we observe cell line-specific differences in chloroquine sensitivity in hypoxia (Figure 5.2.) which could be due to sensitivity to inhibited autophagy activity or sensitivity to inhibited lipid droplet breakdown. In Chapter 4 we observed cell line-specific differences in LDQ following hypoxic chloroquine treatment suggesting that the differences in cell viability are attributable to sensitivity to lipid droplet breakdown inhibition. GBMs are heterogeneous tumours and therefore understanding different drug responses between patients and within tumours will be important to successful therapies. The high chloroquine sensitivity observed in the T98G cell line may offer a therapeutic benefit through targeting hypoxic tumour cells which are not affected by combined chloroquine and temozolomide treatment. However, hypoxic chloroquine treatment increased proliferation in the U87 cell line emphasising the importance of understanding case-specific alterations in lipid droplet metabolism in hypoxia.

Interestingly, in contrast to SRB proliferation assays, the AnnexinV-FITC/PI flow cytometry apoptosis assay indicated that cell viability was decreased by hypoxic chloroquine treatment in the U87.2 cell line (Figure 5.2.B.). The difference may be because the AnnexinV-FITC-PI assay reports cytotoxicity earlier than the SRB proliferation assay as it detects the initial molecular events that lead to cell death. This suggests that, in our assay timeframe, we observed a greater number of early cytotoxic events than cell death events, and that by increasing the length of time of the assay, the SRB assay would detect further cell death. It appears from our data that different hypoxic chloroquine sensitivities may stem from the cell line-specific capacity to compensate for lipid droplet breakdown inhibition. Further investigation is required to confirm the association of this response to impaired lipid droplet

metabolism as opposed to autophagy inhibition whilst hypoxia-induced alterations in lipid droplet metabolism remain unclear. However, this cell line-specific response to chloroquine treatment could represent a potential therapeutic target for exploitation and further emphasises the importance of understanding the genetic background and microenvironment of each patient.

Despite intrinsic drug resistance, manipulation of lipid droplets with chloroquine pre-treatment improved temozolomide cytotoxicity in normoxia. We suggest that drug efficacy is increased through impaired lipid droplet flux and that this may be used to improve the clinical therapeutic efficacy of temozolomide under normoxic conditions. However, the lack of efficacy from chloroquine pre-treatment in hypoxia suggests applying this theory in a clinical setting may prove challenging due to the highly hypoxic nature of GBM. Despite this, the improved efficacy of temozolomide in hypoxia with prior normoxic chloroquine pre-treatment suggests that a clinical benefit can be sought through further understanding of altered hypoxic lipid droplet metabolism. Alternatively, if normoxia is required for treatment efficacy, therapies such as cediranib and bevacizumab can decrease tumour hypoxia by normalising tumour vasculature (281-284). Therefore, lipid droplet manipulation through inhibited lipid droplet breakdown and flux represents an exciting opportunity in the treatment of GBM.

5.3.3. The effect of reducing lipid droplet flux through ATGL inhibition on the cytotoxicity of the chemotherapeutic agent temozolomide

We sought to impair lipid droplet flux through an alternative pathway to confirm that the increased temozolomide cytotoxicity with chloroquine pre-treatment was due to

reduced lipid droplet flux as opposed to altered LDQ. There was a non-significant increase in temozolomide cytotoxicity following pre-treatment with the ATGL inhibitor atglistatin in normoxia in the U343 and U87 cell lines (Figure 5.3.) suggesting that normoxic temozolomide cytotoxicity may be improved through impaired lipid droplet flux from lipid droplet production inhibition. However, the increased temozolomide cytotoxicity following atglistatin pre-treatment is notably smaller than observed with chloroquine pre-treatment. In Chapter 4 our data suggested that inhibition of lipid droplet production pathways such as ATGL induced compensatory activation of alternative lipid droplet production pathways. This compensation would limit the effect of atglistatin in reducing lipid droplet flux, possibly accounting for the smaller improvement in temozolomide cytotoxicity. Nevertheless, despite the comparatively smaller non-significant improvement in temozolomide cytotoxicity observed with atglistatin pre-treatment, our data suggests that reducing lipid droplet flux through inhibiting production and breakdown pathways with atglistatin and chloroquine respectively can increase temozolomide cytotoxicity in normoxia. This further supports the importance of functional lipid droplet flux in cell viability.

Hypoxic temozolomide cytotoxicity was not improved by either normoxic or hypoxic atglistatin pre-treatment, although, as with autophagy inhibition, we observed in Chapter 4 that the role of ATGL in lipid droplet metabolism may be altered in hypoxia. Most notably, LDQ was significantly decreased by hypoxic ATGL inhibition in the U87.2 cell line (Figure 4.12.). If ATGL inhibition further impairs lipid droplet flux in these cells, an improved response to atglistatin pre-treatment in hypoxia may be observed in this cell line; however, this was not investigated. Atglistatin pre-treatment did not increase temozolomide cytotoxicity in the T98G cell line in any oxygen

concentration; however, this cell line has been noted previously to have a different LDQ response to atglistatin treatment in several other experiments in Chapter 4.

Due to the non-significant decrease in cell viability following ATGL inhibition on temozolomide cytotoxicity, this approach would not be appropriate for clinical investigation. Instead, the capacity of ATGL inhibition to increase the cytotoxicity of ROS producing therapies, as discussed in Chapter 4, should be further investigated. Nevertheless, the trend towards improved temozolomide cytotoxicity in normoxia, following prior inhibition of a lipid droplet production pathway, further suggests that reduced lipid droplet flux, rather than single pathway inhibition, is responsible for improved drug efficacy. Therefore, we again propose that lipid droplet manipulation can affect cell viability and temozolomide resistance in normoxia through impeding lipid droplet flux and that this is of greater importance than total LDQ.

5.3.4. The effect of reducing lipid droplet flux through lipid droplet breakdown inhibition on the cytotoxicity of irradiation

Following our findings regarding the impact of inhibiting lipid droplet breakdown on temozolomide cytotoxicity we investigated whether irradiation cytotoxicity, representative of radiotherapy, may also be increased. Exposure to 40Gy of radiation induced a small decrease in cell viability (Figure 5.4.) indicating intrinsic resistance to high doses of irradiation, a common feature of GBM tumours and derived cell lines. However, despite this, inhibition of lipid droplet breakdown through chloroquine pre-treatment increased the cytotoxicity of irradiation in normoxia suggesting that inhibiting lipid droplet flux could improve radiotherapy efficacy in normoxic tumour cells (Figure 5.4.). As with temozolomide, chloroquine pre-

treatment increased LDQ and improved cytotoxic treatment efficacy further supporting that lipid droplets do not provide increased protection through their physical presence. Whilst it is possible that radiation of a larger lipid pool increases the production of toxic lipid groups, radiation-induced lipid damage is predominantly oxidative (285). In contrast to this, we demonstrated a protective role for lipid droplets in the prevention of oxidative lipid damage in Chapter 4. Therefore, as the increased presence of lipid droplets induced by chloroquine pre-treatment is unlikely to directly affect radiation cytotoxicity, we instead propose that this data further supports the importance of effective lipid droplet flux in surviving cytotoxic insult.

As with temozolomide, the improvement of radiation cytotoxicity through inhibition of lipid droplet production could provide further evidence for the importance of lipid droplet flux in maintaining viability. However, in Chapter 4 we demonstrated the role of ATGL in the prevention of unsaturated lipid oxidation, a confounding variable in testing the combination of atglistatin pre-treatment with an oxidative treatment such as irradiation. Therefore, the importance of effective lipid droplet flux in radiation cytotoxicity should be further tested by impairing alternative lipid droplet production pathways such as exogenous lipid uptake.

Due to logistical problems in maintaining hypoxic conditions during irradiation, the effect of chloroquine pre-treatment in hypoxic cells proved impossible to test as cells would have been exposed to re-oxygenation. Re-oxygenation generates ROS and alters cellular metabolism and therefore this investigation was only carried out in normoxia. However, despite demonstrating efficacy in normoxia, chloroquine pre-treatment did not improve temozolomide cytotoxicity in hypoxia and therefore the combination of irradiation and chloroquine pre-treatment in hypoxia must be further investigated. Nevertheless, this data suggests that impairment of lipid droplet flux

can improve the cytotoxicity of irradiation in normoxia and indicates an exciting clinical opportunity to improve radiotherapy efficacy in GBM. Moreover, impairment of lipid droplet flux may prove a useful strategy to improve treatment regimen efficacy in non-hypoxic tumours.

5.3.5. Potential for clinical application

Pharmacological manipulation of LDQ and flux through lipid droplet metabolic pathways provides relevant therapeutic targets with the potential for clinical application. Through inhibition of just one of these pathways, autophagy, the efficacy of two separate therapeutic approaches could be improved, further demonstrating the importance of GBM lipid droplet metabolism. Indeed, autophagy inhibition is not a new concept in cancer therapy and provides a particularly good clinical target for lipid droplet manipulation due to readily available drugs for translational investigations. Several clinical trials have been carried out or are underway investigating chloroquine in GBM treatment regimens. Chloroquine has been shown to improve brain metastases treatment with whole brain irradiation (286) and there are current ongoing trials in both the UK and Netherlands investigating the effect of chloroquine with GBM treatments (287,288). Indeed, inclusion of chloroquine in GBM treatment regimens was observed to improve survival in a small sample of GBM tumours (289). Despite areas of significant hypoxia, other areas of the tumour will remain less hypoxic and these may be more susceptible to the pharmacological impairment of lipid droplet flux with chloroquine.

5.3.6. Summary

Our data suggests that impairing lipid droplet flux through inhibition of lipid droplet metabolic pathways can improve the cytotoxicity of temozolomide and irradiation, representative of chemotherapy and radiotherapy, in normoxia. Indeed, temozolomide cytotoxicity was improved by inhibition of lipid droplet breakdown, despite increased LDQ, further suggesting that the efficacy of treatment is due to lipid droplet flux rather than the physical presence of lipid droplets. However, further investigation is required to confirm that this effect is lipid droplet-specific and not due to autophagy inhibition. We hypothesise that impairment of lipid droplet breakdown through alternative methodologies would induce a similar increase in treatment cytotoxicity. Du et al. (290) demonstrated that lipid droplets accumulate in renal cancer cells in response to HIF-mediated inhibition of mitochondrial β-oxidation through CPT1 down-regulation. Similarly, lipid droplet breakdown may be impaired through targeting regulatory genes uncovered through the RNAseq analysis. This data could also be further supported through concurrently quantifying alterations in LDQ during chloroquine and temozolomide treatment, simultaneously demonstrating impaired lipid droplet breakdown and improved cytotoxicity. Irrespective of this, the evidence emerging from recent clinical trials may support the improvement of treatment efficacy through impaired lipid droplet flux via lipid droplet breakdown inhibition, further demonstrating the clinical importance of lipid droplet metabolism.

However, our results also suggest that therapeutic efficacy would not be improved by chloroquine pre-treatment in hypoxia and this will hinder the effectiveness of targeting lipid droplet metabolism *in vivo*. This is particularly true of the highly hypoxic GBM tumours; however, as discussed in Section 5.3.5, the inclusion of chloroquine in current GBM treatment regimens has shown improved survival in a

small number of cases (289). It is possible that chloroquine co-treatment may improve therapeutic efficacy in peripheral, better oxygenated tumour cells; however, 21% O_2 is not a physiological oxygen concentration and this would require further investigation. Moreover, the partial rescue of cytotoxicity in hypoxia through prior normoxic manipulation of lipid droplet breakdown suggests that efficacy may be restored through improved understanding of hypoxic lipid droplet metabolism. Indeed, this may also reveal complimentary pharmaceutical targets to further improve combined treatment. Our research also revealed cell line-specific sensitivity to autophagy inhibition in hypoxia and this may contribute to the improved survival in some patients. However, we also observed that autophagy inhibition could increase proliferation in some cells and therefore care must be taken to avoid adversely promoting tumour growth. Finally, tumour hypoxia can be decreased through anti-angiogenic therapies potentially enabling normoxic lipid droplet manipulation to influence chemo- and radio-therapy efficacy.

Therefore, we propose that pharmacological manipulation of lipid droplet metabolism enhances temozolomide and radiation cytotoxicity through hindering lipid droplet flux. This will impair down-stream processes such as mitochondrial β-oxidation and membrane synthesis and prevents the full utilisation of lipid droplets in promoting cell viability. Whilst further investigation into this effect is required, impairment of lipid droplet flux represents an exciting prospect for enhancing GBM therapeutic regimens and may provide an increased understanding of basic tumour biology.

Chapter 6

Conclusions

6.1. Summary of project aims

In this project we aimed to investigate the pathways influencing lipid droplet metabolism and their importance in glioma biology. Although lipid droplet metabolic pathways have been defined in other cancers they are yet to be fully explored in glioma. Through the analysis of online clinical data sets and biological *in vitro* investigation we sought to better understand these pathways in glioma and elucidate possible approaches to improve current therapies.

6.2. Summary of data

6.2.1. The importance of lipid droplet metabolic pathways in glioma prognosis

We defined a gene list representing different aspects of lipid droplet biology and metabolism using the current literature and investigated its importance in glioma survival. Genes representative of ATGL, autophagy, membrane synthesis, mitochondrial β-oxidation and lipid droplet-associated proteins were associated with poor prognosis and an increased expression in higher clinical grades. In contrast, high expression of *de novo* fatty acid synthesis genes was associated with good survival and increased expression in lower clinical grades. Representative genes from other pathways that have been observed as important in lipid droplet metabolism in other cancers, such as cholesterol uptake, showed no association with survival. Interestingly, the expression of the different 'survival-associated' genes was found to correlate with each other, indicating that they may represent a coherent aspect of glioma biology. Moreover, gene expression did not cluster when subjected to cluster analysis, suggesting that this common factor is shared between all gliomas

and not limited to a tumour sub-group. These pathways were selected due to their association with lipid droplet metabolism in other cancers and it is therefore likely they are interlinked through lipid droplets.

Gene expression also separated survival curves across grades 2 and 3 in grade-specific a manner; however, this was not observed at grade 4. Although this could suggest that these genes become unimportant in grade 4 tumours, expression of many poor prognosis genes increased greatly in grade 4 tumours suggesting that grade 4 represents an end point for altered gene expression in these pathways. Gene expression would therefore tend towards a similar point in all tumours upon progressing to grade 4 and not separate survival curves. Alternatively, this contrast in survival prediction may represent differences between primary GBM, which comprises the majority of grade 4 tumours, and grade 2 and 3 gliomas and secondary GBM. However, this assumes that these genes are associated with the IDH and TP53 mutations which define secondary GBM, whereas we observed an association between high gene expression in the poor prognosis genes and IDH1 wildtype tumours. Moreover, analysing the expression of a combination of genes within a defined ‘gene set’ increased the prognostic value of gene expression and separated survival curves in our GBM cohort. Therefore, expression of these genes is important across all glioma grades further supporting the importance of these pathways in glioma biology.

Interestingly, poor prognosis grade 2 tumours could be predicted by a “grade 3 like” gene expression profile. As poor prognosis indicates an increased chance of recurrence and increased clinical grade this suggests a role for lipid droplet-associated genes in influencing or responding to tumour progression. However, our data compares gene expression from different tumours across clinical grades as

opposed to measuring tumour gene expression throughout progression and therefore this hypothesis requires further investigation.

We have therefore demonstrated the importance of gene expression in glioma survival across the tumour grades and hypothesise that gliomas refocus their metabolism from pathways such as *de novo* fatty acid synthesis to autophagy, ATGL and lipid droplet metabolism as they increase in clinical grade and severity.

6.2.2. Biological characterisation of the underlying lipid droplet metabolic pathways in GBM cell lines

Having established a strong basis for a hypothesis that lipid droplets play a significant role in the pathogenesis of gliomas, we further sought to test this through a number of biological investigations. Using confocal microscopy, flow cytometry and NMR-based methods we explored the pathways governing lipid droplet metabolism in GBM cell lines. In conjunction with our observations regarding the lipid uptake transporter CD36 in glioma survival and its correlation with lipid droplet markers such as PLIN2, we found that lipid droplets were predominantly produced through uptake of exogenous lipids in both normoxia and hypoxia.

Similarly, the gene encoding ATGL, which correlated with lipid droplet markers and glioma survival, was found to have a role in lipid droplet metabolism in our cell lines. In other cell types, ATGL is frequently associated with lipid droplet breakdown. However, ATGL inhibition decreased LDQ, suggesting a role in lipid droplet production. Due to the localisation of ATGL at cell membranes as well as lipid droplets (189) and the impact of ATGL inhibition on lipid droplet unsaturated content,

we hypothesised an ATGL-mediated unsaturated lipid shuttle system from cell membranes to lipid droplets. Interestingly, this process would require the participation of FABPs which are known to associate with ATGL through CGI58 (192). Moreover, they have been shown to be important factors in GBM cell line lipid droplet production (123). Lipid droplets provide a protective store for vulnerable unsaturated fatty acids during oxidative stress in *Drosophila* glial cells (226). Our data suggest a similar function for lipid droplets in GBM cell lines through this ATGL-mediated lipid shuttle. Indeed, we further observed that oxidative damage could be increased through ATGL inhibition and this may present an interesting clinical target.

In contrast to exogenous lipid uptake and ATGL, our data did not indicate a major role for *de novo* fatty acid synthesis in lipid droplet production. This is supported by Bensaad et al. (123) who similarly did not observe a role for *de novo* fatty acid synthesis in lipid droplet production in GBM cell lines. Moreover, in Chapter 3 we demonstrated an association between expression of the *de novo* fatty acid synthesis gene set and improved survival. In combination with the decreased gene expression observed in higher grade gliomas, this further supports a decreased reliance upon this pathway in high grade glioma lipid droplet metabolism. Interestingly, our data suggests this pathway may compensate for compromised lipid uptake and ATGL activity, a response that has been similarly observed in other cancers (166,167). Therefore, although *de novo* fatty acid synthesis is not the preferred pathway for lipid droplet production, a possible role in maintaining LDQ further demonstrates the importance of effective lipid droplet metabolism.

As in many other cell types and cancers (179,184-188), the major lipid droplet breakdown mechanism in our cell lines was autophagy, although this was less clear

in hypoxia. This finding mirrored our gene expression data as the vital autophagy gene MAP1LC3A was associated with survival in grade 2, 3 and 4 gliomas and strongly correlated with lipid droplet-associated genes. Moreover, autophagy is known to be an important part of glioma biology (172) and, whilst this was presumed to be through cell death prevention, it may be attributable to a role in lipid droplet metabolism. Perhaps most importantly, pharmacological targeting of autophagy is effective and easily translational, as inhibitors have already been through clinical trials for other diseases, increasing the relevance of autophagy and lipid droplet metabolism as clinical targets.

The function of lipid droplets in gliomas has remained largely unaddressed in cancer. However, our preliminary data suggests they provide a source of lipids for mitochondrial β-oxidation and membrane synthesis. Although this data is limited to one qualitative technique in our investigation, this concept is supported in other cancers by the literature wherein lipid droplets fuel energy production and phospholipid synthesis (92,149,215). Moreover, expression of mitochondrial β-oxidation and membrane synthesis genes correlated with lipid droplet-associated markers and was associated with poor survival in Chapter 3, further supporting the importance of these interlinked pathways in glioma.

In summary, our data suggests that lipid droplet metabolism in gliomas occurs through the uptake of exogenous lipids, ATGL-mediated lipid shuttling and autophagic lipid droplet breakdown (Figure 6.1.). Whilst *de novo* fatty acid synthesis may compensate for decreased activity of other pathways, our data does not suggest a major role for this pathway in lipid droplet metabolism and this is supported by the literature (123). Importantly these results correlate with our

observations in Chapter 3, supporting the increased importance of pathways such as autophagy and ATGL in higher grade gliomas as opposed to *de novo* fatty acid synthesis. Therefore, we have further characterised the metabolic pathways underlying lipid droplet production and breakdown in gliomas and suggest that lipid droplet metabolic pathways, as well as lipid droplets, may represent glioma biomarkers and influence tumour survival.

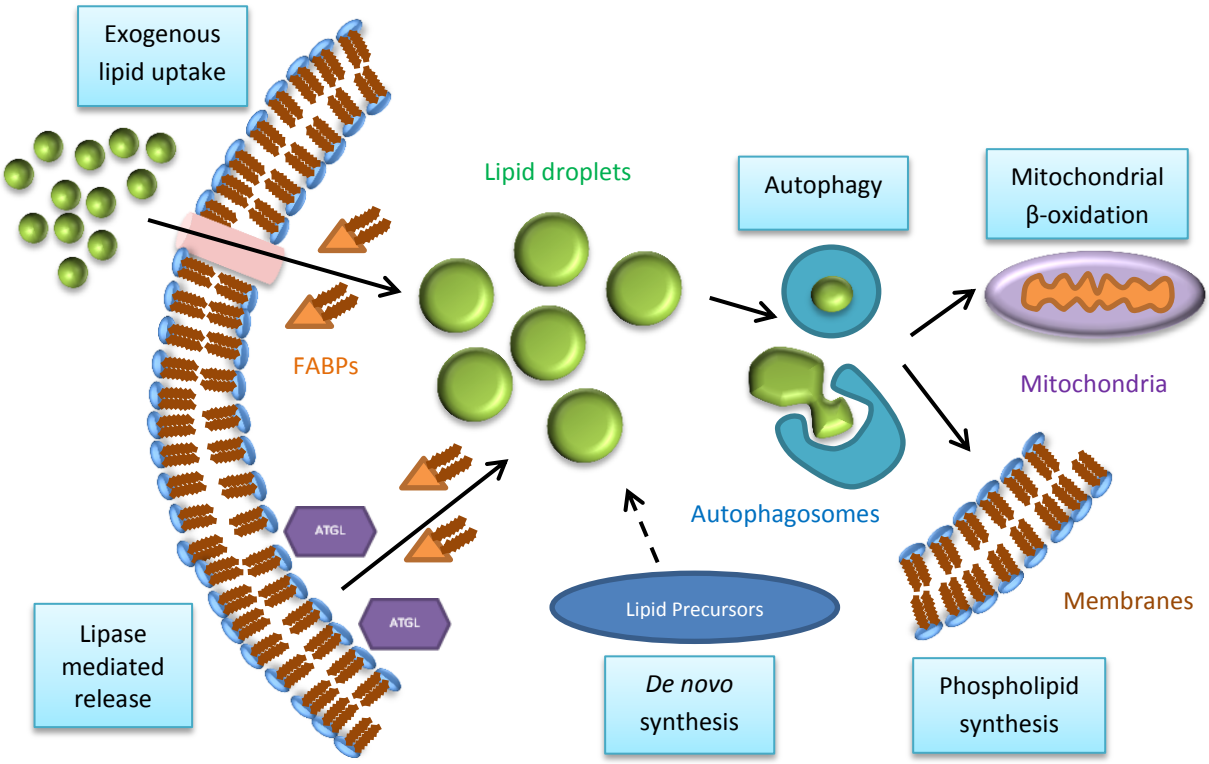

Figure 6.1. A summarised diagram of lipid droplet metabolic pathways in these GBM cell lines. Lipid droplets are produced by exogenous lipid uptake and ATGL-mediated lipid shuttling. *De novo* fatty acid synthesis can contribute to lipid droplet production but does not have a major role in lipid droplet production. Autophagy is the main route of lipid droplet breakdown. Lipid droplet derived lipids can be used to synthesis phospholipids for membranes or produce energy through mitochondrial β-oxidation.

6.2.3. The cytotoxicity of temozolomide and radiation in normoxia can be increased through lipid droplet manipulation

As well as elucidating a relatively unexplored area of glioma metabolism, a better understanding of lipid droplet metabolic pathways in gliomas would enable us to better target lipid droplet metabolism, with the aim to improve current clinical therapies. Lipid droplets have been suggested as important factors in treatment response and resistance, although attempts to target this in GBM have been limited by poor methodology (277). We therefore sought to manipulate LDQ to improve current therapies using the pathways defined in Chapter 4. Despite intrinsic temozolomide and radiation resistance, autophagy inhibition increased temozolomide and irradiation cytotoxicity in normoxia suggesting that lipid droplet manipulation may be of clinical relevance in glioma treatment. Previous studies (238,239,277) suggested that drug efficacy may be improved by inhibiting lipid droplet production, thus decreasing LDQ and drug sequestration. However, we propose that cytotoxicity is improved through interrupted lipid droplet flux as autophagy inhibition impairs lipid droplet breakdown and increases LDQ. As observed in Chapter 4, lipid droplets provide an important source of lipids for energy production and membrane synthesis, and interruption of these processes will further impair cell viability during cytotoxic stress.

Although hypoxia is well established in gliomas and the improved drug cytotoxicity was negated in hypoxia, the partial rescue of this effect by normoxic pre-treatment helps retain the possibility of applying this theory within the clinic. Moreover, tumour hypoxia can be pharmacologically decreased if required whilst tumour resection removes the most significant areas of hypoxia, further supporting the clinical

relevance of lipid droplet manipulation. Finally, this data also highlights the need for *in vitro* studies to be performed in hypoxia when investigating hypoxic tumours.

Interestingly, chloroquine sensitivity varied between cell lines in hypoxia, perhaps reflecting cell line-specific LDQ differences in response to hypoxic autophagy inhibition. Indeed, this may be due to the extent for which impaired lipid droplet metabolism can be compensated for as our data indicated cell death occurs following extended autophagy inhibition. This is further evidence that maintaining effective lipid droplet metabolism is vital in cell survival, particularly during cytotoxic insult. Whilst it could be suggested that the increased cytotoxicity of temozolomide and irradiation is due to the inhibition of general autophagy as opposed to interrupted lipid droplet flux, we have clearly demonstrated the major role autophagy plays in lipid droplet breakdown in these cell lines. Moreover, the correlation between the vital autophagy gene MAP1LC3A and lipid droplet markers and its association with poor survival and increased glioma grade further support the importance of autophagy in lipid droplet metabolism in these cell lines. Therefore, whilst the determination of this effect as lipid droplet-specific requires further confirmation, we suggest that the improved cytotoxicity of temozolomide and irradiation is attributable to inhibition of lipid droplet-specific autophagy.

Temozolomide cytotoxicity was increased through disruption of lipid droplet production with ATGL inhibition, supporting the importance of effective lipid droplet flux in resisting cytotoxic insults. Although we established a role for ATGL in the shuttling of unsaturated fatty acids and the prevention of oxidative stress, as well as lipid droplet production, temozolomide is not thought to cause oxidative stress so this effect is likely due the impairment of lipid droplet flux. Importantly, improved

temozolomide cytotoxicity could be achieved through impaired lipid droplet production as well as breakdown, further supporting interrupted lipid droplet breakdown as the cause for improved temozolomide cytotoxicity with chloroquine treatment, as opposed to general autophagy inhibition.

The improvement of temozolomide and irradiation cytotoxicity by impairing lipid droplet flux represents an exciting clinical opportunity to improve two major aspects of glioma treatment regimens; chemotherapy and radiotherapy. Although this approach remains limited in hypoxia, pharmacological manipulation of hypoxia and further investigation of hypoxic lipid droplet metabolism may reveal alternative and improved strategies to increase treatment efficacy and extend the clinical applicability of combined treatment.

6.3. Future studies

There are several areas within this work which require addressing in future experiments:

Although we show gene expression to alter across tumour grades and be a predictor of survival and prognosis, proving an association with tumour progression requires follow-up gene expression for tumours before and after progression. In such a data set, we hypothesise that expression of the poor prognostic markers; such as PLIN2, PLIN3, MAP1LC3A and PNPLA2, would increase as the tumour progresses, with a corresponding decrease in expression of the good prognostic markers; such as *de novo* fatty acid synthesis enzymes. However, these data are rare and analysis presents its own challenge of separating alterations which are associated with

increased clinical grade and tumour progression versus the effects of exposure to cytotoxic therapies during treatment. Given that paediatric glioma lipid content has been shown to change with treatment (98), there are considerable confounders that would require addressing. Nevertheless, a data set such as this remains vital in monitoring the alterations occurring at each tumour grade and could be further supported using mouse models.

We also need to further explore pathway compensation and the altered lipid droplet metabolism observed in hypoxia. We hypothesise that inhibition of a lipid droplet metabolic pathway will result in a corresponding increase in the activity of alternative pathways. Indeed, this is supported by the minor or conflicting effects on LDQ from inhibiting individual lipid droplet metabolic pathways in hypoxia. We attempted to investigate this through simultaneously inhibiting multiple pathways; however, our results were hindered by the induction of cell stress and death, an effect also observed by Lewis et al. (155). Therefore, future investigations of pathway activity in hypoxia should aim to observe the activation of compensatory pathways non-invasively, for example, through the use of stable isotope-enriched nutrients, such as $^{13}C_{16}$-palmitate, ^{13}C-glucose and ^{13}C-glutamine, to monitor their use by lipid utilising pathways. In these cases, labelled glucose and glutamine incorporation into lipid droplets would be expected to increase upon inhibition of exogenous lipid uptake, with a similar response expected from labelled palmitate upon inhibition of the ATGL-mediated shuttle. Similarly, gene expression of compensatory pathways may increase upon initial pathway inhibition. Lipid droplet breakdown compensation could be further investigated using a pan-lipase inhibitor such as DEUP. We hypothesise that this inhibitor would have no effect on LDQ unless autophagy was simultaneously inhibited, implicating cytoplasmic lipases as a compensatory lipid droplet

mechanism. We further hypothesise that this inhibitor would prevent the LDQ decrease observed upon hypoxic autophagy inhibition in the U343, U87.1 and U87.2 cell lines (Figure 4.14) through preventing the compensatory activation of this pathway as a lipid breakdown mechanism.

The occurrence of cell line-specific responses to lipid droplet metabolic pathway inhibition may reflect the inherent heterogeneity of GBM tumours and could also be further explored through additional RNAseq characterisation of the cell lines. Despite similar gene abundances, the U87 and U87.2 cell lines notably differ in their response to chloroquine or atglistatin treatment in hypoxia, suggesting important mutational or epigenetic differences. We hypothesise that characterisation of these differences may indicate a small list of potential regulatory genes which could be associated with different responses to drug treatment, particularly in hypoxia. This list could then be refined and assessed through targeted gene silencing. Thus, through further characterisation of the genetic profiles of all 5 cell lines, we may extend our understanding of the genetic control underlying lipid droplet metabolic pathways. This could prove vital in maximising the efficacy of impairing lipid droplet flux and in determining effective patient sub-groups for lipid droplet metabolism-associated therapies. Moreover, this data may better inform and caution future studies regarding the significant biological effects that may occur from genetic drift and heterogeneity.

The ATGL-mediated lipid shuttle and its protective role in oxidative stress are supported by both the literature (226) and our investigation, but this area requires considerable further work. We hypothesise that fluorescent-labelled unsaturated fatty acids, ATGL and FABPs will co-localise at membranes, in the cytoplasm during

transport and at lipid droplets providing qualitative evidence for their involvement in a shuttle system. In conjunction with this, we predict that FABP and ATGL knockdown should disrupt this system and decrease unsaturated lipid droplet content, particularly in hypoxia. Finally, as observed with ATGL, inhibition of FABPs should increase ROS damage and therefore interruption of this unsaturated lipid shuttle should decrease viability under oxidative stress. Taken together these experiments could further support our findings and better establish this uncharacterised unsaturated lipid shuttle system.

Our data regarding the use of lipid droplet-derived lipids for mitochondrial β-oxidation and membrane synthesis remains preliminary due the use of a single qualitative technique and therefore requires support from alternative quantitative methodologies. The proportion of lipid droplet-derived lipids catabolised for mitochondrial β-oxidation can be quantified by pharmacologically inhibiting lipid droplet metabolic pathways and observing alterations in oxygen consumption with oxygen probes, such as the Oroboros. Alternatively, the activity of mitochondrial β-oxidation enzymes may also be assessed when deprived of lipid droplet flux. In this case, we hypothesise that mitochondrial β-oxidation would be decreased upon interruption of lipid droplet flux in normoxia but not hypoxia, reflecting the localisation of C16 BODIPY to mitochondria-associated regions in normoxia only. Correspondingly, the role of lipid droplets in membrane synthesis may be investigated through knockdown of membrane synthesis enzymes. We hypothesise that this will result in decreased incorporation of lipid-droplet derived lipids in the cell membrane lipid pool. These experiments could support our data concerning the downstream use of lipid droplets but were not achievable within the timeframe of this project.

We have established the importance of these metabolic pathways in grade 4 glioma cell lines and their relevance in grade 2 and 3 gliomas should also be investigated. From our grade 2 and 3 gene expression data, we would hypothesise an increased reliance upon *de novo* fatty acid synthesis in the lipid droplet metabolism of lower grade tumours and decreased maintenance of lipid droplet flux. Therefore, the experiments of Chapter 4 should be repeated using grade 2 and 3 glioma cell lines to further support the evidence provided in Chapter 3. Moreover, lipid droplet manipulation may also improve current therapies in lower grade tumours, particularly as these tumours are markedly less hypoxic. Similarly, understanding lipid droplet metabolic pathways in grade 2, 3 and 4 glioma cell lines may provide further evidence regarding an association between lipid droplets and tumour progression.

Finally, the clinical significance of this investigation's findings should be further tested using more physiologically relevant models, such as primary cell lines, stem cells and neurospheres, which we predict will continue to demonstrate the importance of these findings.

6.4. Conclusion

Lipid droplets are important metabolically-active structures, capable of impacting a diverse range of processes. Their clinical importance in glioma is well established but the underlying metabolic pathways have remained relatively unexplored. Using gene expression, we demonstrated that lipid droplets and lipid droplet-associated pathways can predict survival and indicate a possible association with tumour progression. Moreover, we demonstrated that glioma lipid droplet production occurs through exogenous lipid uptake and ATGL-mediated unsaturated fatty acid shuttling whilst lipid droplet breakdown occurs through autophagy. We further suggest that lipid droplets can be used to fuel mitochondrial β-oxidation and membrane synthesis and may play a further role in the prevention of oxidative lipid damage. Importantly, we showed that lipid droplet manipulation can improve the current therapies for glioma treatment suggesting that, although they require greater investigation, lipid droplets represent a therapeutic target to complement current treatment regimens. Through analysis of clinical data sets, biological investigation and therapeutic studies, we have elucidated many key areas of lipid droplet metabolism in gliomas and predict that lipid droplets are an important aspect in the improved future treatment of gliomas.

Chapter 7

Appendices

Appendix 7.1. Scripts for generating the correlation heat map in “R”

The correlation heat map was generated using the following script:

```
test.data<-read.table(*data file location*, header=T)

corr.data<-cor(test.data, use="all.obs", method="spearman")

corrplot(corr.data, method="color", type="upper", col=colorRampPalette(c("indian
red", "white", "dark green"))(200))
```

The significance of the correlations was assessed using the following script:

```
test.data<-read.table(*data file location*, header=T)

z<-rcorr(as.matrix(test.data), type="spearman")
```

Appendix 7.2. Correlation heat map data tables

Spearman’s rank r-value correlations

	PLIN2	PLIN3	PNPLA2	CD36	HILPDA	MAP1LC3A	CEPT1	CPT2	ETNK1	PTDSS1	PLIN1	PLIN4	PNPLA3	PNPLA4	ACACA	FASN	SLC25A20
PLIN2	1	0.43	0.17	0.16	0.35	0.17	0.31	0.24	-0.13	-0.03	0.03	0	-0.3	0.27	-0.44	-0.44	0.25
PLIN3	0.43	1	0.19	-0.07	0.25	-0.01	0.51	0.56	-0.13	-0.22	0.22	-0.03	-0.4	0.17	-0.53	-0.52	0.14
PNPLA2	0.17	0.19	1	-0.02	0.14	0.13	-0.07	0.01	-0.32	-0.16	0.01	0.07	-0.24	-0.05	-0.42	-0.06	0.01
CD36	0.16	-0.07	-0.02	1	0.05	-0.17	0.04	0.04	-0.03	0.01	-0.14	-0.16	-0.05	-0.11	-0.01	-0.02	-0.08
HILPDA	0.35	0.25	0.14	0.05	1	0.04	0.27	0.24	-0.11	-0.01	0.03	-0.09	-0.37	0.1	-0.35	-0.34	0.13
MAP1LC3A	0.17	-0.01	0.13	-0.17	0.04	1	-0.1	-0.18	-0.13	0.21	0.08	0.36	0.11	0.66	-0.12	-0.1	0.5
CEPT1	0.31	0.51	-0.07	0.04	0.27	-0.1	1	0.69	0.25	-0.08	0.18	0.08	-0.47	0.19	-0.47	-0.63	0.03
CPT2	0.24	0.56	0.01	0.04	0.24	-0.18	0.69	1	0	-0.08	0.26	0.04	-0.42	0.11	-0.39	-0.5	0.04
ETNK1	-0.13	-0.13	-0.32	-0.03	-0.11	-0.13	0.25	0	1	0.07	-0.09	-0.03	0.05	-0.04	0.1	-0.02	-0.14
PTDSS1	-0.03	-0.22	-0.16	0.01	-0.01	0.21	-0.08	-0.08	0.07	1	-0.3	-0.01	0.21	0.25	0.17	0.05	0.21
PLIN1	0.03	0.22	0.01	-0.14	0.03	0.08	0.18	0.26	-0.09	-0.3	1	0.42	-0.22	0.11	-0.16	-0.14	0.09
PLIN4	0	-0.03	0.07	-0.16	-0.09	0.36	0.08	0.04	-0.03	-0.01	0.42	1	-0.05	0.38	-0.03	-0.02	0.15
PNPLA3	-0.3	-0.4	-0.24	-0.05	-0.37	0.11	-0.47	-0.42	0.05	0.21	-0.22	-0.05	1	0.09	0.62	0.57	0.09
PNPLA4	0.27	0.17	-0.05	-0.11	0.1	0.66	0.19	0.11	-0.04	0.25	0.11	0.38	0.09	1	-0.1	-0.25	0.5
ACACA	-0.44	-0.53	-0.42	-0.01	-0.35	-0.12	-0.47	-0.39	0.1	0.17	-0.16	-0.03	0.62	-0.1	1	0.7	-0.09
FASN	-0.44	-0.52	-0.06	-0.02	-0.34	-0.1	-0.63	-0.5	-0.02	0.05	-0.14	-0.02	0.57	-0.25	0.7	1	-0.18
SLC25A20	0.25	0.14	0.01	-0.08	0.13	0.5	0.03	0.04	-0.14	0.21	0.09	0.15	0.09	0.5	-0.09	-0.18	1

Adjusted p-values (significant correlations are highlighted in red)

	PLIN2	PLIN3	PNPLA2	CD36	HILPDA	MAP1LC3A	CEPT1	CPT2	ETNK1	PTDSS1	PLIN1	PLIN4	PNPLA3	PNPLA4	ACACA	FASN	SLC25A20
PLIN2		0.0001	0.0001	0.0003	0.0001	0.0001	0.0001	0.0001	0.0020	0.4741	0.5054	0.9523	0.0001	0.0001	0.0001	0.0001	0.0001
PLIN3	0.0001		0.0001	0.1191	0.0001	0.8475	0.0001	0.0001	0.0035	0.0001	0.0001	0.4849	0.0001	0.0001	0.0001	0.0001	0.0016
PNPLA2	0.0001	0.0001		0.6472	0.0017	0.0033	0.1058	0.8270	0.0001	0.0002	0.8472	0.1283	0.0001	0.3024	0.0001	0.1882	0.7865
CD36	0.0003	0.1191	0.6472		0.2155	0.0001	0.3440	0.4074	0.4360	0.8925	0.0012	0.0002	0.2457	0.0132	0.7767	0.6683	0.0693
HILPDA	0.0001	0.0001	0.0017	0.2155		0.4141	0.0001	0.0001	0.0090	0.8306	0.5361	0.0302	0.0001	0.0282	0.0001	0.0001	0.0033
MAP1LC3A	0.0001	0.8475	0.0033	0.0001	0.4141		0.0244	0.0001	0.0025	0.0001	0.0729	0.0001	0.0159	0.0001	0.0063	0.0201	0.0001
CEPT1	0.0001	0.0001	0.1058	0.3440	0.0001	0.0244		0.0001	0.0001	0.0685	0.0001	0.0695	0.0001	0.0001	0.0001	0.0001	0.5067
CPT2	0.0001	0.0001	0.8270	0.4074	0.0001	0.0001	0.0001		0.9638	0.0563	0.0001	0.3899	0.0001	0.0099	0.0001	0.0001	0.3911
ETNK1	0.0020	0.0035	0.0001	0.4360	0.0090	0.0025	0.0001	0.9638		0.1285	0.0436	0.4699	0.2898	0.3879	0.0220	0.6927	0.0011
PTDSS1	0.4741	0.0001	0.0002	0.8925	0.8306	0.0001	0.0685	0.0563	0.1285		0.0001	0.8513	0.0001	0.0001	0.0001	0.2466	0.0001
PLIN1	0.5054	0.0001	0.8472	0.0012	0.5361	0.0729	0.0001	0.0001	0.0436	0.0001		0.0001	0.0001	0.0089	0.0002	0.0010	0.0356
PLIN4	0.9523	0.4849	0.1283	0.0002	0.0302	0.0001	0.0695	0.3899	0.4699	0.8513	0.0001		0.2791	0.0001	0.4272	0.6830	0.0004
PNPLA3	0.0001	0.0001	0.0001	0.2457	0.0001	0.0159	0.0001	0.0001	0.2898	0.0001	0.0001	0.2791		0.0389	0.0001	0.0001	0.0418
PNPLA4	0.0001	0.0001	0.3024	0.0132	0.0282	0.0001	0.0001	0.0099	0.3879	0.0001	0.0089	0.0001	0.0389		0.0232	0.0001	0.0001
ACACA	0.0001	0.0001	0.0001	0.7767	0.0001	0.0063	0.0001	0.0001	0.0220	0.0001	0.0002	0.4272	0.0001	0.0232		0.0001	0.0380
FASN	0.0001	0.0001	0.1882	0.6683	0.0001	0.0201	0.0001	0.0001	0.6927	0.2466	0.0010	0.6830	0.0001	0.0001	0.0001		0.0001
SLC25A20	0.0001	0.0016	0.7865	0.0693	0.0033	0.0001	0.5067	0.3911	0.0011	0.0001	0.0356	0.0004	0.0418	0.0001	0.0380	0.0001	

Appendix 7.3. Scripts for generating the cluster analysis

The cluster analysis was generated using the following script:

```
test.data<-read.table(*data file location*, header=T)

heatmap.2(t(test.data),distfun=function(x)dist(x,method="euclidean"),hclustfun=function(x)hclust(x,method="ward.D2"),dendrogram="column",col=redgreen(75),key=TRUE,symkey=FALSE,density.info="none",trace="none",cexRow=1,srtCol=45,labCol=NA)
```

Appendix 7.4. Survival analysis of genes not included in Figure 3.1.

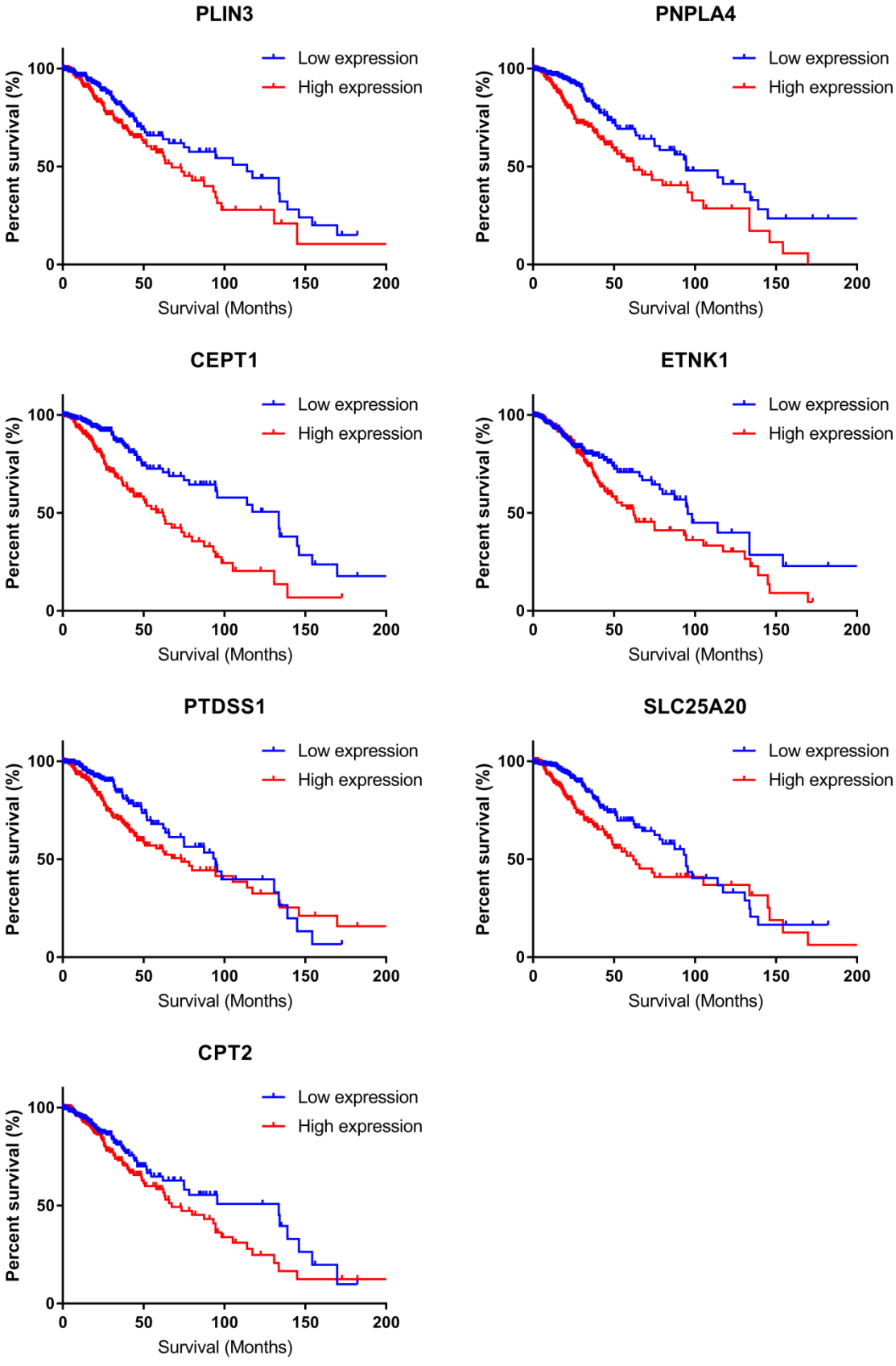

Appendix 7.5. Survival analysis of genes not included in Figure 3.2.

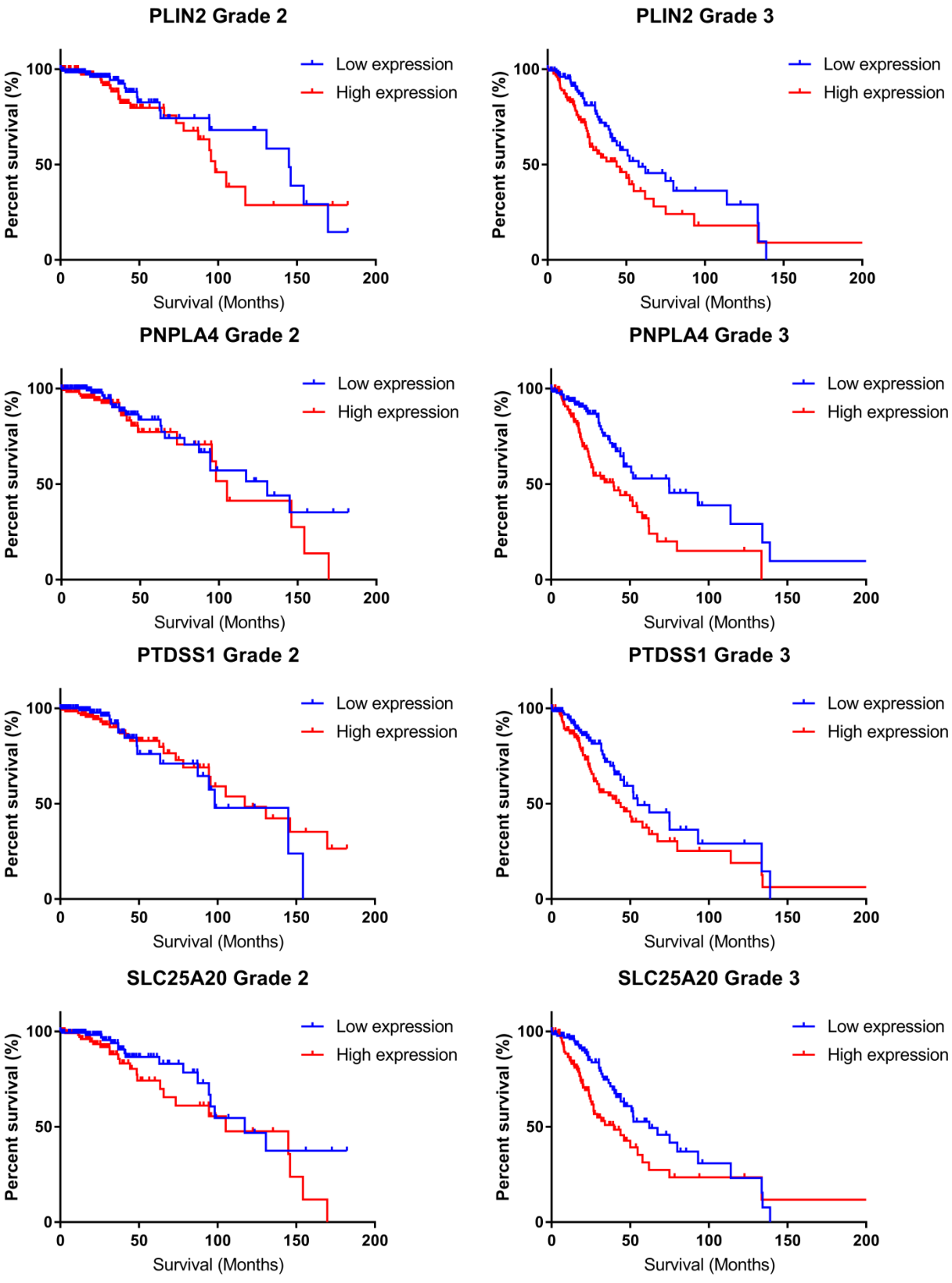

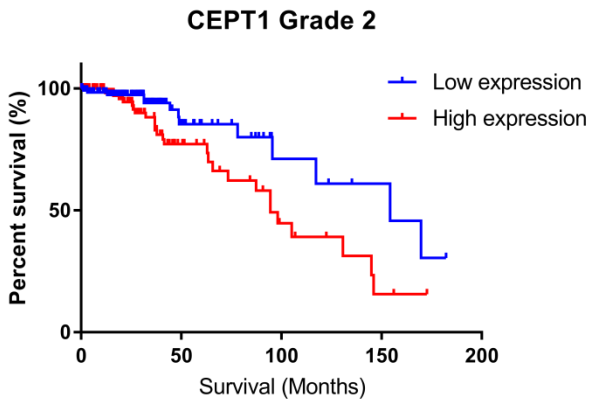
CEPT1 Grade 2
Low expression
High expression
Percent survival (%)
100
50
0
0
50
100
150
200
Survival (Months)

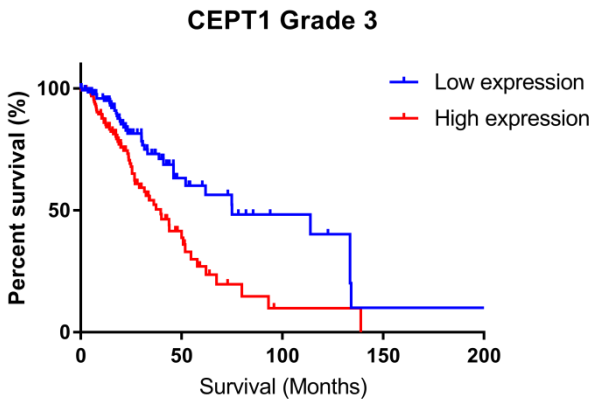
CEPT1 Grade 3
Low expression
High expression
Percent survival (%)
100
50
0
0
50
100
150
200
Survival (Months)

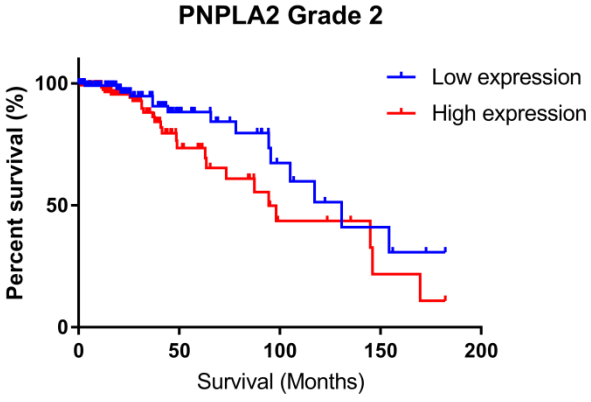
PNPLA2 Grade 2
Low expression
High expression
Percent survival (%)
100
50
0
0
50
100
150
200
Survival (Months)

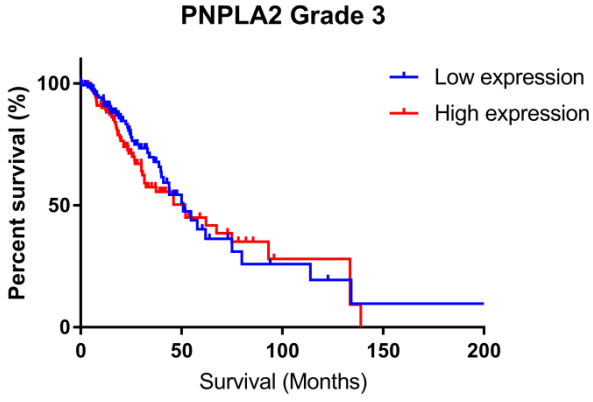
PNPLA2 Grade 3
Low expression
High expression
Percent survival (%)
100
50
0
0
50
100
150
200
Survival (Months)

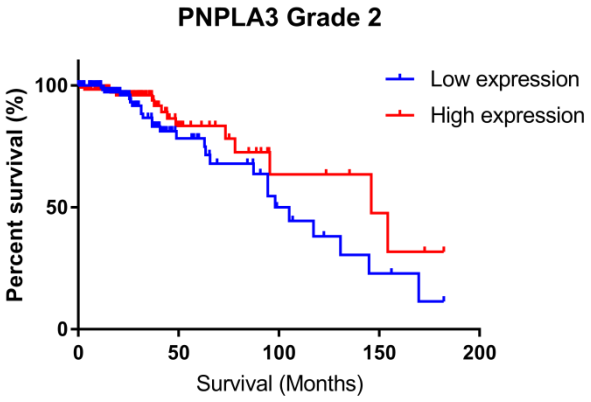
PNPLA3 Grade 2
Low expression
High expression
Percent survival (%)
100
50
0
0
50
100
150
200
Survival (Months)

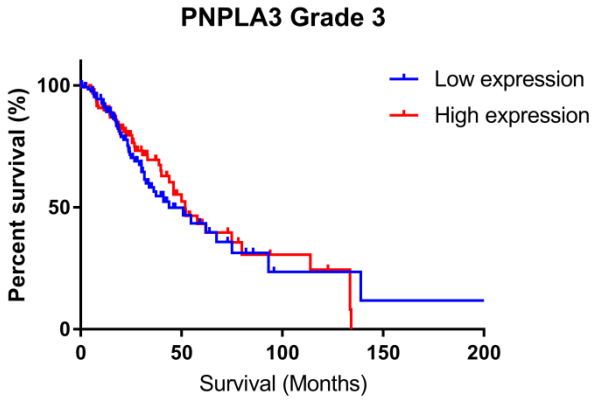
PNPLA3 Grade 3
Low expression
High expression
Percent survival (%)
100
50
0
0
50
100
150
200
Survival (Months)

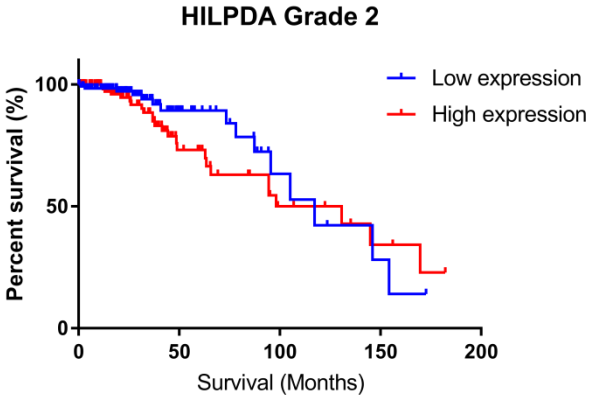
HILPDA Grade 2
Low expression
High expression
Percent survival (%)
100
50
0
0
50
100
150
200
Survival (Months)

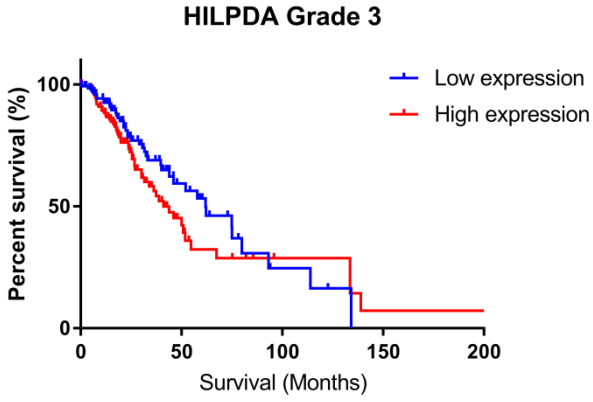
HILPDA Grade 3
Low expression
High expression
Percent survival (%)
100
50
0
0
50
100
150
200
Survival (Months)

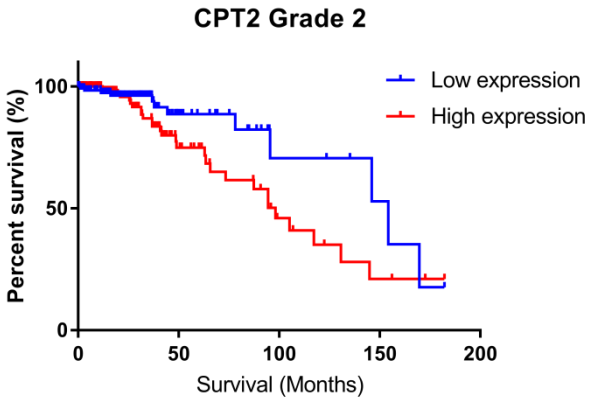
CPT2 Grade 2
Low expression
High expression
Percent survival (%)
100
50
0
0
50
100
150
200
Survival (Months)

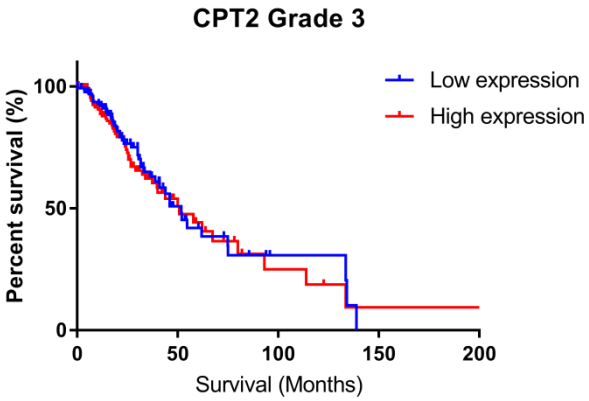
CPT2 Grade 3
Low expression
High expression
Percent survival (%)
100
50
0
0
50
100
150
200
Survival (Months)

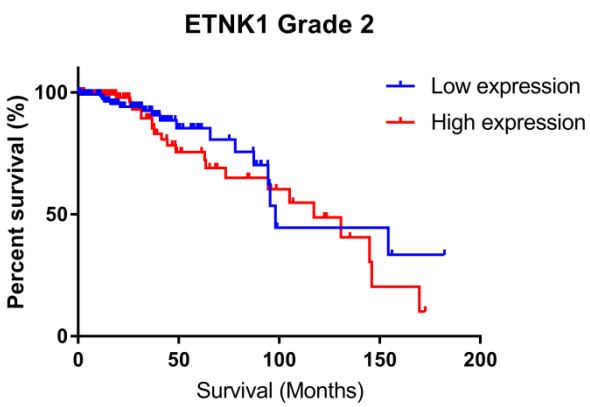
ETNK1 Grade 2
Low expression
High expression
Percent survival (%)
100
50
0
0
50
100
150
200
Survival (Months)

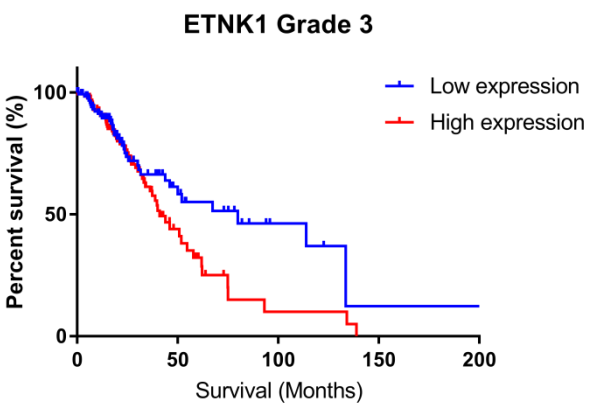
ETNK1 Grade 3
Low expression
High expression
Percent survival (%)
100
50
0
0
50
100
150
200
Survival (Months)

Appendix 7.6. Survival analysis of genes not included in Figure 3.3

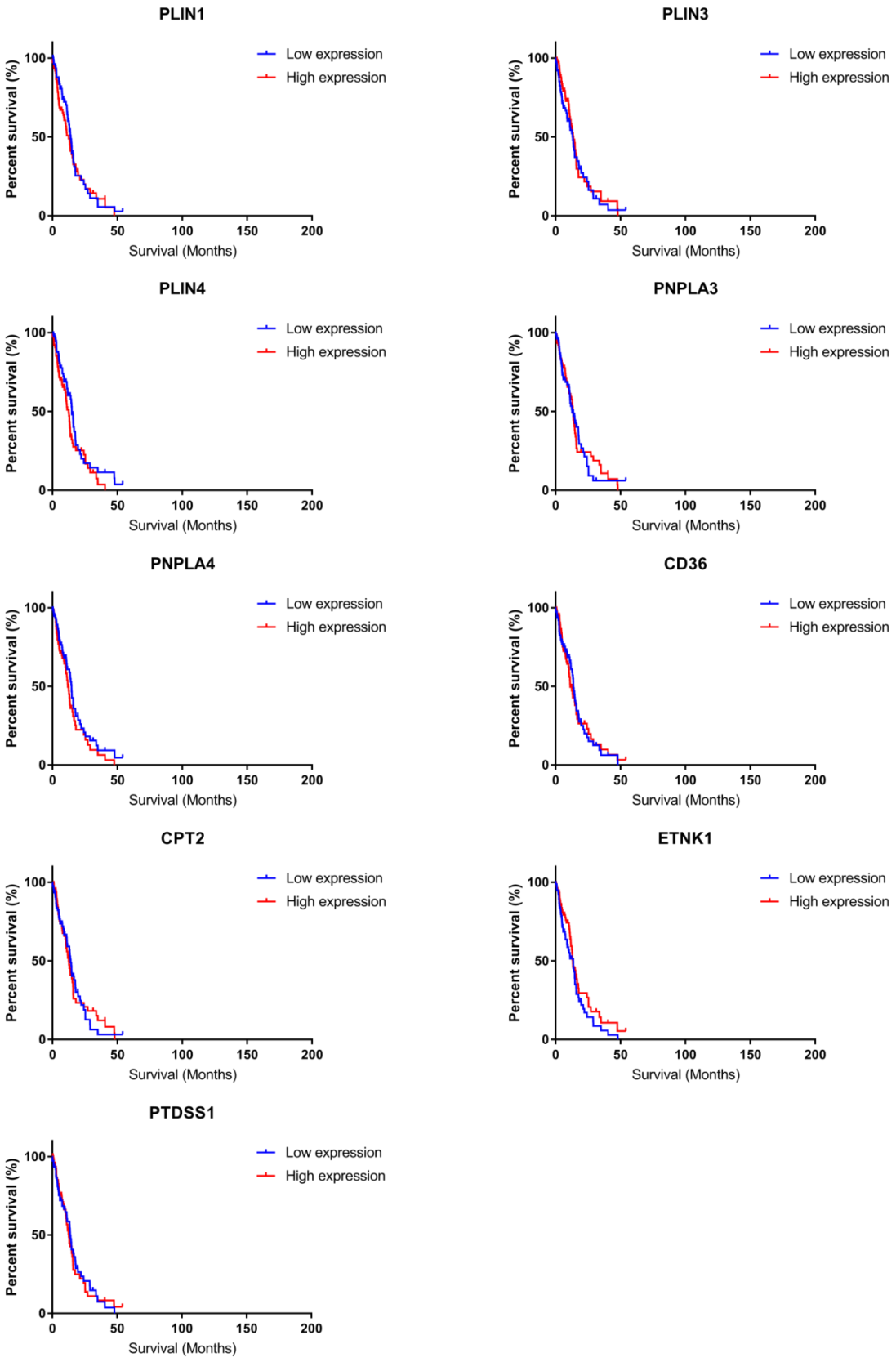

Appendix 7.7. Gene expression boxplots not included in Figure 3.4.

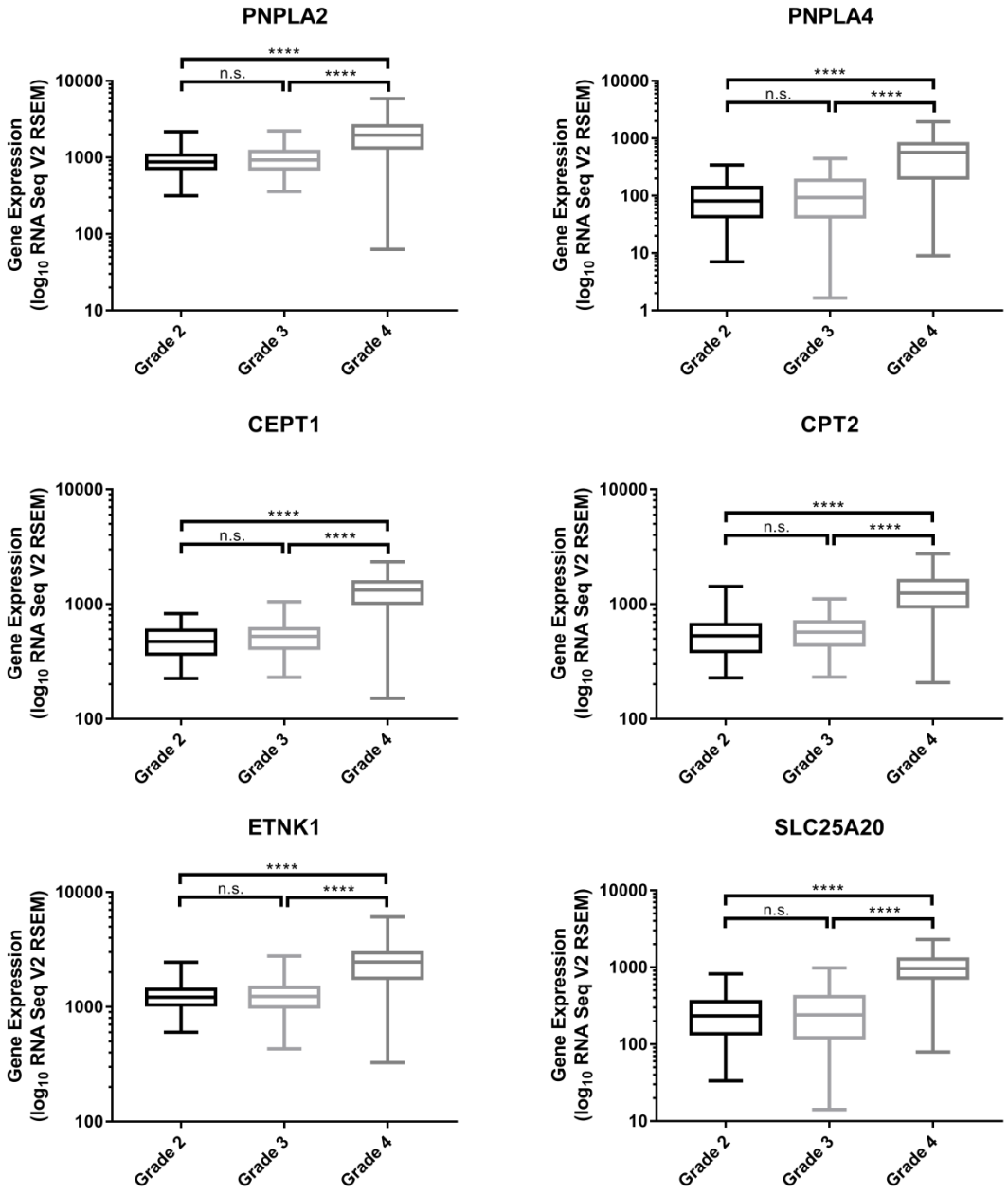

Appendix 7.8. Survival analysis of genes not included in Figure 3.5.

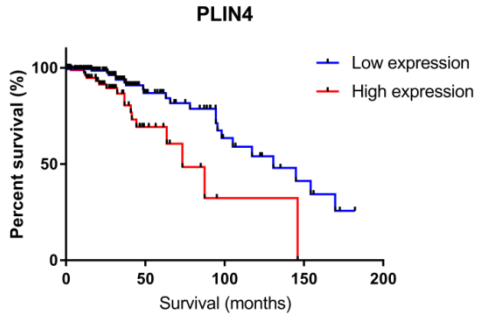

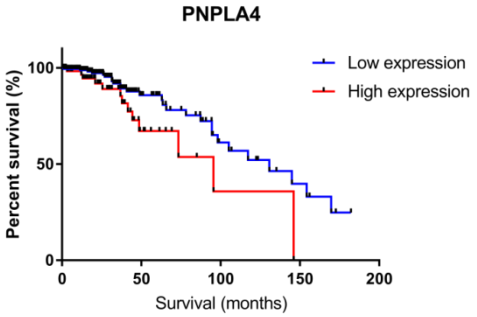

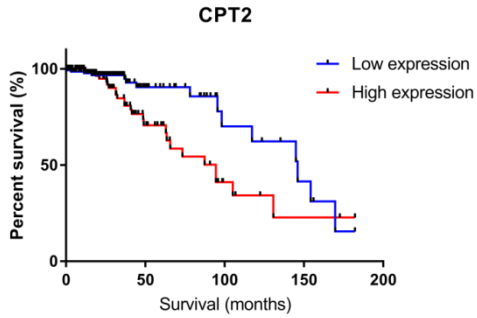

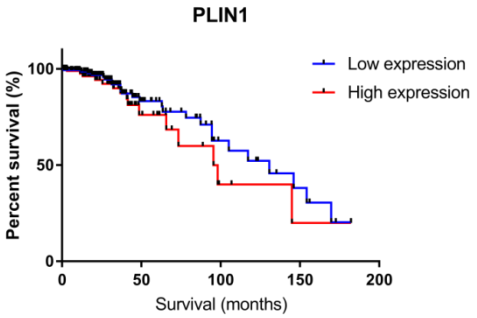

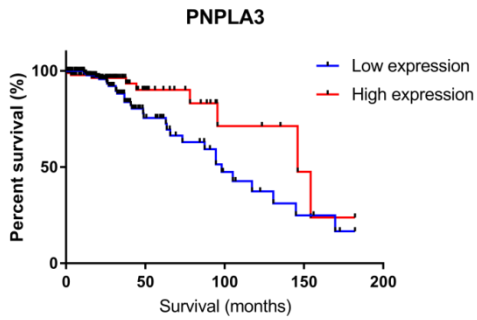

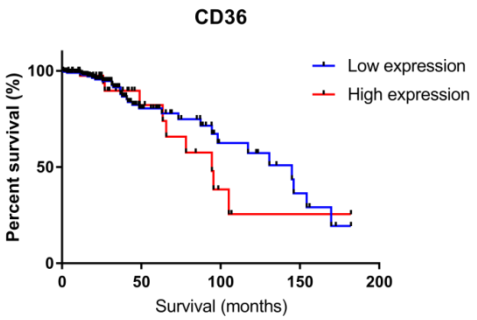

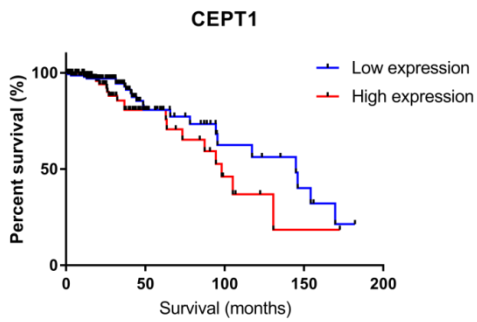

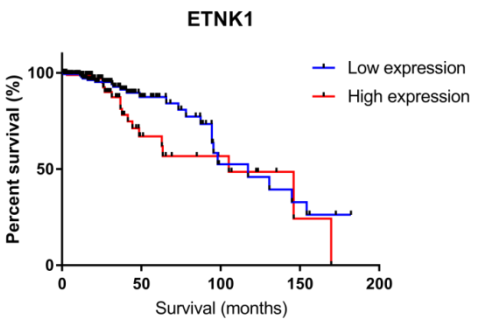

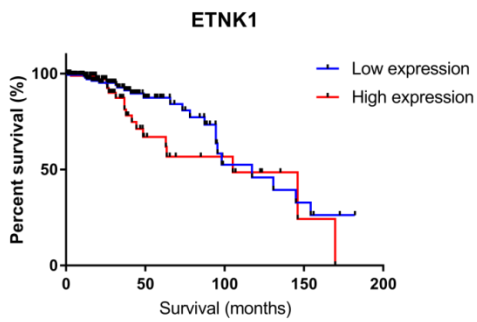

Appendix 7.9. Gene expression boxplots of genes not included in Figure 3.6.

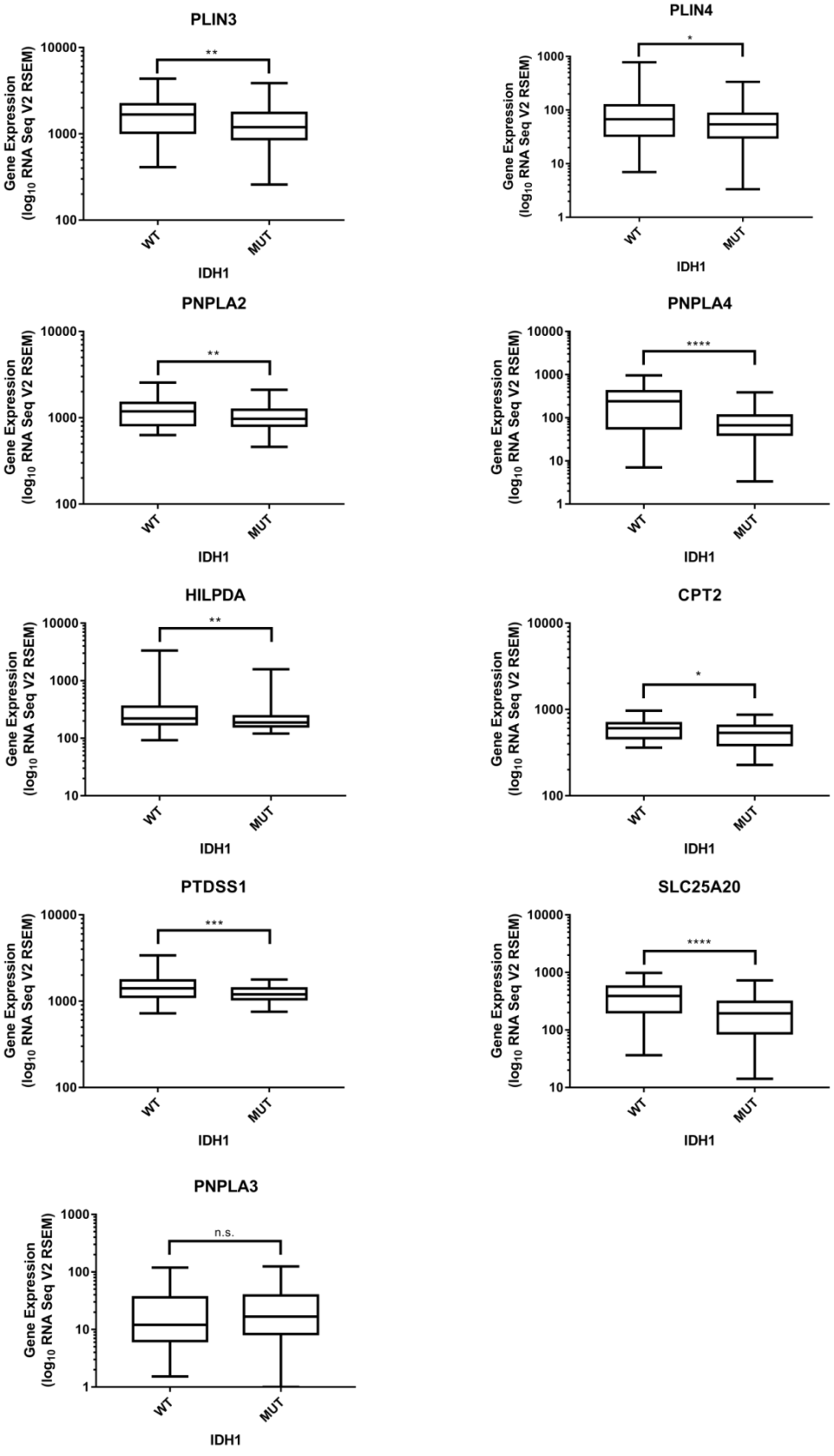

Appendix 7.10. STR profile results

The U87.1 and U87.2 cell lines were found to have the same STR profile. Upon comparison with known STR profiles they were found to match the U87 cell line.

DNA-System	U87.1	U87.2	U87
AM	X, X	X, X	X, X
D3S1358	16, 17	16, 17	16, 17
D1S1656	15, 15	15, 15	15, 15
D6S1043	11, 18	11, 18	11, 18
D13S317	8, 11	8, 11	8, 11
Penta E	7, 14	7, 14	7, 14
D16S539	12, 12	12, 12	12, 12
D18S51	13, 14	13, 14	13, 14
D2S1338	20, 23	20, 23	20, 23
CSF1PO	10, 11	10, 11	10, 11
Penta D	9, 14	9, 14	9, 14
TH01	9.3, 9.3	9.3, 9.3	9.3, 9.3
vWA	15, 17	15, 17	15, 17
D21S11	28, 32.2	28, 32.2	28, 32.2
D7S820	8, 9	8, 9	8, 9
D5S818	11, 12	11, 12	11, 12
TPOX	8, 8	8, 8	8, 8
D8S1179	10, 11	10, 11	10, 11
D12S319	18, 21	18, 21	18, 21
D19S433	15, 15.2	15, 15.2	15, 15.2
FGA	18, 24	18, 24	18, 24

Appendix 7.11. Justification of clonal mutant cell lines

There were 3572 significantly differentially expressed genes between the U87 and U87.1 cell lines. There were 256 significantly differentially expressed genes between the U87 and U87.2 cell lines. There were 3573 significantly differentially expressed genes between the U87.1 and U87.2 cell lines.

First cell line	Second cell line	Significantly differentially expressed genes	Pathways alterations detected by DAVID
U87	U87.1	3572	73
U87	U87.2	256	3
U87.1	U87.2	3573	72

DAVID biochemical pathway analysis of the differentially expressed genes revealed several alterations in key metabolic pathways.

Cell line comparison	Pathway name	Number of alterations
U87 and U87.1	Metabolic pathways	206
	Pathways in cancer	90
	PI3K-Akt signalling	68
	MAPK signalling	47
	Oxidative phosphorylation	32
	HIF-1 signalling	29
	AMPK signalling	25
	Glycolysis/Gluconeogenesis	17
U87 and U87.2	Pathways in cancer	13
U87.1 and U87.2	Metabolic pathways	210
	Pathways in cancer	90
	PI3K-Akt signalling	64
	Oxidative phosphorylation	35
	AMPK signalling	26
	HIF-1 signalling	25
	Glycolysis/Gluconeogenesis	18

An example metabolic Kegg pathway demonstrating significant alterations in gene expression. The image below shows the glycolysis/gluconeogenesis pathway. Red stars denote genes with significant alterations.

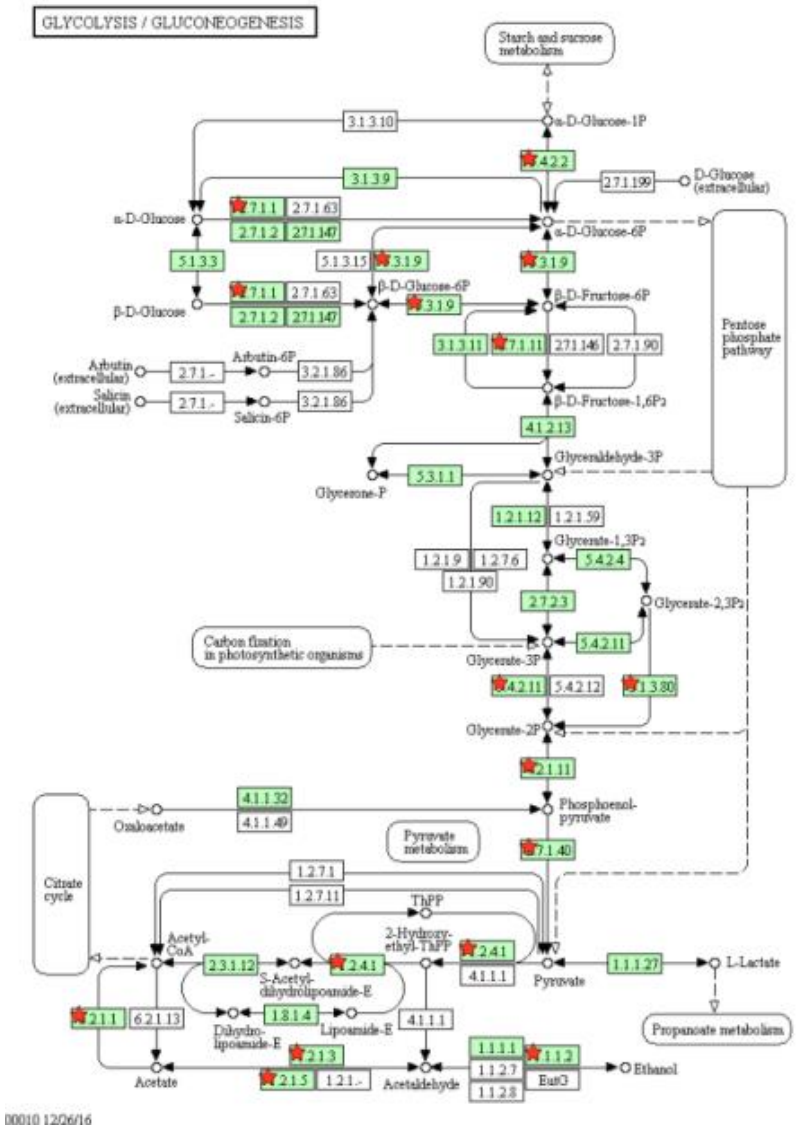

The images below show print screens of the pathways detected by DAVID as containing significant alterations in gene expression. The comparison order is as follows:

U87 vs U87.2

U87 vs U87.1

U87.1 vs U87.2

3 chart records

Download File

Sublist	Category	Term	RT	Genes	Count	%	P-Value	Benjamini
	KEGG_PATHWAY	Pathways in cancer	RT		13	0.0	1.7E-3	2.4E-1
	KEGG_PATHWAY	Rap1 signaling pathway	RT		8	0.0	1.1E-2	5.7E-1
	KEGG_PATHWAY	Focal adhesion	RT		6	0.0	9.0E-2	9.9E-1

Sublist	Category	Term	RT	Genes	Count	%	P-Value	Benjamini
	KEGG_PATHWAY	Metabolic pathways	RT		206	7.4	1.6E-2	1.3E-1
	KEGG_PATHWAY	Pathways in cancer	RT		90	3.2	9.2E-6	1.3E-3
	KEGG_PATHWAY	PI3K-Akt signaling pathway	RT		68	2.4	8.1E-3	9.7E-2
	KEGG_PATHWAY	Endocytosis	RT		54	1.9	5.7E-3	8.8E-2
	KEGG_PATHWAY	Focal adhesion	RT		51	1.8	1.5E-4	1.4E-2
	KEGG_PATHWAY	Regulation of actin cytoskeleton	RT		50	1.8	5.3E-4	2.2E-2
	KEGG_PATHWAY	Proteoglycans in cancer	RT		49	1.8	2.7E-4	1.5E-2
	KEGG_PATHWAY	HTLV-I infection	RT		48	1.7	5.7E-2	2.7E-1
	KEGG_PATHWAY	MAPK signaling pathway	RT		47	1.7	7.5E-2	2.9E-1
	KEGG_PATHWAY	Rap1 signaling pathway	RT		46	1.6	4.7E-3	8.7E-2
	KEGG_PATHWAY	Biosynthesis of antibiotics	RT		43	1.5	2.3E-2	1.5E-1
	KEGG_PATHWAY	Ras signaling pathway	RT		43	1.5	5.9E-2	2.7E-1
	KEGG_PATHWAY	Platelet activation	RT		40	1.4	5.1E-6	1.5E-3
	KEGG_PATHWAY	Tuberculosis	RT		39	1.4	8.7E-3	1.0E-1
	KEGG_PATHWAY	Alzheimer's disease	RT		37	1.3	1.1E-2	1.1E-1
	KEGG_PATHWAY	Calcium signaling pathway	RT		37	1.3	2.8E-2	1.6E-1
	KEGG_PATHWAY	Phagosome	RT		36	1.3	4.1E-3	8.1E-2
	KEGG_PATHWAY	Oxytocin signaling pathway	RT		36	1.3	7.0E-3	9.7E-2
	KEGG_PATHWAY	Protein processing in endoplasmic reticulum	RT		36	1.3	2.0E-2	1.4E-1
	KEGG_PATHWAY	cGMP-PKG signaling pathway	RT		35	1.3	2.5E-2	1.5E-1
	KEGG_PATHWAY	Hepatitis B	RT		33	1.2	1.0E-2	1.1E-1
	KEGG_PATHWAY	Hippo signaling pathway	RT		33	1.2	1.8E-2	1.4E-1
	KEGG_PATHWAY	Oxidative phosphorylation	RT		32	1.1	5.0E-3	8.7E-2
	KEGG_PATHWAY	Adrenergic signaling in cardiomyocytes	RT		32	1.1	1.9E-2	1.4E-1
	KEGG_PATHWAY	Non-alcoholic fatty liver disease (NAFLD)	RT		32	1.1	3.0E-2	1.7E-1
	KEGG_PATHWAY	Tight junction	RT		31	1.1	1.4E-2	1.2E-1
	KEGG_PATHWAY	Parkinson's disease	RT		31	1.1	2.3E-2	1.5E-1
	KEGG_PATHWAY	HIF-1 signaling pathway	RT		29	1.0	2.7E-4	1.9E-2
	KEGG_PATHWAY	Chagas disease (American trypanosomiasis)	RT		28	1.0	1.7E-3	4.8E-2
	KEGG_PATHWAY	TGF-beta signaling pathway	RT		26	0.9	2.8E-4	1.4E-2
	KEGG_PATHWAY	TNF signaling pathway	RT		25	0.9	1.8E-2	1.4E-1
	KEGG_PATHWAY	Toxoplasmosis	RT		25	0.9	5.7E-2	2.8E-1
	KEGG_PATHWAY	Sphingolipid signaling pathway	RT		25	0.9	6.7E-2	2.8E-1
	KEGG_PATHWAY	Lysosome	RT		25	0.9	7.2E-2	2.9E-1
	KEGG_PATHWAY	AMPK signaling pathway	RT		25	0.9	7.8E-2	2.9E-1
	KEGG_PATHWAY	Inflammatory mediator regulation of TRP channels	RT		24	0.9	1.3E-2	1.2E-1
	KEGG_PATHWAY	ErbB signaling pathway	RT		23	0.8	6.2E-3	9.0E-2
	KEGG_PATHWAY	Rheumatoid arthritis	RT		23	0.8	7.1E-3	9.4E-2
	KEGG_PATHWAY	Amoebiasis	RT		23	0.8	5.5E-2	2.7E-1
	KEGG_PATHWAY	ECM-receptor interaction	RT		22	0.8	1.3E-2	1.2E-1
	KEGG_PATHWAY	Hypertrophic cardiomyopathy (HCM)	RT		21	0.8	7.5E-3	9.4E-2
	KEGG_PATHWAY	Dilated cardiomyopathy	RT		21	0.8	1.7E-2	1.4E-1
	KEGG_PATHWAY	Phosphatidylinositol signaling system	RT		21	0.8	7.5E-2	2.9E-1
	KEGG_PATHWAY	Epithelial cell signaling in Helicobacter pylori infection	RT		20	0.7	2.7E-3	7.0E-2
	KEGG_PATHWAY	Adherens junction	RT		20	0.7	5.5E-3	9.0E-2
	KEGG_PATHWAY	Arrhythmogenic right ventricular cardiomyopathy (ARVC)	RT		20	0.7	5.5E-3	9.0E-2
	KEGG_PATHWAY	GnRH signaling pathway	RT		20	0.7	6.7E-2	2.8E-1
	KEGG_PATHWAY	Synaptic vesicle cycle	RT		19	0.7	3.2E-3	7.4E-2
	KEGG_PATHWAY	Bacterial invasion of epithelial cells	RT		19	0.7	3.1E-2	1.7E-1
	KEGG_PATHWAY	Salmonella infection	RT		19	0.7	5.4E-2	2.7E-1
	KEGG_PATHWAY	Fc gamma R-mediated phagocytosis	RT		19	0.7	5.9E-2	2.7E-1
	KEGG_PATHWAY	Small cell lung cancer	RT		19	0.7	6.5E-2	2.8E-1
	KEGG_PATHWAY	NF-kappa B signaling pathway	RT		19	0.7	7.9E-2	2.9E-1
	KEGG_PATHWAY	Gap junction	RT		19	0.7	8.6E-2	3.1E-1
	KEGG_PATHWAY	Vibrio cholerae infection	RT		18	0.6	1.0E-3	3.3E-2
	KEGG_PATHWAY	Pancreatic cancer	RT		18	0.6	1.1E-2	1.1E-1
	KEGG_PATHWAY	Colorectal cancer	RT		17	0.6	1.5E-2	1.3E-1
	KEGG_PATHWAY	Renal cell carcinoma	RT		17	0.6	2.3E-2	1.5E-1
	KEGG_PATHWAY	Glycolysis / Gluconeogenesis	RT		17	0.6	3.0E-2	1.7E-1
	KEGG_PATHWAY	Gastric acid secretion	RT		17	0.6	6.1E-2	2.7E-1
	KEGG_PATHWAY	Long-term depression	RT		16	0.6	2.4E-2	1.5E-1
	KEGG_PATHWAY	Central carbon metabolism in cancer	RT		16	0.6	4.1E-2	2.2E-1
	KEGG_PATHWAY	Malaria	RT		15	0.5	8.8E-3	9.8E-2
	KEGG_PATHWAY	Renin secretion	RT		15	0.5	7.7E-2	2.9E-1
	KEGG_PATHWAY	Acute myeloid leukemia	RT		14	0.5	5.8E-2	2.8E-1
	KEGG_PATHWAY	Collecting duct acid secretion	RT		12	0.4	8.7E-4	3.1E-2

Sublist	Category	Term	RT	Genes	Count	%	P-Value	Benjamini
	KEGG_PATHWAY	Metabolic pathways	RT		210	7.5	9.7E-3	1.0E-1
	KEGG_PATHWAY	Pathways in cancer	RT		90	3.2	1.3E-5	1.2E-3
	KEGG_PATHWAY	PI3K-Akt signaling pathway	RT		64	2.3	4.0E-2	2.0E-1
	KEGG_PATHWAY	Endocytosis	RT		52	1.9	1.6E-2	1.2E-1
	KEGG_PATHWAY	Focal adhesion	RT		49	1.8	6.8E-4	2.8E-2
	KEGG_PATHWAY	Regulation of actin cytoskeleton	RT		48	1.7	2.1E-3	4.5E-2
	KEGG_PATHWAY	Proteoglycans in cancer	RT		47	1.7	1.2E-3	3.0E-2
	KEGG_PATHWAY	Rap1 signaling pathway	RT		47	1.7	3.3E-3	6.1E-2
	KEGG_PATHWAY	Ras signaling pathway	RT		46	1.6	2.1E-2	1.3E-1
	KEGG_PATHWAY	Biosynthesis of antibiotics	RT		44	1.6	1.7E-2	1.2E-1
	KEGG_PATHWAY	Alzheimer's disease	RT		41	1.5	1.2E-3	2.8E-2
	KEGG_PATHWAY	Platelet activation	RT		40	1.4	6.3E-6	9.0E-4
	KEGG_PATHWAY	Phagosome	RT		39	1.4	6.7E-4	3.2E-2
	KEGG_PATHWAY	Protein processing in endoplasmic reticulum	RT		39	1.4	4.6E-3	6.7E-2
	KEGG_PATHWAY	Tuberculosis	RT		39	1.4	1.0E-2	1.0E-1
	KEGG_PATHWAY	Calcium signaling pathway	RT		38	1.4	2.0E-2	1.3E-1
	KEGG_PATHWAY	cGMP-PKG signaling pathway	RT		37	1.3	1.0E-2	1.0E-1
	KEGG_PATHWAY	Oxytocin signaling pathway	RT		36	1.3	8.0E-3	1.0E-1
	KEGG_PATHWAY	Oxidative phosphorylation	RT		35	1.3	7.3E-4	2.3E-2
	KEGG_PATHWAY	Adrenergic signaling in cardiomyocytes	RT		33	1.2	1.3E-2	1.1E-1
	KEGG_PATHWAY	Parkinson's disease	RT		32	1.1	1.5E-2	1.2E-1
	KEGG_PATHWAY	Hippo signaling pathway	RT		32	1.1	3.4E-2	1.8E-1
	KEGG_PATHWAY	Axon guidance	RT		31	1.1	5.3E-3	7.3E-2
	KEGG_PATHWAY	Non-alcoholic fatty liver disease (NAFLD)	RT		31	1.1	5.3E-2	2.3E-1
	KEGG_PATHWAY	Hepatitis B	RT		30	1.1	5.2E-2	2.3E-1
	KEGG_PATHWAY	Tight junction	RT		28	1.0	6.9E-2	2.8E-1
	KEGG_PATHWAY	Rheumatoid arthritis	RT		26	0.9	7.0E-4	2.5E-2
	KEGG_PATHWAY	Chagas disease (American trypanosomiasis)	RT		26	0.9	8.2E-3	9.8E-2
	KEGG_PATHWAY	Vascular smooth muscle contraction	RT		26	0.9	4.1E-2	2.0E-1
	KEGG_PATHWAY	AMPK signaling pathway	RT		26	0.9	5.3E-2	2.3E-1
	KEGG_PATHWAY	TGF-beta signaling pathway	RT		25	0.9	8.2E-4	2.3E-2
	KEGG_PATHWAY	HIF-1 signaling pathway	RT		25	0.9	7.5E-3	9.7E-2
	KEGG_PATHWAY	Inflammatory mediator regulation of TRP channels	RT		24	0.9	1.5E-2	1.2E-1
	KEGG_PATHWAY	Thyroid hormone signaling pathway	RT		24	0.9	7.2E-2	2.8E-1
	KEGG_PATHWAY	Vibrio cholerae infection	RT		23	0.8	2.1E-6	6.0E-4
	KEGG_PATHWAY	Synaptic vesicle cycle	RT		23	0.8	5.4E-5	3.9E-3
	KEGG_PATHWAY	Phosphatidylinositol signaling system	RT		23	0.8	2.7E-2	1.6E-1
	KEGG_PATHWAY	Amoebiasis	RT		23	0.8	5.9E-2	2.5E-1
	KEGG_PATHWAY	TNF signaling pathway	RT		23	0.8	5.9E-2	2.5E-1
	KEGG_PATHWAY	Dilated cardiomyopathy	RT		22	0.8	9.3E-3	1.0E-1
	KEGG_PATHWAY	ECM-receptor interaction	RT		22	0.8	1.4E-2	1.2E-1
	KEGG_PATHWAY	Circadian entrainment	RT		22	0.8	3.6E-2	1.8E-1
	KEGG_PATHWAY	Gastric acid secretion	RT		21	0.8	3.7E-3	6.1E-2
	KEGG_PATHWAY	Hypertrophic cardiomyopathy (HCM)	RT		21	0.8	8.3E-3	9.4E-2
	KEGG_PATHWAY	Epithelial cell signaling in Helicobacter pylori infection	RT		20	0.7	3.0E-3	6.0E-2
	KEGG_PATHWAY	Salmonella infection	RT		20	0.7	3.2E-2	1.8E-1
	KEGG_PATHWAY	ErbB signaling pathway	RT		20	0.7	4.9E-2	2.3E-1
	KEGG_PATHWAY	GnRH signaling pathway	RT		20	0.7	7.2E-2	2.7E-1
	KEGG_PATHWAY	Arrhythmogenic right ventricular cardiomyopathy (ARVC)	RT		19	0.7	1.3E-2	1.1E-1
	KEGG_PATHWAY	Insulin secretion	RT		19	0.7	7.0E-2	2.8E-1
	KEGG_PATHWAY	Small cell lung cancer	RT		19	0.7	7.0E-2	2.8E-1
	KEGG_PATHWAY	Glycolysis / Gluconeogenesis	RT		18	0.6	1.6E-2	1.2E-1
	KEGG_PATHWAY	Adherens junction	RT		18	0.6	2.7E-2	1.6E-1
	KEGG_PATHWAY	Long-term depression	RT		17	0.6	1.2E-2	1.1E-1
	KEGG_PATHWAY	Renin secretion	RT		17	0.6	2.2E-2	1.4E-1
	KEGG_PATHWAY	Pancreatic cancer	RT		17	0.6	2.5E-2	1.5E-1
	KEGG_PATHWAY	Bile secretion	RT		17	0.6	4.2E-2	2.0E-1
	KEGG_PATHWAY	Malaria	RT		16	0.6	3.7E-3	6.4E-2
	KEGG_PATHWAY	Glycerolipid metabolism	RT		16	0.6	1.9E-2	1.3E-1
	KEGG_PATHWAY	Colorectal cancer	RT		16	0.6	3.4E-2	1.8E-1
	KEGG_PATHWAY	Endocrine and other factor-regulated calcium reabsorption	RT		15	0.5	4.2E-3	6.5E-2
	KEGG_PATHWAY	Collecting duct acid secretion	RT		13	0.5	2.1E-4	1.2E-2
	KEGG_PATHWAY	Proteasome	RT		12	0.4	5.2E-2	2.3E-1
	KEGG_PATHWAY	Mineral absorption	RT		12	0.4	6.8E-2	2.8E-1
	KEGG_PATHWAY	N-Glycan biosynthesis	RT		12	0.4	9.9E-2	3.5E-1
	KEGG_PATHWAY	Mucin type O-Glycan biosynthesis	RT		11	0.4	1.1E-2	1.0E-1
	KEGG_PATHWAY	Pentose and glucuronate interconversions	RT		11	0.4	3.2E-2	1.8E-1

Appendix 7.12. siRNA knockdown band densitometry raw data.

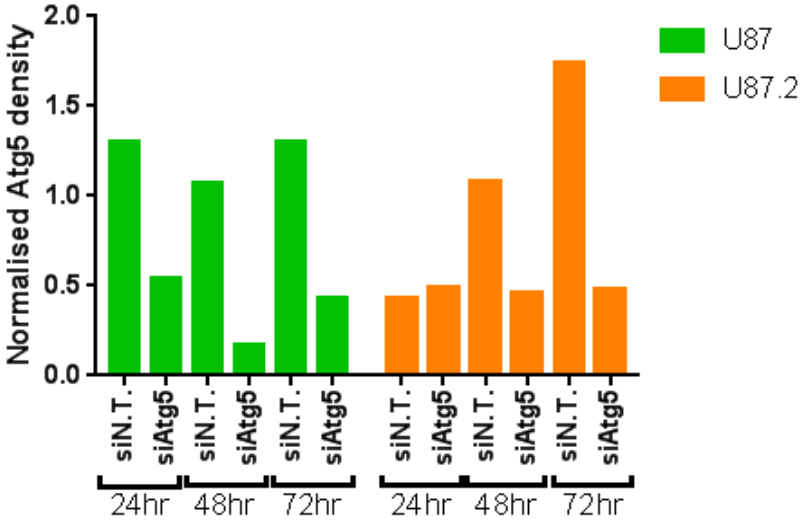

References

(1) WHO. Cancer Fact Sheet. 2017; Available at: http://www.who.int/mediacentre/factsheets/fs297/en/. Accessed 16th August, 2017.

(2) Cancer Research UK. Brain, other CNS and intracranial tumours incidence statistics. 2016; Available at: http://www.cancerresearchuk.org/health-professional/cancer-statistics/statistics-by-cancer-type/brain-other-cns-and-intracranial-tumours/incidence. Accessed 16th August, 2017.

(3) Ostrom QT, Gittleman H, Fulop J, Liu M, Blanda R, Kromer C, et al. CBTRUS Statistical Report: Primary Brain and Central Nervous System Tumors Diagnosed in the United States in 2008-2012. Neuro-oncology 2015;17:iv62.

(4) McKinney PA. Central nervous system tumours in children: Epidemiology and risk factors. Bioelectromagnetics 2005;26(S7):S68.

(5) Bradl M, Lassmann H. Oligodendrocytes: biology and pathology. Acta Neuropathol 2010 Jan;119(1):37-53.

(6) Aguzzi A, Barres BA, Bennett ML. Microglia: scapegoat, saboteur, or something else? Science 2013 Jan 11;339(6116):156-161.

(7) Matyash V, Kettenmann H. Heterogeneity in astrocyte morphology and physiology. Brain Res Rev 2010 May;63(1-2):2-10.

(8) Dolecek TA, Propp JM, Stroup NE, Kruchko C. CBTRUS statistical report: primary brain and central nervous system tumors diagnosed in the United States in 2005-2009. Neuro Oncol 2012 Nov;14 Suppl 5:1.

(9) Louis DN, Perry A, Reifenberger G, von Deimling A, Figarella-Branger D, Cavenee WK, et al. The 2016 World Health Organization Classification of Tumors of the Central Nervous System: a summary. Acta Neuropathol 2016 Jun;131(6):803-820.

(10) Delgado-Lopez PD, Corrales-Garcia EM, Martino J, Lastra-Aras E, Duenas-Polo MT. Diffuse low-grade glioma: a review on the new molecular classification, natural history and current management strategies. Clin Transl Oncol 2017 Aug;19(8):931-944.

(11) Jones DT, Mulholland SA, Pearson DM, Malley DS, Openshaw SW, Lambert SR, et al. Adult grade II diffuse astrocytomas are genetically distinct from and more aggressive than their paediatric counterparts. Acta Neuropathol 2011 Jun;121(6):753-761.

(12) Sanai N, Chang S, Berger MS. Low-grade gliomas in adults. J Neurosurg 2011 Nov;115(5):948-965.

(13) Ostrom QT, Gittleman H, Liao P, Rouse C, Chen Y, Dowling J, et al. CBTRUS statistical report: primary brain and central nervous system tumors diagnosed in the United States in 2007-2011. Neuro Oncol 2014 Oct;16 Suppl 4:63.

(14) Rigau V. Histological Classification. In: Duffau H, editor. Diffuse Low-Grade Gliomas in Adults London: Springer; 2013. p. 31-44.

(15) Rogne SG, Konglund A, Scheie D, Helseth E, Meling TR. Anaplastic astrocytomas: survival and prognostic factors in a surgical series. Acta Neurochir (Wien) 2014 Jun;156(6):1053-1061.

(16) Grimm SA, Pfiffner TJ. Anaplastic astrocytoma. Curr Treat Options Neurol 2013 Jun;15(3):302-315.

(17) Killela PJ, Pirozzi CJ, Reitman ZJ, Jones S, Rasheed BA, Lipp E, et al. The genetic landscape of anaplastic astrocytoma. Oncotarget 2014 Mar;5(6):1452-1457.

(18) Thakkar JP, Dolecek TA, Horbinski C, Ostrom QT, Lightner DD, Barnholtz-Sloan JS, et al. Epidemiologic and molecular prognostic review of glioblastoma. Cancer Epidemiol Biomarkers Prev 2014 Oct;23(10):1985-1996.

(19) Omuro A, DeAngelis LM. Glioblastoma and other malignant gliomas: a clinical review. JAMA 2013 Nov 6;310(17):1842-1850.

(20) Johnson DR, O'Neill BP. Glioblastoma survival in the United States before and during the temozolomide era. J Neurooncol 2012 Apr;107(2):359-364.

(21) Brat DJ. Glioblastoma: biology, genetics, and behavior. Am Soc Clin Oncol Educ Book 2012:102-107.

(22) Rong Y, Durden DL, Van Meir EG, Brat DJ. 'Pseudopalisading' necrosis in glioblastoma: a familiar morphologic feature that links vascular pathology, hypoxia, and angiogenesis. J Neuropathol Exp Neurol 2006 Jun;65(6):529-539.

(23) Mayer A, Schneider F, Vaupel P, Sommer C, Schmidberger H. Differential expression of HIF-1 in glioblastoma multiforme and anaplastic astrocytoma. Int J Oncol 2012 Oct;41(4):1260-1270.

(24) Herrlinger U, Jones DTW, Glas M, Hattingen E, Gramatzki D, Stuplich M, et al. Gliomatosis cerebri: no evidence for a separate brain tumor entity. Acta Neuropathol 2016 Feb;131(2):309-319.

(25) Ohgaki H, Kleihues P. The Definition of Primary and Secondary Glioblastoma. Clin Cancer Res 2013;19(4):764-772.

(26) Verhaak RGW, Hoadley KA, Purdom E, Wang V, Qi Y, Wilkerson MD, et al. An integrated genomic analysis identifies clinically relevant subtypes of glioblastoma characterized by abnormalities in PDGFRA, IDH1, EGFR and NF1. Cancer Cell 2010 Jan 19;17(1):98.

(27) Van Meir EG, Hadjipanayis CG, Norden AD, Shu HK, Wen PY, Olson JJ. Exciting new advances in neuro-oncology: the avenue to a cure for malignant glioma. CA Cancer J Clin 2010;60(3):166-193.

(28) Sturm D, Bender S, Jones DTW, Lichter P, Grill J, Becher O, et al. Paediatric and adult glioblastoma: multiform (epi)genomic culprits emerge. Nat Rev Cancer 2014 Feb;14(2):92-107.

(29) Ohgaki H, Kleihues P. Genetic profile of astrocytic and oligodendroglial gliomas. Brain Tumor Pathol 2011 Jul;28(3):177-183.

(30) Dang L, Yen K, Attar E,C. IDH mutations in cancer and progress toward development of targeted therapeutics. Annals of Oncology 2016;27(4):599-608.

(31) Metallo CM, Gameiro PA, Bell EL, Mattaini KR, Yang J, Hiller K, et al. Reductive glutamine metabolism by IDH1 mediates lipogenesis under hypoxia. Nature 2011;481(7381):380-384.

(32) Bleeker FE, Atai NA, Lamba S, Jonker A, Rijkeboer D, Bosch KS, et al. The prognostic IDH1(R132) mutation is associated with reduced NADP+-dependent IDH activity in glioblastoma. Acta Neuropathol 2010 Apr;119(4):487-494.

(33) Losman JA, Kaelin WG,Jr. What a difference a hydroxyl makes: mutant IDH, (R)-2-hydroxyglutarate, and cancer. Genes Dev 2013 Apr 15;27(8):836-852.

(34) Dang L, Su SM. Isocitrate Dehydrogenase Mutation and (R)-2-Hydroxyglutarate: From Basic Discovery to Therapeutics Development. Annu Rev Biochem 2017;86(1):305-331.

(35) Watanabe T, Nobusawa S, Kleihues P, Ohgaki H. IDH1 mutations are early events in the development of astrocytomas and oligodendrogliomas. Am J Pathol 2009 Apr;174(4):1149-1153.

(36) Lai A, Kharbanda S, Pope WB, Tran A, Solis OE, Peale F, et al. Evidence for sequenced molecular evolution of IDH1 mutant glioblastoma from a distinct cell of origin. J Clin Oncol 2011 Dec 1;29(34):4482-4490.

(37) Cohen A, Holmen S, Colman H. IDH1 and IDH2 Mutations in Gliomas. Current neurology and neuroscience reports 2013;13(5):345.

(38) Rohle D, Popovici-Muller J, Palaskas N, Turcan S, Grommes C, Campos C, et al. An inhibitor of mutant IDH1 delays growth and promotes differentiation of glioma cells. Science 2013 May 3;340(6132):626-630.

(39) Ichimura K, Bolin MB, Goike HM, Schmidt EE, Moshref A, Collins VP. Deregulation of the p14ARF/MDM2/p53 pathway is a prerequisite for human astrocytic gliomas with G1-S transition control gene abnormalities. Cancer Res 2000 Jan 15;60(2):417-424.

(40) Ichimura K. Molecular pathogenesis of IDH mutations in gliomas. Brain Tumor Pathol 2012 Jul;29(3):131-139.

(41) Joerger AC, Fersht AR. The p53 Pathway: Origins, Inactivation in Cancer, and Emerging Therapeutic Approaches. Annu Rev Biochem 2016;85(1):375-404.

(42) Haupt Y, Blandino G. Editorial: Human Tumor-Derived p53 Mutants: A Growing Family of Oncoproteins. Front Oncol 2016;6:10.3389/fonc.2016.00170.

(43) Olivier M, Hollstein M, Hainaut P. TP53 Mutations in Human Cancers: Origins, Consequences, and Clinical Use. Cold Spring Harb Perspect Biol 2010 Jan;2(1):a001008. doi:10.1101/cshperspect.a001008.

(44) Cloughesy TF, Cavenee WK, Mischel PS. Glioblastoma: from molecular pathology to targeted treatment. Annu Rev Pathol 2014;9:1-25.

(45) Bonavia R, Inda M, Cavenee WK, Furnari FB. Heterogeneity Maintenance in Glioblastoma: A Social Network. Cancer Res 2011;71(12):4055-4060.

(46) Nishikawa R, Sugiyama T, Narita Y, Furnari F, Cavenee WK, Matsutani M. Immunohistochemical analysis of the mutant epidermal growth factor, deltaEGFR, in glioblastoma. Brain Tumor Pathol 2004;21(2):53-56.

(47) Inda MM, Bonavia R, Mukasa A, Narita Y, Sah DW, Vandenberg S, et al. Tumor heterogeneity is an active process maintained by a mutant EGFR-induced cytokine circuit in glioblastoma. Genes Dev 2010 Aug 15;24(16):1731-1745.

(48) Srividya MR, Thota B, Shailaja BC, Arivazhagan A, Thennarasu K, Chandramouli BA, et al. Homozygous 10q23/PTEN deletion and its impact on outcome in glioblastoma: a prospective translational study on a uniformly treated cohort of adult patients. Neuropathology 2011 Aug;31(4):376-383.

(49) Friedman JM. Neurofibromatosis 1. In: Adam M, Ardinger H, Pagon R, et al., editors. Gene Reviews Seattle: University of Washington; 2017.

(50) Evans DG, O'Hara C, Wilding A, Ingham SL, Howard E, Dawson J, et al. Mortality in neurofibromatosis 1: in North West England: an assessment of actuarial survival in a region of the UK since 1989. Eur J Hum Genet 2011 Nov;19(11):1187-1191.

(51) Wiestler B, Capper D, Holland-Letz T, Korshunov A, von Deimling A, Pfister SM, et al. ATRX loss refines the classification of anaplastic gliomas and identifies a subgroup of IDH mutant astrocytic tumors with better prognosis. Acta Neuropathol 2013;126(3):443-451.

(52) Ramamoorthy M, Smith S. Loss of ATRX Suppresses Resolution of Telomere Cohesion to Control Recombination in ALT Cancer Cells. Cancer Cell 2015;28(3):357-369.

(53) Clynes D, Higgs DR, Gibbons RJ. The chromatin remodeller ATRX: a repeat offender in human disease. Trends in Biochemical Sciences 2013;38(9):461-466.

(54) Parker NR, Hudson AL, Khong P, Parkinson JF, Dwight T, Ikin RJ, et al. Intratumoral heterogeneity identified at the epigenetic, genetic and transcriptional level in glioblastoma. Scientific Reports 2016;6:22477.

(55) Kloosterhof NK, Bralten LB, Dubbink HJ, French PJ, van den Bent, M J. Isocitrate dehydrogenase-1 mutations: a fundamentally new understanding of diffuse glioma? Lancet Oncol 2011 Jan;12(1):83-91.

(56) Juratli TA, Kirsch M, Robel K, Soucek S, Geiger K, von Kummer R, et al. IDH mutations as an early and consistent marker in low-grade astrocytomas WHO grade II and their consecutive secondary high-grade gliomas. J Neurooncol 2012 Jul;108(3):403-410.

(57) Orringer D, Lau D, Khatri S, Zamora-Berridi GJ, Zhang K, Wu C, et al. Extent of resection in patients with glioblastoma: limiting factors, perception of resectability, and effect on survival. J Neurosurg 2012 Nov;117(5):851-859.

(58) Ghisolfi L, Keates AC, Hu X, Lee DK, Li CJ. Ionizing radiation induces stemness in cancer cells. PLoS One 2012;7(8):e43628.

(59) Asanuma K, Moriai R, Yajima T, Yagihashi A, Yamada M, Kobayashi D, et al. Survivin as a radioresistance factor in pancreatic cancer. Jpn J Cancer Res 2000 Nov;91(11):1204-1209.

(60) Naidu M,D., Mason J,M., Pica R,V., Fung H, Peña L,A. Radiation Resistance in Glioma Cells Determined by DNA Damage Repair Activity of Ape1/Ref-1. Journal of Radiation Research 2010;51(4):393-404.

(61) Mukherjee B, McEllin B, Camacho CV, Tomimatsu N, Sirasanagandala S, Nannepaga S, et al. EGFRvIII and DNA double-strand break repair: a molecular mechanism for radioresistance in glioblastoma. Cancer Res 2009 May 15;69(10):4252-4259.

(62) Al-Dimassi S, Abou-Antoun T, El-Sibai M. Cancer cell resistance mechanisms: a mini review. Clin Transl Oncol 2014 Jun;16(6):511-516.

(63) Barker HE, Paget JTE, Khan AA, Harrington KJ. The Tumour Microenvironment after Radiotherapy: Mechanisms of Resistance and Recurrence. Nat Rev Cancer 2015 Jul;15(7):409-425.

(64) Zhang J, Stevens MF, Bradshaw TD. Temozolomide: mechanisms of action, repair and resistance. Curr Mol Pharmacol 2012 Jan;5(1):102-114.

(65) Villalva C, Cortes U, Wager M, Tourani JM, Rivet P, Marquant C, et al. O6-Methylguanine-methyltransferase (MGMT) promoter methylation status in glioma stem-like cells is correlated to temozolomide sensitivity under differentiation-promoting conditions. Int J Mol Sci 2012;13(6):6983-6994.

(66) Sloan AE, Okada H, Ryken TC, Kalkanis SN, Olson JJ. The role of emerging therapy in the management of patients with diffuse low grade glioma. J Neurooncol 2015 Dec;125(3):631-635.

(67) Chaichana KL, McGirt MJ, Woodworth GF, Datoo G, Tamargo RJ, Weingart J, et al. Persistent outpatient hyperglycemia is independently associated with survival, recurrence and malignant degeneration following surgery for hemispheric low grade gliomas. Neurol Res 2010 May;32(4):442-448.

(68) Gilbert MR, Dignam JJ, Armstrong TS, Wefel JS, Blumenthal DT, Vogelbaum MA, et al. A randomized trial of bevacizumab for newly diagnosed glioblastoma. N Engl J Med 2014 Feb 20;370(8):699-708.

(69) Hamblett KJ, Kozlosky CJ, Siu S, Chang WS, Liu H, Foltz IN, et al. AMG 595, an Anti-EGFRvIII Antibody–Drug Conjugate, Induces Potent Antitumor Activity against EGFRvIII-Expressing Glioblastoma. Mol Cancer Ther 2015;14(7):1614-1624.

(70) Okada H, Butterfield LH, Hamilton RL, Hoji A, Sakaki M, Ahn BJ, et al. Induction of robust type-I CD8+ T-cell responses in WHO grade 2 low-grade glioma patients receiving peptide-based vaccines in combination with poly-ICLC. Clin Cancer Res 2015 Jan 15;21(2):286-294.

(71) Prins RM, Soto H, Konkankit V, Odesa SK, Eskin A, Yong WH, et al. Gene Expression Profile Correlates with T-Cell Infiltration and Relative Survival in Glioblastoma Patients Vaccinated with Dendritic Cell Immunotherapy. Clin Cancer Res 2011;17(6):1603-1615.

(72) Saha D, Martuza RL, Curry WT. Viral Oncolysis of Glioblastoma. In: Reiss C, editor. Neurotropic Viral Infections Cham: Springer; 2016. p. 481-517.

(73) DeLorenze GN, McCoy L, Tsai AL, Quesenberry CP,Jr, Rice T, Il'yasova D, et al. Daily intake of antioxidants in relation to survival among adult patients diagnosed with malignant glioma. BMC Cancer 2010 May 19;10:215.

(74) Schulte A, Liffers K, Kathagen A, Riethdorf S, Zapf S, Merlo A, et al. Erlotinib resistance in EGFR-amplified glioblastoma cells is associated with upregulation of EGFRvIII and PI3Kp110δ. Neuro Oncol 2013 Oct;15(10):1289-1301.

(75) Hanahan D, Weinberg RA. Hallmarks of cancer: the next generation. Cell 2011 Mar 4;144(5):646-674.

(76) Hay N. Reprogramming glucose metabolism in cancer: can it be exploited for cancer therapy? Nature Reviews Cancer 2016;16:635.

(77) Schug ZT, Vande Voorde J, Gottlieb E. The metabolic fate of acetate in cancer. Nature Reviews Cancer 2016;16:708.

(78) Altman BJ, Stine ZE, Dang CV. From Krebs to clinic: glutamine metabolism to cancer therapy. Nature Reviews Cancer 2016;16:619.

(79) Vander Heiden MG, Cantley LC, Thompson CB. Understanding the Warburg Effect: The Metabolic Requirements of Cell Proliferation. Science 2009;324(5930):1029-1033.

(80) WARBURG O. On the origin of cancer cells. Science 1956 Feb 24;123(3191):309-314.

(81) Marquez J, Alonso FJ, Mates JM, Segura JA, Martin-Rufian M, Campos-Sandoval JA. Glutamine Addiction In Gliomas. Neurochem Res 2017 Jun;42(6):1735-1746.

(82) Still ER, Yuneva MO. Hopefully devoted to Q: targeting glutamine addiction in cancer. Br J Cancer 2017 May 23;116(11):1375-1381.

(83) Abramson HN. The lipogenesis pathway as a cancer target. J Med Chem 2011 Aug 25;54(16):5615-5638.

(84) Medes G, Thomas A, Weinhouse S. Metabolism of Neoplastic Tissue. IV. A Study of Lipid Synthesis in Neoplastic Tissue Slices *in Vitro*. Cancer Res 1953;13(1):27-29.

(85) Wu X, Daniels G, Lee P, Monaco ME. Lipid metabolism in prostate cancer. Am J Clin Exp Urol 2014;2(2):111-120.

(86) Clarke NW, Brown MD. The Influence of Lipid Metabolism on Prostate Cancer Development and Progression: Is it Time for a Closer Look? Eur Urol 2007;52(1):3-4.

(87) Suburu J, Chen YQ. Lipids and prostate cancer. Prostaglandins & Other Lipid Mediators 2012;98(1):1-10.

(88) Huang WC, Li X, Liu J, Lin J, Chung LW. Activation of androgen receptor, lipogenesis, and oxidative stress converged by SREBP-1 is responsible for regulating growth and progression of prostate cancer cells. Mol Cancer Res 2012 Jan;10(1):133-142.

(89) Gang X, Yang Y, Zhong J, Jiang K, Pan Y, Karnes RJ, et al. P300 acetyltransferase regulates fatty acid synthase expression, lipid metabolism and prostate cancer growth. Oncotarget 2016 Mar 22;7(12):15135-15149.

(90) Mitra R, Le TT, Gorjala P, Goodman OB,Jr. Positive regulation of prostate cancer cell growth by lipid droplet forming and processing enzymes DGAT1 and ABHD5. BMC Cancer 2017 Sep 6;17(1):6.

(91) Freedland SJ, Aronson WJ. Obesity and prostate cancer. Urology 2005;65(3):433-439.

(92) Wright HJ, Hou J, Xu B, Cortez M, Potma EO, Tromberg BJ, et al. CDCP1 drives triple-negative breast cancer metastasis through reduction of lipid-droplet abundance and stimulation of fatty acid oxidation. Proceedings of the National Academy of Sciences 2017 August 08;114(32):E6565.

(93) Kim S, Lee Y, Koo JS. Differential Expression of Lipid Metabolism-Related Proteins in Different Breast Cancer Subtypes. PLOS ONE 2015;10(3):e0119473.

(94) Opstad KS, Bell BA, Griffiths JR, Howe FA. An investigation of human brain tumour lipids by high-resolution magic angle spinning 1H MRS and histological analysis. NMR Biomed 2008;21(7):677-685.

(95) Delikatny EJ, Chawla S, Leung DJ, Poptani H. MR-visible lipids and the tumor microenvironment. NMR Biomed 2011 Jul;24(6):592-611.

(96) Barbosa AD, Siniossoglou S. Function of lipid droplet-organelle interactions in lipid homeostasis. Biochimica et Biophysica Acta (BBA) - Molecular Cell Research 2017;1864(9):1459-1468.

(97) Pan X, Wilson M, McConville C, Brundler MA, Arvanitis TN, Shockcor JP, et al. The lipid composition of isolated cytoplasmic lipid droplets from a human cancer cell line, BE(2)M17. Mol Biosyst 2012 Jun;8(6):1694-1700.

(98) Mirbahai L, Wilson M, Shaw CS, McConville C, Malcomson RD, Kauppinen RA, et al. Lipid biomarkers of glioma cell growth arrest and cell death detected by 1 H magic angle spinning MRS. NMR Biomed 2012 Nov;25(11):1253-1262.

(99) Grasselli E, Voci A, Canesi L, Salis A, Damonte G, Compalati AD, et al. 3,5-Diiodo-L-Thyronine Modifies the Lipid Droplet Composition in a Model of Hepatosteatosis. Cell Physiol Biochem 2014;33(2):344-356.

(100) Thiam AR, Farese RV, Walther TC. The Biophysics and Cell Biology of Lipid Droplets. Nat Rev Mol Cell Biol 2013 Dec;14(12):775-786.

(101) Walther TC, Farese RV,Jr. Lipid droplets and cellular lipid metabolism. Annu Rev Biochem 2012;81:687-714.

(102) Choudhary V, Ojha N, Golden A, Prinz WA. A conserved family of proteins facilitates nascent lipid droplet budding from the ER. J Cell Biol 2015 Oct 26;211(2):261-271.

(103) Ohsaki Y, Cheng J, Suzuki M, Fujita A, Fujimoto T. Lipid droplets are arrested in the ER membrane by tight binding of lipidated apolipoprotein B-100. J Cell Sci 2008 Jul 15;121(Pt 14):2415-2422.

(104) Wilfling F, Wang H, Haas J, Krahmer N, Gould T, Uchida A, et al. Triacylglycerol Synthesis Enzymes Mediate Lipid Droplet Growth by Relocalizing from the ER to Lipid Droplets. Developmental Cell 2013;24(4):384-399.

(105) Wang CW, Miao YH, Chang YS. Control of lipid droplet size in budding yeast requires the collaboration between Fld1 and Ldb16. J Cell Sci 2014 Mar 15;127(Pt 6):1214-1228.

(106) Fei W, Shui G, Gaeta B, Du X, Kuerschner L, Li P, et al. Fld1p, a functional homologue of human seipin, regulates the size of lipid droplets in yeast. J Cell Biol 2008 Feb 11;180(3):473-482.

(107) Szymanski KM, Binns D, Bartz R, Grishin NV, Li WP, Agarwal AK, et al. The lipodystrophy protein seipin is found at endoplasmic reticulum lipid droplet junctions and is important for droplet morphology. Proc Natl Acad Sci U S A 2007 Dec 26;104(52):20890-20895.

(108) Arisawa K, Mitsudome H, Yoshida K, Sugimoto S, Ishikawa T, Fujiwara Y, et al. Saturated fatty acid in the phospholipid monolayer contributes to the formation of large lipid droplets. Biochem Biophys Res Commun 2016;480(4):641-647.

(109) Bostrom P, Rutberg M, Ericsson J, Holmdahl P, Andersson L, Frohman MA, et al. Cytosolic lipid droplets increase in size by microtubule-dependent complex formation. Arterioscler Thromb Vasc Biol 2005 Sep;25(9):1945-1951.

(110) Pan X, Wilson M, McConville C, Arvanitis TN, Kauppinen RA, Peet AC. The size of cytoplasmic lipid droplets varies between tumour cell lines of the nervous system: a 1H NMR spectroscopy study. MAGMA 2012 Dec;25(6):479-485.

(111) Lahrech H, Zoula S, Farion R, Remy C, Decorps M. In vivo measurement of the size of lipid droplets in an intracerebral glioma in the rat. Magn Reson Med 2001 Mar;45(3):409-414.

(112) Quintero M, Cabanas ME, Arus C. A possible cellular explanation for the NMR-visible mobile lipid (ML) changes in cultured C6 glioma cells with growth. Biochim Biophys Acta 2007 Jan;1771(1):31-44.

(113) Thiele C, Spandl J. Cell biology of lipid droplets. Current Opinion in Cell Biology 2008;20(4):378-385.

(114) Itabe H, Yamaguchi T, Nimura S, Sasabe N. Perilipins: a diversity of intracellular lipid droplet proteins. Lipids in Health and Disease 2017;16(1):83.

(115) Yamaguchi T, Omatsu N, Matsushita S, Osumi T. CGI-58 interacts with perilipin and is localized to lipid droplets. Possible involvement of CGI-58 mislocalization in Chanarin-Dorfman syndrome. J Biol Chem 2004 Jul 16;279(29):30490-30497.

(116) Heid HW, Moll R, Schwetlick I, Rackwitz HR, Keenan TW. Adipophilin is a specific marker of lipid accumulation in diverse cell types and diseases. Cell Tissue Res 1998 Nov;294(2):309-321.

(117) Motomura W, Inoue M, Ohtake T, Takahashi N, Nagamine M, Tanno S, et al. Up-regulation of ADRP in fatty liver in human and liver steatosis in mice fed with high fat diet. Biochemical and Biophysical Research Communications 2006;340(4):1111-1118.

(118) Shiffman D, Mikita T, Tai JT, Wade DP, Porter JG, Seilhamer JJ, et al. Large scale gene expression analysis of cholesterol-loaded macrophages. J Biol Chem 2000 Dec 1;275(48):37324-37332.

(119) Dahlhoff M, Frohlich T, Arnold GJ, Muller U, Leonhardt H, Zouboulis CC, et al. Characterization of the sebocyte lipid droplet proteome reveals novel potential regulators of sebaceous lipogenesis. Exp Cell Res 2015 Mar 1;332(1):146-155.

(120) Russell TD, Palmer CA, Orlicky DJ, Fischer A, Rudolph MC, Neville MC, et al. Cytoplasmic lipid droplet accumulation in developing mammary epithelial cells: roles of adipophilin and lipid metabolism. J Lipid Res 2007 Jul;48(7):1463-1475.

(121) Kaushik S, Cuervo AM. AMPK-dependent phosphorylation of lipid droplet protein PLIN2 triggers its degradation by CMA. Autophagy 2016;12(2):432-438.

(122) Qiu B, Ackerman D, Sanchez DJ, Li B, Ochocki JD, Grazioli A, et al. HIF2alpha-Dependent Lipid Storage Promotes Endoplasmic Reticulum Homeostasis in Clear-Cell Renal Cell Carcinoma. Cancer Discov 2015 Jun;5(6):652-667.

(123) Bensaad K, Favaro E, Lewis CA, Peck B, Lord S, Collins JM, et al. Fatty acid uptake and lipid storage induced by HIF-1alpha contribute to cell growth and survival after hypoxia-reoxygenation. Cell Rep 2014 Oct 9;9(1):349-365.

(124) Patel S, Yang W, Kozusko K, Saudek V, Savage DB. Perilipins 2 and 3 lack a carboxy-terminal domain present in perilipin 1 involved in sequestering ABHD5 and suppressing basal lipolysis. Proc Natl Acad Sci U S A 2014 Jun 24;111(25):9163-9168.

(125) Kuramoto K, Okamura T, Yamaguchi T, Nakamura TY, Wakabayashi S, Morinaga H, et al. Perilipin 5, a lipid droplet-binding protein, protects heart from oxidative burden by sequestering fatty acid from excessive oxidation. J Biol Chem 2012 Jul 6;287(28):23852-23863.

(126) Bosma M, Minnaard R, Sparks LM, Schaart G, Losen M, de Baets MH, et al. The lipid droplet coat protein perilipin 5 also localizes to muscle mitochondria. Histochem Cell Biol 2012 Feb;137(2):205-216.

(127) VandeKopple MJ, Wu J, Baer LA, Bal NC, Maurya SK, Kalyanasundaram A, et al. Stress-responsive HILPDA is necessary for thermoregulation during fasting. Journal of Endocrinology 2017 October 01;235(1):27-38.

(128) Mattijssen F, Georgiadi A, Andasarie T, Szalowska E, Zota A, Krones-Herzig A, et al. Hypoxia-inducible lipid droplet-associated (HILPDA) is a novel peroxisome proliferator-activated receptor (PPAR) target involved in hepatic triglyceride secretion. J Biol Chem 2014 Jul 11;289(28):19279-19293.

(129) Maier A, Wu H, Cordasic N, Oefner P, Dietel B, Thiele C, et al. Hypoxia-inducible protein 2 Hig2/Hilpda mediates neutral lipid accumulation in macrophages and contributes to atherosclerosis in apolipoprotein Edeficient mice. The FASEB Journal 2017 July 31.

(130) Gimm T, Wiese M, Teschemacher B, Deggerich A, Sch&#65533;del J, Knaup KX, et al. Hypoxia-inducible protein 2 is a novel lipid droplet protein and a specific target gene of hypoxia-inducible factor-1. The FASEB Journal 2010 November 01;24(11):4443-4458.

(131) Togashi A, Katagiri T, Ashida S, Fujioka T, Maruyama O, Wakumoto Y, et al. Hypoxia-inducible protein 2 (HIG2), a novel diagnostic marker for renal cell carcinoma and potential target for molecular therapy. Cancer Res 2005 Jun 1;65(11):4817-4826.

(132) Velikkakath AK, Nishimura T, Oita E, Ishihara N, Mizushima N. Mammalian Atg2 proteins are essential for autophagosome formation and important for regulation of size and distribution of lipid droplets. Mol Biol Cell 2012 Mar;23(5):896-909.

(133) Bostrom P, Andersson L, Rutberg M, Perman J, Lidberg U, Johansson BR, et al. SNARE proteins mediate fusion between cytosolic lipid droplets and are implicated in insulin sensitivity. Nat Cell Biol 2007 Nov;9(11):1286-1293.

(134) Andersson L, Bostrom P, Ericson J, Rutberg M, Magnusson B, Marchesan D, et al. PLD1 and ERK2 regulate cytosolic lipid droplet formation. J Cell Sci 2006 Jun 1;119(Pt 11):2246-2257.

(135) Herms A, Bosch M, Reddy BJN, Schieber NL, Fajardo A, Rupérez C, et al. AMPK activation promotes lipid droplet dispersion on detyrosinated microtubules to increase mitochondrial fatty acid oxidation. Nature Communications 2015;6:7176.

(136) Accioly MT, Pacheco P, Maya-Monteiro CM, Carrossini N, Robbs BK, Oliveira SS, et al. Lipid bodies are reservoirs of cyclooxygenase-2 and sites of prostaglandin-E2 synthesis in colon cancer cells. Cancer Res 2008 Mar 15;68(6):1732-1740.

(137) Cabodevilla AG, S&#65533;nchez-Caballero L, Nintou E, Boiadjieva VG, Picatoste F, Gubern A, et al. Cell Survival during Complete Nutrient Deprivation Depends on Lipid Droplet-fueled &#65533;-Oxidation of Fatty Acids. Journal of Biological Chemistry 2013 September 27;288(39):27777-27788.

(138) Boren J, Brindle KM. Apoptosis-induced mitochondrial dysfunction causes cytoplasmic lipid droplet formation. Cell Death Differ 2012 Sep;19(9):1561-1570.

(139) Nakazawa MS, Keith B, Simon MC. Oxygen availability and metabolic adaptations. Nature Reviews Cancer 2016;16:663.

(140) Semenza GL. HIF-1 mediates metabolic responses to intratumoral hypoxia and oncogenic mutations. J Clin Invest 2013 Sep 3;123(9):3664-3671.

(141) Sun RC, Denko NC. Hypoxic regulation of glutamine metabolism through HIF1 and SIAH2 supports lipid synthesis that is necessary for tumor growth. Cell Metab 2014 Feb 4;19(2):285-292.

(142) Wise DR, Ward PS, Shay JE, Cross JR, Gruber JJ, Sachdeva UM, et al. Hypoxia promotes isocitrate dehydrogenase-dependent carboxylation of alpha-ketoglutarate to citrate to support cell growth and viability. Proc Natl Acad Sci U S A 2011 Dec 6;108(49):19611-19616.

(143) Sundelin JP, Stahlman M, Lundqvist A, Levin M, Parini P, Johansson ME, et al. Increased expression of the very low-density lipoprotein receptor mediates lipid accumulation in clear-cell renal cell carcinoma. PLoS One 2012;7(11):e48694.

(144) Glatz JF, Luiken JJ, Bonen A. Membrane fatty acid transporters as regulators of lipid metabolism: implications for metabolic disease. Physiol Rev 2010 Jan;90(1):367-417.

(145) Silverstein RL, Febbraio M. CD36, a Scavenger Receptor Involved in Immunity, Metabolism, Angiogenesis, and Behavior. Sci Signal 2009;2(72):re3.

(146) DeFilippis RA, Chang H, Dumont N, Rabban JT, Chen YY, Fontenay GV, et al. CD36 repression activates a multicellular stromal program shared by high mammographic density and tumor tissues. Cancer Discov 2012 Sep;2(9):826-839.

(147) Kuemmerle NB, Rysman E, Lombardo PS, Flanagan AJ, Lipe BC, Wells WA, et al. Lipoprotein Lipase Links Dietary Fat to Solid Tumor Cell Proliferation. Mol Cancer Ther 2011;10(3):427-436.

(148) Montel V, Gaultier A, Lester RD, Campana WM, Gonias SL. The low-density lipoprotein receptor-related protein regulates cancer cell survival and metastasis development. Cancer Res 2007 Oct 15;67(20):9817-9824.

(149) Wen YA, Xing X, Harris JW, Zaytseva YY, Mitov MI, Napier DL, et al. Adipocytes activate mitochondrial fatty acid oxidation and autophagy to promote tumor growth in colon cancer. Cell Death Dis 2017 Feb;8(2):. Epub 2017 Feb 2 doi:10.1038/cddis.2017.21.

(150) Nieman KM, Kenny HA, Penicka CV, Ladanyi A, Buell-Gutbrod R, Zillhardt MR, et al. Adipocytes promote ovarian cancer metastasis and provide energy for rapid tumor growth. Nature Medicine 2011;17:1498.

(151) Schlaepfer IR, Nambiar DK, Ramteke A, Kumar R, Dhar D, Agarwal C, et al. Hypoxia induces triglycerides accumulation in prostate cancer cells and extracellular vesicles supporting growth and invasiveness following reoxygenation. Oncotarget 2015 Sep 8;6(26):22836-22856.

(152) Giampietri C, Petrungaro S, Cordella M, Tabolacci C, Tomaipitinca L, Facchiano A, et al. Lipid Storage and Autophagy in Melanoma Cancer Cells. International Journal of Molecular Sciences 2017;18(6).

(153) Röhrig F, Schulze A. The multifaceted roles of fatty acid synthesis in cancer. Nature Reviews Cancer 2016;16:732.

(154) Daye D, Wellen KE. Metabolic reprogramming in cancer: unraveling the role of glutamine in tumorigenesis. Semin Cell Dev Biol 2012 Jun;23(4):362-369.

(155) Lewis CA, Brault C, Peck B, Bensaad K, Griffiths B, Mitter R, et al. SREBP maintains lipid biosynthesis and viability of cancer cells under lipid- and oxygen-deprived conditions and defines a gene signature associated with poor survival in glioblastoma multiforme. Oncogene 2015 Oct 1;34(40):5128-5140.

(156) Baenke F, Peck B, Miess H, Schulze A. Hooked on fat: the role of lipid synthesis in cancer metabolism and tumour development. Dis Model Mech 2013 Nov;6(6):1353-1363.

(157) Notarnicola M, Tutino V, Calvani M, Lorusso D, Guerra V, Caruso MG. Serum levels of fatty acid synthase in colorectal cancer patients are associated with tumor stage. J Gastrointest Cancer 2012 Sep;43(3):508-511.

(158) Walter K, Hong SM, Nyhan S, Canto M, Fedarko N, Klein A, et al. Serum Fatty Acid Synthase as a Marker of Pancreatic Neoplasia. Cancer Epidemiol Biomarkers Prev 2009 Sep;18(9):2380-2385.

(159) Lucenay KS, Doostan I, Karakas C, Bui T, Ding Z, Mills GB, et al. Cyclin E Associates with the Lipogenic Enzyme ATP-Citrate Lyase to Enable Malignant Growth of Breast Cancer Cells. Cancer Res 2016.

(160) Xin M, Qiao Z, Li J, Liu J, Song S, Zhao X, et al. miR-22 inhibits tumor growth and metastasis by targeting ATP citrate lyase: evidence in osteosarcoma, prostate cancer, cervical cancer and lung cancer. Oncotarget 2016 Jul 12;7(28):44252-44265.

(161) Chajes V, Cambot M, Moreau K, Lenoir GM, Joulin V. Acetyl-CoA carboxylase alpha is essential to breast cancer cell survival. Cancer Res 2006 May 15;66(10):5287-5294.

(162) Jones JEC, Esler WP, Patel R, Lanba A, Vera NB, Pfefferkorn JA, et al. Inhibition of Acetyl-CoA Carboxylase 1 (ACC1) and 2 (ACC2) Reduces Proliferation and De Novo Lipogenesis of EGFRvIII Human Glioblastoma Cells. PLOS ONE 2017;12(1):e0169566.

(163) Schug ZT, Peck B, Jones DT, Zhang Q, Grosskurth S, Alam IS, et al. Acetyl-CoA synthetase 2 promotes acetate utilization and maintains cancer cell growth under metabolic stress. Cancer Cell 2015 Jan 12;27(1):57-71.

(164) Wilmanski T, Buhman K, Donkin SS, Burgess JR, Teegarden D. 1α,25-dihydroxyvitamin D inhibits de novo fatty acid synthesis and lipid accumulation in metastatic breast cancer cells through down-regulation of pyruvate carboxylase. The Journal of Nutritional Biochemistry 2017;40(Supplement C):194-200.

(165) Wang Q, Hardie RA, Hoy AJ, van Geldermalsen M, Gao D, Fazli L, et al. Targeting ASCT2-mediated glutamine uptake blocks prostate cancer growth and tumour development. J Pathol 2015 Jul;236(3):278-289.

(166) Daniëls VW, Smans K, Royaux I, Chypre M, Swinnen JV, Zaidi N. Cancer Cells Differentially Activate and Thrive on De Novo Lipid Synthesis Pathways in a Low-Lipid Environment. PLOS ONE 2014;9(9):e106913.

(167) Zaidi N, Royaux I, Swinnen JV, Smans K. ATP citrate lyase knockdown induces growth arrest and apoptosis through different cell- and environment-dependent mechanisms. Mol Cancer Ther 2012 Sep;11(9):1925-1935.

(168) Kamphorst JJ, Cross JR, Fan J, de Stanchina E, Mathew R, White EP, et al. Hypoxic and Ras-transformed cells support growth by scavenging unsaturated fatty acids from lysophospholipids. Proc Natl Acad Sci U S A 2013 May 28;110(22):8882-8887.

(169) Galluzzi L, Baehrecke EH, Ballabio A, Boya P, Bravo-San Pedro JM, Cecconi F, et al. Molecular definitions of autophagy and related processes. EMBO J 2017.

(170) White E. Deconvoluting the context-dependent role for autophagy in cancer. Nat Rev Cancer 2012 Apr 26;12(6):401-410.

(171) Dalby KN, Tekedereli I, Lopez-Berestein G, Ozpolat B. Targeting the prodeath and prosurvival functions of autophagy as novel therapeutic strategies in cancer. Autophagy 2010 Apr;6(3):322-329.

(172) Hu Y, DeLay M, Jahangiri A, Molinaro AM, Rose SD, Carbonell WS, et al. Hypoxia-Induced Autophagy Promotes Tumor Cell Survival and Adaptation to Antiangiogenic Treatment in Glioblastoma. Cancer Res 2012;72(7):1773-1783.

(173) Manic G, Obrist F, Kroemer G, Vitale I, Galluzzi L. Chloroquine and hydroxychloroquine for cancer therapy. Mol Cell Oncol 2014;1(1):e29911. doi:10.4161/mco.29911.

(174) Rambold AS, Cohen S, Lippincott-Schwartz J. Fatty acid trafficking in starved cells: regulation by lipid droplet lipolysis, autophagy, and mitochondrial fusion dynamics. Dev Cell 2015 Mar 23;32(6):678-692.

(175) Nguyen TB, Louie SM, Daniele JR, Tran Q, Dillin A, Zoncu R, et al. DGAT1-Dependent Lipid Droplet Biogenesis Protects Mitochondrial Function during Starvation-Induced Autophagy. Developmental Cell 2017;42(1):21.e5.

(176) Guijas C, Rodríguez JP, Rubio JM, Balboa MA, Balsinde J. Phospholipase A2 regulation of lipid droplet formation. Biochimica et Biophysica Acta (BBA) - Molecular and Cell Biology of Lipids 2014;1841(12):1661-1671.

(177) Pucer A, Brglez V, Payre C, Pungercar J, Lambeau G, Petan T. Group X secreted phospholipase A(2) induces lipid droplet formation and prolongs breast cancer cell survival. Mol Cancer 2013 Sep 27;12(1):111.

(178) Wang C. Lipid droplets, lipophagy, and beyond. Biochimica et Biophysica Acta (BBA) - Molecular and Cell Biology of Lipids 2016;1861(8, Part B):793-805.

(179) Singh R, Kaushik S, Wang Y, Xiang Y, Novak I, Komatsu M, et al. Autophagy regulates lipid metabolism. Nature 2009 Apr 30;458(7242):1131-1135.

(180) Schulze RJ, Drizyte K, Casey CA, McNiven MA. Hepatic Lipophagy: New Insights into Autophagic Catabolism of Lipid Droplets in the Liver. Hepatol Commun 2017 Jul;1(5):359-369.

(181) Tsai T, Chen E, Li L, Saha P, Lee H, Huang L, et al. The constitutive lipid droplet protein PLIN2 regulates autophagy in liver. Autophagy 2017;13(7):1130-1144.

(182) Chen E, Tsai TH, Li L, Saha P, Chan L, Chang BH. PLIN2 is a Key Regulator of the Unfolded Protein Response and Endoplasmic Reticulum Stress Resolution in Pancreatic β Cells. Scientific Reports 2017;7:40855.

(183) Martinez–Vicente M, Talloczy Z, Wong E, Tang G, Koga H, Kaushik S, et al. Cargo Recognition Failure is Responsible for Inefficient Autophagy in Huntington's Disease. Nat Neurosci 2010 May;13(5):567-576.

(184) Kaini RR, Sillerud LO, Zhaorigetu S, Hu CA. Autophagy regulates lipolysis and cell survival through lipid droplet degradation in androgen-sensitive prostate cancer cells. Prostate 2012 Sep 15;72(13):1412-1422.

(185) Kaini RR, Hu CA. Synergistic killing effect of chloroquine and androgen deprivation in LNCaP cells. Biochem Biophys Res Commun 2012 Aug 24;425(2):150-156.

(186) Xu G, Jiang Y, Xiao Y, Liu XD, Yue F, Li W, et al. Fast clearance of lipid droplets through MAP1S-activated autophagy suppresses clear cell renal cell carcinomas and promotes patient survival. Oncotarget 2016 Feb 2;7(5):6255-6265.

(187) Mukhopadhyay S, Schlaepfer IR, Bergman BC, Panda PK, Praharaj PP, Naik PP, et al. ATG14 facilitated lipophagy in cancer cells induce ER stress mediated mitoptosis through a ROS dependent pathway. Free Radical Biology and Medicine 2017;104(Supplement C):199-213.

(188) Roy D, Mondal S, Khurana A, Jung DB, Hoffmann R, He X, et al. Loss of HSulf-1: The Missing Link between Autophagy and Lipid Droplets in Ovarian Cancer. Sci Rep 2017;7:10.1038/srep41977.

(189) Zimmermann R, Strauss JG, Haemmerle G, Schoiswohl G, Birner-Gruenberger R, Riederer M, et al. Fat mobilization in adipose tissue is promoted by adipose triglyceride lipase. Science 2004 Nov 19;306(5700):1383-1386.

(190) Schweiger M, Schreiber R, Haemmerle G, Lass A, Fledelius C, Jacobsen P, et al. Adipose triglyceride lipase and hormone-sensitive lipase are the major enzymes in adipose tissue triacylglycerol catabolism. J Biol Chem 2006 Dec 29;281(52):40236-40241.

(191) Taschler U, Radner FPW, Heier C, Schreiber R, Schweiger M, Schoiswohl G, et al. Monoglyceride Lipase Deficiency in Mice Impairs Lipolysis and Attenuates Diet-induced Insulin Resistance. Journal of Biological Chemistry 2011 May 20;286(20):17467-17477.

(192) Hofer P, Boeszoermenyi A, Jaeger D, Feiler U, Arthanari H, Mayer N, et al. Fatty Acid-binding Proteins Interact with Comparative Gene Identification-58 Linking Lipolysis with Lipid Ligand Shuttling. Journal of Biological Chemistry 2015 July 24;290(30):18438-18453.

(193) Eichmann TO, Grumet L, Taschler U, Hartler J, Heier C, Woblistin A, et al. Adipose triglyceride lipase and comparative gene identification-58 are lipid droplet proteins of the hepatic stellate cell-line HSC-T6. J Lipid Res 2015 Oct;56(10):1972-1984.

(194) DiStefano MT, Danai LV, Roth Flach RJ, Chawla A, Pedersen DJ, Guilherme A, et al. The Lipid Droplet Protein Hypoxia-inducible Gene 2 Promotes Hepatic Triglyceride Deposition by Inhibiting Lipolysis. Journal of Biological Chemistry 2015 June 12;290(24):15175-15184.

(195) Nomura DK, Long JZ, Niessen S, Hoover HS, Ng SW, Cravatt BF. Monoacylglycerol lipase regulates a fatty acid network that promotes cancer pathogenesis. Cell 2010 Jan 8;140(1):49-61.

(196) Nomura DK, Lombardi DP, Chang JW, Niessen S, Ward AM, Long JZ, et al. Monoacylglycerol lipase exerts dual control over endocannabinoid and fatty acid pathways to support prostate cancer. Chem Biol 2011 Jul 29;18(7):846-856.

(197) Smirnova E, Goldberg EB, Makarova KS, Lin L, Brown WJ, Jackson CL. ATGL has a key role in lipid droplet/adiposome degradation in mammalian cells. EMBO Rep 2006 Jan;7(1):106-113.

(198) Sathyanarayan A, Mashek MT, Mashek DG. ATGL Promotes Autophagy/Lipophagy via SIRT1 to Control Hepatic Lipid Droplet Catabolism. Cell Reports 2017;19(1):1-9.

(199) Dupont N, Chauhan S, Arko-Mensah J, Castillo EF, Masedunskas A, Weigert R, et al. Neutral lipid stores and lipase PNPLA5 contribute to autophagosome biogenesis. Curr Biol 2014 Mar 17;24(6):609-620.

(200) Houten SM, Violante S, Ventura FV, Wanders RJA. The Biochemistry and Physiology of Mitochondrial Fatty Acid β-Oxidation and Its Genetic Disorders. Annu Rev Physiol 2016;78(1):23-44.

(201) Carracedo A, Cantley LC, Pandolfi PP. Cancer metabolism: fatty acid oxidation in the limelight. Nat Rev Cancer 2013 Apr;13(4):227-232.

(202) Donohoe DR, Collins LB, Wali A, Bigler R, Sun W, Bultman SJ. The Warburg effect dictates the mechanism of butyrate-mediated histone acetylation and cell proliferation. Mol Cell 2012 Nov 30;48(4):612-626.

(203) Camarda R, Zhou AY, Kohnz RA, Balakrishnan S, Mahieu C, Anderton B, et al. Inhibition of fatty acid oxidation as a therapy for MYC-overexpressing triple-negative breast cancer. Nat Med 2016 Apr;22(4):427-432.

(204) Park JH, Vithayathil S, Kumar S, Sung PL, Dobrolecki LE, Putluri V, et al. Fatty Acid Oxidation-Driven Src Links Mitochondrial Energy Reprogramming and Oncogenic Properties in Triple-Negative Breast Cancer. Cell Rep 2016 Mar 8;14(9):2154-2165.

(205) Ye H, Adane B, Khan N, Sullivan T, Minhajuddin M, Gasparetto M, et al. Leukemic Stem Cells Evade Chemotherapy by Metabolic Adaptation to an Adipose Tissue Niche. Cell Stem Cell 2016 Jul 7;19(1):23-37.

(206) Zaugg K, Yao Y, Reilly PT, Kannan K, Kiarash R, Mason J, et al. Carnitine palmitoyltransferase 1C promotes cell survival and tumor growth under conditions of metabolic stress. Genes Dev 2011 May 15;25(10):1041-1051.

(207) Kimmel AR, Sztalryd C. Perilipin 5, a Lipid Droplet Protein Adapted to Mitochondrial Energy Utilization. Curr Opin Lipidol 2014 Apr;25(2):110-117.

(208) Wang H, Sreenivasan U, Hu H, Saladino A, Polster BM, Lund LM, et al. Perilipin 5, a lipid droplet-associated protein, provides physical and metabolic linkage to mitochondria. Journal of Lipid Research 2011 December 01;52(12):2159-2168.

(209) Bhatia H, Pattnaik BR, Datta M. Inhibition of mitochondrial beta-oxidation by miR-107 promotes hepatic lipid accumulation and impairs glucose tolerance in vivo. Int J Obes (Lond) 2016 May;40(5):861-869.

(210) Glunde K, Bhujwalla ZM, Ronen SM. Choline metabolism in malignant transformation. Nat Rev Cancer 2011 Nov 17;11(12):835-848.

(211) Glunde K, Penet MF, Jiang L, Jacobs MA, Bhujwalla ZM. Choline metabolism-based molecular diagnosis of cancer: an update. Expert Rev Mol Diagn 2015 Jun;15(6):735-747.

(212) Ide Y, Waki M, Hayasaka T, Nishio T, Morita Y, Tanaka H, et al. Human Breast Cancer Tissues Contain Abundant Phosphatidylcholine(36∶1) with High Stearoyl-CoA Desaturase-1 Expression. PLoS One 2013;8(4):e61204. doi:10.1371/journal.pone.0061204.

(213) Jia M, Andreassen T, Jensen L, Bathen TF, Sinha I, Gao H, et al. Estrogen Receptor α Promotes Breast Cancer by Reprogramming Choline Metabolism. Cancer Res 2016;76(19):5634-5646.

(214) Trousil S, Kaliszczak M, Schug Z, Nguyen QD, Tomasi G, Favicchio R, et al. The novel choline kinase inhibitor ICL-CCIC-0019 reprograms cellular metabolism and inhibits cancer cell growth. Oncotarget 2016 Jun 14;7(24):37103-37120.

(215) Glunde K, Raman V, Mori N, Bhujwalla ZM. RNA Interference–Mediated Choline Kinase Suppression in Breast Cancer Cells Induces Differentiation and Reduces Proliferation. Cancer Res 2005;65(23):11034-11043.

(216) Yao C, Fowle-Grider R, Mahieu N, Liu G, Chen Y,Jr, Wang R, et al. Exogenous Fatty Acids Are the Preferred Source of Membrane Lipids in Proliferating Fibroblasts. Cell Chemical Biology 2016;23(4):483-493.

(217) Griner EM, Kazanietz MG. Protein kinase C and other diacylglycerol effectors in cancer. Nat Rev Cancer 2007 Apr;7(4):281-294.

(218) Vanhaesebroeck B, Stephens L, Hawkins P. PI3K signalling: the path to discovery and understanding. Nat Rev Mol Cell Biol 2012 Feb 23;13(3):195-203.

(219) Pyne NJ, Tonelli F, Lim KG, Long JS, Edwards J, Pyne S. Sphingosine 1-phosphate signalling in cancer. Biochem Soc Trans 2012 Feb;40(1):94-100.

(220) Park JB, Lee CS, Jang JH, Ghim J, Kim YJ, You S, et al. Phospholipase signalling networks in cancer. Nat Rev Cancer 2012 Nov;12(11):782-792.

(221) Deevska GM, Nikolova-Karakashian MN. The expanding role of sphingolipids in lipid droplet biogenesis. Biochimica et Biophysica Acta (BBA) - Molecular and Cell Biology of Lipids 2017;1862(10, Part B):1155-1165.

(222) Pyne NJ, El Buri A, Adams DR, Pyne S. Sphingosine 1-phosphate and cancer. Advances in Biological Regulation 2017.

(223) Ohsaki Y, Cheng J, Fujita A, Tokumoto T, Fujimoto T. Cytoplasmic lipid droplets are sites of convergence of proteasomal and autophagic degradation of apolipoprotein B. Mol Biol Cell 2006 Jun;17(6):2674-2683.

(224) Keembiyehetty CN, Krzeslak A, Love DC, Hanover JA. A lipid-droplet-targeted O-GlcNAcase isoform is a key regulator of the proteasome. J Cell Sci 2011 Aug 15;124(16):2851-2860.

(225) Koritzinsky M, Wouters BG. The roles of reactive oxygen species and autophagy in mediating the tolerance of tumor cells to cycling hypoxia. Semin Radiat Oncol 2013 Oct;23(4):252-261.

(226) Bailey AP, Koster G, Guillermier C, Hirst EM, MacRae JI, Lechene CP, et al. Antioxidant Role for Lipid Droplets in a Stem Cell Niche of Drosophila. Cell 2015 Oct 8;163(2):340-353.

(227) Zhang X, Zhang K. Endoplasmic Reticulum Stress-Associated Lipid Droplet Formation and Type II Diabetes. Biochem Res Int 2012;2012:247275.

(228) Welte MA. Proteins under new management: lipid droplets deliver. Trends Cell Biol 2007 Aug;17(8):363-369.

(229) Rysman E, Brusselmans K, Scheys K, Timmermans L, Derua R, Munck S, et al. De novo lipogenesis protects cancer cells from free radicals and chemotherapeutics by promoting membrane lipid saturation. Cancer Res 2010 Oct 15;70(20):8117-8126.

(230) Yang Y, Liu H, Li Z, Zhao Z, Yip-Schneider M, Fan Q, et al. Role of fatty acid synthase in gemcitabine and radiation resistance of pancreatic cancers. Int J Biochem Mol Biol 2011 Jan 1;2(1):89-98.

(231) Greening DW, Lee ST, Ji H, Simpson RJ, Rigopoulos A, Murone C, et al. Molecular profiling of cetuximab and bevacizumab treatment of colorectal tumours reveals perturbations in metabolic and hypoxic response pathways. Oncotarget 2015 Nov 10;6(35):38166-38180.

(232) Potcoava MC, Futia GL, Aughenbaugh J, Schlaepfer IR, Gibson EA. Raman and coherent anti-Stokes Raman scattering microscopy studies of changes in lipid content and composition in hormone-treated breast and prostate cancer cells. J Biomed Opt 2014;19(11):111605.

(233) Mesti T, Savarin P, Triba MN, Le Moyec L, Ocvirk J, Banissi C, et al. Metabolic impact of anti-angiogenic agents on U87 glioma cells. PLoS One 2014 Jun 12;9(6):e99198.

(234) Pan X, Wilson M, McConville C, Arvanitis TN, Griffin JL, Kauppinen RA, et al. Increased unsaturation of lipids in cytoplasmic lipid droplets in DAOY cancer cells in response to cisplatin treatment. Metabolomics 2013 Jun;9(3):722-729.

(235) Montopoli M, Bellanda M, Lonardoni F, Ragazzi E, Dorigo P, Froldi G, et al. "Metabolic reprogramming" in ovarian cancer cells resistant to cisplatin. Curr Cancer Drug Targets 2011 Feb;11(2):226-235.

(236) Zietkowski D, Payne GS, Nagy E, Mobberley MA, Ryder TA, deSouza NM. Comparison of NMR lipid profiles in mitotic arrest and apoptosis as indicators of paclitaxel resistance in cervical cell lines. Magn Reson Med 2012 Aug;68(2):369-377.

(237) Tirinato L, Liberale C, Di Franco S, Candeloro P, Benfante A, La Rocca R, et al. Lipid droplets: a new player in colorectal cancer stem cells unveiled by spectroscopic imaging. Stem Cells 2015 Jan;33(1):35-44.

(238) Verbrugge SE, Al M, Assaraf YG, Kammerer S, Chandrupatla, D M S H, Honeywell R, et al. Multifactorial resistance to aminopeptidase inhibitor prodrug CHR2863 in myeloid leukemia cells: down-regulation of carboxylesterase 1, drug sequestration in lipid droplets and pro-survival activation ERK/Akt/mTOR. Oncotarget 2016 Feb 2;7(5):5240-5257.

(239) Schlaepfer IR, Hitz CA, Gijon MA, Bergman BC, Eckel RH, Jacobsen BM. Progestin modulates the lipid profile and sensitivity of breast cancer cells to docetaxel. Mol Cell Endocrinol 2012 Nov 5;363(1-2):111-121.

(240) Kohe S, Colmenero I, McConville C, Peet A. Immunohistochemical staining of lipid droplets with adipophilin in paraffin-embedded glioma tissue identifies an association between lipid droplets and tumour grade. Journal of Histology and Histopathology 2017;4(1):4.

(241) Wilson M, Cummins CL, MacPherson L, Sun Y, Natarajan K, Grundy RG, et al. Magnetic resonance spectroscopy metabolite profiles predict survival in paediatric brain tumours. Eur J Cancer 2013 Jan;49(2):457-464.

(242) Vicente J, Fuster-Garcia E, Tortajada S, Garcia-Gomez JM, Davies N, Natarajan K, et al. Accurate classification of childhood brain tumours by in vivo (1)H MRS - a multi-centre study. Eur J Cancer 2013 Feb;49(3):658-667.

(243) Pan X, Wilson M, Mirbahai L, McConville C, Arvanitis TN, Griffin JL, et al. In vitro metabonomic study detects increases in UDP-GlcNAc and UDP-GalNAc, as early phase markers of cisplatin treatment response in brain tumor cells. J Proteome Res 2011 Aug 5;10(8):3493-3500.

(244) Zanotto-Filho A, Braganhol E, Klafke K, Figueiró F, Terra SR, Paludo FJ, et al. Autophagy inhibition improves the efficacy of curcumin/temozolomide combination therapy in glioblastomas. Cancer Letters 2015;358(2):220-231.

(245) Gao J, Aksoy BA, Dogrusoz U, Dresdner G, Gross B, Sumer SO, et al. Integrative analysis of complex cancer genomics and clinical profiles using the cBioPortal. Sci Signal 2013 Apr 2;6(269):pl1.

(246) Cerami E, Gao J, Dogrusoz U, Gross BE, Sumer SO, Aksoy BA, et al. The cBio Cancer Genomics Portal: An Open Platform for Exploring Multidimensional Cancer Genomics Data. CANCER DISCOVERY 2012;2(5):401-404.

(247) Greenspan P, Mayer EP, Fowler SD. Nile red: a selective fluorescent stain for intracellular lipid droplets. J Cell Biol 1985;100(3):965-973.

(248) Koizume S, Miyagi Y. Lipid Droplets: A Key Cellular Organelle Associated with Cancer Cell Survival under Normoxia and Hypoxia. International Journal of Molecular Sciences 2016;17(9).

(249) Geng F, Guo D. Lipid droplets, potential biomarker and metabolic target in glioblastoma. Intern Med Rev (Wash D C) 2017 May;3(5):10.18103/imr.v3i5.443.

(250) Amelot A, De Cremoux P, Quillien V, Polivka M, Adle-Biassette H, Lehmann-Che J, et al. IDH-Mutation Is a Weak Predictor of Long-Term Survival in Glioblastoma Patients. PLoS One 2015;10(7):e0130596. doi:10.1371/journal.pone.0130596.

(251) Chen JR, Yao Y, Xu HZ, Qin ZY. Isocitrate Dehydrogenase (IDH)1/2 Mutations as Prognostic Markers in Patients With Glioblastomas. Medicine (Baltimore) 2016 Mar;95(9):e2583. doi:10.1097/MD.0000000000002583.

(252) Dhani N, Fyles A, Hedley D, Milosevic M. The Clinical Significance of Hypoxia in Human Cancers. Seminars in Nuclear Medicine 2015;45(2):110-121.

(253) Jensen RL. Brain tumor hypoxia: tumorigenesis, angiogenesis, imaging, pseudoprogression, and as a therapeutic target. J Neurooncol 2009 May;92(3):317-335.

(254) Chamoun Z, Vacca F, Parton RG, Gruenberg J. PNPLA3/adiponutrin functions in lipid droplet formation. Biol Cell 2013 May;105(5):219-233.

(255) Martin S, Parton RG. Lipid droplets: a unified view of a dynamic organelle. Nat Rev Mol Cell Biol 2006 May;7(5):373-378.

(256) Eales KL, Hollinshead KER, Tennant DA. Hypoxia and metabolic adaptation of cancer cells. Oncogenesis 2016;5:e190.

(257) Nguyen LK, Cavadas MAS, Scholz CC, Fitzpatrick SF, Bruning U, Cummins EP, et al. A dynamic model of the hypoxia-inducible factor 1α (HIF-1α) network. J Cell Sci 2013;126(6):1454-1463.

(258) Vance JE. Phospholipid Synthesis and Transport in Mammalian Cells. Traffic 2015;16(1):1-18.

(259) Liu Y, Ma Z, Zhao C, Wang Y, Wu G, Xiao J, et al. HIF-1α and HIF-2α are critically involved in hypoxia-induced lipid accumulation in hepatocytes through reducing PGC-1α-mediated fatty acid β-oxidation. Toxicology Letters 2014;226(2):117-123.

(260) Marullo R, Werner E, Degtyareva N, Moore B, Altavilla G, Ramalingam SS, et al. Cisplatin induces a mitochondrial-ROS response that contributes to cytotoxicity depending on mitochondrial redox status and bioenergetic functions. PLoS One 2013 Nov 19;8(11):e81162.

(261) Chen RF. Removal of Fatty Acids from Serum Albumin by Charcoal Treatment. Journal of Biological Chemistry 1967 January 25;242(2):173-181.

(262) Helledie T, Antonius M, Sørensen RV, Hertzel AV, Bernlohr DA, Kølvraa S, et al. Lipid-binding proteins modulate ligand-dependent trans-activation by peroxisome proliferator-activated receptors and localize to the nucleus as well as the cytoplasm. Journal of Lipid Research 2000 November 01;41(11):1740-1751.

(263) Penrose H, Heller S, Cable C, Makboul R, Chadalawada G, Chen Y, et al. Epidermal growth factor receptor mediated proliferation depends on increased lipid droplet density regulated via a negative regulatory loop with FOXO3/Sirtuin6. Biochem Biophys Res Commun 2016;469(3):370-376.

(264) Abe H, Yamashita S, Satoh T, Hoshi H. Accumulation of cytoplasmic lipid droplets in bovine embryos and cryotolerance of embryos developed in different culture systems using serum-free or serum-containing media. Mol Reprod Dev 2002;61(1):57-66.

(265) Opstad KS, Wright AJ, Bell BA, Griffiths JR, Howe FA. Correlations between in vivo 1H MRS and ex vivo 1H HRMAS metabolite measurements in adult human gliomas. Journal of Magnetic Resonance Imaging 2010;31(2):289-297.

(266) Mayer N, Schweiger M, Romauch M, Grabner GF, Eichmann TO, Fuchs E, et al. Development of small-molecule inhibitors targeting adipose triglyceride lipase. Nat Chem Biol 2013 Dec;9(12):785-787.

(267) Yang P, Liu K, Ngai MH, Lear MJ, Wenk MR, Yao SQ. Activity-Based Proteome Profiling of Potential Cellular Targets of Orlistat − An FDA-Approved Drug with Anti-Tumor Activities. J Am Chem Soc 2010;132(2):656-666.

(268) Gbelcova H, Sveda M, Laubertova L, Varga I, Vitek L, Kolar M, et al. The effect of simvastatin on lipid droplets accumulation in human embryonic kidney cells and pancreatic cancer cells. Lipids Health Dis 2013 Aug 21;12:126.

(269) Antalis CJ, Arnold T, Rasool T, Lee B, Buhman KK, Siddiqui RA. High ACAT1 expression in estrogen receptor negative basal-like breast cancer cells is associated with LDL-induced proliferation. Breast Cancer Res Treat 2010 Aug;122(3):661-670.

(270) Petiot A, Ogier-Denis E, Blommaart EF, Meijer AJ, Codogno P. Distinct classes of phosphatidylinositol 3'-kinases are involved in signaling pathways that control macroautophagy in HT-29 cells. J Biol Chem 2000 Jan 14;275(2):992-998.

(271) Kimura T, Takabatake Y, Takahashi A, Isaka Y. Chloroquine in cancer therapy: a double-edged sword of autophagy. Cancer Res 2013 Jan 1;73(1):3-7.

(272) Hashimoto T, Yokokawa T, Endo Y, Iwanaka N, Higashida K, Taguchi S. Modest hypoxia significantly reduces triglyceride content and lipid droplet size in 3T3-L1 adipocytes. Biochem Biophys Res Commun 2013;440(1):43-49.

(273) Zhang H, Sun T, Jiang X, Yu H, Wang M, Wei T, et al. PEDF and PEDF-derived peptide 44mer stimulate cardiac triglyceride degradation via ATGL. J Transl Med 2015 Feb 21;13:1.

(274) Villa G, Hulce J, Zanca C, Bi J, Ikegami S, Cahill G, et al. An LXR-Cholesterol Axis Creates a Metabolic Co-Dependency for Brain Cancers. Cancer Cell 2016;30(5):683-693.

(275) Egnatchik RA, Leamy AK, Noguchi Y, Shiota M, Young JD. Palmitate-induced Activation of Mitochondrial Metabolism Promotes Oxidative Stress and Apoptosis in H4IIEC3 Rat Hepatocytes. Metabolism 2014 Feb;63(2):283-295.

(276) Peck B, Schulze A. Lipid desaturation – the next step in targeting lipogenesis in cancer? The FEBS Journal 2016;283(15):2767-2778.

(277) Zhang I, Cui Y, Amiri A, Ding Y, Campbell RE, Maysinger D. Pharmacological inhibition of lipid droplet formation enhances the effectiveness of curcumin in glioblastoma. European Journal of Pharmaceutics and Biopharmaceutics 2016;100(Supplement C):66-76.

(278) Mizumoto M, Yamamoto T, Takano S, Ishikawa E, Matsumura A, Ishikawa H, et al. Long-term survival after treatment of glioblastoma multiforme with hyperfractionated concomitant boost proton beam therapy. Practical Radiation Oncology 2015;5(1):e16.

(279) Hauswald H, Rieken S, Ecker S, Kessel KA, Herfarth K, Debus J, et al. First experiences in treatment of low-grade glioma grade I and II with proton therapy. Radiat Oncol 2012 Nov 9;7:189.

(280) Stupp R, Hegi ME, Mason WP, van den Bent, Martin J, Taphoorn MJ, Janzer RC, et al. Effects of radiotherapy with concomitant and adjuvant temozolomide versus radiotherapy alone on survival in glioblastoma in a randomised phase III study: 5-year analysis of the EORTC-NCIC trial. The Lancet Oncology 2009;10(5):459-466.

(281) Sorensen AG, Emblem KE, Polaskova P, Jennings D, Kim H, Ancukiewicz M, et al. Increased Survival of Glioblastoma Patients Who Respond to Antiangiogenic Therapy with Elevated Blood Perfusion. Cancer Res 2012;72(2):402-407.

(282) Batchelor TT, Gerstner ER, Emblem KE, Duda DG, Kalpathy-Cramer J, Snuderl M, et al. Improved tumor oxygenation and survival in glioblastoma patients who show increased blood perfusion after cediranib and chemoradiation. Proceedings of the National Academy of Sciences 2013 November 19;110(47):19059-19064.

(283) McIntyre A, Harris AL. Metabolic and hypoxic adaptation to anti-angiogenic therapy: a target for induced essentiality. EMBO Mol Med 2015 Apr;7(4):368-379.

(284) Schiffmann LM, Brunold M, Liwschitz M, Goede V, Loges S, Wroblewski M, et al. A combination of low-dose bevacizumab and imatinib enhances vascular normalisation without inducing extracellular matrix deposition. British Journal Of Cancer 2017;116:600.

(285) Reisz JA, Bansal N, Qian J, Zhao W, Furdui CM. Effects of Ionizing Radiation on Biological Molecules—Mechanisms of Damage and Emerging Methods of Detection. Antioxid Redox Signal 2014 Jul 10;21(2):260-292.

(286) Rojas-Puentes LL, Gonzalez-Pinedo M, Crismatt A, Ortega-Gomez A, Gamboa-Vignolle C, Nuñez-Gomez R, et al. Phase II randomized, double-blind, placebo-controlled study of whole-brain irradiation with concomitant chloroquine for brain metastases. Radiat Oncol 2013;8:209.

(287) ClinicalTrials.gov. A Randomised Trial Investigating the Additional Benefit of Hydroxychloroquine(HCQ)to Short Course Radiotherapy (SCRT) in Patients Aged 70 Years and Older With High Grade Gliomas (HGG) (HCQ). 2016; Available at: https://clinicaltrials.gov/ct2/show/NCT01602588.

(288) ClinicalTrials.gov. The Addition of Chloroquine to Chemoradiation for Glioblastoma (CHLOROBRAIN). 2017; Available at: https://clinicaltrials.gov/ct2/show/NCT02378532.

(289) Sotelo J, Briceno E, Lopez-Gonzalez MA. Adding chloroquine to conventional treatment for glioblastoma multiforme: a randomized, double-blind, placebo-controlled trial. Ann Intern Med 2006 Mar 7;144(5):337-343.

(290) Du W, Zhang L, Brett-Morris A, Aguila B, Kerner J, Hoppel CL, et al. HIF drives lipid deposition and cancer in ccRCC via repression of fatty acid metabolism. Nature Communications 2017;8(1):1769.

(291) Yang H, Ye D, Guan K, Xiong Y. *IDH1* and *IDH2* Mutations in Tumorigenesis: Mechanistic Insights and Clinical Perspectives. Clin Cancer Res 2012;18(20):5562-5571.

(292) Rao JS. Molecular mechanisms of glioma invasiveness: the role of proteases. Nature Reviews Cancer 2003;3:489.

(293) Melendez A, Levine B. Autophagy in C. elegans. WormBook 2009 Aug 24:1-26.

(294) Singh R, Maria Cuervo A. Lipophagy: Connecting Autophagy and Lipid Metabolism. ; 2012.

(295) Prados MD, Seiferheld W, Sandler HM, Buckner JC, Phillips T, Schultz C, et al. Phase III randomized study of radiotherapy plus procarbazine, lomustine, and vincristine with or without BUdR for treatment of anaplastic astrocytoma: final report of RTOG 9404. International Journal of Radiation Oncology • Biology • Physics 2004;58(4):1147-1152.

Outputs from this research

Scientific research papers

Manuscript in preparation

Poster presentations at conferences

Keystone Metabolism and Hypoxia – Whistler, Canada 2017

Metabolic pathways influencing glioblastoma lipid droplet biology

Lipid droplets are rapidly emerging as key components of cancer metabolism however the cellular pathways governing these dynamic organelles remain unclear. Although preferred mechanisms are often tissue specific, they can include uptake of exogenous serum lipids, lipophagy, lipase activity and de novo lipid synthesis. A number of tumour types exhibit an increase in lipid droplets in hypoxia, notably glioblastoma (GBM), where they are associated with treatment resistance and poor survival. Our understanding of lipid droplet biology remains incomplete and we therefore investigated potential mechanisms using four human GBM cell lines (T98G, U87, HGG01 and HGG03). We found that lipid droplets were increased in hypoxia (0.3% O2) in all cell lines, measured using microscopy, flow cytometry and NMR-based methods. We show a role for adipose triglyceride lipase (ATGL) and a cellular reliance upon the uptake of exogenous serum lipids in lipid droplet production and maintenance. Lipid droplet degradation was observed through the combined action of lipophagy (lipid droplet-specific autophagy) and ATGL. We suggest that the action of these mechanisms provide the core of a lipid droplet metabolic pathway within these cell lines and that the hypoxia-induced lipid droplet increase is reliant upon differential activity of these mechanisms. Therapeutic options remain highly limited in GBM and our data suggest that manipulation of lipid droplets with pharmacological inhibitors can alter the in vitro cytotoxic efficacy of temozolomide, the major chemotherapeutic agent. Our data further illuminates the metabolic mechanisms governing lipid droplet metabolism in GBM and suggests the application of lipid droplet manipulation may greatly improve current and future clinical therapies.

International Symposium on Paediatric Neuro-Oncology (ISPNO) – Liverpool, UK 2016

Hypoxia and lipid droplets in glioblastoma: A story of two paths.

Glioblastoma is a highly malignant disease with limited therapeutic options and a poor prognosis which affects both children and adults. An area of recent interest in glioblastoma is lipid droplets which are quickly emerging as an influential facet of cancer cell biology. Considered dynamic organelles composed of a neutral lipid core and single-layer phospholipid membrane they are associated with higher grade and poorer prognosis in astrocytomas. Furthermore, highly hypoxic areas in glioblastomas are known to alter lipid metabolism as well as being resistant to treatments such as radiotherapy. However the impact of hypoxia on lipid droplets and the mechanisms for lipid droplet formation in glioblastoma is yet to be elucidated. Changes in lipid droplet number between normoxia and hypoxia (0.3% O2) were investigated using confocal fluorescence microscopy. Pharmacological targeting of autophagy and lipid synthesis and degradation was employed to investigate the cellular role of lipid droplets in both adult (T98G and U87) and paediatric (HGG01 and HGG03, Hulleman VUMC, NL) immortalised glioblastoma cell lines. Acute and chronic hypoxic incubation significantly increased lipid droplet expression whilst pharmacological inhibition of lipid synthesis failed to abrogate lipid droplet formation. Instead lipid droplet formation was reliant upon autophagy and lipase function in the U87 and HGG03 cell lines and exogenous uptake from serum in the T98G and HGG01 cell lines. Taken together our data suggests that hypoxia induces an increased level of lipid droplet expression through either autophagy or exogenous uptake from serum and raises the possibility of pharmacological targeting.

Mitox – Oxford, UK 2015

The Role of Hypoxia on Lipid Droplet Production in Glioblastoma.

Lipid droplets are quickly emerging as an important and influential facet of cancer cell biology. Composed of a neutral lipid core and single-layer phospholipid membrane, they were originally considered simple energy stores but are now thought of as dynamic organelles with a significant impact upon cellular metabolism. Lipid droplets have been particularly linked to glioblastoma, a very severe and malignant form of brain cancer, and are shown to increase with clinical grade and chemotherapeutic response. Moreover glioblastomas contain very hypoxic areas which are known to alter lipid metabolism and are believed to influence lipid droplet expression. The impact of hypoxia on lipid droplets has been only briefly investigated and the methods by which any alterations could occur remain unknown.

We investigated changes in lipid droplet number between normoxia and hypoxia (0.3% O2) using confocal fluorescence microscopy and observed that, in both adult and paediatric immortalised glioblastoma cell lines (U87, T98G, HGG01 and HGG03), lipid droplet number increased significantly in acute hypoxia (16 hours). Chronic hypoxic incubation further increased lipid droplet number whilst pharmacological inhibition of both glutaminolysis, through BPTES, and fatty acid synthesis, through Orlistat, failed to abrogate lipid droplet formation. Where possible we used data acquired through high-resolution magic-angle spinning (HRMAS) nuclear magnetic resonance spectroscopy (NMR) and analysed with Mestrenova peak analysis to support induced metabolic alterations.

Taken together our data suggests that hypoxia induces an increasing level of lipid droplet expression through a cellular mechanism other than de novo synthesis, indicating an alternative and potentially pharmacologically-targetable pathway for investigation.